Enhancing Recovery After Spinal Cord Injury with Combinational Activity-Based Therapy and Anti-Nogo-A, and Targeting Gamma Motor Neurons Which Could Mediate this Recovery

Richard Gabriel Dickson

Submitted in accordance with the requirements for the degree of Doctor of Philosophy

The University of Leeds

School of Biomedical Sciences

Intellectual property rights and declaration

The candidate confirms that the work submitted is his own and that appropriate credit has been given where reference has been made to the work of others.

Acknowledgments

I would first like to thank my supervisors Drs. Ronaldo Ichiyama and Samit Chakrabarty. Thank you Ronaldo for all the wide-ranging chats on motor learning and for the excitement whenever we discussed something new. Your time and investment in my career has been above and beyond. Thanks to Samit and Ronaldo, your enthusiasm for science is an inspiration. For all the long days of surgery with a playlist of Shostakovich for Samit, Britney for Ronaldo, and the Chainsmokers/Lion King soundtrack for Roger. Jessica Kwok has been an invaluable resource for any and all questions I have had. Without her scientific guidance everything would have been that much harder.

To all the Ichiyama lab members, Varinder, Calvin, Yazi, Kinon, Aleks, Roger, Natalie, Nicole and Supti. For all the morning lab meetings with Ronaldo buying the best croissants and for all the lab meetings derailed. For everyone in the 5.55 ‘office’ hallway, Sian, Luke, Sylvain, Gareth, Pip, Giuliano, Ashleigh, Stuart, Jan, Raphael, Josh, Abigail, and Linda. For putting up with my cheese toasties and coffee and for always popping round my desk for a chat. Thanks especially to Chun Yue for being there throughout this whole writing process and pandemic.

Special thanks to Piyanee and Tom, members of 5.55 before it was cool. Thanks for all the late nights at the Fenton and the space to vent. To my best friends, Erika and Jaime, for all the weekends spent not thinking about science.

Finally, I would like to thank my dad and Anna for always supporting me. To all my family, but especially Miguel for all the debates and discussions, and to Christia for keeping me grounded.

Abstract

Sequential Anti-Nogo-A therapy with the antibody 11C7 and step training has previously been shown to improve locomotor function and increase axonal sprouting of afferents and descending pathways after partial spinal transection in a rat (Maier et al., 2009, Chen et al., 2017). Separately, step training under electrical epidural stimulation (ES) has been shown to improve locomotor function after complete spinal transection in rats and humans with clinically motor complete lesions (Ichiyama et al., 2005, Angeli et al., 2018, Wagner et al., 2018). Combinational treatments involving activity-based rehabilitation and plasticity enhancing therapies are needed to improve locomotor function beyond the modest recovery observed with individual treatments in severe lesions (Dickson et al., 2019). Therefore, we have investigated a combinational therapy with the plasticity enhancing 11C7 antibody followed by sequential training under ES in a severe contusion injury model. In order to combine therapies it is necessary to understand the mechanisms of each therapy individually and in combination with other therapies. For that reason we have studied all possible combinations of training, 11C7, and ES and investigated kinematic, electrophysiological, local spinal, and descending pathway changes between groups.

Adult Sprague-Dawley rats (~250 g) received a severe spinal contusion injury (250 kilodyne) (T9/10) and epidural implantation at segmental levels L2 and S1. An intrathecal catheter attached to a mini-osmotic pump delivered 11C7 or control IgG (cyclosporin) for two weeks after injury. Rats were randomly assigned to groups of cage control, training, ES, or combinational training under ES (CB). Three weeks after injury animals in treatment groups were given 8 weeks of therapy 5 days a week for 20 minutes a day. Treatment consisted of step training under body weight support (7-18 cm/s) or ES (0.2 ms pulses at 40 Hz, 0.5-5 V), or step training under ES for the CB group. The 11C7 treated training and CB groups had the most animals demonstrating weight supported stepping in the final four weeks of treatment. Kinematic analysis showed that the 11C7 treated CB group had the least percentage of toe dragging. Principal component analysis of kinematics revealed that for the first principal component the combination of 11C7 followed by step training, ES, or step training under ES were not statistically significantly different from naïve controls.

Afferent input to MNs was reduced in the CB 11C7 group, along with an increase of afferent inputs receiving clusters of 3+ presynaptic inhibitory P boutons. Thus indicating that there is more modulation of afferent input with this more behaviourally effective combinational treatment.

γ-MNs modulate the activity of muscle spindle afferents. These spindle afferents are vital for recovery after spinal cord injury (SCI) (Takeoka et al., 2014). However, the role of γ-MNs, which control these afferents, has not been determined. Their separate descending and segmental control from α-MNs mean these neurons may be activated by different pathways even if input to α-MNs is impaired. Earlier evidence suggests that these neurons may be more plastic than α-MNs, they lack plasticity restricting perineuronal nets (Smith et al., 2015, Al'joboori et al., 2020), have less neurite outgrowth inhibiting Nogo-A (unpublished observations), and are known to lose synaptic coverage and then regain this input after training in a neonatal transection (Ichiyama et al., 2011). Taken together this suggests γ-MNs are an integral part of circuit reorganization and recovery after SCI. We therefore attempted to selectively target γ-MNs with adeno associated virus molecularly in order to trace their immediate inputs and thereby uncover some of their function (Wickersham et al., 2007). AAVs with promotors for the apparently γ-MN specific estrogen related receptor γ (Err3) (Friese et al., 2009), or the serotonin receptor 5-HT_{1D} were not able to selectively target γ-MNs. Further investigation of γ-MN specific targeting via the small proximal branch of the soleus muscle has indicated this pathway could be suitable for tracing experiments. In order to uncover some of the function of γ-MNs, we have also determined the proportion of γ-MNs in various forelimb and hindlimb muscles. There is a lower proportion of γ-MNs in extensors, and in forelimb muscles. The greater reliance of extensors on Golgi tendon organs, and the greater visual guidance of forelimb muscle could be why we have observed lower numbers in these areas. Further experiments, perhaps with genetically modified mice, may allow us selective access to γ-MNs, in order to uncover their inputs, and role in movement, learning, and SCI recovery.

In conclusion, we have demonstrated combinational potential for 11C7 with sequential step training or step training under ES for improved locomotor recovery. Our combinational treatment for SCI with 11C7 could have an immediate impact as clinical

trials of anti-Nogo-A in humans are underway (Kucher et al., 2018) and our data suggest it is only effective in severe contusion injuries if followed by locomotor training. In addition, we have determined some differences in the relative proportion of γ-MNs despite our unsuccessful selective targeting studies. This is one further step to understanding the function of these neurons which present a uniquely attractive target to enhance motor recovery after SCI.

Table of contents

Table of Figures

List of Abbreviations

5-HT-Serotonin

5-HT$_{1D}$-Serotonin receptor 1D

α-MN-Alpha motor neuron

β-MN-Beta motor neuron

γ-MN-Gamma motor neuron

γ$_d$-dynamic gamma motor neurons

γ$_d$-static gamma motor neurons

AAV-Adeno associated viruses

AR-Antigen retrieval

ASIA-American Spinal Injury Association

ASPA-Animals (Scientific Procedures) Act

BBB-Basso, Beattie and Bresnahan

BDA-Biotinylated Dextran Amine

BDNF-Brain Derived Neurotrophic Factor

BK-Bradykinin

BWS-Body Weight Support

cAMP-Cyclic adenosine monophosphate

CB-Combination treatment

cDNA-Complementary deoxyribonucleic acid

CGCT-cage control treated

ChABC-Chondroitinase

ChAT-Choline Acetyl Transferase

CNS-Central nervous system

CPG-Central Pattern Generator

CREB-Cyclic AMP response binding element

CSPG-Chondroitin Sulphate Proteoglycan

CST-Corticospinal tract

CTB-Cholera toxin subunit β

DCM-Dichloromethane

DH-Dorsal horn

DIG-Digoxigenin

DRG-Dorsal Root Ganglion

EMG-Electromyography

EphaA4-erythropoietin-producing hepatocellular

Err3-Estrogen related receptor γ

ES-Epidural stimulation

F:E-Flexor:extensor

FDD-Frequency dependent depression

GABA-Gamma-Aminobutyric acid

GAD65-glutamic acid decarboxylase 65 kDa isoform

GDNF-Glial derived neurotrophic factor

GFP-Green fluorescent protein

GS-Gastrocnemius

GTO-Golgi tendon organ

Ia IN- Ia inhibitory interneuron

IHC-Immunohistochemistry

IMZ-Intermediate zone

INs-Interneurons

L:R-Left:right

L-Dopa-Levodopa

MAG-Myelin-associated glycoprotein

MesADC-Mesencephalic area for dynamic control

MLR-Mesencephalic locomotor region

MN-Motor neuron

MSR-Mono-synaptic reflex

mTOR-Mammalian target of rapamyacin

NDS-Normal donkey serum

NgR-Nogo receptor

NKAα3-Na^+/K^+ ATPase alpha 3 subunit

NMDA-N-methyl-D-aspartate receptor

NMJ-Neuromuscular junction

Nogo-A-Neurite outgrowth inhibitor

NT3-Neurotrophic factor 3

OCT-Optimal cutting temperature compound

OMgp-Oligodendrocyte-myelin glycoprotein

PB-Phosphate buffer

PBS-Phosphate buffer saline

PBST-Phosphate buffer saline with Triton X-100

PC-Principal component

PCA-Principal component analysis

PFA-Paraformaldehyde

PNN-Perineuronal nets

PNS-Peripheral nervous system

PTEN-Phosphate and tensin homolog

RC-Renshaw cell

ReST-Reticulospinal tract

rhoA-Ras homolog gene family member A

ROCK-RhoA kinase

RST-Rubrospinal tract

S1PR2-Sphingosine-1-phosphate receptor 2

SA1-Slow adapting type 1 mechanoreceptor

SCI-Spinal cord injury

SD-Standard deviation

SEM-Standard error mean

SNpr-Substantia nigra pars reticulata

TBS-Tris buffered saline

TH-Tyrosine hydroxylase

TNS-Tris non saline

TR-Training

VGAT-Vesicular GABA transporter

VGluT1-Vesicular glutamate transporter 1

VGluT2-Vesicular glutamate transporter 2

VH-Ventral horn

1 General introduction

1.1 Introduction

This thesis has two foci of attention, both gamma motor neurons (γ-MNs) and spinal cord injury (SCI). I will attempt to explain the connection between γ-MNs and spinal cord injury (SCI) and in the process shed some light on both topics individually.

The spinal cord locomotor network receives input from supraspinal centres and sensory afferents from the periphery and has outputs to both the supraspinal centres and to the muscles. The role of γ-MNs in this is to change the firing properties of the proprioceptive afferents inputting to this network. We know proprioceptive information is vital for SCI recovery as mice without muscle spindles were unable to recover any locomotor ability following a unilateral hemisection (Takeoka et al., 2014). While it is unknown whether γ-MNs are also vital for this recovery, it does seem likely, as they are responsible for the control of these spindles. Further hints at the role of γ-MNs in SCI include research by Ichiyama et al. (2011) who showed that there was a decrease in synaptic coverage on γ-MNs following neonatal transection. This, along with the lack of plasticity restricting perineuronal nets on γ-MNs (Smith et al., 2015) , and the reduced amount of neurite outgrowth inhibitor Nogo-A seen in γ-MNs following SCI (unpublished observations), has led us to believe that γ-MNs present a uniquely plastic and important target for SCI recovery. Thus it is worth studying both their inputs and their changes following SCI.

There are both γ-MN and SCI experimental chapters within this document. The introduction will start with an overview of the spinal locomotor network along with a thorough investigation of the current knowledge of γ-MNs and their role in SCI. The SCI section will cover background and pathology with emphasis on local spinal changes after combinatorial plasticity enhancing treatments.

1.2 Spinal control of movement

1.2.1 Spinal cord structure

The spinal cord is involved in practically all motor control caudal to the neck. However, in this thesis much of the focus will be on the lumbar spinal cord with emphasis on structures involved in locomotion.

The spinal cord projects caudally from the brain with spinal roots extending out every segment. In the rat there are 34 segments. From rostral to caudal they are the cervical, thoracic, lumbar, and sacro-coccygeal. The spinal cord consists of white matter tracts and grey matter divided into a ventral and dorsal horn. Additionally, in the thoracic spinal cord there is an intermediate lateral horn for autonomic control. The dorsal horn components are involved in more sensory functions and the ventral horn more motor functions. The spinal cord grey matter is divided into Rexed Laminae by cellular structure as shown in Figure 1.1 (Rexed, 1952, Molander et al., 1984). Laminae I-VI contain most sensory integration interneurons, Laminae VII-VIII contain many of the interneurons involved in pattern formation and rhythm generation of spinal motor output. Lamina IX contains the MNs while lamina X around the central canal contains many autonomic neurons. These different areas of the spinal cord receive, integrate and transmit information to and from supraspinal centres and the periphery. Within the spinal cord are multiple neurons involved in each of these tasks, these neurons will be covered in the section on spinal interneuronal networks and central pattern generators (page 3).

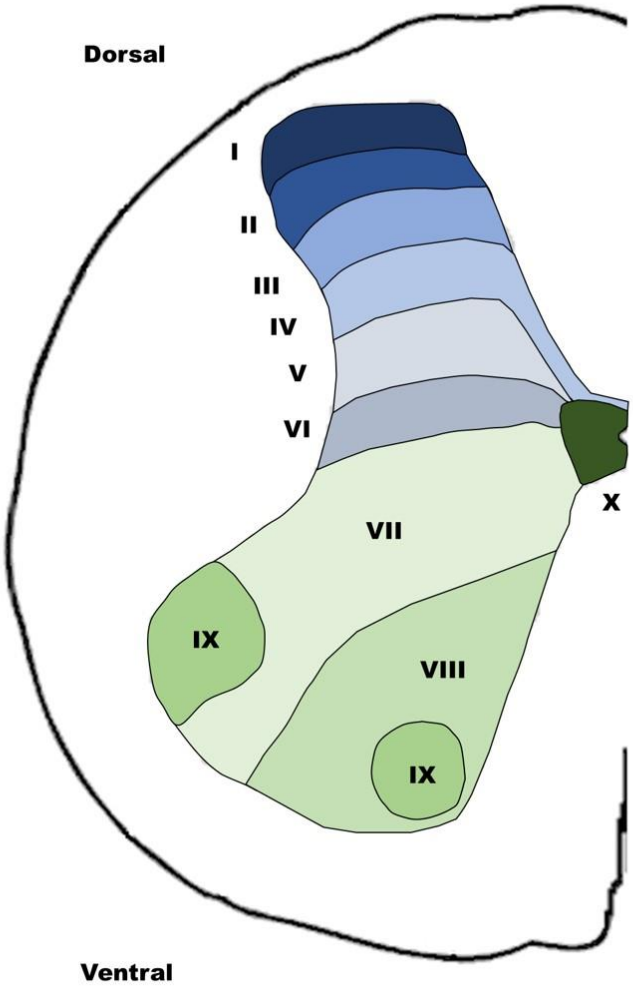

Figure 1.1 Rexed laminae of the spinal cord
The spinal cord divided into the ten Rexed Laminae with Laminae I-V being largely confined to the dorsal horn, Lamina X around the central canal. Lamina VII covers much of the intermediate zone and some ventral horn. Lamina VIII includes many pre-motor neurons while Lamina IX includes the motor neurons.

1.2.2 Spinal locomotor networks

1.2.2.1 Monosynaptic reflex and H-reflex

The locomotor network in the spinal cord is complex with many different interneurons involved. These interneuron networks are often termed central pattern generators (CPGs). The various components of the CPG are detailed more below (Section 1.2.2.2, page 6). The complexity of this network and the inability to target individual components has meant that detailed study is a relatively recent phenomenon. Due to its accessibility, study of spinal

sensorimotor circuitry has often focused on the relatively simple mono-synaptic reflex arc (MSR). The pathway begins from muscle spindles responding to stretch. Primary muscle spindle afferents are activated by this stretch, and they then synapse to directly excite homonymous or synergist α-MNs leading to a contraction in the muscle (Figure 1.2). The contraction allows the muscle to counteract the original force causing the reflex and thus maintain a constant length. The MSR is a way of accessing the 'final common pathway' of the motor neuron to the muscle. The MSR is modulated by supraspinal and segmental inputs, thus it is often used to study changes in these inputs and how they alter the CPG.

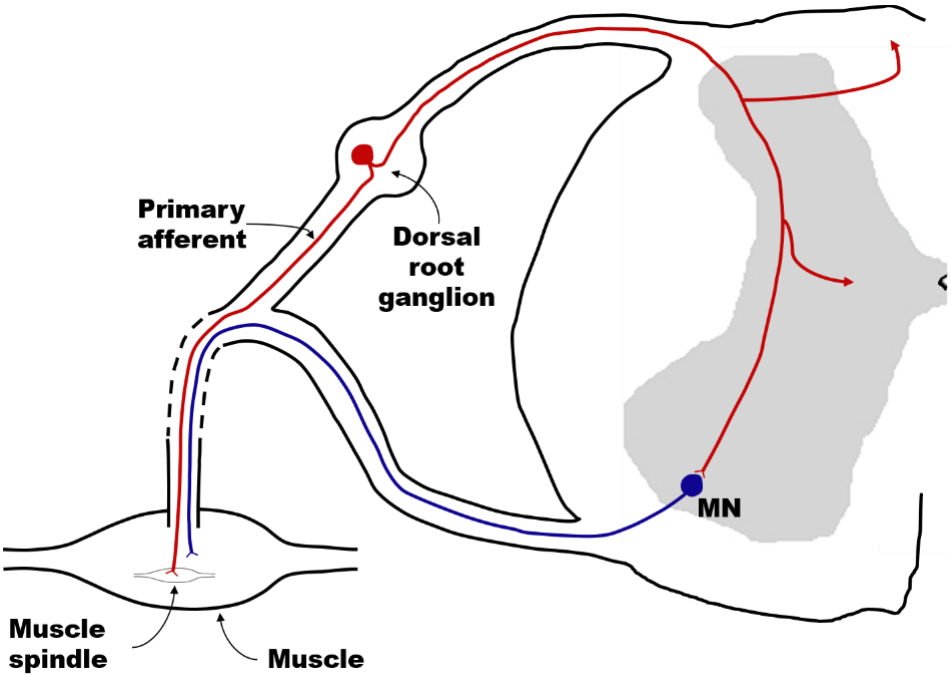

Figure 1.2 The MSR arc
MNs (blue) are contacted with excitatory synapses from primary muscle spindle afferents (red) which respond to stretch.

The electrical analogue of the MSR is the H-reflex (Hoffmann, 1918) (Figure 1.3). This is the method by which the MSR is often probed. The H-reflex is observed when a nerve is stimulated at a strength high enough to excite the primary sensory afferents and cause a muscle reaction. This has the advantage of bypassing the muscle spindle and thus any changes in sensitivity of the spindle which may have occurred. The maximum H reflex response is often normalised to the maximum M response, which is the direct motor axon stimulation causing a muscle response. Studies on humans have shown a reduction in the Hmax:Mmax ratio following skill acquisition (Perez et al., 2005) and an increase following

SCI (Phadke et al., 2010). Changes in the H-reflex have been studied intensively and have aided in many of the studies described below.

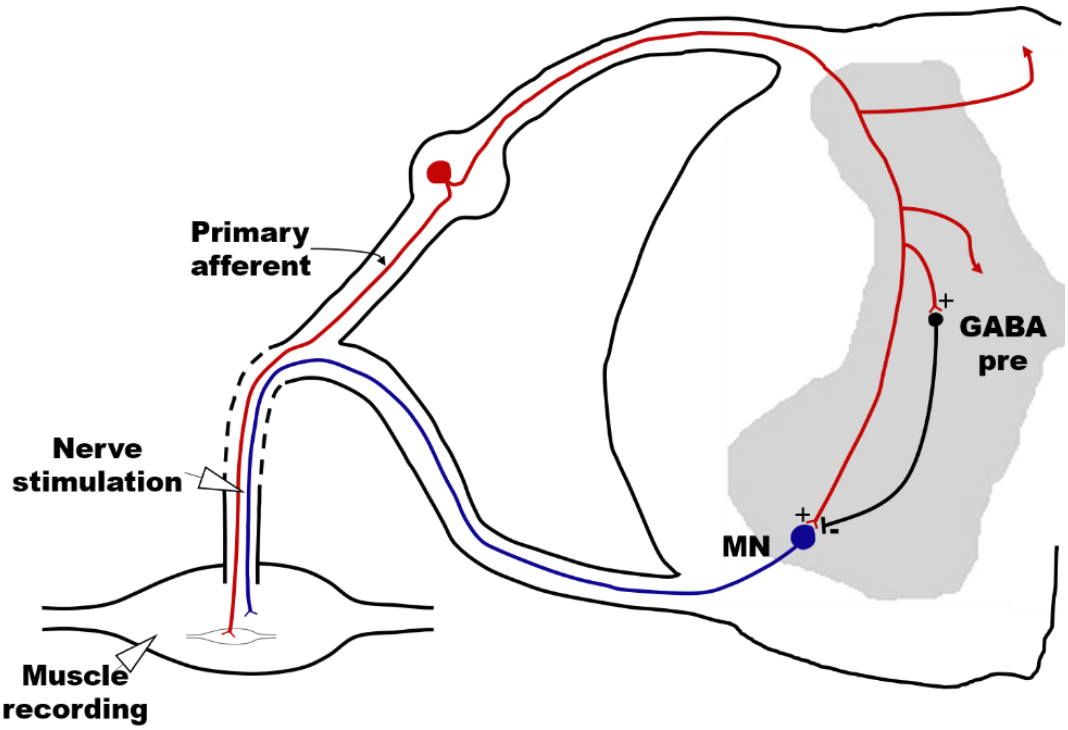

Figure 1.3 H-reflex and presynaptic inhibition
The electrical analogue of the MSR in Figure 1.2 is the H-reflex. A mixed nerve is stimulated which leads to primary afferent activation and subsequent MN and then muscle response recorded by electromyography (EMG). Pre-synaptic inhibition of this reflex by GABA-pre interneurons is often studied with the H-reflex.

What is causing the increase in Hmax:Mmax after SCI is most likely loss of pre-synaptic inhibition. Pre-synaptic inhibition is a phenomenon first discovered by Frank and Fuortes (1957), which is modulated by supraspinal as well as primary afferent input (Ménard et al., 1999). This presynaptic inhibition filters sensory stimulation and ensures smooth movement, as without presynaptic inhibition oscillations in movement occur (Fink et al., 2014). The inhibition comes from what are termed GABApre interneurons (Betley et al., 2009) which have synapses on the primary afferent inputs to motor neurons (P boutons) (Figure 1.3). Changes in this network drive H-reflex changes after SCI, such as a reduction in P boutons following sacral transection in rat (Kapitza et al., 2012). More recently, also in rats, a complete thoracic transection reduced pre-synaptic inhibition from

afferent inputs (Caron et al., 2020). Treadmill training returned this pre-synaptic inhibition to normal. Anatomical evidence backs this up, as another complete transection rat study found that training increased P bouton density (Khalki et al., 2018). The mechanism for the increase in pre-synaptic inhibition and P boutons probably relies on increased afferent activity from training. This is because afferent glutamatergic activity is known to drive P bouton formation, probably via brain derived neurotrophic factor (BDNF) (Mende et al., 2016, Betley et al., 2009). Some of the training induced changes in H-reflex are also described in section 1.3.3.3 on Locomotor training. We have also studied changes in the H-reflex and P boutons in our SCI study in chapter 3.

In summary, studies on the MSR circuitry, via its electrical analogue the H-reflex, are a crucial window into the spinal locomotor network. The H-reflex and the neural network responsible for it, allow us access to uncover electrophysiological and anatomical changes in the local spinal circuitry. Of course this is only a small part of the locomotor circuitry, and more detailed knowledge of other individual components are described below.

1.2.2.2 The central pattern generator and its known components

A central pattern generator (CPG) is a network that can produce rhythmic output without the need for segmental or supraspinal input. The first evidence for this came from Brown (1911). In Brown's model a groups of excitatory interneurons projects to motor neurons activating extensors or flexors. These excitatory interneurons also project to inhibitory interneurons which contact the antagonist motor neurons and antagonist pre-motor neurons. This ensure that antagonist excitatory interneurons and motor neurons could not be firing at the same time (Figure 1.4A). This theory paved the way for much further research, however it is oversimplified. The details of this model, including the necessity of reciprocal inhibition, have been questioned (Kiehn, 2006). Other more complex CPG models have been postulated, including one by McCrea and Rybak (Figure 1.4B). This model can account for more observed behaviour with its separate rhythm generation and pattern formation layers. Rather than relying on reciprocal inhibition the model's rhythmicity relies on a slowly inactivating persistent inward sodium current (Rybak et al., 2006). Advances in genetic targeting has allowed us to identify many of the

components which contribute to spinal CPGs shown in Figure 1.4B. This section will cover some of these components and the role they play in the spinal control of movement.

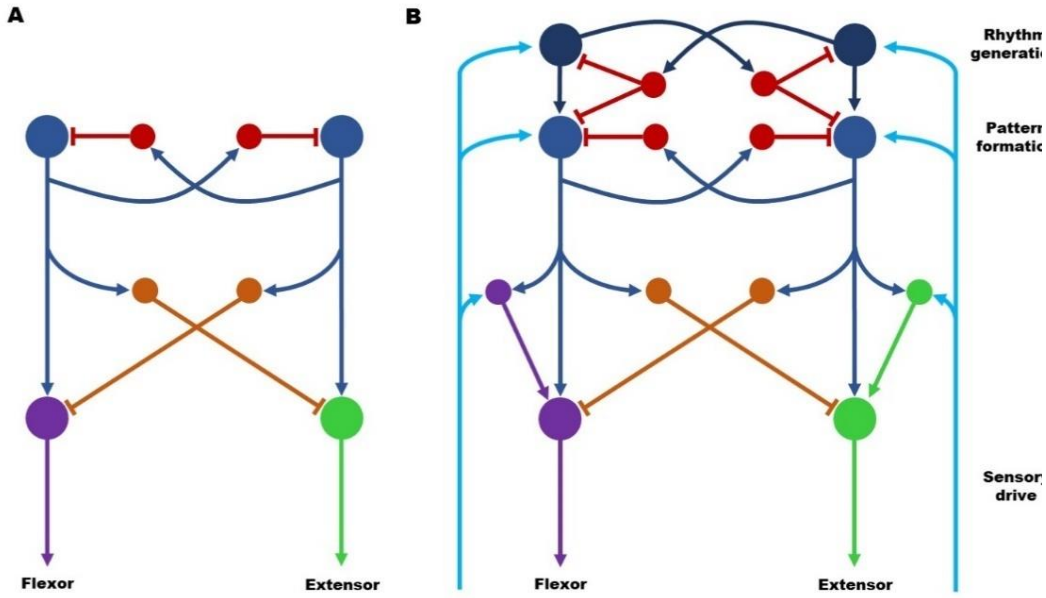

Figure 1.4 Different models for CPGs

Brown's early model for a CPG (A) consisted of two excitatory interneurons (blue) connected to inhibitory interneurons (orange and red) to ensure only the flexor or extensor of each limb was active at one time. McCrea and Rybak (2008) have an updated model which has separate rhythm and pattern generation layers, with sensory drive (light blue) also taken into account (B). Arrows indicate excitation while caps indicate inhibition.

There are numerous distinct subtypes of interneurons that make up the spinal locomotor network. During development these subtypes differentiate based on their relative distance from signalling hubs. The first such division is the dorso-ventral pattern which emerges due to Sonic hedgehog ventrally and dorsal bone morphogenetic protein dorsally (Jessell, 2000). This leads to six dorsal progenitors (dI1-dI6), and four ventral progenitors (V0-V3) alongside Hb9 expressing cells which include MNs. The ventral interneurons are all involved in the locomotor network while the dorsal interneurons are primarily involved in sensory circuits. Signalling along these gradients leads to a cascade of transcription factors which are mutually inhibitory, thus leading to cell types which are robust and well defined once their fate has been chosen (Balaskas et al., 2012).

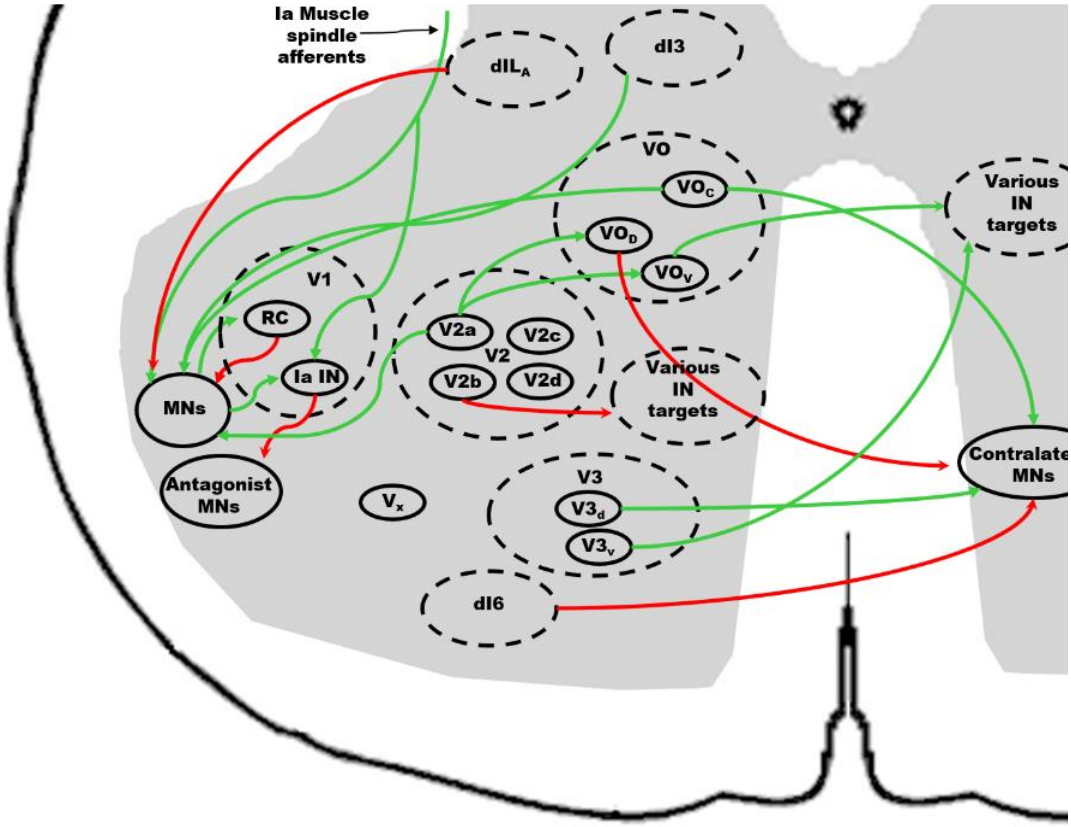

Figure 1.5 Ventral interneuron connections

Some of the various known spinal interneuron connections. V1 interneurons include two inhibitory subtypes receiving direct input from MNs, while the VO group includes both excitatory and inhibitory commissural interneurons. The dIL$_A$ interneuron population provide pre-synaptic inhibition to Ia propriospinal afferents. Populations of progenitor domains are not spatially precise. RC=Renshaw cell, Ia IN=reciprocal inhibition interneurons. Red is GABA/glycine while green is glutamate/acetylcholine.

The dorso-ventral progenitors domains mentioned earlier can be further divided into multiple subtypes with differing projection patterns. Figure 1.5 shows some of the interneurons directly involved in the locomotor network along with a few of their connections. Some of these cell types were reviewed by Catela et al. (2015) and a brief overview of the interneurons shown (Figure 1.5) and their connectivity and roles are provided here. These interneurons are not the focus of my thesis, however an overview of the whole locomotor network is necessary to understand any single part of it. Understanding how these interneurons may interact with γ-MNs and how they contribute

to recovery from SCI is important for any discussion of either γ-MNs or recovery of locomotor function after SCI.

V0 interneurons are derived from Dbx1 HD expressing progenitors. These can be largely divided into three subclasses which are $V0_D$ (inhibitory), $V0_v$ (largely excitatory), and $V0_C$ (cholinergic). $V0_D$ is a commissural interneuron involved in left:right (L:R) coordination, while $V0_v$ INs are largely excitatory and may contact INs in the intermediate zone for di-synaptic inhibition (Pierani et al., 2001). $V0_v$ and $V0_d$ INs are involved in L:R coordination at high and low speeds respectively (Talpalar et al., 2013). Cholinergic interneuron activation is known to decrease spike afterhyperpolarisation and increase the frequency of MN firing (Miles et al., 2007). The interneuron responsible for this is the $V0_c$ subtype. These neurons are phase locked with MN firing in fictive locomotion (Zagoraiou et al., 2009). $V0_c$ INs are probably involved in modulating MN firing frequency as inactivating them impairs the swimming induced increase in gastrocnemius EMG normally observed. Of course, the congenital knockout of $V0_c$ cholinergic activity means that there could have been compensatory changes in the locomotor circuitry, thus obscuring further behavioural changes which may have occurred otherwise.

The V1 subtype is marked by expression of En1 and includes Renshaw cells (expressing calbindin and OC2/3) for recurrent inhibition, and Ia inhibitory INs (Ia IN) (expressing FoxP2) for reciprocal inhibition. The fact that Renshaw cells and Ia INs are such a small proportion of known V1 cells (~22% (Alvarez et al., 2005)) indicates that there is a huge variety of distinct subtypes for each progenitor domain. A developmental knockout of Renshaw cell transmission had no discernible behavioural changes (Enjin et al., 2017a); this points to the plasticity of the motor system to compensate for missing components and underlines the need for adult conditional knockout or knockdown models. Another study by Gosgnach et al. (2006) found that deletion of Ia IN inhibition actually slows the speed of fictive locomotion and does not disrupt L:R or flexor extensor (F:E) coordination. This shows the simple wiring of spinal circuitry is not always indicative of the circuit function.

The V2 subtype is marked by Lhx3 expression and includes excitatory V2a (expressing Chx10 and Sox14), inhibitory V2b (Gata3), and V2c (Sox1). V2b and V2c

interneurons are closely related, although not much is known about their projection patterns or role. However, co-disruption of V2b and V1 INs did disrupt F:E coupling in a fictive locomotion preparation, as a subset of V2b INs are Ia INs (Zhang et al., 2014). V2a INs project to commissural interneurons involved in L:R coordination and their embryonic ablation led to L:R coordination deficits without disrupting F:E coordination (Crone et al., 2008). A major caveat with the study is that only fictive locomotion preps were used as mice were not viable into adulthood. The V2a population also provides evidence for the multiple subdivisions within classes. Hayashi et al. (2018) found two distinct types of V2a INs based on their projections patterns and regulation of Chx10 expression. Class I V2a INs projected locally to MNs and INs and were found in greater number in the lumbar spinal cord, while class II V2a INs had both local and supraspinal projections and were more prominent in the cervical spinal cord. These classes also expressed different genes based on their motor pool. This diversity points to problems when trying to discover the role of any one IN and they may have different roles depending on their position in the spinal cord.

While V2a INs have been pinned as the major rhythmogenic components of the CPG, research by Crone et al. (2008) showed that the spinal cord maintains its rhythmicity without their activity. Non MN HB9 INs may play a role, as deletion of glutamatergic transmission in HB9 cells reduces locomotor frequency (Caldeira et al., 2017), although this has been recently questioned (Koronfel et al., 2021). Other research has shown another IN population expressing Short-stature homeobox 2 (Shox2) also plays a role in rhythm generation. This population is not restricted to a particular progenitor domain as 25% of the neurons are not V2a (Dougherty et al., 2013). Blocking Shox2 cells transmission decreased rhythmic frequency in a fictive locomotion preparation while not affecting L:R or F:E coordination. The study above showed that dI3 and dI5 progenitor domains contributed to the Shox2 expressing neurons. This diversity of neurons involved in the same role has made the CPG difficult to study, and with each new study on distinct IN types there are further questions which need to be answered. That there is a population of V2a INs involved in L:R coordination while another population is involved in rhythm generation is a cautionary tale about what can be determined from the broad progenitor domain knockouts we have seen thus far.

V3 neurons (expressing Nkx2.2, Nkx2.9, and Sim1) are divided into V3d (expressing OC2/3) and V3v (Olig3). All V3 cells express VGlut2 and ~80% are commissural interneurons. V3 neurons are involved in spike coordination of the left and right spinal cords in a fictive locomotion prep (Zhang et al., 2008). The majority of V3 interneurons do not have oscillatory responses to NMDA, serotonin (5HT) or dopamine. Their role has been hypothesised to stabilise the rhythm of the CPG by ensuring even activation across the networks needed. The more dorsal V3d INs receive more diverse inputs from afferents and are involved in weight bearing gaits where they transmit contralaterally to INs, while V3v contacts contralateral MNs and are involved in all types of locomotion (Borowska et al., 2013).

Some of these ventral subtypes do appear to match up to components of the CPG as described by McCrea and Rybak (2008) and shown in Figure 1.4. Components such as the V2a and Hb9 INs for the rhythm generation, VO_v for gait switching at higher speeds, and VO_D and some V2a with the help of V3 INs for L:R coordination, and the V1 and V2b subtypes for F:E coordination. While there is evidence of the above tasks there is also clear evidence showing that they are not wholly responsible for any of the functions they fulfil. This could be down to insufficient controls and mis-timing of knockouts leading to developmental compensation. It is also possible there are multiple areas of redundancy within the spinal network, with some INs playing multiple roles with overlap in function. The fact that there is overlap in some transcription factors may point to a greater problem we have defining cells by progenitor domains. There is massive variation in MNs across the spinal cord, with each motor pool being guided by series of distinct transcription factors during development (Catela et al., 2015). There is every likelihood that there is similar diversity of INs. Indeed, Francius et al. (2013) found multiple differences across the rostro-caudal extent of the spinal cord with different transcription factors identifying multiple subtypes of all the cardinal ventral class INs. The diversity underlines the need for further work into the subsets of interneurons involved in different types of movements and different muscles. This is one reason we have attempted to study the prevalence of gamma motor neurons in various muscles in order to determine whether there is an expression difference in different muscle types as there is with RCs. This may allow us to make some assertations as to their role.

The locomotor CPG contains the ability to work with just general drive from various supraspinal structures, epidural electrical stimulation, or pharmacological stimulation. Of course, many of the above ventral INs also receive direct input from afferents and supraspinal pathways. In normal locomotion there is the need for supraspinal and sensory integration. The next two sections cover a brief overview of first the descending pathways and then some of the sensory integration neurons in the spinal cord.

1.2.2.3 Descending input

Supraspinal input is not the focus of this thesis, but a very brief overview is useful when discussing inputs to the spinal locomotor network. What follows is a description of some of the more important descending pathways for motor control. The pathways are named based on their origin and destination as well as their neurotransmitter type. The corticospinal tract (CST) and brainstem pathways will be covered with a focus on rat anatomy. For a fuller review of the CST including comparisons of species and the developmental aspects of descending input see Lemon (2008).

The CST projects from the cortex with 90% of fibres decussating at the base of the pyramids, the CST terminates primarily in Laminae VI and VII in the rat. In primates there is a direct cortico-MN pathway but this is not present in the rat (Alstermark et al., 2004). In the rat there are direct rubrospinal tract (RST) inputs to MNs which are involved in control of distal limb muscles (Küchler et al., 2002). The CST and RST in the rat have some overlapping functions with both primarily providing input to pre-motor interneuron controlling distal limb muscles with a focus on flexor muscles. The CST and RST tract are both glutamatergic with the CST expressing vesicular glutamate transporter 1 (VGluT1) and the RST expressing vesicular glutamate transporter 2 (VGlut2) (Du Beau et al., 2012).

The reticular formation consists of nuclei in the pons and medulla. In the rat these receive thalamic, cortical and cerebellar input and project bilaterally to pre-motor interneurons. The reticulospinal tract (ReST) is involved in locomotion with one pathway exciting the central pattern generator interneurons and the other pathway activating inhibitory interneurons to inhibit spinal reflexes (Takakusaki, 2013). The ReST tract has two neurotransmitters, with the majority of fibres positive for the excitatory VGluT2 and around 20% positive for the inhibitory vesicular GABA transporter (VGAT) (Du Beau et

al., 2012). The VGlut2 positive vestibulospinal tract is important for postural control where it projects ipsilaterally from the vestibular nuclei with a focus on extensors (Du Beau et al., 2012). Kuypers (1981) divided the brainstem pathways into group A and group B pathways. Group A pathways such as the ReST and vestibulospinal tract are involved in more whole body and multilimbed movements while group B pathways such as the rubrospinal tract contact individual motor pools and pre-motor interneurons. There is evidence for a less clear distinction for the ReST, at least in primates where there are direct ReST connections to individual hand motor neurons (Riddle et al., 2009). This tract may be important in SCI as the ReST is found to sprout extensively after SCI (Baker et al., 2015).

There is also mono-aminergic input to the spinal cord. A raphespinal tract provides 5 hydroxy-triptamine (5-HT) to the spinal cord, while the locus coeruleus provides noradrenergic input. There are some local spinal dopaminergic neurons (Hou et al., 2016a) which supplement dopaminergic input from anatomical group A11 (Sharples et al., 2014). The mono-aminergic pathways provide broadly excitatory or potentiating input. Where they may not directly activate circuitry they can increase excitability for other stimuli.

The different descending pathways often have similar redundancies as the ventral interneuron subtypes mentioned earlier. The CST and rubrospinal tract in the rat are good examples of this with similar functions carried out by both pathways. This redundancy is good if you are trying to regain function after something like SCI. If neural insults occur sometimes new pathways can take over the function of the old one, such as the cortico-reticulo-spinal pathway which becomes prominent following CST loss and combined training with epidural stimulation (Asboth et al., 2018).

1.2.2.4 Sensory and supraspinal integration networks

The ventral progenitor domains make up much of the CPG. However, the dorsal subtypes also play a role in movement, especially in integration of descending and sensory input. The spinal locomotor CPG may be activated without peripheral or supraspinal stimulation in fictive locomotor or spinal preparations. However, in real locomotion and movement we know supraspinal and peripheral information are crucial for a fully functional locomotor system. The interneurons described below are involved in integrating

this information. Some of the studies have shown interesting results with their models, however the same caveats from the section on ventral CPG components apply here. Namely, redundancies in networks, timing of deletion, and full behavioural analysis. The behavioural aspect is doubly important as in many of these studies the impact on sensory processing is subtle. This requires more than just fictive locomotor preparations and sometimes needs very sophisticated behavioural tests to observe any significant changes. As with the ventral subtypes the possible functional overlap of dorsal interneuron subtypes also needs to be considered.

dI1 and dI2 are somatosensory relay neurons targeting the cerebellum and thalamus, but are not known to contact the CPG components as of yet (Helms and Johnson, 2003). dI3 neurons are involved in di-synaptic excitatory transmission from cutaneous afferents to MNs but do not impact normal locomotion when deleted (Bui et al., 2016). However, mice were unable to recover overground locomotion after SCI following this deletion. This underlines the need for sensory input after spinal cord injury, which is a major component of this thesis. This also shows the importance of studying these INs in all conditions and determining how they may be involved in the spinal locomotor system in health and disease.

Subsets of dI4 and dI5 INs both project ipsilaterally to MNs. They receive direct Ia inputs and are needed to ensure L:R alteration during swimming, but not during walking (Satoh et al., 2016). This again underlines the need for robust behavioural testing after interneuron manipulation, if walking alone was used then this deficit would not have been picked up. This also suggests that during walking there is redundancy in L:R control interneurons responding to stretch, where Golgi tendon organs and Ib afferents may be contacting other L:R alternation interneurons. There are multiple subsets of dI6 INs. There are at least two excitatory subtypes types, with one probably involved in pattern formation projecting to ipsilateral MNs, and one involved in rhythm generation projecting to Hb9 and V2a INs (Dyck et al., 2012). Another subset of neurons derived from dI4-6 progenitors expresses Dmrt3. This subset is predominantly inhibitory and projects to MNs, RCs, VO_C and other cell types and receives just as diverse inputs (Perry et al., 2019). These neurons are involved in L:R coordination especially at higher speeds (Andersson et al., 2012). They

offer another example of the diversity of rhythm generating and pattern formation neurons in the spinal cord.

Some neurons progenitor domains are not yet known. Interneurons such as GABA pre neurons involved in pre-synaptic inhibition of the H-reflex (Fink et al., 2014), probably consist of mostly dIL_A INs (Pillai et al., 2007). If there is overlap in the functional divisions of the ventral progenitor domains, there is an equal amount here. Many of the dorsal progenitor domains contain INs involved in sensory relay, propriospinal networks, and the central pattern generator. Many of the studies into dorsal sensory relay INs has found that they do not conform to the cardinal progenitor domains. INs not confined to one progenitors domain include RORα INs, Zic2 INs integrating light touch, and Sat2B INs integrating proprioceptive limb (Bourane et al., 2015, Hilde et al., 2016, Paixão et al., 2019). Some of these sensory integration neurons may need to be looked at more holistically, and subdivided more on function and projection rather than just genetic lineage (Graham and Hughes, 2020).

The advance in genetic targeting and knockout studies has exponentially increased our understanding of the CPG network and what role each component plays. While much of the research in this field is excellent, there are some issues which need to be considered. Knockout timing is vital, as if the knockout is pre-natal, we know there can be compensation from other interneurons. Thus, the small changes which may occur due to deletion of specific interneuron populations are masked by compensatory mechanisms during development. If inducible knockouts are used, then control animals must be fully phenotyped to insure Cre expression has not led to significant neural changes. While spinal preparations and fictive locomotion can be used, they may not always reflect the true role of the neurons analysed. For this reason full behavioural analysis is preferable, with dynamic and challenging behavioural tasks and detailed analysis of the kinematics of the movements. The fact that interneurons can be further subdivided into smaller and smaller classes is also important. This is because one interneuron type may contain subclasses for each task they accomplish, and one interneuron in the class might not be accomplishing both functions.

We know the locomotor CPG can produce timed and phased activity in the absence of sensory feedback. However, we also know that the CPGs activity is regulated by sensory feedback in normal walking. Also that proprioceptive sensory input specifically is needed for recovery from SCI (Takeoka and Arber, 2019). γ-MNs are the controllers of this sensory feedback via their control of the muscle spindle. We have looked in more detail below at their structure, innervation and function. γ-MNs have a wide array of segmental inputs, presumably many of the interneurons above are relaying this sensory input to γ-MNs. However at this point there are no studies which have defined which interneurons are projecting this information to γ-MNs. Uncovering this would improve our understanding of the locomotor system and how its sensory integration and control function.

1.2.3 Gamma motor neurons in movement control

As discussed previously, sensory input is necessary for normal locomotion and is responsible for modulating CPG output. The neuron controlling much of this sensory input is the γ-MN. γ-MNs control the gain of muscle spindle afferents and respond to segmental and supraspinal stimuli in order to adjust the sensitivity and firing rate of group I and II spindle afferents. The muscle spindle is the only sensory body with its own motor control, this unique system allows for another layer of control over the sensory feedback need for locomotion and movement in general. We will look at what is known of γ-MN's structure and innervation, and theories as to their role in locomotion and learning.

1.2.3.1 Muscle spindle structure and innervation

Much of the research examining γ-MNs has been done in the context of muscle spindle research; therefore an understanding of the research on muscle spindles is vital to understanding the history of research on γ-MNs. Muscle spindles were first identified by Weissman (1861) with Kerschner in 1888 first describing the spindle as a sensory organ. Sherrington in 1894 confirmed this sensory innervation. Secondary, primary and plate endings on spindles were described by Ruffini (1898) and motor innervation of the muscle spindles was suggested by Cipollone (1898). The first to distinguish γ-MNs from α-MNs was Hinsey (1934). This was confirmed by Leskell (1945) who found that stimulating these small "γ-efferents" increased spindle afferent firing while causing no extrafusal contraction (Barker et al., 1974, Matthews, 1964, Hunt and Kuffler, 1951).

Figure 1.6 shows a stylised mammalian muscle spindle. The typical spindle consists of 6-10 intrafusal fibres within the muscle with a length of about 10-20% of extrafusal fibre length (~0.5-10mm). The polar regions of the intrafusal fibres are the contractile portions and they are attached to the extrafusal fibres surrounding the spindle (Banks and Stacey, 1988). There are two types of afferent fibres innervating the non-contractile central region of the intrafusal fibres. These afferent fibres are Ia (primary) and II (secondary) afferents. There are usually 1-2 primary afferents innervating the equatorial region of the spindle and 1-5 secondary afferents innervating the juxta-equatorial region of the spindle fibres. These afferent fibre sensory endings are located in a central capsular enlargement of the spindle which protects the sensory endings from electrolyte changes caused by extrafusal contraction (Prochazka, 1996). The muscle spindle has motor innervation from 4-12 γ-MN axons and often a β-MN axon, and each β and γ MN innervate multiple spindles (Emonet-Denand et al., 1992). A β-MN is a motor neuron with axons innervating both the intrafusal and extrafusal fibres.

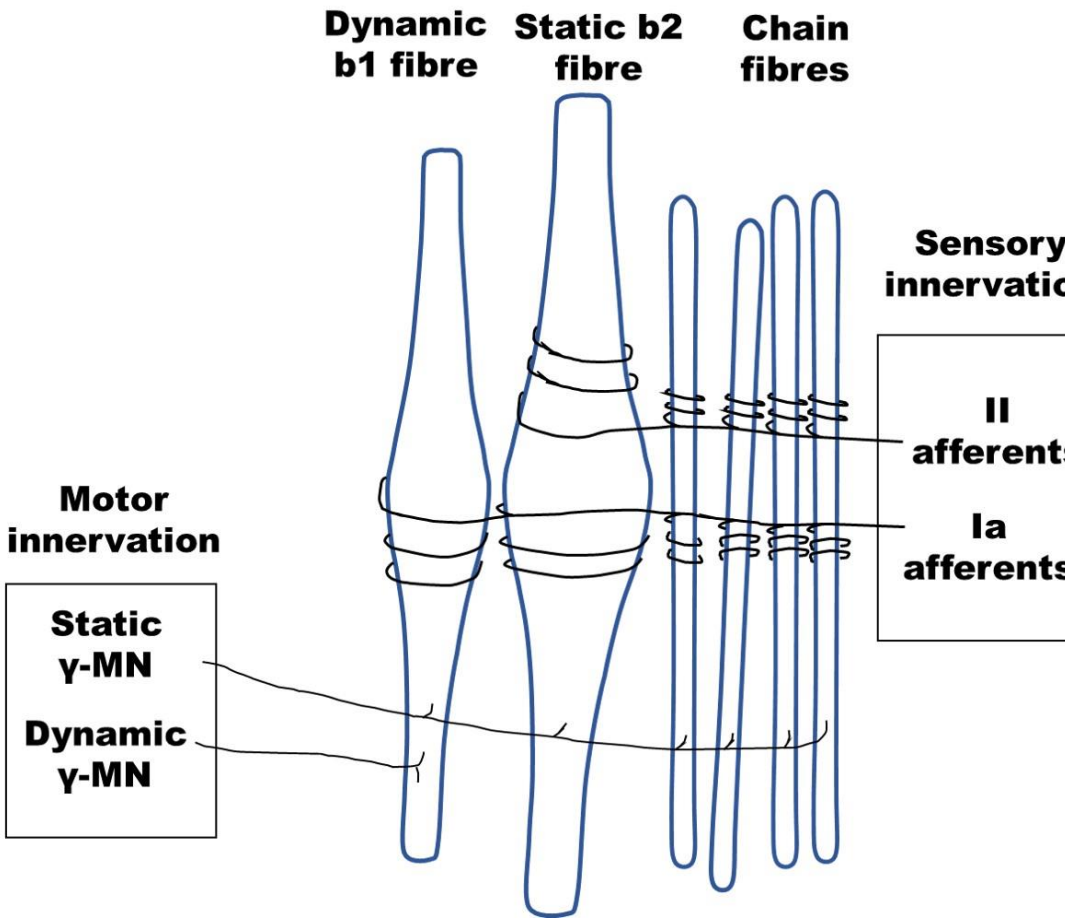

Figure 1.6 Muscle spindle sensory and motor innervation
The muscle spindle receives motor input from static and dynamic γ-MNs and sensory innervation from primary (Ia) and secondary afferents (II). The b1 fibres only receive input from dynamic γ-MNs while all fibres receive static γ-MN input. Primary afferents contact all the intrafusal fibres while secondary afferents are not in contact with b1 fibres.

Intrafusal fibres are classed as either bag or chain based on how the nuclei in the intrafusal fibres are arranged (Barker, 1948). The typical spindle contains a dynamic bag fibre (b_1), a static bag fibre (b_2), and 2-10 chain fibres (c) (Matthews, 1964). Bag_2 fibres are distinguished from bag_1 fibres by an increased level of elastin and a reduction in mitochondria (Walro and Kucera, 1987), b_2 fibres also contain more glycogen and have more ATPase activity than b_1 fibres (Boyd, 1981). Motor control of b_1 fibres is from dynamic γ-MNs (γ_d) and dynamic β-MNs (β_d) and motor control of b_2 and c intrafusal fibres is from static γ-MNs (γ_s) and static β-MNs (β_s) (Barker et al., 1973). Kucera and Hughes (1983) proposed a further subdivision into long and short chain fibres, with β_s motor neurons selectively innervating long chain fibres in the cat hind limb (Jami et al., 1982).

Primary muscle spindle afferents (Ia) have sensory terminals on b_1, b_2 and c intrafusal fibres and secondary spindle afferents have sensory terminals on b_2 and c spindle fibres (Emonet-Dénand et al., 1977). Primary spindle afferents fire more during the application of stretch while primary and secondary afferents signal the length of stretch, with secondary afferents having a sustained higher firing rate until the return of the muscle to resting length (Harvey and Matthews, 1961).

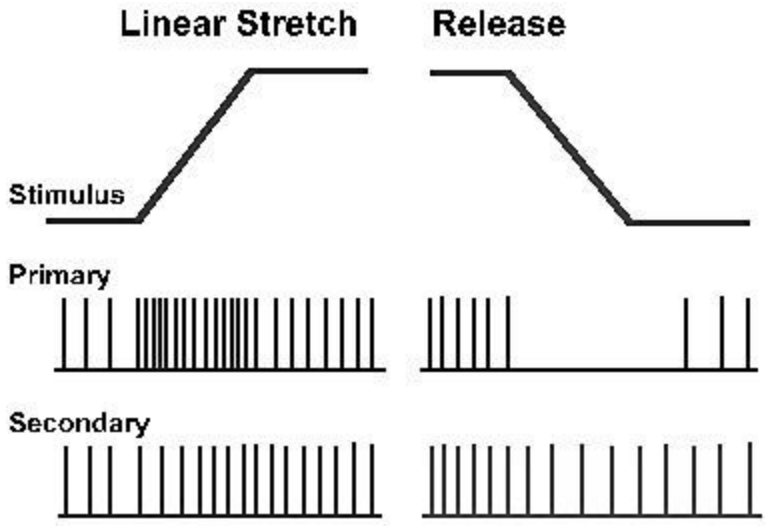

Figure 1.7 Primary and secondary spindle afferent firing properties
Primary afferents responding by increasing firing during the application of stretch with a reduction in firing after stretch is released. Secondary afferents have no increased firing during stretch, but the amount the muscle is stretched does correspond to firing. So the secondary afferent acts as a more positional sensor. (Matthews, 1964)

Dynamic and static responses of primary and secondary spindle afferents to stretch are not linear, and there are conditions which alter the sensitivity and gain of secondary and especially primary spindle afferents. During small movements the dynamic sensitivity of primary afferents is high, while during large movements the dynamic sensitivity decreases (Baumann et al., 1982). Stuck actin-myosin cross-bridges in intrafusal fibres has been suggested to be responsible for the high sensitivity of primary afferents to small stretch (Brown, 1971). The decrease in this high sensitivity during large movements is postulated to be the breakdown of these cross-bridges (Hunt and Wilkinson, 1980). This gain compression was observed by recording afferents during small sinusoidal stretches while the muscle was undergoing concomitant large triangular stretches (Baumann and Hulliger,

1991). In the above study higher velocity triangular stretches were also found to decrease dynamic sensitivity of spindle afferents. The implications for research on dynamic sensitivity are large, as the dynamic response of spindle afferents during stationary tests will not be the same as the response during natural (faster and larger) movements.

When studying γ-MNs it is important to keep the muscle spindle properties in mind. As γ-MNs only have a role insomuch as they modify the function of the muscle spindle components, and thus the sensory output which proceeds from them.

Potential information can also be found looking at muscle spindle distribution. There are approximately 27,000 spindles in the human, with some muscles such as the diaphragm, larynx and the posterior belly of the digastric sphincter containing no spindles at all (Prochazka, 1996). There are no spindles in the extraocular muscles of the cat, dog, rabbit, and horse, however there are extraocular muscle spindles in the human, chimpanzee, most ungulates, and possibly the rat (Enjin et al., 2012, Matthews, 1972). The number of spindles per muscle increases with size, however the density of spindles is lower in larger compared to smaller muscles (Banks, 2006). Taking size differences into account the spindle density of each muscle still varies; the neck muscles have increased numbers of spindles while the shoulder girdle muscles have fewer spindles. The reason for the lack of spindles in some muscles may be because less feedback is necessary or because there is an alternate source of feedback to the central nervous system. Determining the presence and number of spindles per muscle could help illuminate spindle function. However, the amount of labour required for this means that detailed quantitative data is not yet available. Determining the number of γ-MNs in each muscle may also be beneficial for the same reason. Advances in 3D clearing and imaging of tissue may mean that this is currently a possibility. INs and MNs show genetic variation in transcription factors across muscle pools. There is no reason to believe that these differences are not also present in γ-MNs.

1.2.3.2 Structure and types of γ-MNs

There are two widely distinguished types of γ-MN, dynamic and static. Dynamic γ-MNs increase the sensitivity to stretch of the spindle primary afferents and lead to a pronounced drop in primary afferent firing after stretch termination (Emonet-Dénand et al., 1977). Static γ-MNs increase the base rate of spindle afferent firing while decreasing the

stretch sensitivity. Static γ-MNs also attenuate the drop in firing after stretch termination. During muscle shortening γ_s activity acts to limit the decrease in spindle afferent firing (Prochazka et al., 1979). γ_s activity is able to occlude the effects of γ_d activity on Ia spindle afferents during small sinusoidal movements (Hulliger et al., 1977). This means that during small movements γ_d activity may be hidden if afferents are studied during co-activation of dynamic and static γ-MNs. There has been no difference found between dynamic and static γ-MN ratios in different muscles, as γ_d make up around a third of γ-MNs in any given muscle in the cat (Matthews, 1972), although the data are sparse, with limited muscles and only the one species studied.

The picture is even more complicated as distinguished by Emonet-Dénand et al. (1977), who found that not all dynamic or static γ-MNs displayed the same action on separate primary spindle afferents. Figure 1.8 displays the variety of effects on different muscle spindles observed by stimulating single γ-MNs. All the ranges of effects were able to be replicated by stimulating dynamic and static γ-MNs together at various intensities. The action of static γ-MNs in particular appear to have some not entirely homologous effects on separate spindles. Static γ-MN differences were investigated by Boyd (1986), who found that 79% of all γ_s motor neurons innervated either b_2 or c intrafusal fibres preferentially. 48% of γ_s axons had functional connections with only chain fibres in all of the spindles they innervated, and 31% of γ_s axons had functional connections with only b_2 intrafusal fibres. This separation is not fully supported by anatomical evidence as the majority of γ_s MNs observed by Barker et al. (1973) had endings on both b_2 and c fibres. However it is possible that not all of the endings observed were functionally active. Further evidence for γ_s subdivisions was found stimulating certain areas of the cortex to cause b_2 intrafusal fibre contraction without chain fibre contraction (Gladden, 1981). This subdivision of γ_s MNs is not necessarily surprising as the closer a cell population is studied, the more subdivisions appear. The IN diversity observed in the previous section is likely to occur in γ-MNs as well. It is important to take the various subdivision of γ-MNs into account, as blunt studies looking at the activity of the population as whole could lead to inconclusive and unsatisfactory results.

Briefly, β-MNs are MNs which contact both intrafusal and extrafusal muscle fibres. While they are not the focus of the current research, a little background is needed as to their role as some of their functions overlap with γ-MNs. Approximately 30-40% of muscle spindles in the cat hind limb muscles are innervated by β-MNs, with around 10% of large motor neurons innervating both intrafusal and extrafusal muscle fibres (McWilliam, 1975). There are both dynamic and static β-MNs (Laporte et al., 1981). Smaller dynamic β-MNs innervate intrafusal b_1 and slow oxidative extrafusal fibres. While larger static β-MNs innervate intrafusal chain and extrafusal fast fatigue resistant fibres (Jami et al., 1982). According to Henneman's size principle (Henneman et al., 1965), the smaller dynamic β-MNs being activated first during small muscle movements would lead to increased dynamic sensitivity during small movements. While β-MN innervation is significant, the effect of β-MN stimulation may be small due to the smaller number of synaptic contacts each β-MN has on the muscle spindle. One possible reason to be aware of β-MNs is that if static β-MNs are activated at the same time as α-MNs this may lead to the occlusion of dynamic γ-MN effects during large movements. Due to the confirmed separate control of α and γ motor neurons (during some conditions at least), the role of γ-MNs has the potential to act as more than just a spindle gain control, or a mechanism to maintain the sensitivity of spindles during contraction. For this reason it is of more interest to study γ rather than β motor neurons. Although there is the currently unstudied possibility of separate control of α and β motor neurons which may make them an attractive target for investigations.

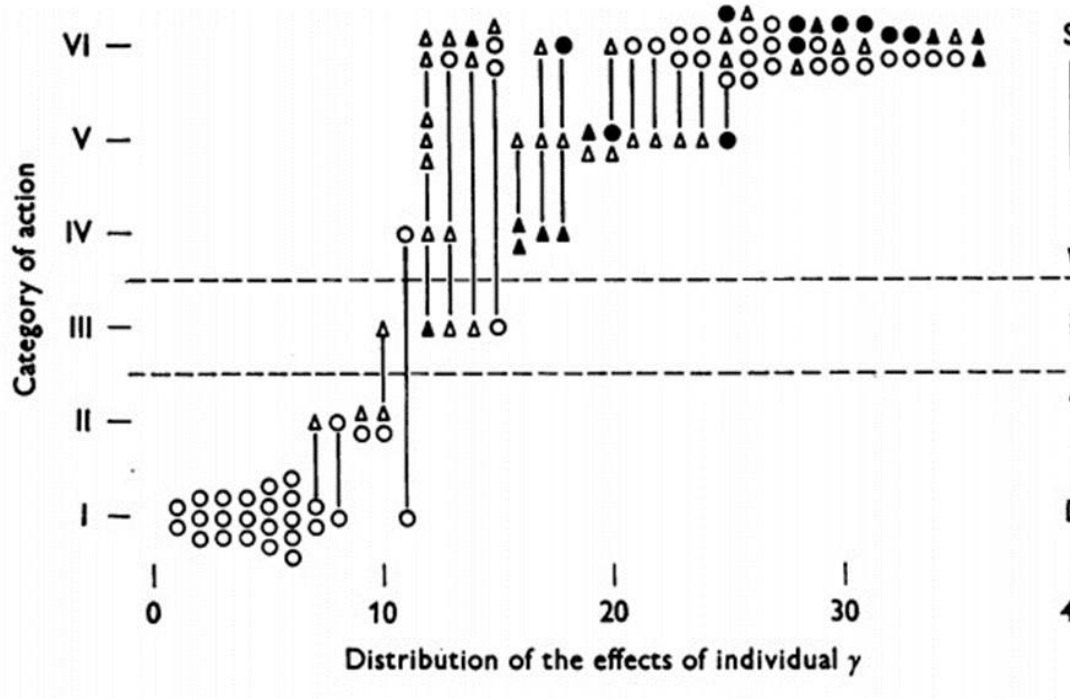

Figure 1.8 Static and dynamic γ-MN subdivision of actions
The effects of stimulating 36 γ-MN axons. 67% of γ-MN axons have pure dynamic or static action with the rest displaying a mix of both types in different muscle spindles. The symbols indicate the effect of stimulation on the afferent firing rhythm. ○, regular firing; Δ, moderate irregular firing; ▲, considerable irregular firing; ●, 1:1 driving. (Emonet-Dénand et al., 1977)

It is important to note the differences between γ-MNs. However, due to limitations identifying the two types anatomically, the following structural description and markers describe both γ_s and γ_d MNs. First off, γ-MNs (<400μm^2 generally) are smaller than α-MNs, with some overlap (Friese et al., 2009). γ-MN dendrites extend up to 1.5 mm from the cell body and are longer, thinner, and less branched than α-MN dendrites (Ulfhake and Cullheim, 1981, Moschovakis et al., 1991). In cats γ-MNs have half the somatic synaptic coverage as α-MNs (Johnson, 1986), while more synaptic coverage was found in rat γ-MNs which have comparable number of contacts and synaptic coverage percentage as α-MNs (Ichiyama et al., 2006). γ-MNs have only S-type (round synaptic vesicles containing glutamate) and F-type (flat synaptic vesicles containing GABA or glycine) synaptic terminals while α-MNs have S and F type terminals as well as C (cistern containing acetylcholine) and M types (presynaptic bouton contacting synapses) (types classified by Conradi (1969)) (Lagerback et al., 1986). γ-MNs have fewer and smaller glycinergic

receptor clusters on their somas compared to α-MNs or V1 INs (Alvarez et al., 1997). Finally γ-MNs have biophysical properties intermediate to fast and slow type α-MNs (Enjin et al., 2012).

The discovery of a few markers for γ-MNs has allowed us to study their contacts with more ease than was possible before. Although some of the markers are more reliable than others. Certain antibodies appear to label γ-MNs primarily. After postnatal day 10 the continued higher expression of oestrogen related receptor gamma (Err3) becomes more selective for γ-MNs (Friese et al., 2009). γ-MNs lack Hb9 and the nuclear protein Neuronal nuclei (NeuN) and express the glial derived neurotrophic factor (GDNF) receptor subunit α-1 (Gfrα1). Interestingly large Gfrα1 and Hb9 expressing motor neurons may mark β-MNs (Shneider et al., 2009). GDNF is vital for γ-MN survival and increasing or decreasing GDNF expression leads to a concurrent change in γ-MN innervation of muscle spindles (Whitehead et al., 2005). The serotonin (5-HT) receptor 5-HT1d (Enjin et al., 2012), the signalling molecule Wnt7a from embryonic day 17 to postnatal day 21 (Ashrafi et al., 2012), and the sodium potassium pump subunit NKAα3 (Edwards et al., 2013) are also expressed highly in γ and not α motor neurons. These markers are all potential targets for studying γ-MNs, although some are limited to certain developmental timepoints.

1.2.3.3 Inputs to γ-MNs

Understanding the innervation of γ-MNs is of great importance in determining their function. The huge range of segmental and supraspinal input they receive points to their role in integrating feed forward and feedback mechanisms in the spinal cord. The following sections will cover what is currently known about this innervation. The missing links in their segmental innervation are shown in Figure 1.9 (below). It is important to discover which of the IN populations described earlier innervate γ-MNs. This would allow us to determine how γ-MNs are integrated in the CPG system and potentially how they may be involved in learning.

The first thing to note is that γ-MNs are not monosynaptically innervated by Ia afferents, and may in fact be inhibited by them (Eccles et al., 1960). This inhibition may be due to α-MN recurrent inhibition of γ-MNs (Kemm and Westbury, 1978, Ellaway and Murphy, 1981). If there was a strong functional connection between Ia and γ-MNs this

could cause an unstable positive feedback loop between the sensory and sensorimotor system. If γ-MNs were excited by Ia axons they would in turn increase spindle firing leading to higher and higher firing rates of Ia and γ-MNs. Static and dynamic γ-MNs both receive some recurrent inhibition from γ and α antidromic volleys (Appelberg et al., 1983d). From the evidence it appears that there is a moderate degree of recurrent inhibition from α to γ motor neurons, but a much more limited recurrent inhibition from γ to γ-MNs (Cullheim and Kellerth, 1978, Westbury, 1982, Ulfhake and Cullheim, 1981). The absence of a positive sensory to sensorimotor feedback loop and the presence of some recurrent inhibition could be important to stabilize MN firing rates, especially during precise or small postural movements during which a stable discharge rate is needed (Granit et al., 1957, Eccles et al., 1961).

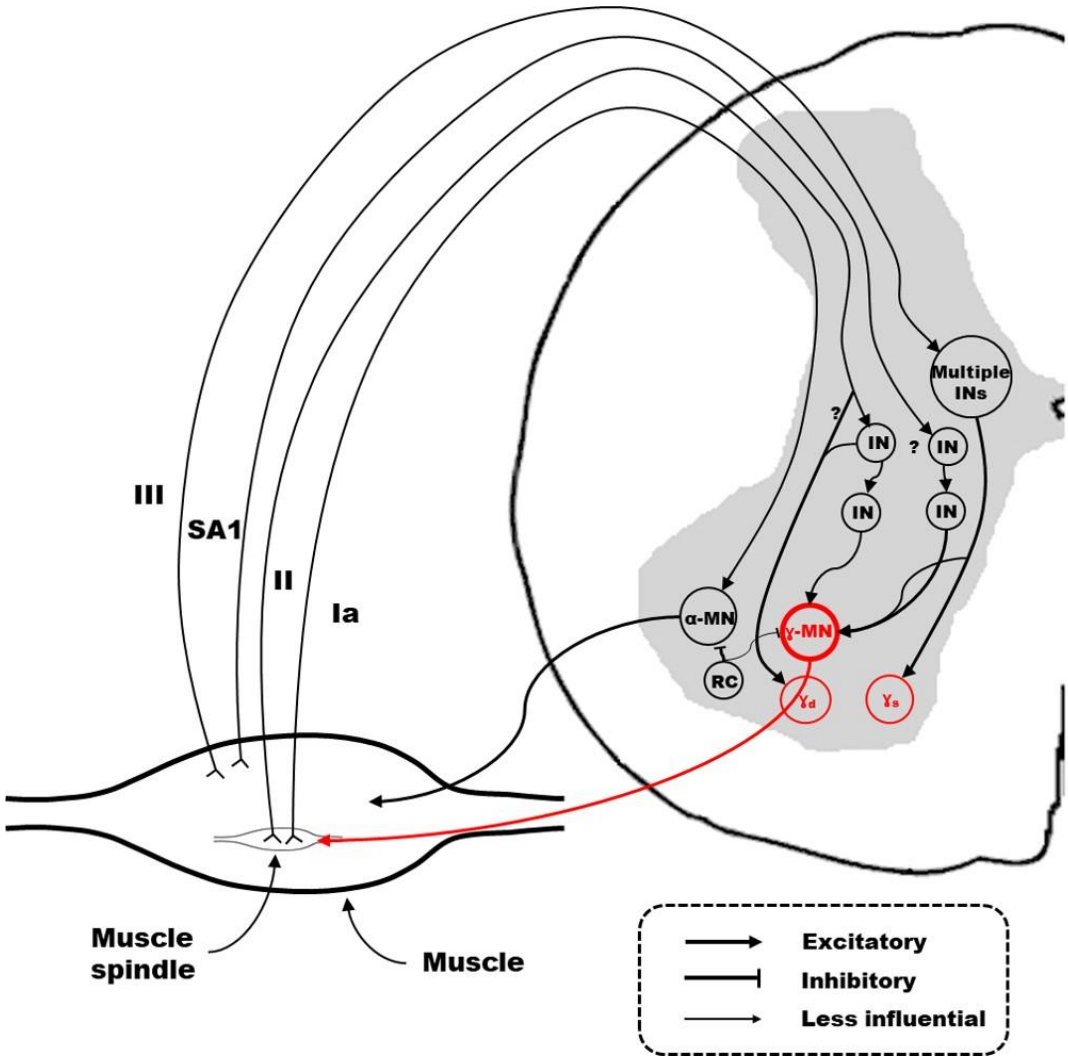

Figure 1.9 Segmental inputs to γ-MNs

Interneurons (INs) are estimates with some tri and poly-synaptic connections not shown. Question marks over whether there are mono-synaptic connections between group II and ɣ-MNs, and how many and what types of INs are involved in transmitting the sensory signals are still unclear. SA1=Slow adapting type 1 mechanoreceptor, RC=Renshaw cell, α-MN=alpha motor neuron, and γ_d and γ_s =dynamic and static ɣ-MNs respectively

Moving on from Ia afferents to group II. Intracellular recordings from identified γ-MNs in the cat found that stimulation of different nerve fibres at Group II strength was found to excite the majority of γ_d MNs (Appelberg et al., 1977). Whether it is exclusively secondary spindle afferents, and not other group II units exciting γ-MNs, is yet to be confirmed. Although homonymous γ-MNs are definitely excited by muscle stretch in a decerebrate cat model (Noth, 1981), this does not exclude other group II units, which may also respond to stretch, from being involved. Appelberg et al. (1983b) did not observe

mono-synaptic group II to γ-MN inputs. However, following homonymous and heteronymous group II afferent stimulation, monosynaptic (1.4-2.7 ms latency) responses were observed in one third of γ-MNs by Gladden et al. (1998). Intracellularly recorded excitatory post synaptic potentials (EPSPs) in γ-MNs were used by Gladden et al., while Appelberg et al. pooled together extra and intracellularly recorded EPSPs. This may have led to the differing conclusions between the two groups. This monosynaptic sensory input is still not confirmed, although it is unlikely that there is any monosynaptic input for II afferents in the rat. This is because no direct contacts on γ-MNs are observed using the tracer Cholera toxin subunit β which should be transported in secondary afferents. An interesting note from the experiments by Gladden et al. was that medial gastrocnemius (MG) γ-MNs received inputs from heteronymous group II afferents while group II afferents from the MG did not excite synergistic muscles such as the lateral gastrocnemius and soleus muscles. Thus, caution is needed when pooling together data from different muscles to generalise conclusions. This muscle pool variation is another cautionary tale of generalising the results of one set of γ-MNs to the whole spinal cord.

There is also segmental input from the smaller group III afferents. Stimulating the gastrocnemius medialis nerve of the hind limb at a strength sufficient for group III afferents was found to have an excitatory effect on homonymous and heteronymous γ-MNs (Ellaway et al., 1982). The central delay of 3 ms observed indicates a polysynaptic coupling of this reflex. Group III afferents that excite γ-MNs are probably the ones which respond to light muscle contraction and skin stimulation, as light touches on the muscle were found to excite γ-MNs. There is a higher proportion of γ_s than γ_d MNs which receive input from group III afferents, and this input is more likely to be excitatory than the group III to γ_d action (Appelberg et al., 1983c). Group III excitation of γ-MNs could be acting as an event marker to the onset of contraction as they are found to fire in response to muscle twitch. The reasons why Group III units would act as event markers is unclear at present. It is possible that increasing the activity of static γ-MNs may cause the spindle afferents to have a more ‘servo-assistance’ mode of action, and thus would act more effectively to offset spindle unloading during contraction.

γ-MNs also respond to chemoreceptor stimulation. Bradykinin (BK) and 5-HT are both released in the muscle in response to contraction (Stebbins et al., 1990). BK and 5-HT injections into a hindlimb or forelimb muscle increased the spindle afferent activity during sinusoidal stretches in anaesthetised cats (Djupsjobacka et al., 1995, Jovanovic et al., 1990). 5-HT was found to increase static γ-MN firing only, while BK increased both static and dynamic γ-MN firing. The above studies also found that lactic acid injections also increased γ-MN firing rates, indicating that this pathway may play some role in central fatigue processing and the tendency for pain and stiffness to spread from one muscle to another (Simons, 1988). As BK, and 5-HT are known to excite group III and IV afferents (Mense and Meyer, 1988), this indicates that the group III to γ-MN input observed by Ellaway et al. (1982) and Appelberg et al. (1983c) may not just be the group III afferents responding to touch.

Appelberg et al. (1983a) found that stimulation of group I afferents did not have a consistent significant effect on most γ-MN firing rates. However, slow adapting type 1 (SA1) mechanoreceptors in the leg have been found to cause periods of synchrony and raised firing rates in gastrocnemius γ-MNs (Davey and Ellaway, 1989). The estimated central latency of the response was 2.7-5.6 ms indicating a di or tri synaptic coupling of the reflex. This discrepancy may be due to the preparation used by Appelberg et al. as they did not denervate the contralateral limb and thus there may have been tonic effects masking any group I to γ-MN facilitation. Choralose was also used in Appelberg's preparation and the diffuse effects of this anaesthetic could disrupt the normal polysynaptic γ-MN response to certain group I afferents. By simply recording firing rate increases Appelberg et al. may have missed some effects observed by Davey and Ellaway measuring γ-MN firing synchrony. The discrepancy of results does point to the limitations of purely electrophysiological studies in determining the innervation of γ-MNs and underlines the need for anatomical studies to solve some of these disputes.

The possible group II to γ-MN connection is the only monosynaptic segmental input to γ-MNs found to date. There are presumably many interneuronal connections, including Renshaw cells, and dorsal horn interneurons such as dI3 which are found to excite α and

possibly γ-MNs in response to cutaneous stimulation (Bui et al., 2013). However, the identity and origin of the vast majority of these interneuronal connections remain elusive.

In summary γ-MNs are influenced by SA1 mechanoreceptors, secondary muscle spindle afferents, group III afferents responding to stretch or skin stimulation, and 5-HT and BK intramuscular injections probably via group III and IV afferents. The influences are many with different inputs to dynamic and static γ-MNs which will have an effect on their function during movement. Recurrent inhibition and the lack of primary spindle afferent input to γ-MNs also prevent any potentially unstable feedback loops. The only other potentially unstable loop would be between secondary spindle afferents and γ-MNs and this pathway may be involved in disorders of muscle tone such as Parkinson's disease and spasticity. Figuring out the segmental inputs to γ-MNs would open a new window to study the spinal locomotor system and the role of γ-MNs in the CPG and SCI recovery.

As γ-MNs receive input from multiple segmental sources they also receive a large amount of supraspinal input. Here again, the limitations of purely electrophysiological studies are observed. The diverse input they receive once again points to their role integrating signals from multiple sources. There is a similar dearth of information about the INs involved in the relay pathway from supraspinal centres as there was with segmental relay neurons (Figure 1.10).

The early research on supraspinal inputs to γ-MNs relied on outputs from the muscle spindle, and not direct recordings from the neurons themselves. The first such study looking at spindle afferents was by Eldred et al. (1953). They found an inhibitory and excitatory contralateral influence on spindle afferent firing from stimulating the internal capsule and inferior colliculus respectively. Early on, two brainstem to γ-MN pathways were described, with one 'fast' pathway which was disrupted with lateral column incision in the spinal cord and one slow pathway Granit and Holmgren (1955). The slow pathway was not found to drive spikes in γ-MN activity but rather provided a protracted excitatory response. This slow pathway persisted with extensive sectioning of the cord displaying a diffuse pattern which was unable to be interrupted without full transection of the spinal cord. Granit and Kaada (1953) recorded from both Ia spindle afferents and γ-MNs directly while stimulating various supraspinal structures. Their results pointed to the reticular

formation and pyramidal tract as having excitatory effects on Ia spindle afferents. While stimulating the anterior lobe of the cerebellum was found to inhibit Ia spindle afferent firing. While the above studies were important, the difference between dynamic and static γ-MN activity had not yet been discovered and as such changes in firing rates were probably masked by discrepancy among the γ-MN populations.

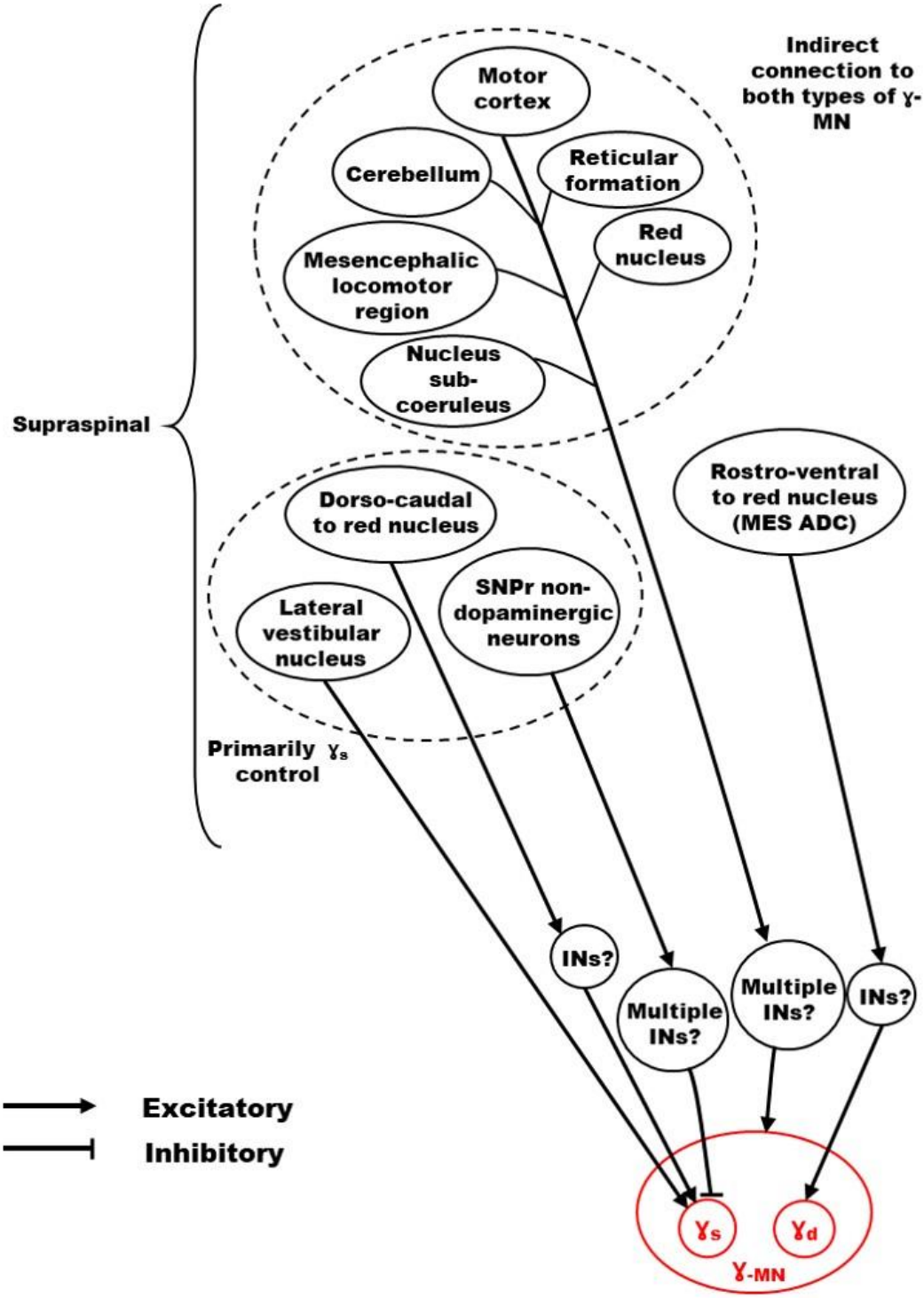

Figure 1.10 Known supraspinal inputs to γ-MNs.
γ-MNs receive input from many of the same brain areas as α-MNs. But there are areas not found to excite α-MNs which do modify γ-MN firing. Areas like the MesADC.

There are a few areas in which co-excitation of α and γ motor neurons is seen in response to supraspinal stimulation. Most locations within the mesencephalic locomotor region (MLR) were found to co-excite γ_s and α motor neurons in de-afferented cats (Eldred and Fujimori, 1958). Besides the α-γ co-activation seen during MLR stimulation, reticular stimulation also co-excites γ_s and α motor neurons in flexors (Bergmans and Grillner, 1968), and red nucleus stimulation di-synaptically co-excites flexor α and γ motor neurons while co-inhibiting extensor α and γ motor neurons (Appelberg et al., 1975). Monosynaptic excitatory connections between the lateral vestibular nucleus and γ-MNs were recorded intracellularly in half of all γ-MNs in an extensor muscle (Grillner et al., 1969). As only γ_s motor neurons are assumed to be mono-synaptically excited from supraspinal stimulation (Bergmans and Grillner, 1968), these γ-MNs were probably of the static type . The motor cortex was also found to mono-synaptically co-excite 1/3 of γ-MNs along with α-MNs in the forearm and hand of monkeys (Clough et al., 1971).

While α-γ co-activation has been seen during stimulation of a number of sites, this is not always the case; indeed if it were, what need would there be for separate γ and α motor neurons, instead of just β-MNs as are seen in the amphibian. Selective control of γ and α-MNs was demonstrated by Granit et al. (1955). Here, ablating the anterior lobe of the cerebellum was shown to decrease γ-MN firing while increasing the firing rate of α-MNs. Gilman and Ebel (1970) found that base firing of individual γ-MNs reduced after cerebellar ablation. Here the sensory evoked increase in γ-MNs firing rate was the same regardless of cerebellar ablation, suggesting that the cerebellum is not involved in descending control γ-MNs segmental response. However it is hard to make conclusions as to the role of the cerebellum in γ-MN and spindle control, as further research is needed to discover which type (dynamic or static) of γ-MN the cerebellum controls and which cerebellar areas are involved in this control.

The distinction between the actions of dynamic and static γ-MNs made earlier is important because their actions have sometimes opposing effects. Thus looking at the innervation of γ-MNs as a whole does not tell the whole picture. In fact, looking at the distinct innervation differences between γ-MN types can be beneficial. For example, fusimotor set (the state of readiness or arousal during the learning of a motor task) probably

includes increased spindle sensitivity (Prochazka and Wand, 1981) and thus probably dynamic γ-MN action (Prochazka, 1989). Looking at areas responsible for increasing the dynamic γ-MN activity could reveal the areas involved in fusimotor set and arousal.

One such area for exclusive γ_d control was found by stimulating an area ventro-rostral to the red nucleus (Appelberg and Jeneskog, 1972). This area is termed the mesencephalic area for dynamic control (MesADC). The MesADC could be involved in fusimotor set, and is potentially responsible for the increased dynamic sensitivity of muscles in the cat during moderately opposed movements (Prochazka et al., 1988). The pathway was found to have collaterals to the inferior olive and stimulation also excited the climbing fibres of the posterior cerebellum (Appelberg and Molander, 1967). The MesADC to γ_d pathway has been found to proceed through the dorsal lateral funiculus of the spinal cord. However, destruction of the rubro-spinal tract or corticospinal tract did not attenuate the dynamic effect of MesADC stimulation (Appelberg and Jeneskog, 1969), thus the MesADC pathway is not confined to the pathway of either tracts. MesADC stimulation has been used frequently to identify dynamic γ-MNs in cats.

Static γ-MNs have a number of different supraspinal inputs which γ_d neurons do not have. For example, the aforementioned vestibular nucleus (Grillner et al., 1969), and an area dorso-caudal to the red nucleus (Taylor et al., 1993, Donga et al., 1993). An interesting area of static γ-MN control are non-dopaminergic substantia nigra pars reticulata (SNpr) neurons. Chemical excitation with Picrotoxin, or electrical stimulation of the caudo-lateral SNpr caused a decrease in static γ-MN activity (Wand et al., 1981, Schwarz et al., 1984a). Another study by Schwarz et al. (1984b) found that non dopaminergic SNpr neurons fired in response to limb perturbations, especially during movement to overcome an unexpected impediment during treadmill walking. These two studies point to the SNpr as an important output centre for basal ganglia control of spindle bias and sensitivity during movement. By decreasing the amount of static γ-MN activity the dynamic sensitivity of the spindles will increase if there is an unexpected limb perturbation, this should allow the reflexes a greater ability to counteract the perturbation. These studies underline the importance of taking the differences between static and dynamic γ-MNs into account, as in this case the inhibition of static γ-MNs is potentially leading to an increase in dynamic sensitivity.

The above research looked at spindle afferent firing and direct γ-MN activity. While this is useful it does have limitations; a novel approach looking at neuron firing synchrony enabled the discovery of other supraspinal inputs, in particular monoaminergic input. In a normal decerebrate cat there is no γ-MN firing synchrony and discharges are dispersed. However, when brainstem input was removed there was an increase in γ-MNs firing synchrony (Davey and Ellaway, 1988). This increase in synchrony was reversed by the application of either levodopa (L-DOPA) or the 5HT precursor 5 hydroxytryptophan. Thus suggesting that dopaminergic and serotonergic pathways are the brainstem structures involved in γ-MN control. γ-MN synchrony is due to segmental inputs such as SA1 , type II, and type III afferents (Davey and Ellaway, 1989). Further investigation into brainstem structures involved in γ-MN control was completed by Baker et al. (1991). γ-MN firing synchrony was measured after electrolytic lesions of various brainstem structures. Lesions to the subcoeruleus nucleus were found to increase synchrony of γ-MN firing, while lesioning the locus coeruleus, central raphe nucleus, and periaqueductal grey had no effect. This, along with evidence showing increased synchrony of firing in response to monoamine depletion in the spinal cord (Ellaway et al., 1989), indicates that there is monoaminergic control of γ-MN firing patterns.

To summarise, there are structures such as the lateral vestibular nucleus, reticular formation, and certain areas in the MLR which have similar effects on α and γ motor neurons. However, selective control of γ and not α motor neurons has been observed from areas including the subcoeruleus nucleus, SNpr, MesADC, and anterior cerebellum. Differences in supraspinal areas for dynamic and static control are also observed with the MesADC exciting γ_d only, and an area dorsal and caudal to the red nucleus exciting γ_s only. The SNpr and vestibular nucleus also exert control on γ_s and not γ_d. This separate control of γ and α-MNs makes sense as there would be no reason to have separate systems if they were always activated at the same time. Further, the separate areas of control for γ_s and γ_d may be useful as the two γ-MN types often display opposite effects on spindle afferents. During small movements or postural tasks it may be useful to have a high dynamic spindle sensitivity so that if there is a small change in muscle length the afferent system would react strongly and quickly enough to resist the change. During larger rhythmic movements decreased spindle sensitivity would be useful so that the antagonist muscles would not be

receiving strong Ia input causing them to oppose the movement. The evidence presented here suggests that there is such control, figuring out the spinal networks involved in this control could allow us to further understand spinal motor control.

1.2.3.4 γ-MN role in movement

Severin et al. (1967) was the first to show that spindle firing increased with voluntary contraction during locomotion in a decerebrate cat. The idea of α-γ co-activation was furthered with a study on de-afferented and decorticated cats when both α and γ motor neurons were found to fire in phase during L-DOPA induced locomotion (Sjöström and Zangger, 1976). While there was no distinction made between static and dynamic γ-MNs within this study it has been shown that dopamine selectively excites γ_s motor neurons (Grillner et al., 1967). While α-γ_s co-activation appears common, there is more debate as to whether γ_d motor neurons are co-activated with α-MNs. This lack of α-γ_d co-activation was seen during breathing as γ_d motor neurons of the intercostal muscles were tonically active throughout the cycle, while γ_s motor neurons were phasically co-activated with α-MNs (Greer and Stein, 1990).

Extensors and flexors have possibly different types of γ-MN control during locomotion in the decerebrate cat, with extensors observed to have predominantly dynamic control and flexors predominantly static control (Cabelguen, 1981). This was found by recording primary afferents response to sinusoidal and ramp stretches. γ_s activity was presumed when primary afferents maintained their firing rates during contraction. γ_d activity was presumed when primary afferents increased their firing rate more during the application of stretch and then reduced their firing almost completely after stretch termination. This difference in predominant action may be due to the role of these muscles during locomotion, flexors may benefit from more ‘servo-assistance’ from γ_s action during contraction. The increased dynamic action raising spindle sensitivity in extensors, could assist in the counteraction to lengthening which occurs during the stance phase of locomotion. γ_d activity is also found to dominate in the extensors of resting cats (Bennett et al., 1996). As extensors are more involved in postural control than flexors, this predominance of γ_d action in extensors during rest appears appropriate to condition the extensors to respond to small disturbances. The predominance of γ_s action in flexors and

during locomotion appears well suited to offset spindle and extrafusal length mismatch during shortening.

Murphy and Hammond (1993) stated that there were two types of γ-MN activity occurring in the decerebrate cat during locomotion as measured by direct small MN axons from the anterior branch of the flexor tibialis anterior (TA) nerve. One type was phasic with TA electro-neurogram activity, while the other was tonically active during locomotion. Murphy and Hammond argued that the phasic activity was γ_s and that the tonic activity was γ_d. However, this was simply based on muscle afferent firing rates, and there were no direct recordings from identified static or dynamic γ-MNs to confirm this. In fact, one of the same authors concluded the opposite in an earlier study (Murphy et al., 1984). Others, (Greer and Stein, 1990, Appenteng et al., 1980), have also attempted to link phasic or tonic γ-MN activity with either dynamic or static γ-MNs. In most cases there is an assumption that one or the other is involved without actually stimulating any of the γ-MNs they recorded from in order to confirm type. The limited direct recordings from identified dynamic or static γ-MNs led to a variety of theories as to the role of γ-MNs during locomotion, and a general lack of clarity as to the true picture.

The most robust and complete investigations of γ-MN activity during locomotion were completed by Taylor et al. (2004) in their series of experiments. During locomotion in the decerebrate cat, single γ-MNs innervating spindles in an ankle flexor (tibialis anterior) were recorded from. They were identified in the resting state as either dynamic or static by their effect on spindle afferent firing and their response during MesADC stimulation. During locomotion, in phase γ_s activity with EMG was observed, with rapidly increasing γ_d activity observed after the onset of shortening, which began a slow after half decay at the onset of lengthening (Taylor et al., 2006). The results were similar for an experiment done in the extensor medial gastrocnemius, with the only differences being a phase advance of γ_s activity in the extensor muscle prior to shortening (Taylor et al., 2000). While γ_s activity could be maintaining muscle spindle firing rates during contraction γ_d action at the phase seen is probably preparing the spindle to detect the onset of stretch during the stance phase. Two separate types of γ_s action were also seen in their earlier studies with a lesser and more highly modulated firing rate distinguishing the two types (Taylor et al., 2000). These two

types of γ_s activity were assumed to be from γ_s motor neurons selective for b_2 fibres (less modulated) and c fibres (highly modulated). This was the first study in locomoting animals to observe and define the two types of γ_s activity which were identified earlier by Boyd (1986) in resting cats.

The difficulty of identifying and recording from single γ-MNs during normal locomotion led to a lack of clarity as to their role. The majority of studies prior to those by Taylor et al. were only able to record from afferents and calculate the difference in firing rate compared to passive movements; this led to unclear theories surrounding the activity of the different γ-MN types during locomotion. With the studies by Taylor et al., the picture is clearer, although locomotion in the decerebrate cat is not the same as natural movement. The limitations of the preparation mean that much about the role of γ-MNs in locomotion is still yet to be uncovered.

1.2.3.5 The role of γ-MNs in spinal cord injury

Although it is known that spindle afferent feedback is necessary for recovery of locomotion following spinal cord injury in a rat (Takeoka et al., 2014), the role of γ-MNs in this is yet to be elucidated. The data in this field are incredibly limited. With a study by Ichiyama et al. (2011) one of the very few to look at synaptic changes after injury. The study found loss of synaptic input to γ-MNs after injury while locomotor training returned synaptic inputs closer to normal. Barring this one study the role of γ-MNs in recovery is unknown. The wide array of sensory inputs that γ-MNs receive does point to their importance in SCI. Adding to the possible importance of γ-MNs in SCI is their lack of plasticity inhibiting perineuronal nets (Smith et al., 2015). Potentially pointing to their more plastic nature as shown earlier (Ichiyama et al., 2011).

There is far greater research into the effects of γ-MNs on spasticity after injury. Our SCI experiments did not look at spasticity, however it would be remiss to not mention their possible role in this area. One prominent theory on clonic spasticity suggests that reflexes remain at high ‘default parameters’ in patients with spasticity, and that the reflex sensitivity is not able to be reduced or controlled by supraspinal centres (Prochazka, 1989). Evidence to support this theory was found by Powers et al. (1989) studying patients with hemiparetic clonic spasticity. Patients were able to consciously mimic spasticity in their non-affected

limb so that the response to stretch was the same as their spastic limb. However, patients were not able to change or reduce the reflex sensitivity on their affected side. There is also some evidence against the role of γ-MNs in spasticity as well. Two studies using microneurography found no increase in spindle firing in spastic patients (Hagbarth et al., 1973, Hagbarth et al., 1975). Although the small number of patients and small number of neurons recorded from does limit the conclusions that can be drawn. The evidence from the studies by Hagbarth et al. (1973 and 1975) and from Macefield (2013) point to a lack of increased static γ-MN activity. However, it is more complicated to study the effects of dynamic γ-MNs on spasticity as measuring single afferents in humans does limit the type of actions that can be completed. Some evidence of increased γ_d activity was suggested by Szumski et al. (1974) as they found higher firing levels and a pronounced double twitch of single unit action potentials in Ia afferents during the relaxation phase of clonus. Thus providing some possible evidence that it was increased dynamic γ-MN action sensitising the spindle to the onset of stretch.

Decreased monoaminergic control from the brainstem may be implicated in SCI induced spasticity. Earlier it was mentioned that removing the brainstem was found to increase γ-MN synchrony (Davey and Ellaway, 1988), probably due to lack of modulation of reflex inputs. Systemic clonidine application, or direct L-DOPA or tizanidine (another α-$_2$adrenergic receptor agonist) administration all decrease secondary afferents input to γ-MNs (Jankowska et al., 1998). Of the three, only clonidine reduced spontaneous γ-MN firing rates. Thus suggesting that some of the antispastic effects of L-DOPA and tizanidine on γ-MNs is probably via their effect on reducing the secondary spindle afferent to γ-MN reflexes. As γ_d MNs may be more affected by secondary spindle afferents than γ_s MNs, this agrees with the theory of increased γ_d action in patients with spasticity. Of course, all the drugs above are also known to affect α-MNs as well, so it is unlikely they are acting solely through their effect on γ-MNs.

While γ-MN dysfunction may be an important factor in clonic spasticity, there are other working theories. Dysfunctional CPGs (Beres-Jones et al., 2003), increased spinal excitability (Little and Halar, 1985), generally reduced supraspinal inhibition (Ditunno et al., 2004), and 5-HT_{2c} receptor overactivity (Murray et al., 2010) have all been suggested

as possible causes for SCI induced clonic spasticity. The different theories need not be mutually exclusive, and there is some evidence supporting a role for γ-MNs in SCI induced clonic spasticity. There is certainly insufficient evidence presently to rule out a role for dynamic γ-MNs in spasticity.

1.2.3.6 Conclusion

The γ-MN is a critical part of the motor system. Controlling the spindle feedback the locomotor network receives allows them to alter the response of the motor system to external and internal influences. The separate control allows for adaptation of the reflexes responses in different environments and during different levels of arousal. This allows the dynamic γ-MNs to increase spindle responsiveness in resting states in order to counteract small postural differences. And allows the static γ-MNs to increase and maintain spindle firing during contraction in order to assist in force production. Unfortunately, the lack of recordings made from clearly identified static and dynamic γ-MNs in naturally moving animals or humans has limited the conclusions that can be made as to their role. With studies in decerebrate cats providing the clearest picture (Taylor et al., 2004). However informative the above studies, the preparation used is probably not completely representative of γ-MN activity in normal movement. At present there is still much debate as to γ-MNs' role in normal movement and locomotion, learning, clonic spasticity, and postural control. This appears unlikely to be resolved in the near future due to the technical difficulties involved in continuously recording from identified γ-MNs in awake normally moving animals or humans. Looking at their changing inputs after SCI, and attempting to determine their innervation would enhance our understanding of this fascinating neuron. And in so doing add to our understanding of the spinal motor network in general.

1.3 Spinal cord injury

1.3.1 Introduction

Spinal cord injury causes the impairment of motor and autonomic functions as well as sensory processing. This greatly impacts the approximately 50,000 people in the UK living with some kind of SCI. The cost to the NHS over the lifetime of a patient range in the millions with the ~1,200 new patients per year estimated to cost 1.43 billion (McDaid et al., 2019). The life changing and costs aspects of SCI could be ameliorated by recovery of

voluntary movement and autonomic function. Among the priorities for SCI patients are hand function, bladder control, sexual function, pain, and recovery of locomotion (Anderson, 2004). It is the recovery of locomotion we are focusing on here.

SCI is a complex problem with no solution currently available. In this section I will briefly cover spinal cord pathology before taking a deeper dive into the current therapies to enhance plasticity and restore locomotor capacity.

1.3.2 Pathology

SCI may be caused by a few different primary physical mechanisms. These mechanisms include a laceration, a compression, or a contusion. Of these the contusion injury is most common (49% of SCI cases) (Ribak et al., 2008). Of note the majority of SCI's are not full transections, with some spared tissue almost always present. The clinically relevant contusion injury was used in our study, and it is this injury type that will be the focus of this section. The pathology of a contusion is complex, with numerous related cascading events stemming from the original injury. The various timepoints are subdivided slightly differently by different authors. Here the injury pathology is divided into acute, subacute, and chronic with a summary of some of the process seen in Figure 1.11.

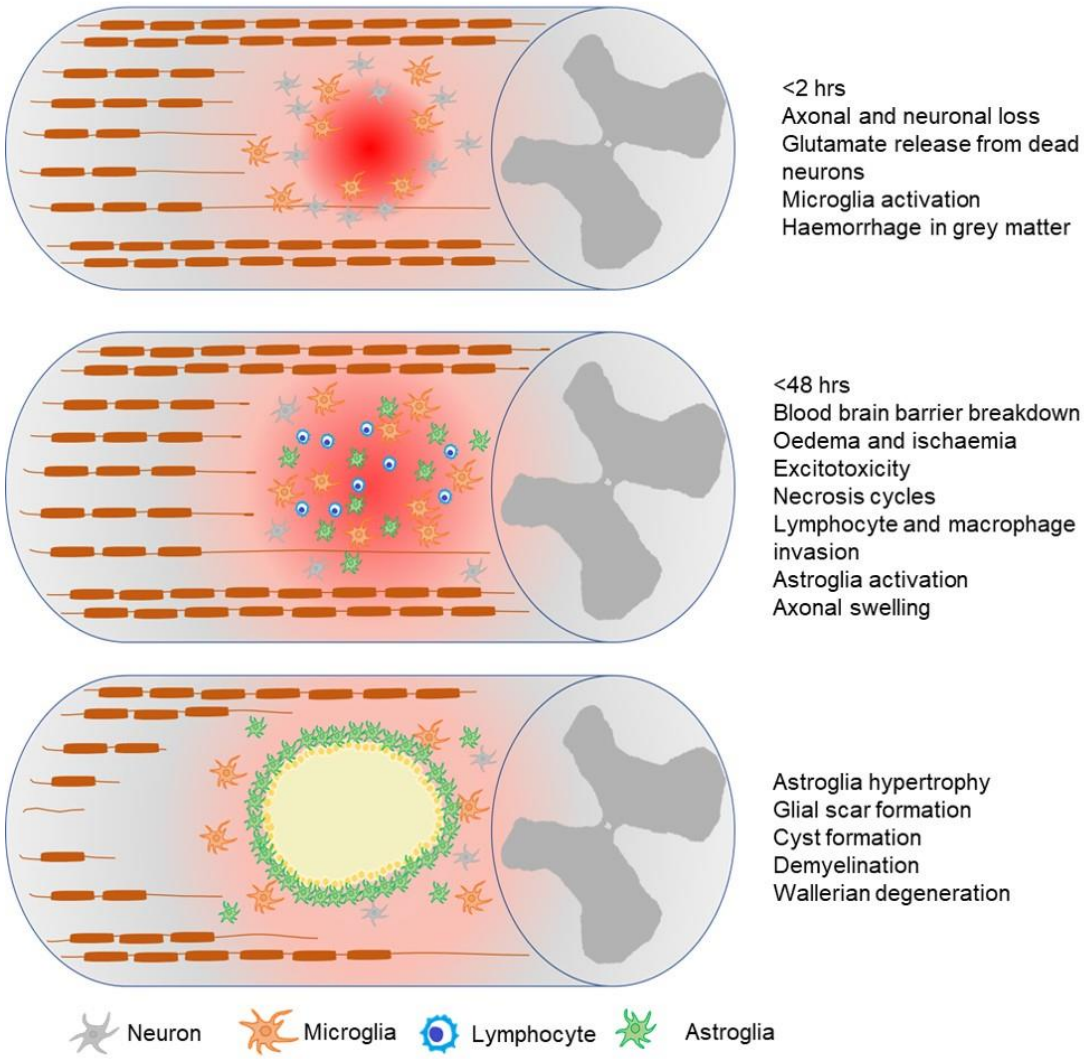

Figure 1.11 Pathology of SCI

There are numerous processes involved in SCI pathology. There is the immediate damage to cells and axons. There is the microglia activation leading to cytokine production. There is the grey matter haemorrhage and blood brain barrier breakdown leading to oedema and further inflammation and necrosis. Later astrocytes are activated with some beginning to seal off the injury site with the formation of a glial scar.

The immediate damage to spinal cord causes cell death via direct mechanical disruption. Spinal shock occurs almost immediately after the initial damage with the loss of spinal reflexes (Ditunno et al., 2004). A number of other processes occur in rapid succession. Grey matter haemorrhage from the injury leads to rapid haemorrhagic necrosis and oedema (Rowland et al., 2008). The oedema increases ischaemia in the spinal cord

leading to further necrosis. Microglia activation is almost immediate with cytokines like TNF-α and IL-β upregulated within minutes (Pineau and Lacroix, 2007). The immediate cell death and membrane damage also leads to glutamate release which in turn causes excitotoxicity (Wrathall et al., 1996). There is often quite limited damage visible at this stage with the later stages causing most of the injury. The secondary damage is especially important in contusion injuries, where in the rat the damage and cell death can spread >4 mm on either side of the lesion epicentre (Grossman et al., 2001).

In the acute stage there are many different processes occurring simultaneously with cascading events leading to secondary damage due to some of these cascades. The blood brain barrier breakdown leads to plasma accumulating in the extracellular space. This plasma accumulation causes pressure induced ischaemia and further necrosis. The necrosis causes more release of glutamate and reactive oxygen species leading to a further cycles of cell death. Axonal swelling also accompanies the necrosis at this stage (Kakulas, 2004). Lymphocyte invasion along with the plasma causes more cell death and immune neurotoxicity due to the production of free radicals (Hausmann, 2003). The time course for the blood brain barrier breakdown shows a peak at 24 hrs which is under control within two weeks (Noble and Wrathall, 1989). While some of the immune response and inflammation is harmful, some of the processes described here are not always detrimental. A certain amount of astrocyte activation, or immune response are probably useful to prevent even worse damage or infection (Anderson et al., 2016).

The sub-acute stage up to two weeks after injury is known to be a critical period during which plasticity is high and interventions are often administered. During this stage phagocytes clear debris from the injury site. Astrocytes at the lesion core experience cytotoxic oedema and die, while some astrocytes on the lesion border become hypertrophic and start to form the glial scar (Okada et al., 2018). There is some apoptosis of oligodendrocytes at earlier stages and this continues along with demyelination at this later stage (Rowland et al., 2008).

In the chronic stages there is continued cyst formation, mesenchymal fibrous scar formation, further demyelination, and importantly Wallerian degeneration. Wallerian degeneration in the CNS is a slow and progressive degeneration of the axon. The slowness

of Wallerian degeneration in the CNS compared to the peripheral nervous system (PNS) is due to the slow clearing of myelin debris (Vargas and Barres, 2007). This slow clearing leaves myelin associated growth inhibitors to retard the growth of axons in the CNS. These inhibitors will be discussed in the following section, they are one reason there is less regeneration in the CNS compared with the PNS.

The complexity of SCI pathology has provided multiple opportunities to limit its damage. As such there are numerous treatments targeting the damage cascade above. This is vitally important, however, we focus more on regeneration after injury, and as such the following sections will cover some of the regenerative approaches taken after SCI.

1.3.3 Plasticity enhancing treatments

Plasticity and axonal regeneration within the spinal cord is vital in order to achieve any functional recovery. However, following SCI the spinal cord is an inhibitory environment not setup for the plasticity needed. Before we move into therapies to enhance plasticity it is useful to understand what we are referring to with plasticity and what it is we want to achieve following SCI. After injury there are three major mechanisms to repair or recover lost connections (Figure 1.12). Axonal regeneration of injured neurons, axonal sprouting from spared neurons, and plasticity of synaptic connections. Axonal regeneration and sprouting of spared fibres are important for recovery. However, within our study much of the focus is on the synaptic plasticity, specifically spinal plasticity below the lesion.

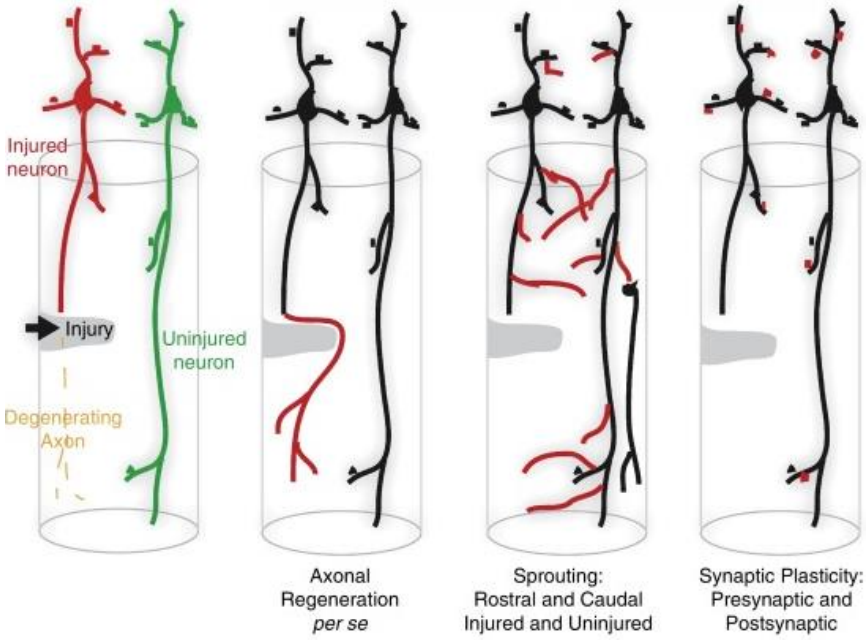

Figure 1.12 Axonal regeneration, sprouting, and plasticity after SCI
After injury there are three important mechanisms for neural repair and recovery. Axonal regeneration of lost axons, sprouting from spared fibres, and synaptic plasticity. (Schwab and Strittmatter, 2014)

Following SCI there is some spontaneous regeneration and neural plasticity. The following section will cover this spontaneous regeneration and then current treatments to enhance this. The final section will cover locomotor training. This training is key as without task-specific rehabilitative training many of the plasticity enhancing therapies have little functional benefit. In the following sections it is worth noting the interplay between plasticity enhancing interventions and rehabilitation (Figure 1.13) (Dickson et al., 2019). Without the mix of these two the functional recovery that can be achieved is greatly limited. Indeed, spontaneous reorganisation in the absence of training can often lead to maladaptive plasticity and negative behavioural results (Beauparlant et al., 2013).

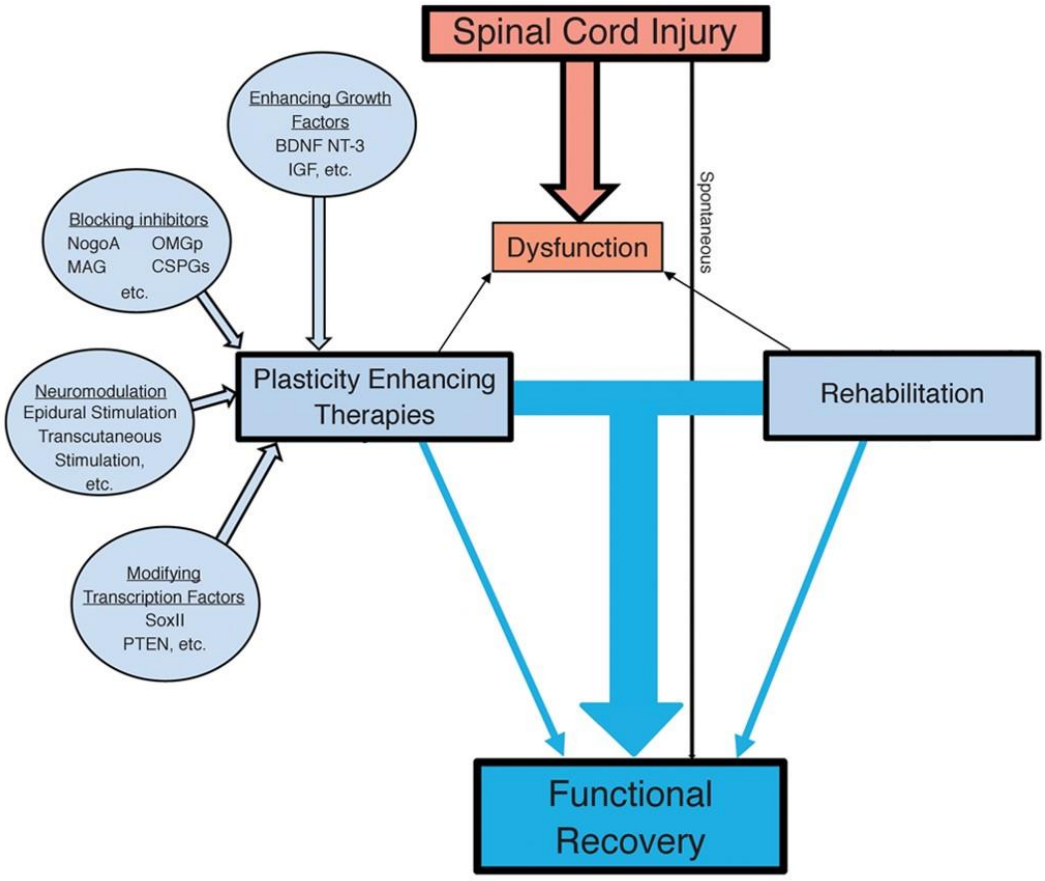

Figure 1.13 Interplay between plasticity enhancing interventions and rehabilitation
The many plasticity enhancing interventions interact with rehabilitation to result in functional recovery. The results of this interaction are not always positive, with some plasticity enhancing interventions and some rehabilitative therapies sometimes resulting in dysfunction. (Dickson et al., 2019)

1.3.3.1 Spontaneous regeneration and modulating intrinsic growth factors

There is some spontaneous axonal regeneration and recovery following SCI. This is especially true in rodent models which likely self-train after incomplete injury (Caudle et al., 2011). Some of these changes have been studied recently using previously unavailable chemogenetic silencing techniques. Spared dorsolateral CST sprouting (Hilton et al., 2016), reticulospinal sprouting onto propriospinal neurons (Filli et al., 2014, May et al., 2017), and a new rubro-raphe pathway (Siegel et al., 2015) have all been implicated in motor recovery following incomplete SCI. The types of neural reorganisation shown in Figure 1.12 are all at play in spontaneous regeneration.

The spontaneous recovery following SCI is important. However, the functional recovery from this is often limited. Therefore, finding ways to enhance this spontaneous plasticity and regeneration are vital. Recent reviews by van Niekerk et al. (2016) and Tedeschi and Bradke (2017) have discussed the mechanisms by which this spontaneous regeneration occurs. Numerous targets present in spontaneously regenerating neurons have been recently identified (Fink et al., 2017). The potential for further manipulation of the spontaneous regenerative capacity of the spinal cord is a large and growing field. However, many of these treatments lead to axonal growth and reorganisation without any functional improvement. One example of this is viral overexpression of the transcription factor Sox11 which increased CST sprouting but actually impaired functional recovery (Wang et al., 2015b). There has been some limited behavioural improvements and axonal growth using Docosahexaenoic acid (Liu et al., 2015), a combination of insulin like growth factor-1 (IGF-1), osteopontin and 4-AP-meOH (Liu et al., 2017a), epothilone B treatment (Ruschel et al., 2015) or histone deacetylase inhibition (Zhang et al., 2018). All these studies have attempted to modify the intrinsic growth mechanisms within the spinal cord with varying degrees of success.

There is massive growth in this field with many promising interventions. However, there is limited functional recovery using any of these interventions alone. Figuring out how these therapies interact with rehabilitative training and other neuromodulatory interventions will be vital to take the field further.

1.3.3.2 Inhibitors

As mentioned earlier, the environment in the adult spinal cord is not especially conducive to axonal growth. After injury there may be a short window where growth is promoted, but this quickly reverts to the spinal cord's normal inhibitory state (Poplawski et al., 2020). After SCI there are three major inhibitors of axonal growth. First there are many inhibitory factors within neurons such as phosphatase and tensin homolog (PTEN)(Park et al., 2008) and poly(ADP-ribose) polymerases (Byrne et al., 2016). These are not the focus of this thesis, and are reviewed here (He and Jin, 2016) and here (Filous and Schwab, 2018). Second, there are extracellular matrix components chondroitin sulphate proteoglycans (CSPGs). And finally there are myelin associated factors such as

Nogo-A. I will briefly discuss CSPGs and how current treatment are attempting to blend rehabilitation with individual therapies. The later parts will cover the myelin associated Nogo-A as this is the target we have pursued in our study.

CSPGs are a major component of the extracellular matrix in the CNS. These CSPGs are also found attached to cell membranes where they form part of perineuronal nets (PNNs) and are also found concentrated in the glial scar after SCI. CSPGs are implicated in a large range of plasticity inhibiting functions (Zimmermann and Dours-Zimmermann, 2008), and interventions to remove or inhibit their action are a major source of study in the SCI field. CSPG sidechain digestion by the bacterial enzyme chondroitinase ABC (ChABC) has shown some promising effects on recovery following SCI (Bradbury et al., 2002, Caggiano et al., 2005, Tester and Howland, 2008, Lee et al., 2010). ChABC treatment has been combined with training in order to achieve significant improvements in forepaw function (Garcia-Alias et al., 2009, Wang et al., 2011). ChABC treatment is promising, however it has also been found that removing the glial scar completely (Rasouli et al., 2009, Faulkner et al., 2004), or removing the glial scar forming astrocytes (Anderson et al., 2016) has negative effects on recovery from SCI.

As alluded to earlier, after SCI, there is myelin debris adding to inhibition of axonal growth. The causes of the inhibition are several proteins enriched within CNS myelin. Some of these factors are myelin associated glycoprotein (MAG), oligodendrocyte myelin glycoprotein (OMgp), semaphorins, ephrins, CSPGs, and importantly for us, the neurite outgrowth inhibitor (Nogo-A) (Schwab, 2004). It is this Nogo-A which we have targeted as part of our combinational treatment.

Nogo-A is not just present in myelin, in the developing nervous system it is enriched in many projecting neurons where it acts to enhance fasciculation (Schwab, 2010). In the adult CNS Nogo-A acts to limit axonal growth and is a stabilising factor on neuronal wiring (Huber et al., 2002). Nogo-A has two inhibitory domains, the nogo-66 domain acting on the nogo receptor NgR-1 complex, and the Δ20 domain or ‘amino nogo domain’ acting on the sphingosine-1-phosphate receptor 2 (S1PR2) (Oertle et al., 2003) (Figure 1.14). Interactions between Nogo-A and both of these receptors leads to the activation of RhoA and Rho-associated, coiled-coil containing protein kinase 1 (ROCK) (Fournier et al., 2003).

This activation leads to growth cone collapse via disruption of the actin cytoskeleton (Schmandke et al., 2007). This first growth cone collapse function of Nogo-A is also supplemented by a later action of an internalised nogo-Δ20 causing reduction in growth associated transcription factors (Joset et al., 2010). This dual inhibitory role is one reason Nogo-A is such a promising therapeutic target.

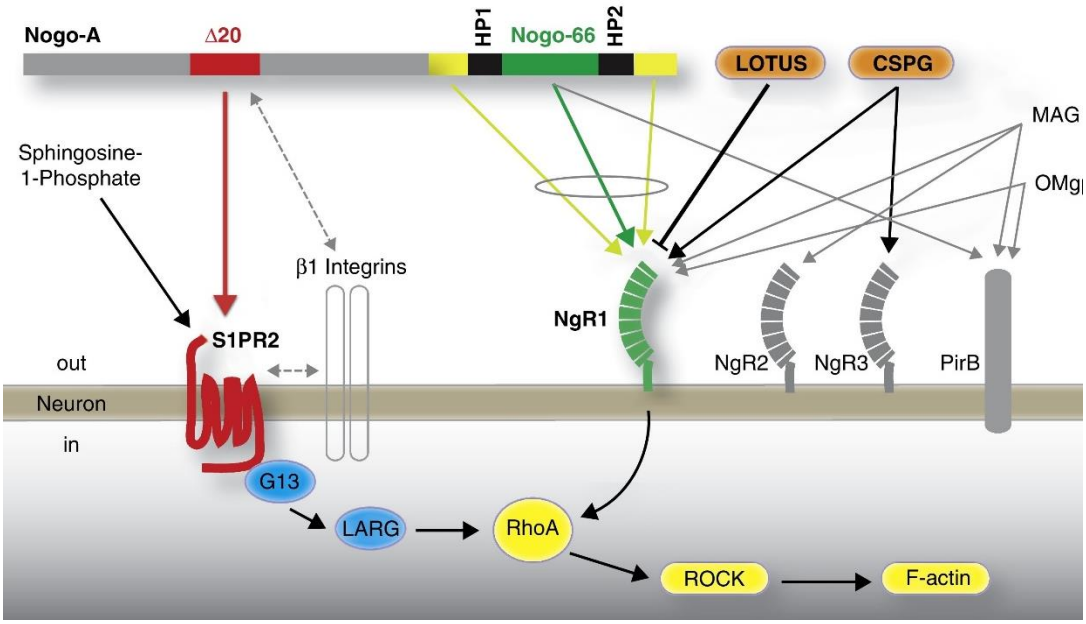

Figure 1.14 Nogo-A inhibitory pathway
The nogo-66 domain interacts with the NgR-1 complex, and the Δ20 domain interacts with S1PR2. RhoA is the downstream pathway for both receptors and the result is the collapse of the neurite outgrowth through effects on the actin cytoskeleton. (Schwab and Strittmatter, 2014)

Nogo-A inhibition has proven a promising therapy for SCI (Zörner and Schwab, 2010). Axonal sprouting and some functional recovery is observed in a number of different animal models with different lesions (Müllner et al., 2008, Bregman et al., 1995, Freund et al., 2009). Anti-Nogo-A is also currently in clinical trials for acute SCI treatment (Kucher et al., 2018). There are two important points about anti-Nogo-A antibody therapy. One is that the most recovery is seen following acute rather than delayed treatment (Gonzenbach et al., 2012). The other is that synchronous anti-Nogo-A therapy and locomotor training actually has a negative combinational effect on recovery (Maier et al., 2009). It has since been shown that sequential treatment first with anti-Nogo-A and then locomotor training does enhance recovery after SCI (Chen et al., 2017).

As seen above, anti-Nogo-A therapy in various combinational treatments is widely studied. Indeed the effectiveness of anti-Nogo-A therapy has led to multiple attempts at combinational treatment. Combined deletion of the inhibitors PTEN and Nogo resulted in limited behavioural recovery (Geoffroy et al., 2015). More successfully, combined treatment with anti-Nogo-A and then ChABC followed by rehabilitative training also produced synergistic effects not just on axonal sprouting, but on behavioural recovery as well (Zhao et al., 2013). One of the things which is novel in our study is the type and severity of injury. No one has, to date, attempted to use anti-Nogo-A with the clinically relevant contusion injury, or attempted to use the therapy in such a severe injury as our experiments outlined in chapter 3.

1.3.3.3 Locomotor training

We know from numerous studies that treadmill training or wheel running leads to some recovery of locomotor function after SCI (Barbeau and Rossignol, 1987, Lovely et al., 1986, Engesser-Cesar et al., 2007). What we do not know is precisely how this is working. Our knowledge is also limited with regards to training timing and training modality, and crucially, how to combine it with other treatments. What follows is a general description of the role of exercise training, before looking at specific circuitry changes following locomotor training.

The role of activity dependant plasticity in locomotor recovery is key. The idea that use of a pathway ensures its survival, and that lack of use leads to its loss. Some evidence for this comes from cat developmental studies inhibiting either regions of the motor cortex or specific muscles (Martin et al., 2007). There is a loss of stable synaptic connection between the motor cortex and motor neurons by inhibiting either one or the other during critical periods of development. More evidence of activity dependant spinal plasticity is seen when one hemisphere of the motor cortex is inhibited during development. Here, the inhibition led to a lack of refinement of CST to interneuron connections, and left CST terminations resembling the immature spinal cord (Chakrabarty et al., 2009). The spinal circuitry is especially plastic during development and may be more susceptible to activity dependant plasticity during this stage. Supporting this is evidence that early training and constraint induced therapy is able to restore normal cholinergic interneurons after unilateral

motor cortex inhibition, whereas later training did not have this effect (Friel et al., 2012). While CST was not shown to have a critical period in this study, it does appear that there is critical period for development for the cholinergic interneuron subtype. Further, following SCI, the transcriptional state of many neurons is returned to a developmental phenotype (Poplawski et al., 2020). Thus indicating activity dependant circuitry remodelling may be even more important during this stage. Indeed cortical reorganisation has been observed following cycling with 5-HT agonists in a rat SCI model (Ganzer et al., 2016). Activity therapy has also been shown to increase certain developmentally important transcription factors which are normally repressed in adults. Factors such as the mammalian target of rapamyacin (mTOR), which is upregulated following cycle training (Liu et al., 2012).

As mentioned, our knowledge of the mechanisms causing exercise induced plasticity is limited. It is known that exercise training is found to upregulate several plasticity enhancing transcription factors. Brain derived neurotrophic factor (BDNF) is among the most studied. It has been shown to increase axonal growth (Bregman et al., 1997) and dendritic spine formation (McAllister et al., 1995). BDNF expression is not always upregulated with training (Macias et al., 2009) but most studies suggest that it is (Hutchinson et al., 2004) and that this increase is associated with enhanced neurite sprouting and behavioural recovery (Wang et al., 2015a). Overexpression of BDNF has also been shown to increase locomotor ability following SCI, although this was negated by increased spasticity in those rats receiving treatment (Boyce et al., 2012). Another neurotrophic factor upregulated by exercise is glial derived neurotrophic factor (GDNF) (Detloff et al., 2014). This factor has been found crucial to facilitate sprouting of propriospinal neurons across a severe lesion (Anderson et al., 2018). The combination of these factors presents a possible mechanism whereby training induces axonal reorganisation.

While this general plasticity enhancement is noted, there are several questions regarding the timing and task specificity of training. If the increased plasticity is not guided correctly there may be negative behavioural effects. Negative transfer occurs when training one task is found to interfere in the function of another task. This negative transfer is

observed with stand and step training, (Leon et al., 1998), with pellet training and the horizontal ladder (Girgis et al., 2007), and with enriched environment and pellet reaching with ChABC therapy (Garcia-Alias et al., 2009). Getting the timing of rehabilitative intervention right may be important to discourage negative transfer. It has previously been shown that delaying training by three months resulted in less training induced behavioural recovery in a rat (Norrie et al., 2005). However, by delaying training 12 days, Krajacic et al. (2009) observed that reach training did not negatively impact horizontal ladder ability also in rats. Further, mixing step and stand training also resulted in no negative transfer in SCI rats (Ichiyama et al., 2009), and is supported by human studies (Gill et al., 2018). Thus it appears the timing and combination of training are important considerations when designing effective rehabilitative treatments.

For locomotor training it appears that changes in spinal sensory integration are the key driver of locomotor recovery. This is mentioned later in the electrical epidural stimulation section (1.3.3.4). The concept of the locomotor CPG is key. Understanding the ability of sensory input to drive the central pattern generator is important to understand locomotor training induced recovery. This sensory driven CPG was demonstrated in spinalised cats walking on a treadmill (Forssberg et al., 1980). Here cats were able to modulate their limb speed independently of each other with a split treadmill. Thus proving the ability of afferent information to robustly modify locomotor output in the absence of supraspinal input. This theory of locomotor training portends that epidural stimulation, and/or pharmacological stimulation simply modulate the spinal cord in a way that allows for sensory input to drive the CPG (Edgerton et al., 2008). The idea of modulation allowing for sensory activation is also observed in studies using clonidine (Chau et al., 1998), or the 5-HT agonist quipazine (Fong et al., 2005). Neither of which directly activate the CPG, but both of which allow for activation of the CPG by sensory inputs.

The theory of sensory driven recovery is well evidenced. With research showing that sensory changes are a key driver of recovery following locomotor training. Changes in the MSR and its electrical analogue, the H reflex, are a mechanism whereby we can study changes in the sensory circuitry (section 1.2.2.1 Monosynaptic reflex and H-reflex). After SCI there is an increase in the H-reflex, this higher H-reflex is restored to more normal

levels following wheel running (Skinner et al., 1996). Ia and II input during cycling were found to mediate this response, as removing their input during cycling training resulted in no modulation of the H-reflex following spinal transection (Ollivier-Lanvin et al., 2010). Frequency dependant depression (FDD) occurs when repeated stimulation of the H-reflex at smaller intervals results in decreased response to the second stimulus. This is probably caused by pre-synaptic inhibition of sensory input to MNs. FDD of the H-reflex is also reduced following SCI, and this FDD is restored with training (Reese et al., 2006). The same FDD reduction also occurs in humans and is returned with cycle training (Kiser et al., 2005). The exercise mediated return of FDD has also been tied to the potassium chloride transporter KCC2, which is downregulated after SCI and upregulated following training (Côté et al., 2014). These changes in local circuitry have allowed us a closer look at spinal changes. Further studies into sensorimotor circuitry changes after treatment could allow us to tease out these specific changes leading to recovery. At present much of the research suggests Ia afferent changes after training. However, this research has not causally linked these afferent changes with specific kinematic and/or behavioural changes following SCI and treatment.

At present our understanding of training induced recovery is limited. Much more research is needed into the mechanisms and modalities best suited for locomotor recovery after SCI. Although we can say that training is necessary. Our lack of understanding has not limited our use of training in combination with other treatments as seen below.

1.3.3.4 Electrical epidural stimulation

In order to achieve synergistic effects on recovery, we are attempting to combine some already moderately successful therapies together. Electrical epidural stimulation (ES) is one of these therapies.

The central pattern generator of the spinal cord contains much of the circuitry necessary for movement. By exciting this circuitry with ES one is able to elicit locomotor type movement in the absence of supraspinal input (Iwahara et al., 1992). By activating this network in SCI it is possible to modulate and train the CPG to act with the limited spared supraspinal input and rely more on sensory input. The role of sensory input in

modulating the CPG is crucial, as such nearly all the studies below combine locomotor training with ES in order to activate the spinal locomotor CPG.

The first such study to tap into this network was completed on neonatal rats. Here ES was able to elicit fictive locomotion (Iwahara et al., 1991). This was followed up with ES on spinally transected cats in order to elicit locomotion on a treadmill (Iwahara et al., 1992). The first studies on ES and training after SCI in rats were completed by V. Reggie Edgerton's lab at UCLA (Ichiyama et al., 2005). These pioneering studies showed that stimulation of the spinal cord at L2 produced consistent stepping on a treadmill with body weight support in rats. Further research combined ES and step training with 5-HT agonists (Gerasimenko et al., 2007, Ichiyama et al., 2008a, Ichiyama et al., 2008b, Courtine et al., 2009), or a cocktail of 5-HT, and dopamine agonists (van den Brand et al., 2012). These studies all point to the importance of training alongside ES as a key for recovery. Exactly how epidural stimulation acts to remodel the spinal circuitry is still not fully understood.

Various theories have been put forward for the mechanisms by which ES elicits motor recovery. First, it is very clear that sensory information is vital, as de-afferented regions showed no activity following ES (Lavrov et al., 2008). Computer modelling ES has backed this up, with a suggestion that large myelinated sensory axons are the primary target of epidural stimulation (Capogrosso et al., 2013). The necessity of proprioceptive information has been shown clearly in other studies. Including one where mice lacking muscle spindles were unable to recover function from a hemisection, whereas mice with muscle spindles were able to regain control of the affected limb (Takeoka et al., 2014). Recovery of a long latency reflex after spinal cord transection has also been suggested as a possible mechanism for ES. This was suggested as ES and step training were found to recover this reflex, which was correlated with better stepping (Lavrov et al., 2006). Step training with ES and a 5-HT agonist was also found to reduce the number of active interneurons during locomotion (Ichiyama et al., 2008a). This reduced activation was suggested to be due to improved sensorimotor specificity leading to a more selective and stable excitation pattern. An argument has been put forward that the main role of ES is to alter the state of the CPG such that sensory input is more easily integrated into locomotion (Sławińska et al., 2012). This argument portends that there is no voluntary recovery of

locomotion, but it is postural changes leading to activation of the CPG by sensory activation. Possible evidence against this is a more recent study suggesting that supraspinal changes are important in ES induced locomotor recovery. Here, in a contusion injury , a cortico-reticular-spinal pathway was shown to be vital for locomotor recovery following ES, step training, and 5-HT agonist treatment (Asboth et al., 2018).

Understanding the changes occurring in the spinal cord due to ES is incredibly important, especially when looking to combine therapies. The past decade has seen several new studies into the therapeutic use of ES in humans. From recovery of locomotion (Harkema et al., 2011, Angeli et al., 2014, Angeli et al., 2018, Wagner et al., 2018), to bladder function (Herrity et al., 2018), to blood pressure control (Harkema et al., 2018). The large increase in the therapeutic use of ES has increased the need for more understanding of this field. While the exact mechanisms for ES mediated recovery is unclear, human studies using ES have demonstrated the need for combinational rehabilitation with stimulation (Angeli et al., 2018). How to best combine rehabilitation with ES is still a very live debate. Classically negative transfer has been observed during training. In a rat model, step training has led to reduced standing ability, and stand training has led to reduced stepping ability (Ichiyama et al., 2009). However in humans, multimodal step and stand training with ES has proved effective in locomotor recovery after SCI (Gill et al., 2018). The above study found no negative transfer of ability from one task to another. Sustained recovery was also observed using ES timed to the desire of patients (Wagner et al., 2018). Studies like those above are rapidly advancing the field. However, further, mechanistic insights are needed to determine the interplay between rehabilitation, epidural stimulation, and other plasticity enhancing therapies.

1.3.3.5 Combinatorial treatments

After SCI there is a period of increased plasticity, during which many interventions seek to extend or enhance this plasticity for behavioural recovery. We do know however, that plasticity itself is not always beneficial. In the absence of training maladaptive plasticity can occur with aberrant synaptic connections causing motor dysfunction following SCI (Beauparlant et al., 2013). Training, as described above, seeks to modulate this plasticity and lead to functional networks.

Combinatorial therapy has been a constant presence in research into ES. Training along with ES and 5-HT agonists has been described in detail above. Combinatorial therapies with other treatments are more limited with mixed results. ChABC and reaching training has been combined for improved forelimb function (Wang et al., 2011, Garcia-Alias et al., 2009). Anti-Nogo-A and sequential locomotor training has also shown increased locomotor capability (Chen et al., 2017). While the treatments above have been mentioned before, there is more recent evidence demonstrating the effectiveness of plasticity enhancing treatments with training. Recovery in a reaching task was only significant following a C4 lesion when a CST specific protein kinase A inhibitor was combined with reaching training (Wei et al., 2016). Either an antibody against or a motor cortex specific knockout of the repulsive Wnt receptor RyK increased CST sprouting following a cervical dorsal column lesion in a mouse (Hollis Ii et al., 2016). However, cortical reorganization and motor improvements in a reaching task were only seen if animals were given weekly reaching testing in combination with this knockout. Rehabilitative reaching training was also found to be vital with increased reaching accuracy and increased CST sprouting observed when reaching training was combined with a mild inflammatory lipopolysaccharide following a dorsal column lesion (Torres-Espín et al., 2018) The neurite growth enhancer docosahexaenoic acid and reaching training were similarly found to have a synergistic effect on CST and serotonergic sprouting, as well as on reaching task (Liu et al., 2017b).

The above studies demonstrate the ability of training to guide recovery in concert with other treatments. However, the evidence is limited regarding mechanisms. Training also seems to be effective in guiding locomotor recovery following stem cell treatment. Here, there does appear to be a possible mechanism of action. Increased glutamic acid decarboxylase 65 kDa isoform (GAD65) expressing inhibitory interneurons were found with treadmill training and neural stem cell treatment (Tashiro et al., 2016). These inhibitory interneurons are a possible source of rhythmic inhibition during fictive locomotion (Wilson et al., 2010) and there is a reduction in these neurons following SCI (Kapitza et al., 2012). Thus, restoring these neurons could be important to restore the capacity of the locomotor CPG to produce stepping after injury. However, understanding changes in this circuitry are constrained due to limited targeting ability of the various

interneurons in adults. Slightly easier to study are Ia afferent inputs to MNs. Ia afferents on MNs are increased after Anti-Nogo-A treatment, but following locomotor training these are decreased (Chen et al., 2017). Changes in this Ia to MN network appear to be pivotal for training induced recovery, and this probably applies in combinational treatment as well.

1.3.4 Conclusion

The spinal networks controlling locomotion are complex, as described in section 1.2. The pathology and treatments for SCI are equally complex. Overcoming the inhibitory environment and promoting axonal growth is just one step for recovery. Epidural electrical stimulation and locomotor training are both important tools to activate the locomotor CPG and enhance recovery. Both the above treatments are attempting to reconfiguring spinal circuitry so that it can function without the need for fully intact supraspinal inputs. A key driver of this reconfiguration is sensory modulation. We know this as without muscle spindles providing proprioceptive information mice are unable to recover from SCI (Takeoka et al., 2014). The neurons controlling this proprioceptive information are γ-MNs. Their separate supraspinal control, broad spectrum segmental inputs, and potentially unique capacity for synaptic plasticity make these neurons attractive targets.

1.4 Aims and objectives

There are no current treatments for SCI at present. The substantial personal and economic cost of the disease make finding a cure an imperative. The Anti-Nogo-A antibody 11C7 is one treatment showing beneficial effects on recovery. We are the first group to test this antibody in the more clinically relevant contusion injury rodent model. By combining this drug with epidural stimulation and locomotor training we aim to enhance recovery more than with any of the individual interventions alone. We have interrogated changes on a behavioural, structural, and electrophysiological level. We aimed to determine which factors were important in recovery and which factors were changed by individual treatments. The overall hypothesis was that combinatorial treatment would result in the best locomotor recovery. We aimed to do this by increasing axonal growth and sprouting with Anti-Nogo-A antibody and then harnessing this plasticity with a training paradigm assisted by epidural stimulation. As proprioceptive sensory input is necessary for

recovery we have interrogated changes in this network via electrophysiological and structural methods.

On the theme of sensory changes we have specifically targeted γ-MNs to determine their inputs. These neurons control the sensory output from muscle spindles and as such are key regulators of the locomotor CPG. Their role in recovery from spinal cord injury is currently unknown, but it is very likely they play a key role. We have targeted them using multiple methods.

1.4.1 Aims

1.4.1.1 Spinal cord injury aims

i) We aimed to discover which combination of anti-Nogo-A antibody treatment, locomotor training and epidural stimulation would result in the greatest functional recovery.
   (1) To do this we investigated kinematic changes in body weight supported locomotion as well as open field behaviour

ii) As reviewed in previous sections, plasticity enhancing treatments and rehabilitative therapy lead to sensory changes in the spinal cord. We aimed to interrogate these changes by measuring structural and electrophysiological differences in afferent networks between treatment groups. Training and epidural stimulation would lead to changes in afferent and pre-synaptic inhibition circuitry.
   (1) We aimed to determine whether combinational treatment resulted in reduced H-reflex response
   (2) We studied sensory fibre innervation changes by immunohistochemistry of the vesicular glutamate transporter 1 (VGluT1) found in primary muscle spindle afferents
   (3) We studied changes in pre-synaptic inhibition via immunohistochemistry and 3D reconstruction for accuracy

iii) Anti-Nogo-A antibody treatment and training can both lead to axonal sprouting after SCI. We aimed to determine if this took place in our study, and if there was any increase in CST or monaminergic fibres below the lesion.

(1) We aimed to determine if any CST fibres had crossed the lesion or if any spared fibres had increased sprouting after treatment
(2) We aimed to study 5HT expression changes below the lesion
(3) We determined whether any of our treatments led to an increase in 5HT fibres in close apposition with α-MNs
(4) We also investigated tyrosine hydroxylase expression below the lesion and attempt to determine whether dopaminergic/noradrenergic fibre sprouting had occurred

1.4.1.2 γ-MN study aims

i) We aimed to investigate γ-MN expression in various muscles as this may enable us to determine more about their function.
   (a) To do this we have injected cholera toxin subunit β (CTB) into seven different muscles and have imaged stained tissue with light sheet microscopy after applying tissue clearing
ii) In order to study γ-MNs we have attempted to specifically target them and their inputs via virus tracing. We aimed to determine if it was possible to target γ-MNs via adeno associated viruses (AAVs) with γ-MN specific promotors.

1.5 Hypotheses

1.5.1.1 Spinal cord injury hypotheses

i) Combinational treatment would result in the highest behavioural recovery
   (1) Open field behavioural (BBB) score will be highest in the combination ES, training, and 11C7 antibody group
   (2) Changes in kinematics will elucidate and expand on this recovery
ii) Local sensory changes measured with immunohistochemistry and electrophysiology will be modulated differently in various treatments
   (1) The H-reflex amplitude should be reduced in the trained groups and should be correlated with locomotor recovery
   (2) Changes in direct sensory innervation (VGluT1) could be mediating this and should be correlated with H-reflex results

(3) Pre-synaptic inhibition of these sensory inputs measured by GAD65+ p boutons should be increased in trained groups

iii) Axonal sprouting caudal to the lesion will increase with 11C7 treatment and exercise

(1) BDA tracing should show more corticospinal tract sprouting after treatment with 11C7

(2) 5-HT should also increase with 11C7 and with training

(3) Tyrosine Hydroxylase (TH) will increase with 11C7

1.5.1.2 γ-MN study hypotheses

i. γ-MN expression will vary by muscle type. More postural muscles will contain a higher proportion of γ-MNs

(a) A higher proportion of γ-MNs will be observed in postural muscles

(b) Fewer γ-MNs will be observed in more distal fine control muscles

ii. An AAV with the Err3 promotor will specifically target γ-MNs and allow us to determine their inputs and potentially manipulate their behaviour via optogenetic stimulation

2 General methods

Specific methods are contained within experimental chapters. Common surgery, tissue preparation, and immunohistochemistry methods for both chapters are below.

2.1 Animals and Surgeries

44 Adult (200-250 g) female Sprague Dawley rats (Charles River) were used for SCI experiments. For SCI experiments animals were housed individually under a 12 h light/dark cycle with food and water access ad libitum. A mix of Sprague Dawley (Charles River), and Wistar (in house) animals were used for γ-MN experiments. These were multiply housed under a 12 h light/dark cycle with food and water access ad libitum. All procedures were performed in accordance with the United Kingdom's Animal (Scientific Procedures) Act 1986 (ASPA) under project licence PPL 70/8085 and P7DD7EE20.

For surgeries, animals were anaesthetised with inhalable 5% isoflurane for induction and 1.5-2.5% for maintenance with O2 flow at ~1.5 litres/minute. Animals were placed on heat pads for the duration of the surgeries and left in warmed incubation chambers post-surgery. Animals were given subcutaneous pain relief (0.015 mg/kg, Vetergesic®) and antibiotic (2.5 mg/kg, Baytril®) immediately following all surgeries.

2.2 Perfusion and tissue preparation

Animals were deeply anaesthetised with intraperitoneal injection of sodium pentobarbital (100 mg/kg). When the rats became unresponsive they were then transcardially perfused with 0.1 M phosphate buffer (PB) before perfusion with 4% paraformaldehyde (PFA) in PB. Spinal columns (and brains where applicable), were removed and post-fixed overnight at 4 ^{o}C in 4% PFA in PB. Spinal cords were then dissected out of columns. Care was taken to retain all dorsal root ganglia from T13 caudally to identify spinal segments (Figure 2-1). Spinal cords were then left overnight at 4 ^{o}C in 30% sucrose in PB. They were then cryoprotected for at least a further two nights in fresh 30% sucrose in PB at 4 ^{o}C. Spinal cords and brains were stored in 30% sucrose in PB at 4 ^{o}C with a drop of 4% PFA until further processing.

Areas of interest were briefly washed in PB before being embedded in FSC 22 Frozen Section Media (Leica, USA) for 1 hr at room temperature before being frozen on crushed dry ice. Tissue was stored at -80 ^{o}C for at least one night or until further use. Transverse sections of spinal cord were cut on a cryostat at -20 ^{o}C. 25 µm sections were cut free floating unless otherwise stated. Samples were stored in cryoprotectant at -20 ^{o}C until immunohistochemical analysis. For *in-situ* hybridisation experiments sections were cut directly onto slides and stored at -80 ^{o}C.

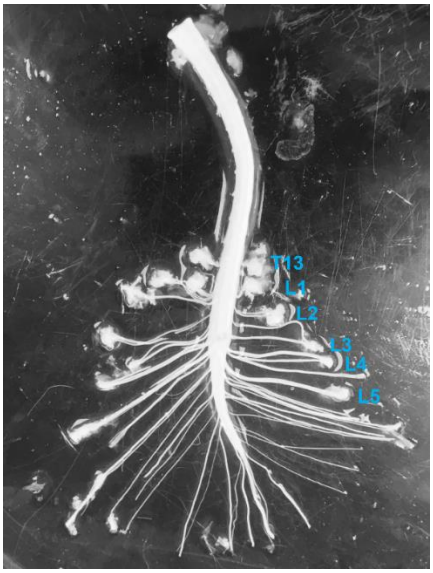

Figure 2-1 Dissection with lumbar enlargement DRGs

2.3 Immunohistochemistry and imaging

After removal from -20 ^{o}C storage, free floating sections were washed three times ten minutes in 0.1 M phosphate buffered saline (PBS) at room temperature (RT). Sections were incubated in primary antibody solution at 4 ^{o}C for 16-48 hrs depending on the antibody requirements. After this, sections were washed three times ten minutes in PBS before 2 hrs incubation of secondary antibody all at RT. Sections were washed two times ten minutes PBS, before a final two times ten minutes wash in 0.1 M tris non saline to remove background from salts. Sections were mounted on glass slides (SuperFrost Plus™, Fisher Scientific, UK) with mounting media (FluorSave reagent, Millipore, Germany) and glass coverslips before storage at RT.

Carl Zeiss Zen Black (Germany) was used for image capture with a confocal microscope (LSM 700, LSM 880, or LSM 880 inverted, Zeiss, Germany). All imaging settings were identical for each individual experiment investigating one structure.

3 Combinational treatment for spinal cord injury

3.1 Introduction

Spinal cord injury results in a cascade of events which can lead to severe loss of motor, sensory and autonomic function. Restoring locomotion after spinal cord injury is a high priority for those affected (Anderson, 2004). However, at present there is still no effective treatment. The most common type of injury, the contusion injury, leads to a cascade of secondary damage. First there is the immediate mechanical damage and cell death before a breakdown of the blood brain barrier. This breakdown and the accompanying cell death leads to oedema and further necrosis (Rowland et al., 2008). The acute secondary damage increases the lesion size, this larger lesion then undergoes gliosis and then mesenchymal scar formation (Okada et al., 2018). Slow Wallerian degeneration of axons in the CNS leads to further loss of function (Vargas and Barres, 2007). These cascades of injury lead to disconnection between the brain and spinal cord.

After and during the process briefly described above there is some spontaneous reorganisation of network in the spinal cord. During this time some neurons transiently return to a more developmental transcriptional state (Poplawski et al., 2020). This period of increased plasticity can lead to some behavioural improvements. However, in the absence of training, this plasticity is often maladaptive and can lead to negative behavioural results (Beauparlant et al., 2013, Dickson et al., 2019). There are many therapies aiming to augment endogenous plasticity by targeting various transcription factors and inhibitors. One such inhibitory target is the Nogo-A pathway. In the adult CNS this pathway acts to limit axonal growth and stabilize neuronal pathways (Huber et al., 2002). Nogo-A acts on various receptors on the cell surface to activate the Rho/Rock pathway and leads to growth cone collapse via disruption of the actin cytoskeleton (Schmandke et al., 2007). A section of Nogo-A is also internalized where it leads to a reduction in growth associated transcription factors (Joset et al., 2010). These various well documented effects of Nogo-A are the reason why it has been so heavily targeted as a treatment for SCI and stroke (Müllner et al., 2008, Bregman et al., 1995, Freund et al., 2009, Gonzenbach et al., 2012, Kucher et al., 2018).

There are various experimental therapies for SCI, however at present the only widely used clinical intervention is rehabilitative therapy. Combining locomotor training and anti-Nogo-A requires sequential anti-Nogo-A and then locomotor training to enhance recovery after SCI (Chen et al., 2017). Synchronous anti-Nogo-A therapy and locomotor training actually has a negative combined effect on recovery (Maier et al., 2009). There is a growing push to combine plasticity enhancing therapies with rehabilitation. Rehabilitative training has been combined with inhibition of the repulsive Wnt receptor RyK (Hollis Ii et al., 2016), digestion of chondroitin sulphate proteoglycans with ChondroitinaseABC (Wang et al., 2011, Garcia-Alias et al., 2009), mildly inflammatory lipopolysaccharide (Torres-Espín et al., 2018), and docosahexaenoic acid (Liu et al., 2017b) among others (reviewed in Dickson et al. (2019)). Determining the individual and combinatorial changes occurring is important for the eventual application of combinational therapies for enhanced behavioural recovery.

Electrical epidural stimulation (ES) is one treatment with combinatorial potential. ES has been combined with training to induce locomotor stepping after complete spinal transection (Ichiyama et al., 2005). Further treatments combined ES and training with 5-HT agonists (Gerasimenko et al., 2007, Ichiyama et al., 2008a, Ichiyama et al., 2008b, Courtine et al., 2009). This early research has led to human studies which often combined ES with training for lasting behavioural improvements. (Harkema et al., 2011, Angeli et al., 2014, Angeli et al., 2018, Wagner et al., 2018).

The exact mechanisms governing recovery following training or ES are not entirely clear. Following SCI, exercise increases expression of neurotrophic factors such as BDNF and GDNF (Detloff et al., 2014, Wang et al., 2015a). These neurotrophic factors are both associated with axonal growth and sprouting (Anderson et al., 2018, Wang et al., 2015a). Proprioceptive afferents are a potential source for some increase in neurotrophic factors. As neurotrophic factor 3 (NT3) and to a lesser extent BDNF are both increased in the spinal cord following afferent stimulation (Gajewska-Woźniak et al., 2013). This proprioceptive driven increase in growth factors is probably a key driver in training and ES induced plasticity.

Proprioceptive afferents are a key driver of locomotor recovery following ES or training. The spinal network responsible for the control of locomotion is termed the central pattern generator (CPG). This network is able to control stepping in the absence of supraspinal control using just sensory input from a treadmill (Forssberg et al., 1980). In the absence of proprioceptive feedback there is a degradation of locomotor pattern, including interjoint and flexor extensor coordination (Akay et al., 2014). Proprioceptive feedback plays an important role in locomotor recovery following SCI. Indeed, proprioceptive input is vital for locomotor recovery after SCI in mice, as without muscle spindles animals do not recover (Takeoka et al., 2014). Sensory feedback is also vital for recovery of movement following epidural stimulation, as without sensory input ES has no effect (Lavrov et al., 2008).

Changes in afferent input occur after SCI and training. Increased proprioceptive input is observed after unilateral CST transection in the rat (Tan et al., 2012). This increased direct sensory input (as measured by VGluT1 boutons on MNs) is hypothesized to contribute to spasticity after SCI. Another, full transection study found decreased VGluT1 fibres in the medial Lamina VII interneuronal area (Kapitza et al., 2012). So there appears to be some difference in afferent changes between full transection and more targeted lesions. Locomotor training has been shown to reduce VGluT1 boutons in the ventral horn and on MN dendrites of rats given 11C7 after a T-lesion (Chen et al., 2017). Although this reduced VGluT1 input is not always the case, and an increase in VGluT1 boutons has also been observed following training with a 5-HT agonist in a separate full transection study (Khalki et al., 2018). Further investigation of sensory changes in the clinically relevant contusion model are needed to understand how ES and training are modulating spinal cord circuitry.

The H-reflex is one method whereby we can probe sensory changes following SCI. In rats SCI increases the amplitude of the H-reflex and exercise training returns the reflex to more normal levels (Skinner et al., 1996). Sensory feedback is critical for this training induced recovery of H-reflex in spinally transected rats (Ollivier-Lanvin et al., 2010). In the Ollivier-Lanvin et al. (2010). study exercise did not lead to a reduction H-reflex if afferent signalling was blocked during training. We have investigated both H-reflex

changes and modulation of VGluT1 input in the spinal cord. We have also investigated presynaptic inhibition in our study, as SCI has been shown to decrease pre-synaptic inhibition of sensory input (Caron et al., 2020). After a full transection and training with 5-HT agonists, there is an increase in the density of the inhibitory P boutons causing pre-synaptic inhibition (Khalki et al., 2018). Thus providing both anatomical and electrophysiological evidence of SCI induced reduction in pre-synaptic inhibition, and training induced increase in boutons mediating this inhibition.

Plasticity of local afferent networks are not the only changes after SCI and treatment. Given the loss of descending inputs, supraspinal pathways reorganisation is important for recovery (Asboth et al., 2018). We have investigated supraspinal descending pathway fibre sprouting in the lumbar cord. In rats, the CST terminates primarily in Laminae VI and VII and not directly on MNs as it does in primates (Alstermark et al., 2004). In rodents the CST primarily provides input to pre-motor interneuron controlling distal limb muscles with a focus on flexor muscles (Lemon, 2008). Given its role in control of movement the CST is often a target for plasticity enhancing treatments (Hollis Ii et al., 2016, Liu et al., 2017b, Geoffroy et al., 2015). Fine movements are especially influenced by CST loss, and regeneration of the CST is correlated with recovery of fine motor control (Jin et al., 2015). 11C7 therapy has been shown to increase CST sprouting following a targeted lesion (Chen et al., 2017, Maier et al., 2009). To determine whether there are similar changes following a severe contusion injury we have investigated cortical sprouting with biotinylated dextran amine injections into the sensorimotor cortex.

We have also quantified serotonergic and dopaminergic/noradrenergic fibre expression to see if there are any monoaminergic fibre changes. The mono-aminergic pathways provide broadly excitatory input, where they may not directly activate circuitry they can increase excitability for other stimuli (Schmidt and Jordan, 2000). Serotonergic sprouting is correlated with locomotor recovery in a rat spinal hemisection model (Saruhashi et al., 1996). Both wheel running and treadmill training have both been shown to increase 5-HT sprouting after SCI (Engesser-Cesar et al., 2007, Maier et al., 2009), although this is not always the case (Chen et al., 2017). 11C7 has also been shown to increase serotonergic sprouting in a targeted lesion (Chen et al., 2017, Maier et al., 2009).

We aim to determine if this also occurs after a severe contusion injury. Tyrosine hydroxylase (TH) is an enzyme responsible for dopamine and noradrenaline synthesis, and is found in noradrenergic and dopaminergic cells and fibres (Yamamoto et al., 2011). We have investigated TH in the lumbar spinal cord to determine fibre sprouting. TH immunoreactivity below the lesion is correlated with swimming recovery in a lamprey spinal cord transection (Kuscha et al., 2012). Locus coeruleus noradrenergic neurons were recently implicated in motor learning in a autism spectrum disorder mouse model (Yin et al., 2021). Thus indicating both of these catcholamines are important for locomotor function and recovery.

In our study we have combined a plasticity enhancing treatment, (the anti-Nogo-A antibody 11C7), with locomotor training and epidural stimulation. The goal was to increase axonal sprouting with anti-Nogo-A, and then refine and modulate this new growth into functional networks with locomotor training and electrical epidural stimulation. We are the first group to investigate anti-Nogo-A antibody treatment in a contusion injury rat model, and the first to combine anti-Nogo-A antibody therapy with training and epidural stimulation.

3.2 Aims

In this study we aimed to determine if combinatorial therapy would increase locomotor behaviour above a single therapy. We attempted to elucidate what could be mediating this recovery by observing kinematic, electrophysiological, and anatomical changes. We also aimed to study interactions of the treatments and their effects individually and in combination.

3.3 Hypothesis

i) Combinational treatment will result in the highest behavioural recovery
   (1) BBB score will be highest in CB 11C7 group
   (2) Changes in kinematics will show improved step consistency and reduced drag

ii) Local sensory changes measured with immunohistochemistry and electrophysiology will be modulated differently in different treatments and this will underly the behavioural changes
    (1) The H-reflex amplitude will be reduced in the trained groups and will be correlated with locomotor recovery
    (2) Changes in direct sensory innervation of MNs (VGluT1) will mediating this H-reflex reduction
    (3) Training will increase pre-synaptic inhibition of these sensory inputs
iii) Axonal sprouting from supraspinal input will increase with 11C7 treatment and exercise
    (1) Biotinylated dextran amine (BDA) tracing will show more corticospinal tract sprouting after treatment with anti-Nogo-A
    (2) 5-HT below the lesion will increase with 11C7 and with training
    (3) 5-HT contacts on MNs below injury will increase with 11C7 and training
    (4) Tyrosine Hydroxylase may increase with 11C7
iv) Analysing all this together will allow us to link the local spinal changes with behavioural improvements associated with the individual and combined therapies

3.4 Methods

3.4.1 Study plan

First all animals received implants and injuries and were divided into treatment groups (Figure 3.1A). The timeline for the study is shown in Figure 3.1B. After injury animals were then left for two weeks before mini osmotic pumps containing anti-Nogo-A or control IgG were removed. One week after pump removal animals started to receive therapeutic interventions based on their group. Therapy continued for 8 weeks. Kinematic experiments were then completed within two days of the last training session. Shortly after this, tracer injections were injected into the sensorimotor cortex. Animals were then left between 12-16 days for terminal electrophysiology and perfusions. For the first cohort, cortical, epidural and electromyography wires were implanted one week before injury and pump implantation.

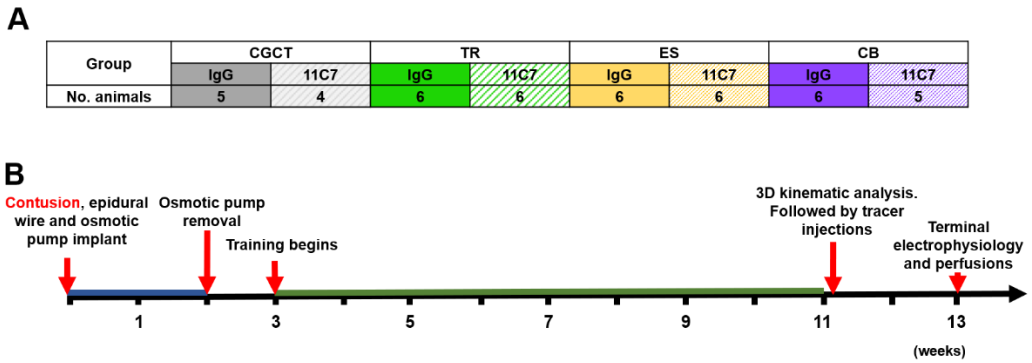

Figure 3.1 Timeline of experiments and groups

3.4.2 Surgical procedures

3.4.2.1 Spinal cord injury

44 Adult (200-250 g) female Sprague Dawley rats (Charles River) were used for SCI experiments. Animals were anaesthetised with inhalable isoflurane as per the general methods (Chapter 2). After shaving and sterilisation of the surgical site, a large midline skin incision was made from mid thoracic (~T4) through lumbar (L1-L6) up to mid sacral level (~S3). Partial laminectomies were completed at T8/T9, T12/T13 and L2 vertebrae (Figure 3.2A). After laminectomies the spinal column was secured with stereotaxic holders just rostral (T6/T7) and caudal (T10/T11) to the injury site at T8/T9 vertebral level corresponding to T9/T10 spinal cord (Figure 3.2B). Injury was completed at a proscribed

force of 250 kilodynes using the Infinite Horizon impactor (Precision Systems & Instrumentation, Lexington, KY, USA).

3.4.2.2 Epidural wire implantation

Another ~2 cm skin incision was made at the skull and wires were passed under the skin to the back. The epidural wires were then implanted on the midline of the spinal cord at spinal levels L2 and S1 (Figure 3.2C). These were Teflon coated stainless steel wires (AS632, Cooner Wire, Chatsworth, CA, USA) connected to 16-channel amphenol connectors (MCS-16-SS; Omnetics, Minneapolis, MN, USA). Wires were passed caudally between the spinous process and the dura from the laminectomy rostral to implantation. For stimulation approximately 1 mm of stainless steel was exposed around 1 cm from the end of the insulated wire. A small suture (Ethilon 9.0, Ethicon) was then placed either side of the exposure in order to secure the wires. A third wire was left in the subcutaneous space of the back as a common ground. To secure the amphenol connector to the skull, three screws (0-9.0 X 3/32; Otto Frei, USA) were anchored to the skull in holes drilled for this purpose. Cold cure dental acrylic (Simplex Rapid; Kemdent, Swindon, Wiltshire, UK) was used to secure the connector to the screws.

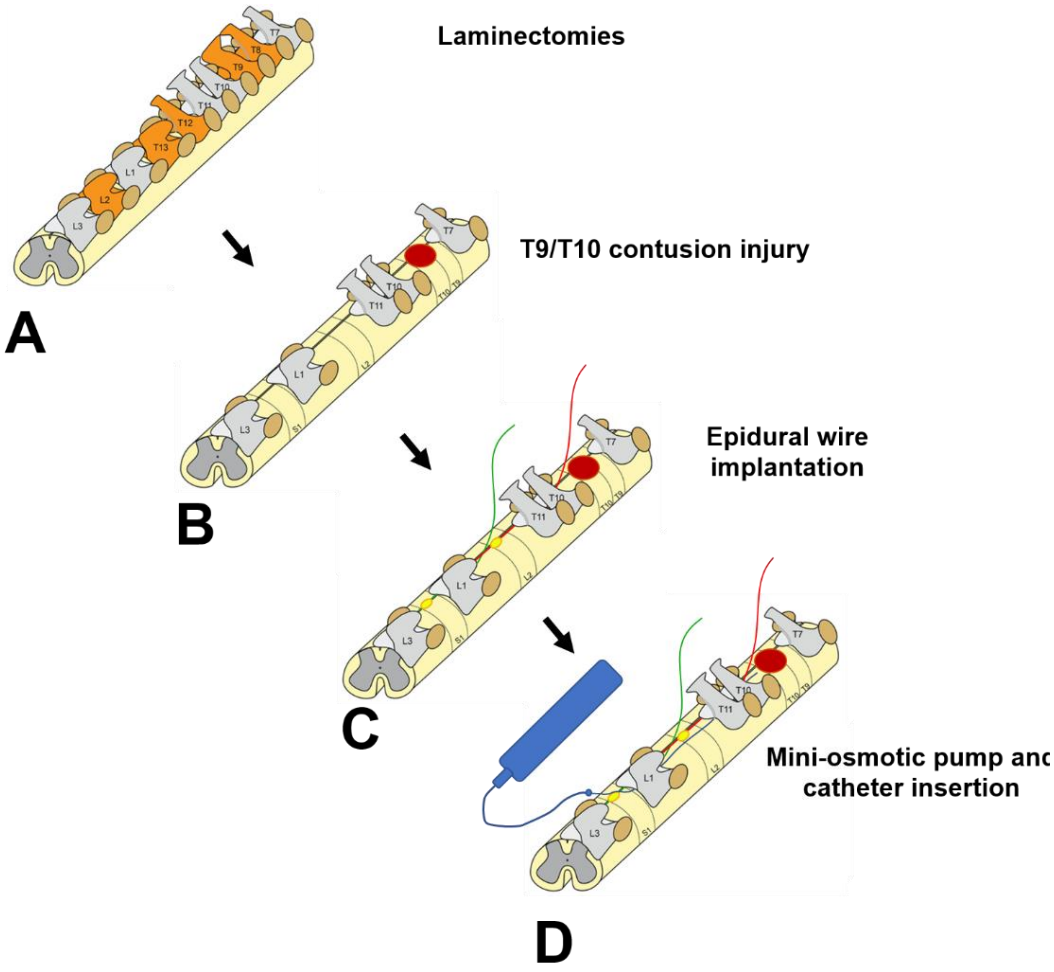

Figure 3.2 Spinal epidural implantation, injury and catheter implant

Partial laminectomies were completed at T9/T10, T12/T13 and L2 (A) Before injury at T9/T10 spinal level (B). Epidural wires were then implanted (C), before insertion of the mini-osmotic pump catheter (D). Adapted from Al'Joboori (2016).

3.4.2.3 Mini-osmotic pump implant

Drug delivery was by mini osmotic pumps (Alzet 2ML2, Durect Co., Cupertino, USA). These pumps were filled with 2 ml of 11C7 (University of Zurich) or control antibody mouse monoclonal IgG1 anti-cyclosporin A (University of Zurich) (both 3 mg/ml) and pumps were blinded by a third party. Attached to the pumps were custom made silicon catheters (0.702 mm inner diameter, 00702, Detakta, Norderstedt, Germany and 0.108 mm inner diameter, 0041, ReCathCo, Allison Park, USA). The day before surgery, pumps were placed in sterile saline water baths at 37 ^{o}C. The body of the pump was

implanted subcutaneously in the back of the rats. The larger end of the catheter was passed through a paravertebral muscle and secured with sutures. The smaller catheter was inserted from the L2 laminectomy site through a hole in the dura into the subdural space. The catheter was then passed rostrally to the injury site at T9/T10 (Figure 3.2D). The anti-Nogo-A or control antibody were delivered intrathecally at a rate of 5 μl/hour before removal after two weeks. A roughly equal number of 11C7 and control IgG pumps were implanted every day of surgery.

3.4.2.4 Recording electrode implantation

A small subset of animals received left hemisphere cortical implants to chronically test cortical responses and right side electromyography (EMG) electrodes in the tibialis anterior, gastrocnemius soleus and spinodeltoid for muscle responses (Figure 3.3). The cortical electrode consisted of five gold electrodes with a polymer base placed on the dura of the sensorimotor cortex after removal of a section of the cranium (Figure 3.3A). EMG electrodes in the hindlimb and forelimb were implanted in order to test chronic cortex responses (Figure 3.3B). The EMG and cortical wires were connected to the Amphenol connector mentioned previously. These extra recording wires were discontinued in later cohorts as no cortical to hindlimb response was ever observed in chronic recordings.

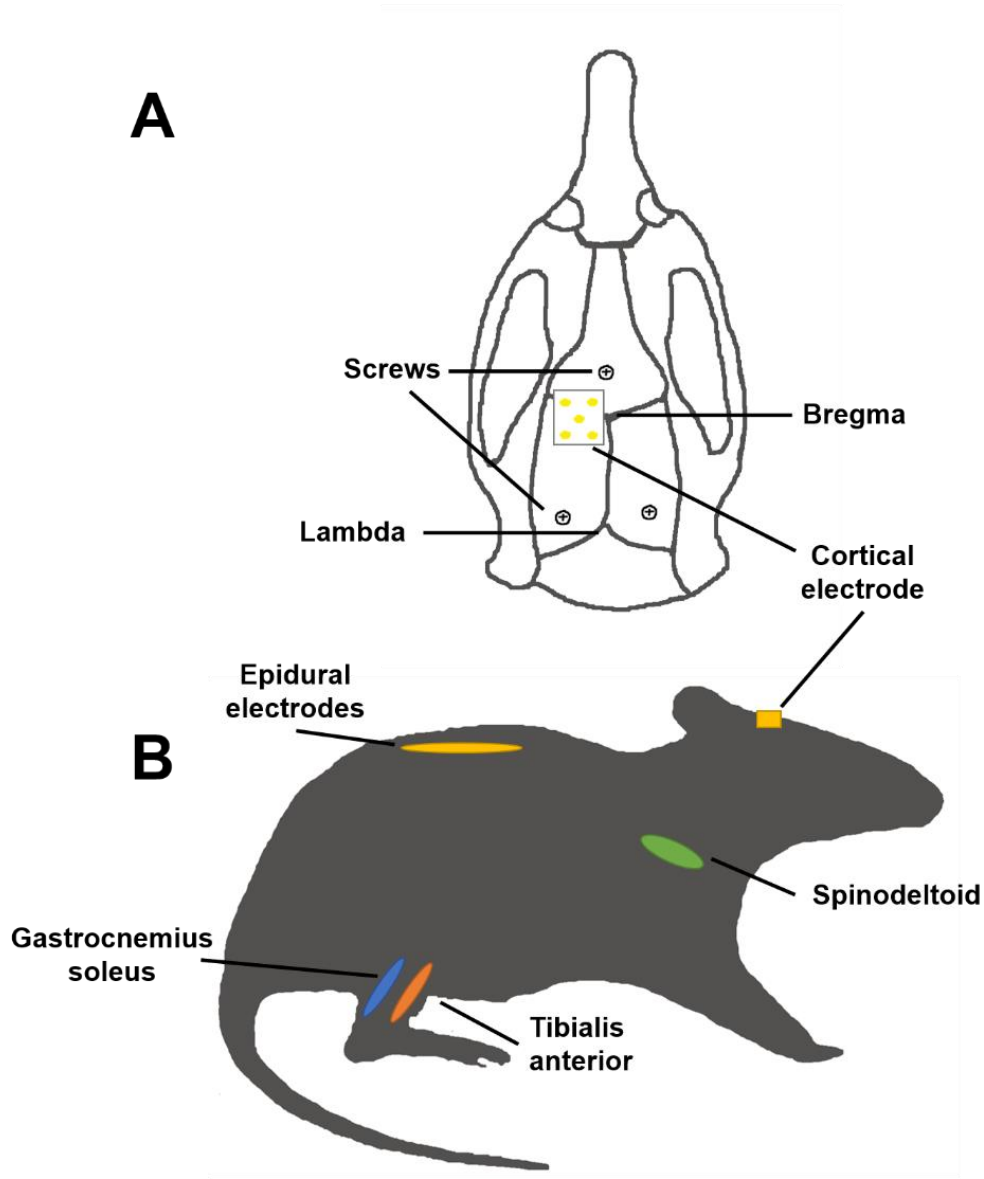

Figure 3.3 Electromyography and cortical electrode placement
A subset of animals had cortical implants over the sensorimotor cortex (A), and EMG electrode implants in the tibialis anterior, gastrocnemius soleus and spinodeltoid muscles.

3.4.2.5 Post-operative animal care

All animals were given subcutaneous saline, pain relief (0.015 mg/kg, Vetergesic®) and antibiotic (2.5 mg/kg, Baytril®) for 3 days post-surgery. Animals were manually expressed twice daily until the end of the study, or until they were able to evacuate their bladder autonomously.

3.4.3 Treatment groups and interventions

The mini-osmotic pump delivering 11C7 or control IgG was removed after two weeks. After this there was a one week break to have the wash out period, as synchronous 11C7 therapy and training have proven to have a negative combinatorial effect on locomotor recovery after stroke and SCI (Wahl et al., 2014, Maier et al., 2009). Rats were randomly divided into treatment groups as seen above (Figure 3.1). Animals were either cage control (CGCT), trained (TR), given electrical epidural stimulation (ES), or a combination of epidural stimulation and training (CB). All these groups had an 11C7 and control IgG cohort.

3.4.3.1 Epidural stimulation

The amphenol connector on the rats skull was attached via a cable and an isolator unit (SIU-V Isolation unit; Astro-Med®, Inc. Grass instruments, Middleton, WA, USA) to a Grass stimulator (S88X stimulator; Astro-Med®, Inc. Grass instruments, Middleton, WA, USA). Electrical stimulation consisted of 0.2 ms rectangular pulses at 40 Hz using a protocol designed by Ichiyama et al. (2005) for rats. Stimulation strength ranged from 0.5-5 volts. The threshold for L2-S1 stimulation or the reverse S1-L2 was determined by feeling for movement in the hindlimbs. Animals were then stimulated at sub movement threshold. Stimulation took place alongside training in the CB group or without training in the ES alone group. Therapy consisted of ten minutes stimulation/training, a ten minute break, and then ten minutes stimulation/training. Training took place five days a week for eight weeks and was always completed after behavioural assessments.

3.4.3.2 Locomotor training

Training consisted of the same ten minutes on, ten minutes rest, and ten minutes on again as the above epidural stimulation. This distributed practice is so that animals do not fatigue during training and is also supported by evidence showing distributed practice results in faster and more permanent skill acquisition (Lee and Genovese, 1988). For training, rats were placed in an upper body harness and suspended by a body weight support system over a treadmill (Robomedica; Irvine, CA, USA) (Figure 3.4B). Animals were moved from a more bipedal to quadrupedal position over the course of the session, and

body weight support was adjusted to ensure rats were able to weight bear while walking. Speeds ranged from 7-21 cm/s according to ability.

3.4.4 BBB scoring

The Basso, Beattie and Bresnehan scoring system is a widely used open field scoring system for SCI rats (Basso et al., 1995). The assessment requires relatively little time and equipment and because of this it can provide a general overview of behaviour over time. Rats are placed on a round table of ~1 metre diameter with clear sides for unobstructed view. Animals are assessed for a range of tasks of both hindlimbs for a period of four minutes. The BBB scale is not linear, and ranges from small limb movements (1) to full range of movement (7) to body weight supported stepping (10) to coordinated stepping (14) to full trunk stability, toe clearance, and parallel paw placement (21). This test was completed one week after injury and for the subsequent 11 weeks until the end of training.

3.4.5 Kinematics

Kinematic recordings of the hindlimb were made one or two days after the final training session. Six Vicon motion systems infrared cameras recorded at 100 Hz, along with one video camera (Figure 3.4A) (Bonita cameras, Vicon, Oxford, UK). Reflective markers were placed bilaterally on the shaved skin overlaying the fifth digit of the distal phalange (toe), lateral malleolus (ankle), lateral epicondyle of femur (knee), greater trochanter (hip) and iliac crest (crest), along with one marker over the midline spine (Figure 3.4B).

All recordings were made with animals receiving no stimulation, however, body weight support was provided and optimised for each rat. Ten consecutive steps were recorded for each speed (7,14 and 21 cm/s). Not all animals were able to walk at 21 cm/s and 7 cm/s was too slow for others, therefore we have used 14 cm/s recordings for all analysis. Recordings were processed using Vicon Nexus 7 to label and then export data as excel files with cartesian coordinates. Custom MATLAB (MathWorks, Natick, USA) scripts were used to extract variables before further analysis (Figure 3.5).

Overall, 90 variables were used for analysis. Not all are reported individually here, however they are available in the appendix (Figure 7.1, Figure 7.2). First, the swing phase

was determined by the toe marker leaving the z-plane of the treadmill, the stance phase began after the toe marker returned to the treadmill. Other variables were calculated using this definition for swing and stance. One variable compared here is swing height, which was defined as mean toe marker height (z value) during the swing phase. Stride length was calculated as the y value of the marker at end of the swing phase minus the y value at the beginning of the swing phase.

Toes drag does not normally occur in uninjured rats, however SCI animals frequently display this behaviour (Chen et al., 2017, Maier et al., 2009). Toe drag was defined as the percentage of the swing phase during which the toe marker was less than 1 mm above the treadmill level. Consistency scores were also calculated for each individual point using methods described in Chen et al. (2017). These scores measure how repeatable each step is compared to the last and is calculated by resampling the x, y and z positions of the marker. The higher the score the more consistent a step was in the combined xyz positions (Fong et al., 2005). M score is an average of the individual toe, ankle, knee, hip and iliac crest consistency scores.

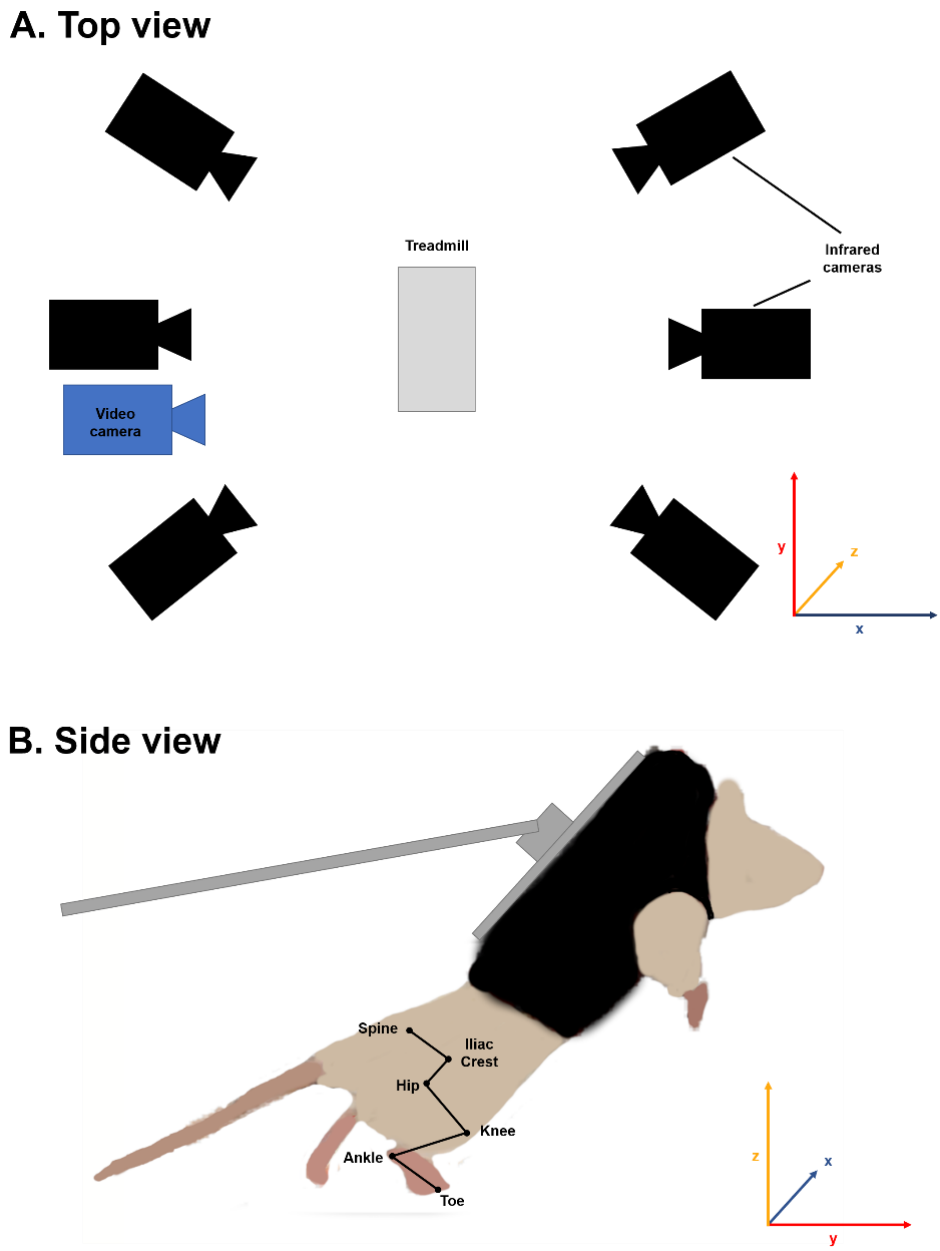

Figure 3.4 Kinematic recordings

Kinematics were recorded with 6 infrared one video camera (A). Reflective markers were placed on the toe, ankle, knee, hip, iliac crest, and the middle of the spine (B). Recordings were made of ten consecutive steps at 14 cm/s. Animals were unstimulated but were given body weight support.

As mentioned earlier, 90 different kinematic variables were computed. Principal component analysis (PCA) was undertaken in order to reduce these multiple dimensions (Figure 3.5). There can be no missing data when doing PCA with R (R Core Team, 2020), therefore data had to be imputed for the few missing variables. Missing variables were rare,

however, left right couplings and coupling variation were missing for a few animals. The 'R' package 'mice' along with the package 'dplyr' were used for imputation (van Buuren and Groothuis-Oudshoorn, 2011, Hadley et al., 2020) (see appendix). Multivariate imputation by chained equations (mice) uses the surrounding variables to predict the values for missing data, while the package 'dplyr' is a grammar system for general data manipulation. For PCA the package 'ggbiplot' was used (Vu, 2011). SPSS was used to visualize factor loading, by determining the correlation between variables and the individual principal components. Animals individual principal component scores were extracted and group and subgroup means were then graphed (Figure 3.5).

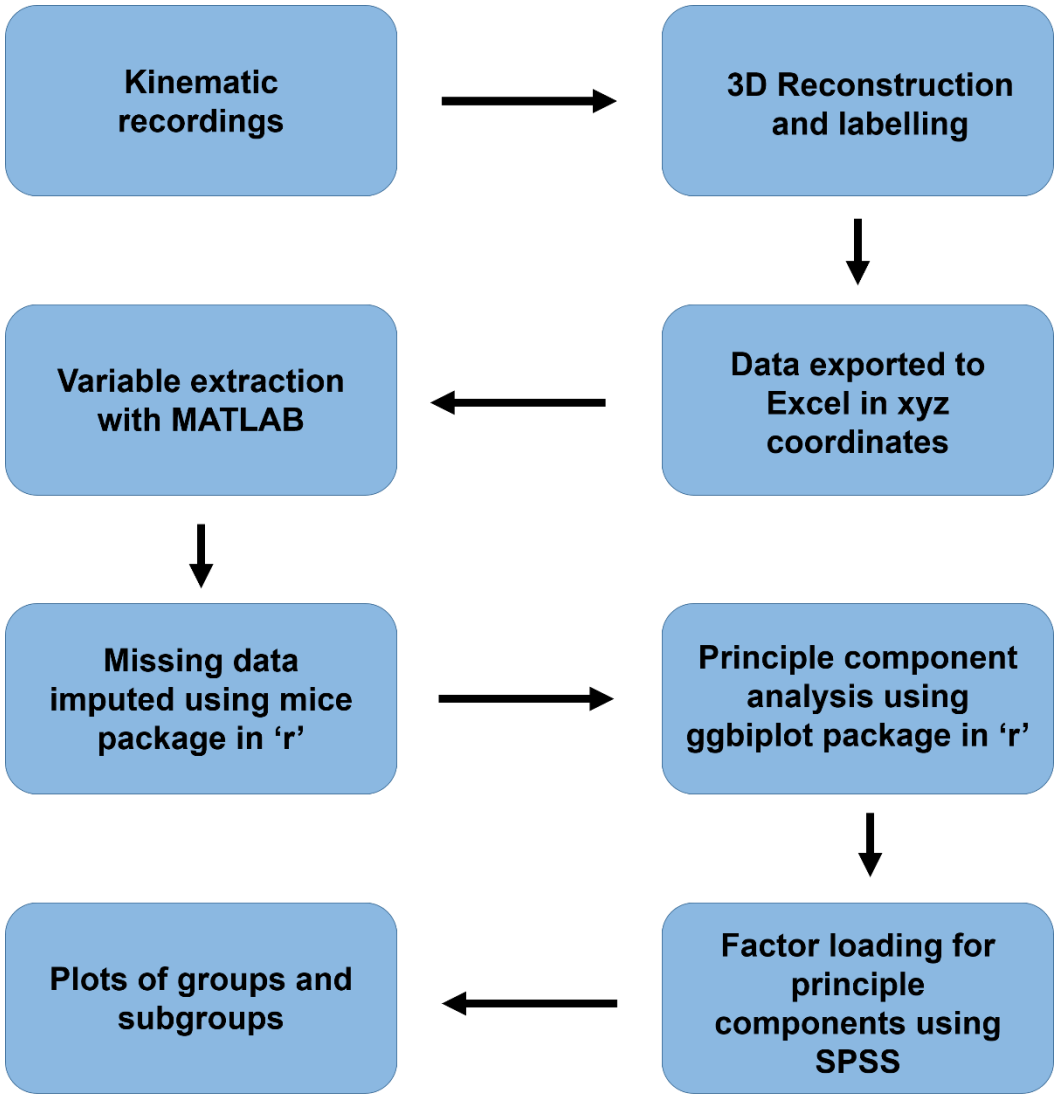

Figure 3.5 Workflow for kinematic data analysis

3.4.6 BDA tracing

After kinematic recording tracer injections into the sensorimotor cortex were completed using biotinylated dextran amine (10,000 MW; Invitrogen, Carlsbad, USA). Animals were anaesthetised as before with inhalable isoflurane. Headplugs were removed and a small piece (3 mm by 3 mm) of skull was removed (~1-4 mm lateral and ~0.5-3.5 mm posterior to bregma). ~400 nl of 10% BDA in 10 millimolar PBS was injected into nine sites as shown in Figure 3.6. All injections were 1.3 mm deep and were spaced so as to cover the hindlimb CST projection neurons in layer V (Paxinos and Watson, 2006). Pulled glass pipettes (1.5 mm outer diameter, 0.84 mm inner diameter, 1B150-4. WPI, Sarasota, USA.) were back filled using Hamilton needles and injections were completed by air pressure using the Pneumatic PicoPump (SYS-PV830, WPI, Sarasota, USA). After 400 nl was injected pipettes were left for two minutes before withdrawal from the cortex.

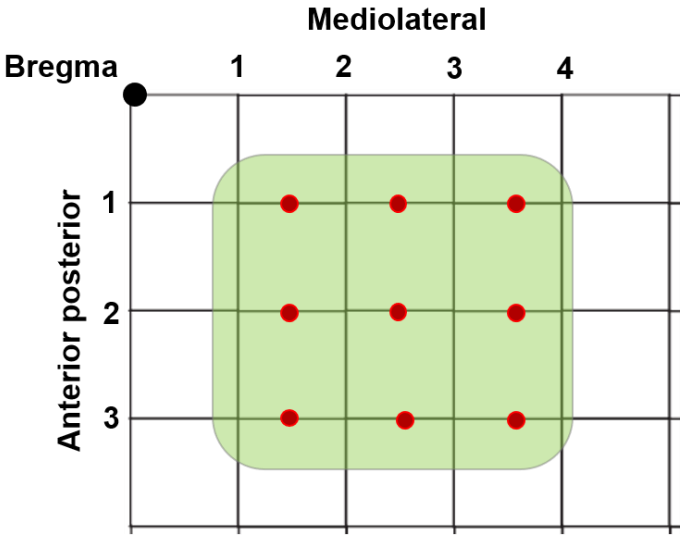

Figure 3.6 BDA tracing sites
A total of 3.6 µl of 10% BDA was injected into nine sites of the right sensorimotor cortex. The 400 nl injections were made at a depth of 1.3 mm from the surface of the dura. Shaded green shows removed skull portion.

3.4.7 Electrophysiology

Electrophysiological investigations were not completed by me. Therefore, what follows is a brief description of only one portion of this study, for which results are mentioned later. These studies were terminal and were performed under a ketamine (200

mg/kg) and xylazine (80mg/ml) injectable anaesthetic by way of a jugular vein catheter. H-reflex recordings were made from the intrinsic foot muscles in response to medial plantar nerve stimulation. The maximum H and maximum M wave response were recorded, and these are the data referred to in section **Error! Reference source not found.**. In addition t o this, paired pulse depression, and H-reflex response to cortical stimulation was also recorded. However these data are not included in this thesis.

3.4.8 Immunohistochemistry

Perfusions, tissue preparation and storage were completed as per the general methods (Chapter 2). The primary and secondary antibodies used are presented in Table 3.1.

Table 3.1 Antibodies and concentrations

Primary antibodies

Name	Target	Host	Dilution	Supplier
Anti-ChAT	Choline acetyltransferase	Goat	1:500	Millipore
Anti-NeuN	Neuron specific nuclear protein	Mouse	1:500	Millipore
Anti-VGLUT1	Vesicular glutamate transporter 1	Guinea pig	1:15,000	Millipore
Anti-TH	Tyrosine hydroxylase	Mouse	1:100	Millipore
Anti-5-HT	5-hydroxytriptamine	Rabbit	1:15,000	Immunostar
Anti-GAD65	Glutamic acid decarboxylase 65 kDa	Mouse	1:10,000	Invitrogen

Secondary antibodies

Target	Fluorophore	Host	Dilution	Supplier
Goat	488	Donkey	1:500	Invitrogen
Mouse	488	Donkey	1:500	Invitrogen
Rabbit	555	Donkey	1:500	Invitrogen
Goat	555	Donkey	1:500	Invitrogen
Mouse	555	Donkey	1:500	Invitrogen
Guinea pig	555	Donkey	1:500	Invitrogen
Rabbit	647	Donkey	1:250	Invitrogen
Mouse	647	Donkey	1:250	Invitrogen

3.4.8.1 Double VGluT1 ChAT staining

Three replicate sections of L4 lumbar spinal cord were analysed for each animal. Sections were incubated in ChAT for 48 hours and VGluT1 for 24 hours in phosphate buffered saline 0.2% triton x-100 (T8787-100ML, Sigma) and 3% normal donkey serum (NDS) (D9663-10ML, Sigma). The secondary antibodies used were donkey anti-Goat-555 and donkey anti-guinea pig-488. After mounting, slides were imaged at 20x with a confocal microscope (LSM 880, Zeiss) using Zen 3.2 tile scan function. Settings were kept the same for all imaging completed for each experiment. VGluT1 integrated density was calculated in three regions of interest using ImageJ. The three regions of interest were two 300 µm square regions of the lateral ventral horn (VH) and intermediate zone (IMZ), and one 100 µm by 400 µm region of the dorsal horn (DH) (Figure 3.17). Integrated density measurements were normalised to the mean of the IMZ of CGCT IgG animals. VGluT1 boutons in close apposition to MNs and their proximal dendrites were counted manually. Counts were normalised to 100 µm of cell perimeter and only boutons in close apposition to large (>100 µm circumference) ChAT positive ventral horn neurons with a visible nucleus were measured. This is because smaller γ-MNs do not receive direct Ia proprioceptive input.

3.4.8.2 Double 5-HT/ChAT and TH/ChAT staining

Three replicate sections of L4 were used for the 5-HT analysis. The protocol was similar to that above, with 48 hour anti-ChAT and then 24 hour anti-5-HT with the same buffer. In this case an anti-goat-488 and an anti-rabbit-555 secondary were used. After mounting, slides were imaged at 20x with a confocal microscope (LSM 700, Zeiss) using the same Zen 3.2 tile scan function. Integrated density was calculated for the entire grey matter of the ventral horn and date were normalised to the CGCT IgG group mean. Axons were quantified after thresholding with imageJ and were included for integrated density analysis if they were larger than 0.5 µm in total area. 5-HT fibres in close apposition to MNs and their proximal dendrites were counted manually and normalised to 100 µm cell perimeter.

Tyrosine hydroxylase staining was completed as above, but with TH instead of 5-HT primary antibody, and with anti-mouse-555 instead of anti-rabbit-555 secondary. Imaging and analysis were the same for integrated density measurements, with all data normalised to the mean CGCT IgG group mean. Axons were quantified after thresholding with imageJ and were included for integrated density analysis if they were larger than 0.5 µm in total area. The sparsity of fibres precluded an analysis of TH innervation of MNs as the vast majority of MNs had no TH in close apposition to either the soma or proximal dendrites.

3.4.9 3D reconstruction of p boutons

The immunohistochemistry protocol was similar to those above and the general methods (chapter 2). Briefly, three replicate sections of L5 were used for analysis. Sections were incubated 48 hours in ChAT, and 24 hours in VGluT1 and GAD65. Antibodies were diluted in phosphate buffered saline with no triton or blocking serum. After mounting, slides were imaged with a confocal microscope (inverted LSM 880, Zeiss) at 63x with oil immersion. MNs were imaged using Z-stacks with .5 µm steps and 2 times averaging. At least ten lateral ventral horn MNs per animal were imaged and subsequently analysed with IMARIS after 3D reconstruction.

3.4.10 Statistical analysis

For BBB improvement week over week a repeated measures analysis of variance (ANOVA) was used (Greenhouse-Geisser corrected for lack of sphericity). Data were tested for normality using a Shapiro-Wilk test. If data were not normally distributed (Pbouton off, Pbouton 3+, TH expression) a non-parametric Kruskall-Wallis test was used. For normally distributed kinematic, VGluT1, and 5-HT data a one-way ANOVA was used followed by a LSD *post hoc* test. A pearsons correlation was completed to compare principal components with kinematic parameters. All statistical analysis was completed using SPSS 26 (IBM, Chicago, USA).

3.5 Results

3.5.1 Injury and lesion volume

A higher impact force results in less sparing of tissue and worse behavioural outcomes (Scheff et al., 2003). All animals received an impact set to 250 kilodyne. The IH impactor use should reduce variability as there is a force sensor which immediately withdraws the impactor once a specific force is reached. Stereotaxic arms holding the spinal cord level and tight should also minimise variability. Impact force recorded from the device shows the actual impact was 270 kilodyne ±5 SEM. There were no differences between groups ($p = .641$). Animals which were not fully injured, as evidenced by same day lower limb movement after injury, were excluded from the study.

Lesion volumetrics have not been completed yet. Spinal cord tissue is currently in China where it is being analysed. BDA cortical tracing is also taking place at Beihang University Beijing.

3.5.2 BBB

Behavioural testing was completed each week using the Basso Beattie and Bresnahan scoring system (BBB) (Basso et al., 1995). The test is a simple and easy way of monitoring recovery over time. However, the scale is not linear and there is limited scoring discrimination between some very different behaviour. One week after injury all animals had a score of 7 or below, this indicates that none of the animals could produce a sweeping or stepping movement. Those animals that could step or sweep at this stage were excluded from further study and are not included in results.

The BBB score for all groups are shown in Figure 3.7A below. All groups improved from their week one scores ($p < .001$). There was a general trend of improved scores in the CB 11C7 vs the ES 11C7 group ($p = .099$) and between the CB 11C7 and the TR IgG group ($p = .115$). Interestingly 11C7 treatment had no effect in the untrained cage control or in the ES without training group. In fact, there appears to be a negative interaction between non trained ES animals and 11C7. Unfortunately, none of these data reached statistical significance, so any conclusions from these data need to be understood as such.

As mentioned, the BBB scale is not linear and there is limited scoring discrimination between some very different behaviour. Large functional improvements may be masked by the low scoring discrimination of the BBB scoring system. Due to the lack of distinction in raw BBB scores we have also looked to divide the animals based on more clinically relevant cut-off points. Weight supported plantar stepping achieves a score of at least 10 on the BBB scale. We divided our animals into those that averaged ≥10 in the last four weeks or those that did not. The results can be seen in Figure 3.7B. This further analysis did not change results between the 11C7 and IgG cage groups. However, the TR 11C7 groups had more animals averaging weight supported stepping than their TR IgG counterparts ($p = .009$), than the CB IgG group ($p = .045$), and than the ES 11C7 group ($p = .009$). The CB 11C7 groups had more animals averaging weight supported stepping than the TR IgG group ($p = .023$) and the ES 11C7 group ($p = .023$). The negative interaction between untrained ES animals and 11C7 is again seen here with no animals averaging weight supported stepping in this group.

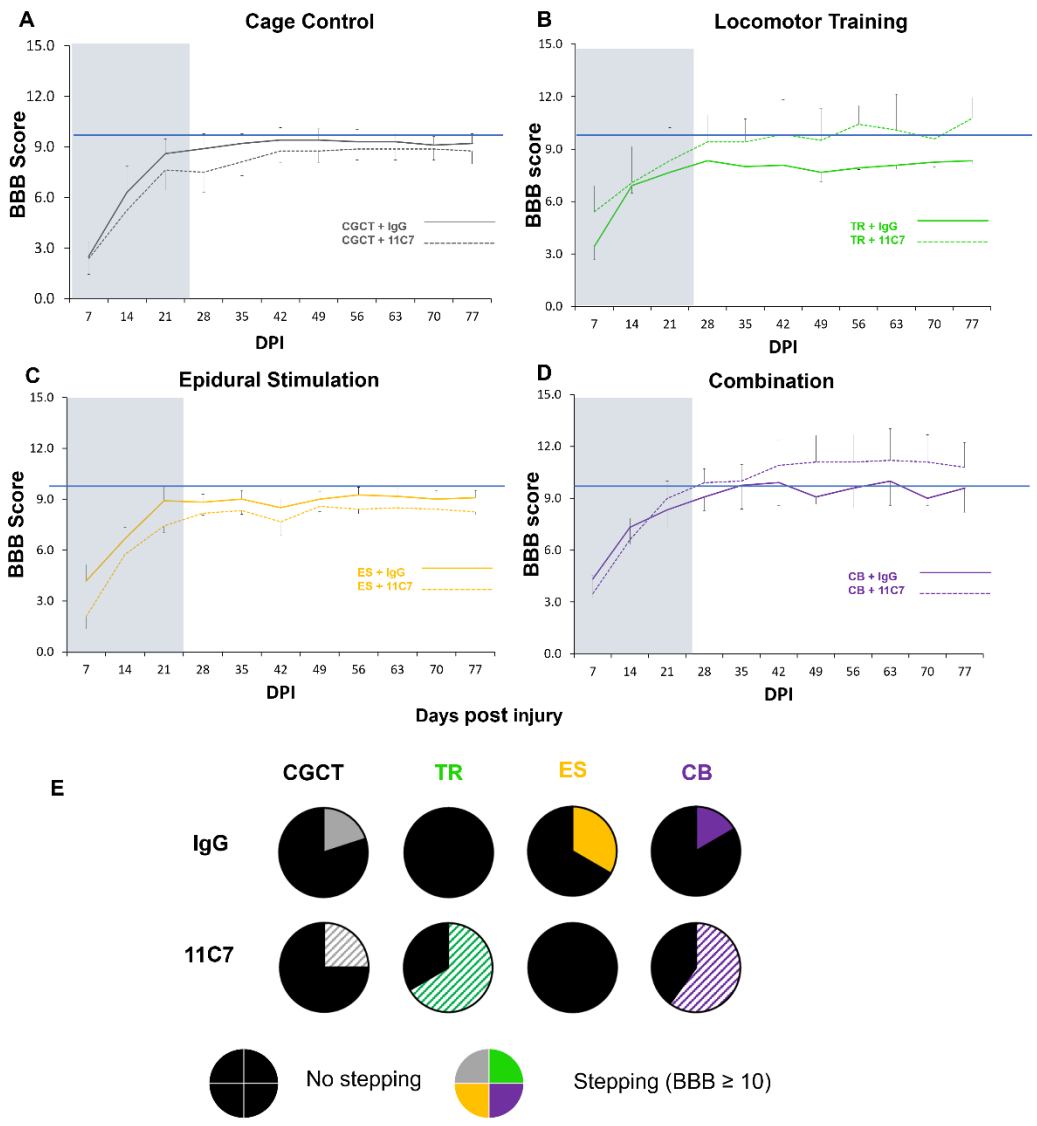

Figure 3.7 BBB score over time

The blue line marks the point at which weight supported stepping occurs, and the shaded area at the beginning indicates that training had not yet started at this point (A-D). There was a general trend of improved score in the CB 11C7 group (D). However, results did not reach statistical significance. More animals in the CB and TR 11C7 group averaged a BBB ≥ 10 in the last four weeks of the intervention (E). CGCT IgG (n=5), CGCT 11C7 (n=4), TR IgG (n=6), TR 11C7 (n=6), ES IgG (n=6), ES 11C7 (n=6),CB IgG (n=6), CB 11C7 (n=5). Error bars ± SEM

3.5.3 Kinematics

3.5.3.1 Independent kinematic variables

Kinematic analysis can expand on the rough picture given by the BBB scores. We have highlighted step height and stride length, as both these variables have been shown to increase after training under ES in SCI rats (Lavrov et al., 2008). In the above study kinematic measurements were taken during ES assisted stepping. However, in our study we investigated stepping in the absence of ES. We have also investigated the percentage of toe dragging during the step cycle. After SCI rats often display toe dragging behaviour (Basso et al., 1995) and toe dragging is reduced following 11C7 treatment (Chen et al., 2017, Maier et al., 2009).

For swing height there were no statistically significant differences between treatment groups or between injured and naïve animals (Figure 3.8A). For stride length the TR 11C7 group had a significantly longer stride than either the ES IgG ($p = .003$) or CB IgG ($p = .05$) groups. The ES IgG group had a shorter stride length than the naïve control ($p = .013$) (Figure 3.8B). Normalised stride length and step height show the clear difference between the longer strides and lower step height of the TR 11C7 group and naïve controls, and the higher step height and concurrent lower stride length of the ES IgG group (Figure 3.8C). All groups bar ES IgG ($p = .051$) and CB 11C7 ($p = .133$) had a higher percentage of toe drag during swing as compared to naïve controls (Figure 3.8D). The CB 11C7 group also had less drag than CGCT 11C7 ($p = .046$).

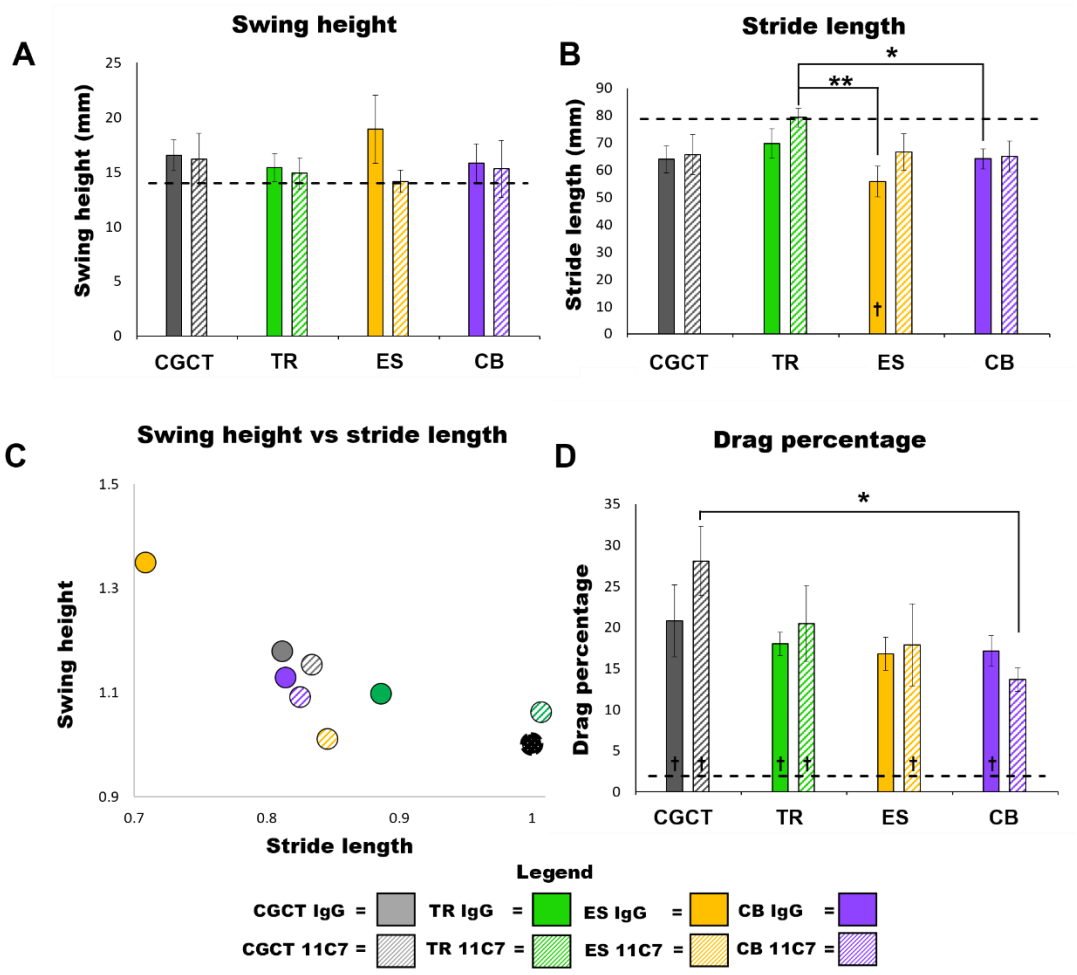

Figure 3.8 Individual kinematic parameters

The key kinematic measures of swing height (A) and stride length (B) were compared between treatment groups and naïve controls. The dashed lines represent naïve animal kinematics (A, B, and D) with † representing significant differences between the experimental groups and naïve controls. For swing height there were no statistically significant differences between groups or between injured and naïve animals (A). The TR 11C7 group had a longer stride length than either the ES IgG or CB IgG group and the ES IgG group had a shorter stride length than the naïve control (B). Normalised stride length and step height show the clear difference between the longer strides and lower step height of the TR 11C7 group and naïve controls, and the higher step height and concurrent lower stride length of the ES IgG group (C). All groups bar ES IgG ($p = .051$) and CB 11C7 ($p = .018$) had a higher percentage of toe drag during swing as compared to naïve controls (D). The CB 11C7 also had less drag than the CGCT 11C7 group. CGCT IgG (n=5), CGCT 11C7 (n=4), TR IgG (n=6), TR 11C7 (n=5), ES IgG (n=6), ES 11C7 (n=6), CB IgG (n=6), CB 11C7 (n=5), Naïve control (n=3). Error bars ± SEM. * $p < .05$. ** $p < .005$.

To test for step consistency all markers were sampled every step and compared to other steps in the cycle. All points were then given a consistency score and these were averaged for a general M score (Figure 3.9). The toe, knee, and crest points are shown in Figure 3.9A-C. The ES 11C7 groups had higher toe ($p = .032$) and knee ($p = .006$) scores than the ES IgG group (Figure 3.9A-C). Indicating that here 11C7 did improve step consistency even if it did not improve weight supported stepping (Figure 3.7E). The ES IgG group also had a significantly worse knee scores than TR11C7 ($p = .006$), CB IgG ($p = .028$), and naïve controls ($p = .018$) (Figure 3.9C). The TR 11C7 group had significantly higher toe scores than CGCT 11C7 ($p = .041$), ES IgG ($p = .003$), and CB IgG ($p = .036$) (Figure 3.9A). In addition to the ES IgG group, the naïve control group also had higher toe scores than CGCT 11C7 ($p = .027$), TR IgG ($p = .047$) and CB IgG (.024) groups (Figure 3.9A). There were no significant differences for crest scores (Figure 3.9C). The ES IgG group had less consistent overall step kinematics than either TR 11C7 ($p = .019$), ES 11C7 ($p = .036$), or the naïve controls ($p = .027$) (Figure 3.9F).

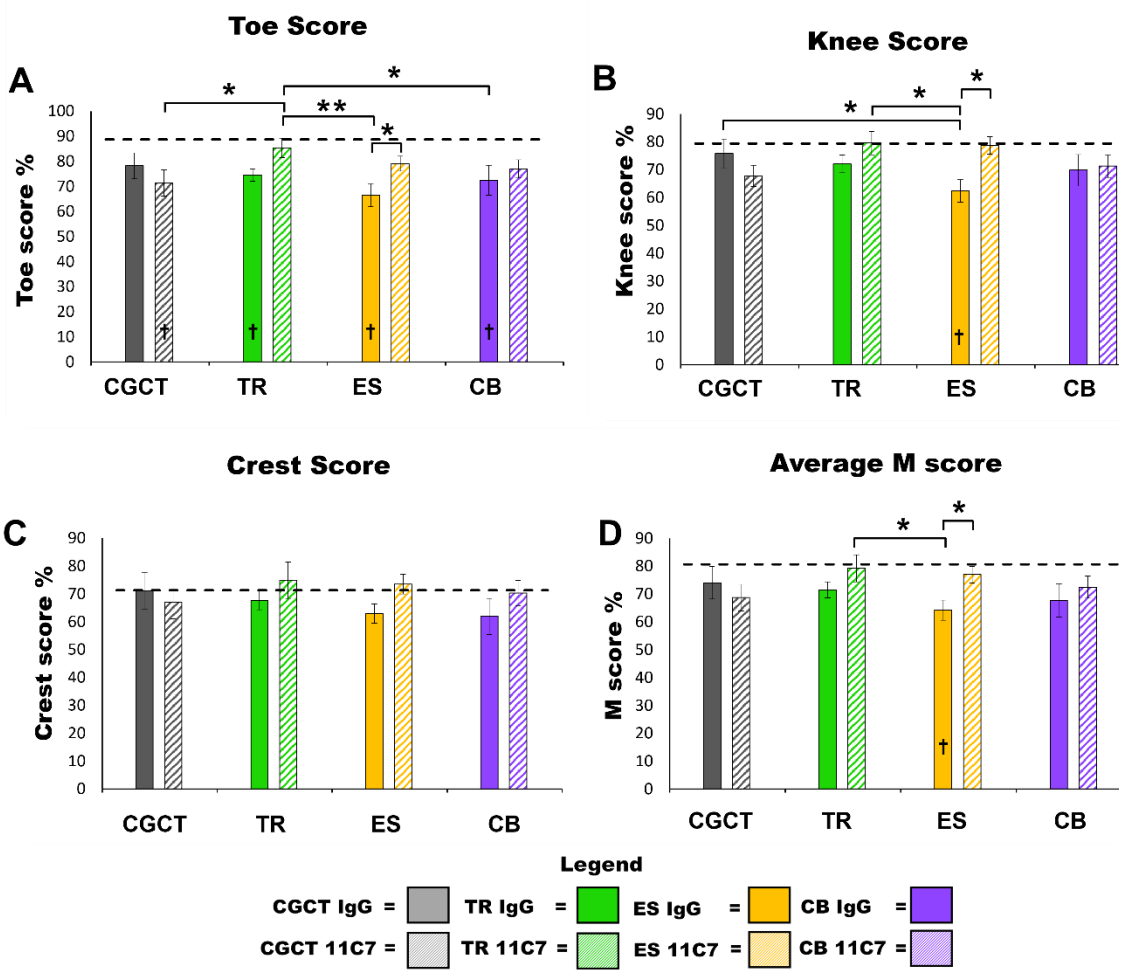

Figure 3.9 Step consistency

Consistency scores for each marker as described in the methods (section 3.4.5 above). The dashed lines represent naïve animal kinematics (A-F) with † representing significant differences between the experimental groups and naïve controls. The ES IgG group had less consistent step kinematics than either TR 11C7 ($p = .019$), ES 11C7 ($p = .036$), or the naïve controls ($p = .027$) (F). CGCT IgG (n=5), CGCT 11C7 (n=4), TR IgG (n=6), TR 11C7 (n=5), ES IgG (n=6), ES 11C7 (n=6), CB IgG (n=6), CB 11C7 (n=5), Naïve control (n=3). Error bars ± SEM. * $p < .05$.

3.5.3.2 Kinematics PCA

PCA was completed to add another level of analysis to the individual gait parameters. The first two principal components (PCs) were chosen for initial analysis as PCs below them accounted for less than 10% of variance each. PC1 and PC2 accounted for 22.1 and 11.8% of variance respectively.

The eigenvectors indicate the weighting and direction each variable provides to the PCA, and the eigenvectors for the first two PCs are shown in Figure 3.10. The length of the arrow indicates how much influence each variable has on the PC. Another way to visualise this is by looking at correlations between individual variables and the PCs. The PC1 correlations are shown in Figure 3.11A along with the percentage of variance explained by the PC (Figure 3.11B). The most correlated factors with PC1 included the standard deviation of many parameters, including variation in gait timing and variation in step height, and length. PC1 was negatively correlated with the step consistency scores for individual joints and the average step consistency. The PC2 correlations are shown in Figure 3.12A along with the percentage of variance explained by the PC (Figure 3.12B). PC2 was correlated with many of the drag related parameters including drag length in mm, drag time in seconds, and drag as a percentage of length and time.

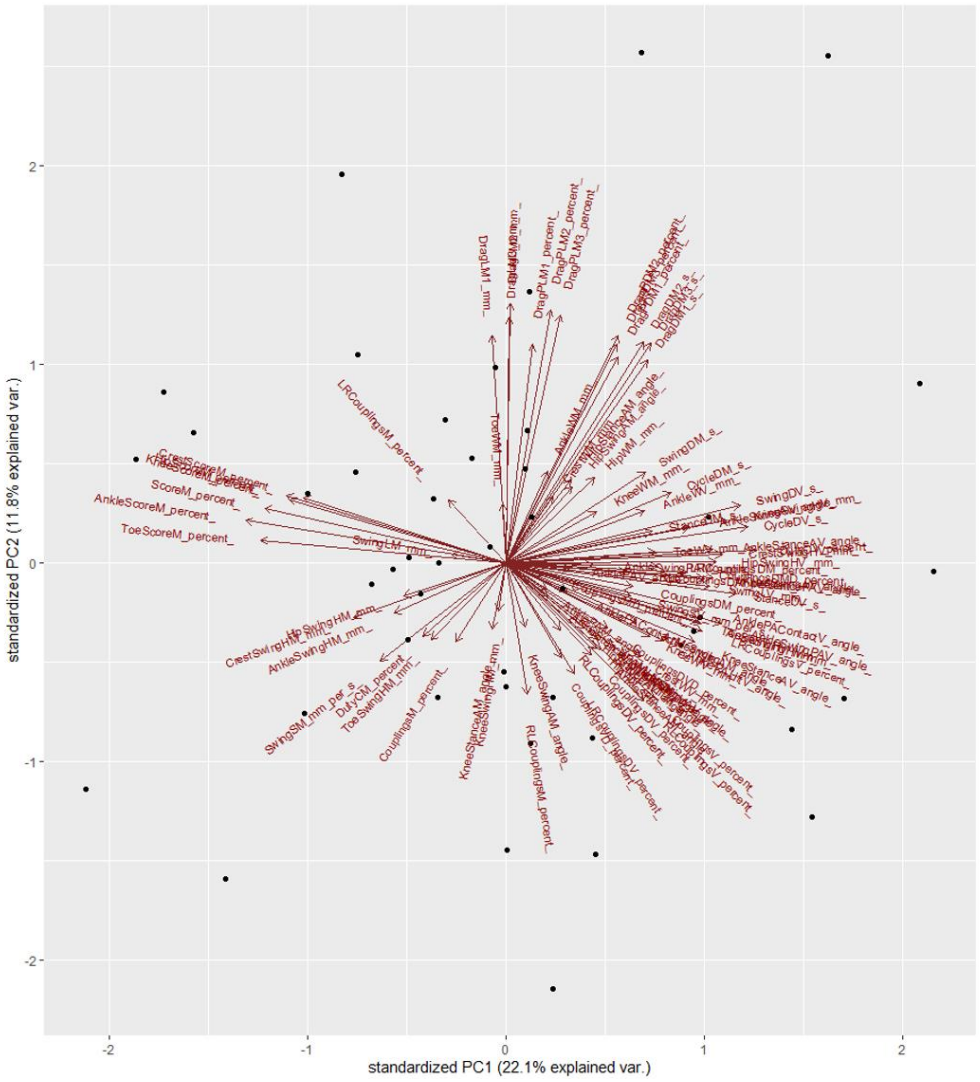

Figure 3.10 PCA 1 and 2 eigenvectors

The eigenvectors for the first two PCs are shown. The length of the arrow indicates how much influence each variable has on the PC. The dots are individual animals.

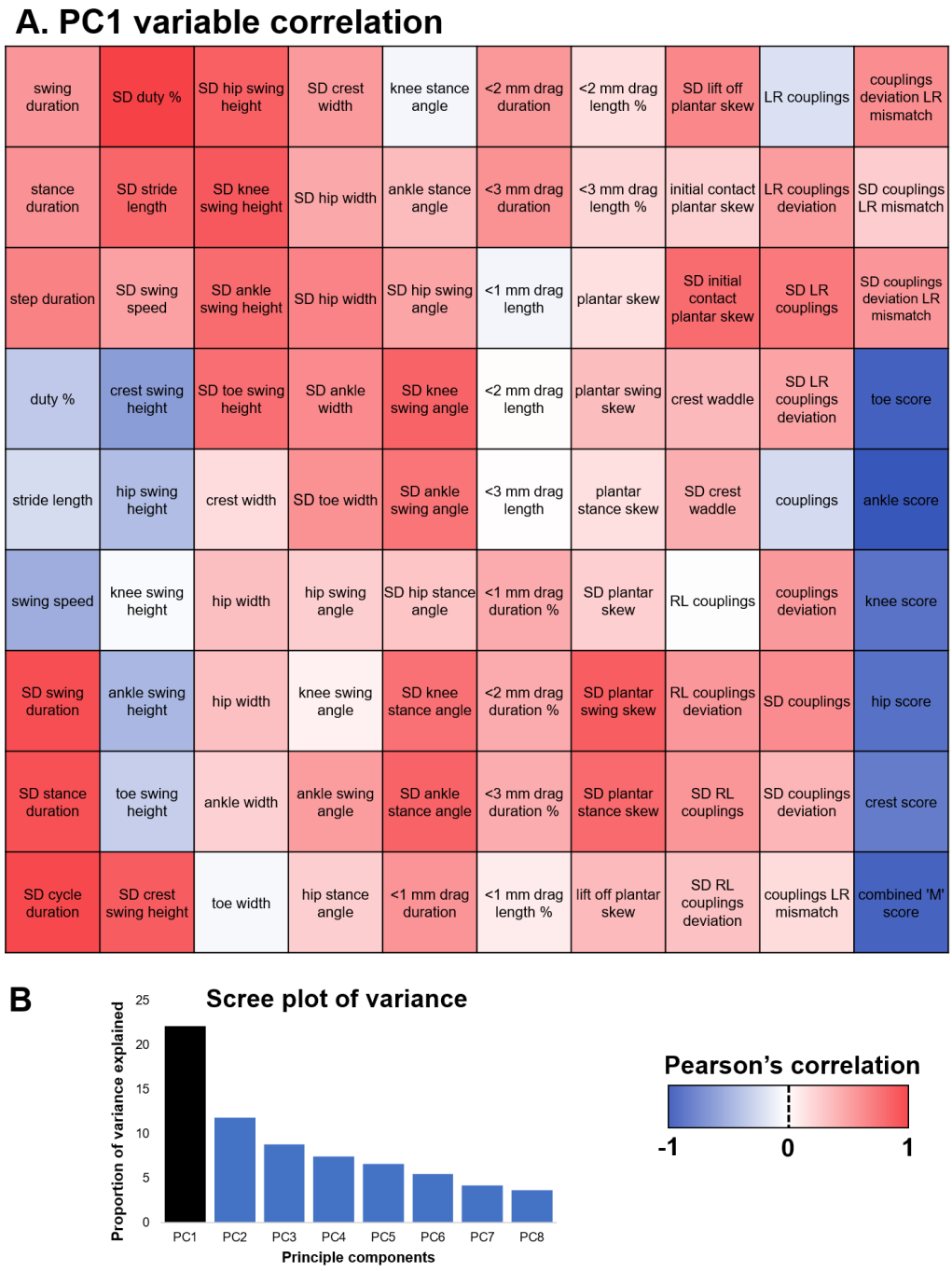

Figure 3.11 PC1 correlations and scree plot

PC1 was positively correlated with many variability related factors and negatively correlated with the step consistency variables (A). The percentage of overall variance explained by this PC was 22.1% (B)

A. PC2 variable correlation

swing duration	SD duty %	SD hip swing height	SD crest width	knee stance angle	<2 mm drag duration	<2 mm drag length %	SD lift off plantar skew	LR couplings	couplings deviation LR mismatch
stance duration	SD stride length	SD knee swing height	SD hip width	ankle stance angle	<3 mm drag duration	<3 mm drag length %	initial contact plantar skew	LR couplings deviation	SD couplings LR mismatch
step duration	SD swing speed	SD ankle swing height	SD hip width	SD hip swing angle	<1 mm drag length	plantar skew	SD initial contact plantar skew	SD LR couplings	sd couplings deviation LR mismatch
duty %	crest swing height	SD toe swing height	SD ankle width	SD knee swing angle	<2 mm drag length	plantar swing skew	crest waddle	SD LR couplings deviation	toe score
stride length	hip swing height	crest width	SD toe width	SD ankle swing angle	<3 mm drag length	plantar stance skew	SD crest waddle	couplings	ankle score
swing speed	knee swing height	hip width	hip swing angle	SD hip stance angle	<1 mm drag duration %	SD plantar skew	RL couplings	couplings deviation	knee score
SD swing duration	ankle swing height	hip width	knee swing angle	SD knee stance angle	<2 mm drag duration %	SD plantar swing skew	RL couplings deviation	SD couplings	hip score
SD stance duration	toe swing height	ankle width	ankle swing angle	SD ankle stance angle	<3 mm drag duration %	SD plantar stance skew	SD RL couplings	SD couplings deviation	crest score
SD cycle duration	SD crest swing height	toe width	hip stance angle	<1 mm drag duration	<1 mm drag length %	lift off plantar skew	SD RL couplings deviation	couplings LR mismatch	combined 'M' score

B

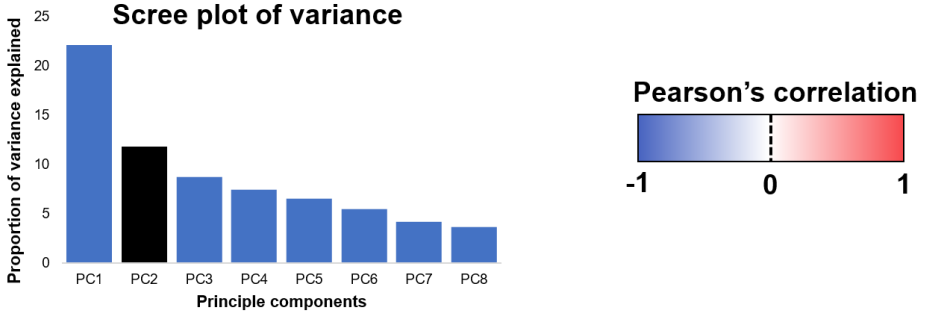

Figure 3.12 PC 2 correlations and scree plot

PC2 was positively correlated with many of the drag related variables, and negatively correlated with some coupling related variables (A). The percentage of overall variance explained by this PC was 11.8% (B).

There were no statistically significant group differences between any of the treatment groups for PC1 and PC2 (Figure 3.13). However, there were differences between naïve controls and treatment groups. For PC1 naïve controls were significantly lower than CGCT IgG, CGCT 11C7, TR IgG, ES IgG, and CB IgG ($p = .042$, .010, .016, .005 and .019 respectively) (Figure 3.13B). This difference did not reach statistical significance for the TR 11C7, ES 11C7, and CB 11C7 groups ($p = .069$, .064, and .056 respectively). For PC2 naïve controls were significantly lower than CGCT 11C7 ($p = .018$) and TR 11C7 ($p = .024$) (Figure 3.13C). The difference did not reach statistical significance for the CGCT IgG, TR IgG, ES IgG, ES 11C7, CB IgG, and CB 11C7 ($p = .076$, .341, .243, .057, .051, and .102 respectively).

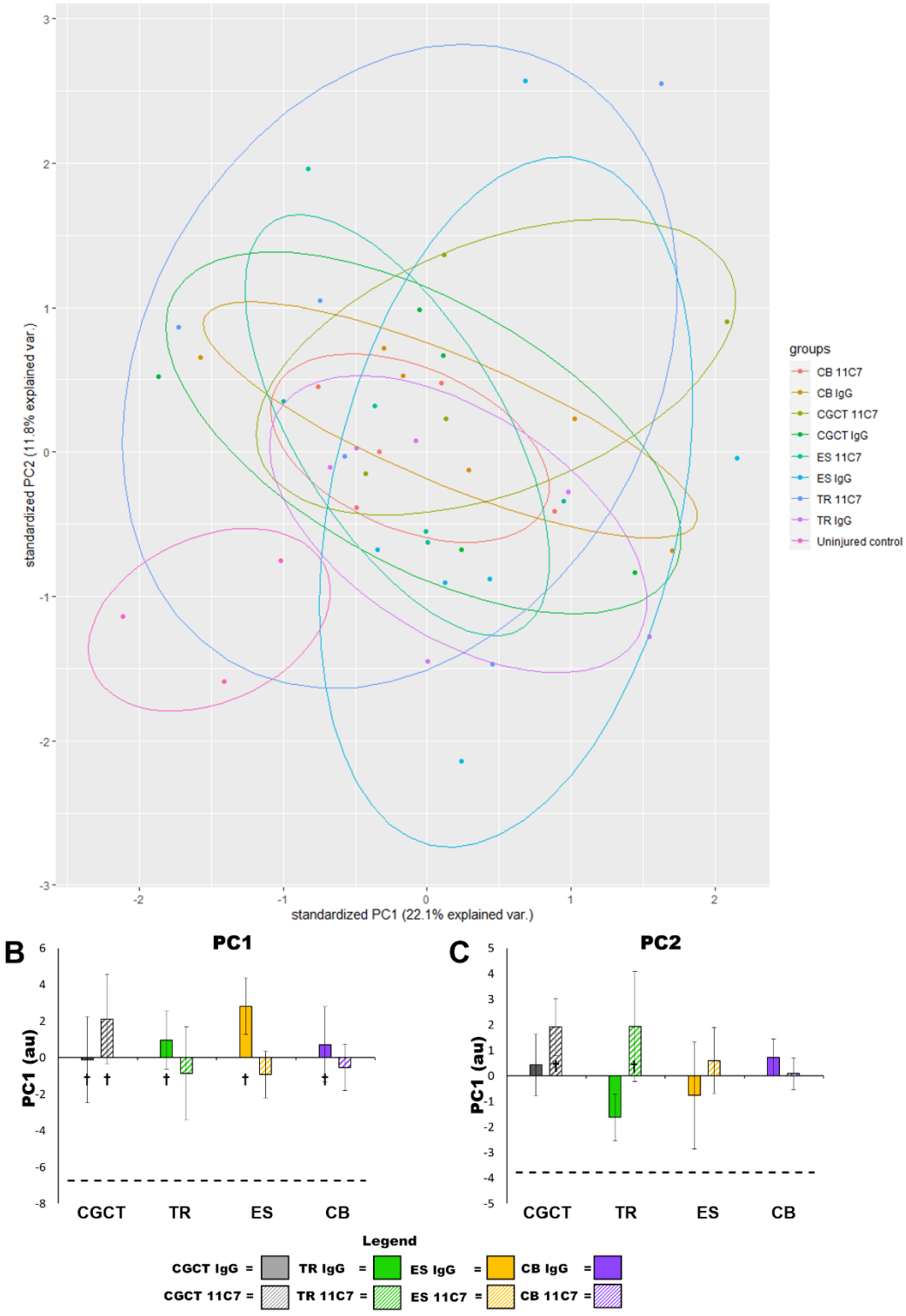

Figure 3.13 Kinematic PC1 and PC2 by group

PC1 (x axis) and PC2 (y axis) showed that groups were largely overlapping (A). Naïve controls are represented by the dashed lines in B and C) with † representing significant differences between the experimental groups and naïve controls. The

naïve controls were statistically significantly lower than all IgG groups and the CGCT 11C7 group in PC1 (B). However, the naïve control group was not statistically significantly different than the TR 11C7, ES 11C7, or CB 11C7 groups. For PC2, only the CGCT 11C7 and TR 11C7 were statistically significantly different from the naïve controls (C). CGCT IgG (n=5), CGCT 11C7 (n=4), TR IgG (n=6), TR 11C7 (n=5), ES IgG (n=6), ES 11C7 (n=6), CB IgG (n=6), CB 11C7 (n=5), Naïve control (n=3). Error bars ± SEM. * p <.05.

Subgroup analysis of different treatments showed that there were no statistically significant differences between animals given IgG or 11C7 (Figure 3.14). However, both IgG (p = .010) and 11C7 (p = .037) treated animals were higher on PC1 than naïve controls (Figure 3.14B). For PC2, the IgG treated animals were not statistically significantly higher than naïve controls (p = .083), whereas 11C7 treated animals were (p = .014) (Figure 3.14C). Subgroup analysis of different treatments showed that there were no statistically significant differences between animals given treadmill training or untrained (Figure 3.15). For PC1, both trained (p = .010) and untrained (p = .005) animals were statistically significantly different from naïve controls (Figure 3.15B). For PC2, both trained (p = .046) and untrained (p = .042) animals were significantly higher than naïve controls (Figure 3.15C). Subgroup analysis of different treatments showed that there were no statistically significant differences between animals given ES or unstimulated animals (Figure 3.16). Both animals receiving epidural stimulation (p = .007) and those with no stimulation (p = .008) were significantly higher than naïve controls in PC1 (Figure 3.16B). For PC2, there was a statistically significant difference between naïve controls and non-stimulated animals (p = .035), but this did not reach statistical significance for those receiving epidural stimulation (p = .053) (Figure 3.16C).

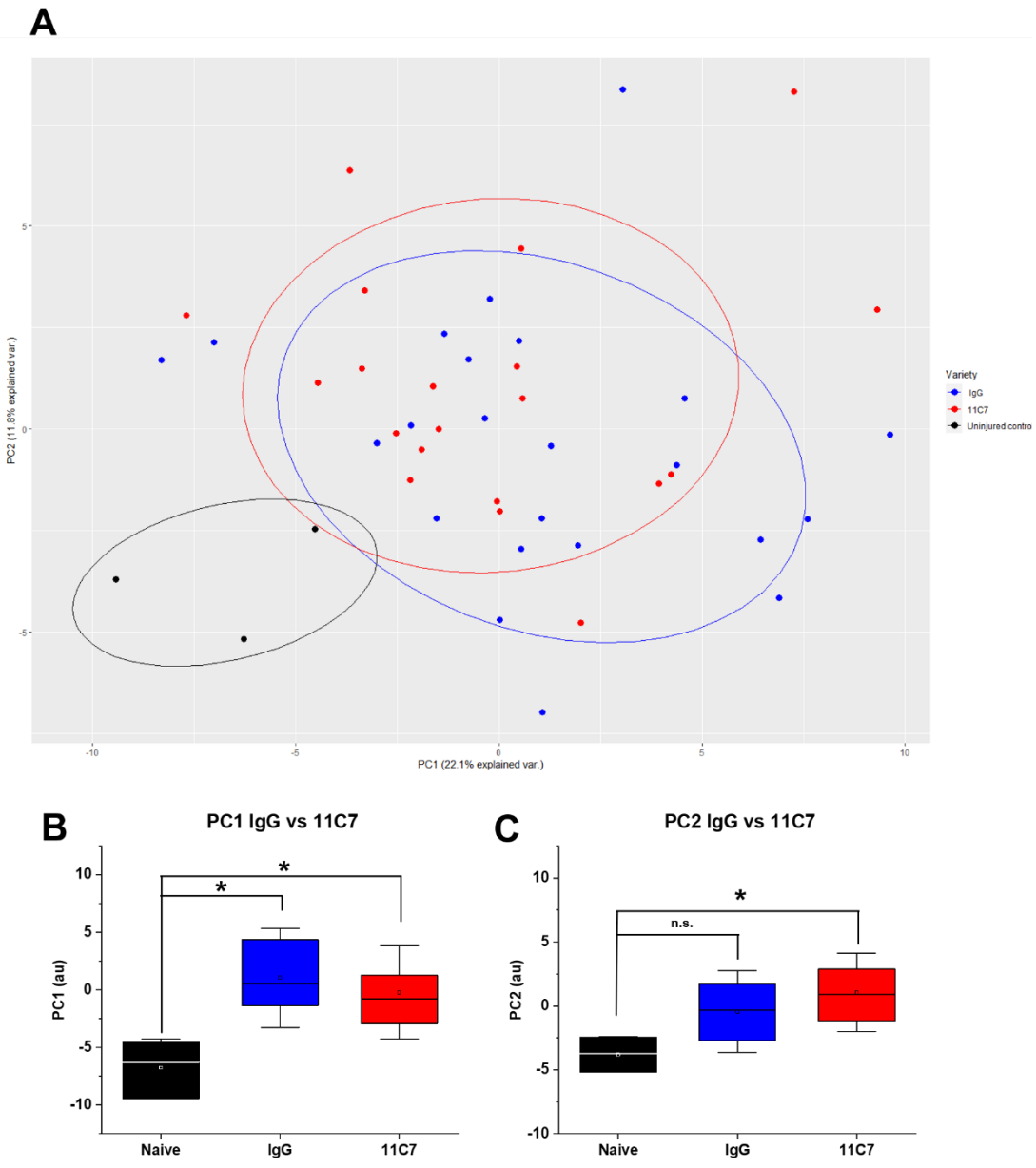

Figure 3.14 PC1 and PC2 by 11C7 vs IgG

PC1 and PC2 analysis showed that there were no statistically significant differences between subgroups (A-C). However there was a significant difference between naïve controls and injured animals. For PC1, both groups were statistically significantly higher than naïve controls (B). While for PC2, the IgG group was not significantly higher than naïve controls (C). IgG (n=23), 11C7 (n=20), naïve control (n=3). Error bars ± SD. * $p < .05$

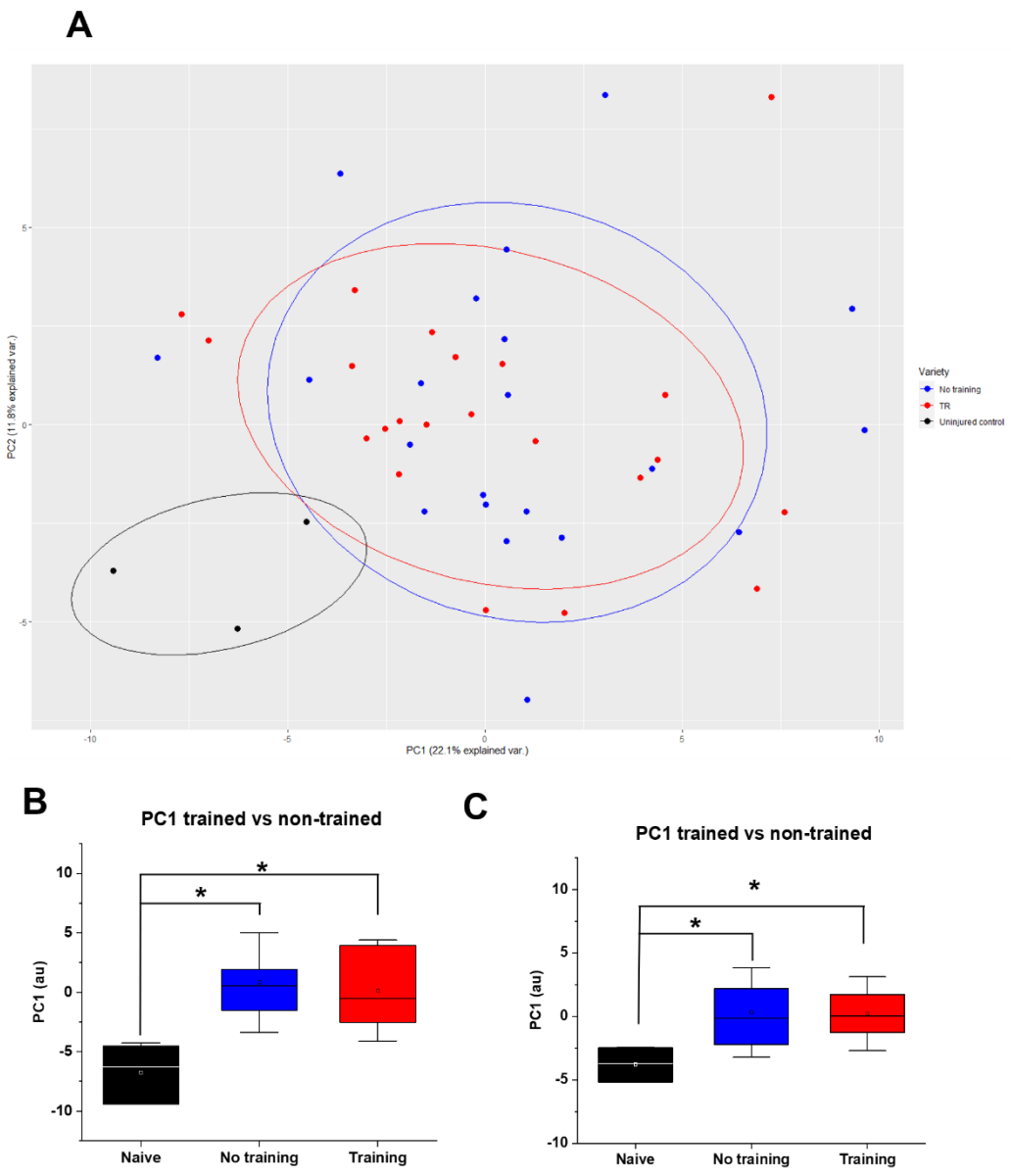

Figure 3.15 PC1 and PC2 trained vs non-trained

PC1 and PC2 analysis showed that there were no statistically significant differences between trained and non-trained animals (A-C). However, there was a significant difference between naïve controls and injured animals in both PCs. For PC1 and PC2 both groups were statistically significantly higher than naïve controls (B-C). Non trained (n=21), trained (n=22), naïve control (n=3). Error bars ± SD. * p <.05

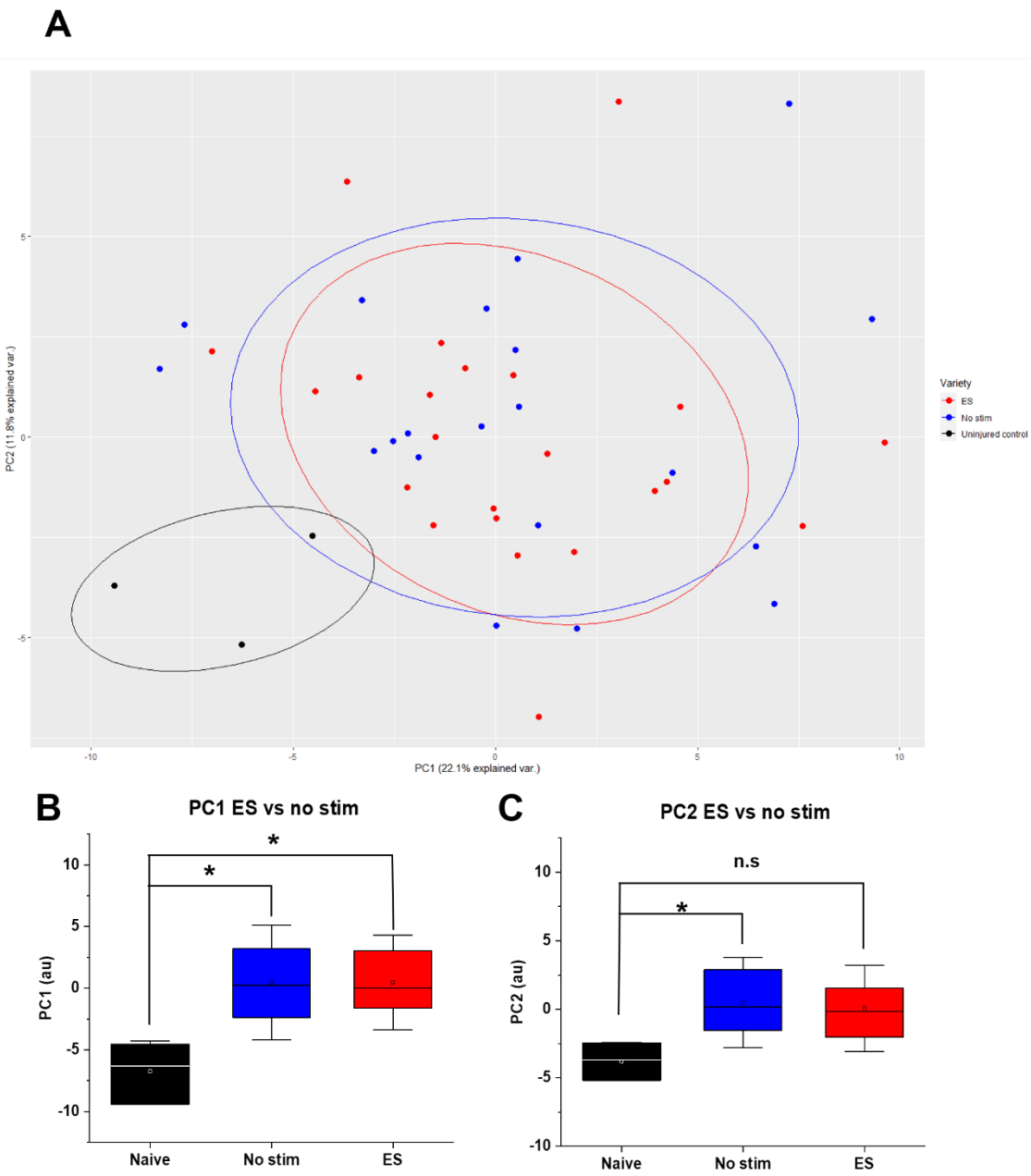

Figure 3.16 PC1 and PC2 ES vs unstimulated

PC1 and PC2 analysis showed that there were no statistically significant differences between animals receiving epidural stimulation and those without (A-C). However, there was a significant difference between naïve controls and injured animals of either group. For PC1, both animals given ES and those unstimulated were statistically significantly higher than naïve controls (B). For PC2 animals receiving ES were not statistically significantly different than naïve controls (C). No stimulation (n=20), epidural stimulation (n=23), naïve control (n=3). Error bars ± SD. * p <.05

3.5.4 Sensory input in lumbar spinal cord

Vglut1 is a marker for synaptic input from proprioceptive afferents. VGluT1 is also present in the descending CST. However, with the severity of our injury there is very limited amount of descending input remaining. Thus it can be inferred that the vast majority of VGluT1 immunoreactivity is due to sensory input from muscles.

We have analysed three areas within the spinal cord. The dorsal horn around laminae II-III, the intermediate zone around Laminae IV-VI, and the lateral ventral horn Lamina IX/Lamina VII (Figure 3.17A). Integrated density of these discreet areas was measured using ImageJ and normalised to the intermediate zone of the CGCT IgG group. The dorsal horn (Figure 3.17B) had the most variability between animals with no clear pattern in dorsal horn VGluT1 immunostaining. The large variability here precludes comment on possible trends. The intermediate zone (Figure 3.17C) data were also highly variable. However, there is a trend with the TR 11C7 group expressing higher amounts of VGluT1 than the TR IgG, CB IgG, and CB 11C7 groups ($p = .089$, .058, and .057 respectively). There were no statistically significant differences in ventral horn VGluT1 density (Figure 3.17D). Examples of ventral horn VGluT1 can be seen in Figure 3.17E.

To summarise, it appears there is little to no inter-group differences in proprioceptive innervation to Laminae II and III. There is a trend for increased innervation in the IMZ of the TR 11C7 group. VGluT1 innervation in the medial ventral horn Lamina IX has been shown to increase following 11C7 treatment with training (Chen et al., 2017). However, there were no statistically significant changes in ventral horn VGluT1 in any of our treatment groups

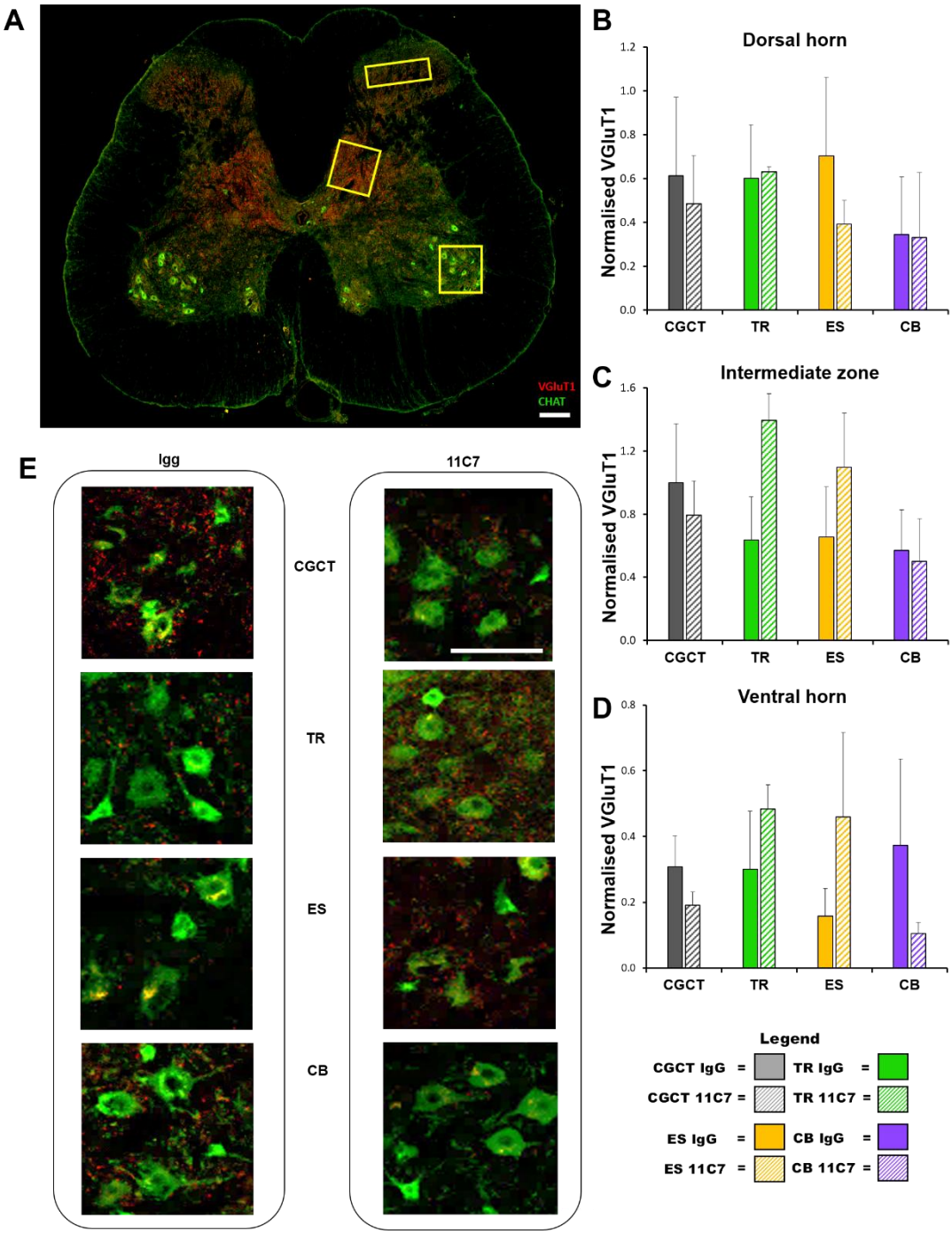

Figure 3.17 Sensory input in lumbar spinal cord

Proprioceptive input as measured by VGluT1 integrated density. All data are normalized to the intermediate zone of the cage control IgG. Three discreet areas were analysed, (A). The dorsal horn (B) had the most variability with no clear pattern in VGluT1 differences. The intermediate zone data were also highly variable (C). However, there is a trend for increased density in TR 11C7 group. The ventral horn VGluT1 differences were not statistically significant (D). Representative samples shown in E. CGCT IgG (n=3), CGCT 11C7 (n=4), TR

IgG (n=5), TR 11C7 (n=3), ES IgG (n=4), ES 11C7 (n=4), CB IgG (n=6), CB 11C7 (n=4). Red = VGluT1, green = ChAT. Scale bar in A = 200 μm, in E =100 μm. Error bars ±SEM

Also quantified were VGluT1 inputs to individual α-MNs at L5. Contacts in close apposition to the cell body and proximal dendrites of large (>100 μm perimeter) Chat+ MNs were counted. Data were reported as boutons per 100 μm cell perimeter. Post hoc analysis revealed a few differences between groups (Figure 3.18 A). Notably, there was a reduced number of VGluT1 boutons in the CB 11C7 group as compared to the CGCT IgG ($p = .023$) and the TR 11C7 ($p = .032$) groups. These results are broadly similar to those in Figure 3.17 D for VGluT1 density in the ventral horn. The results are also very similar to the H-reflex experiments (Figure 3.18A). Where the ratio between Hmax and Mmax aligns closely with numbers of VGluT1 boutons on MNs (Figure 3.18C).

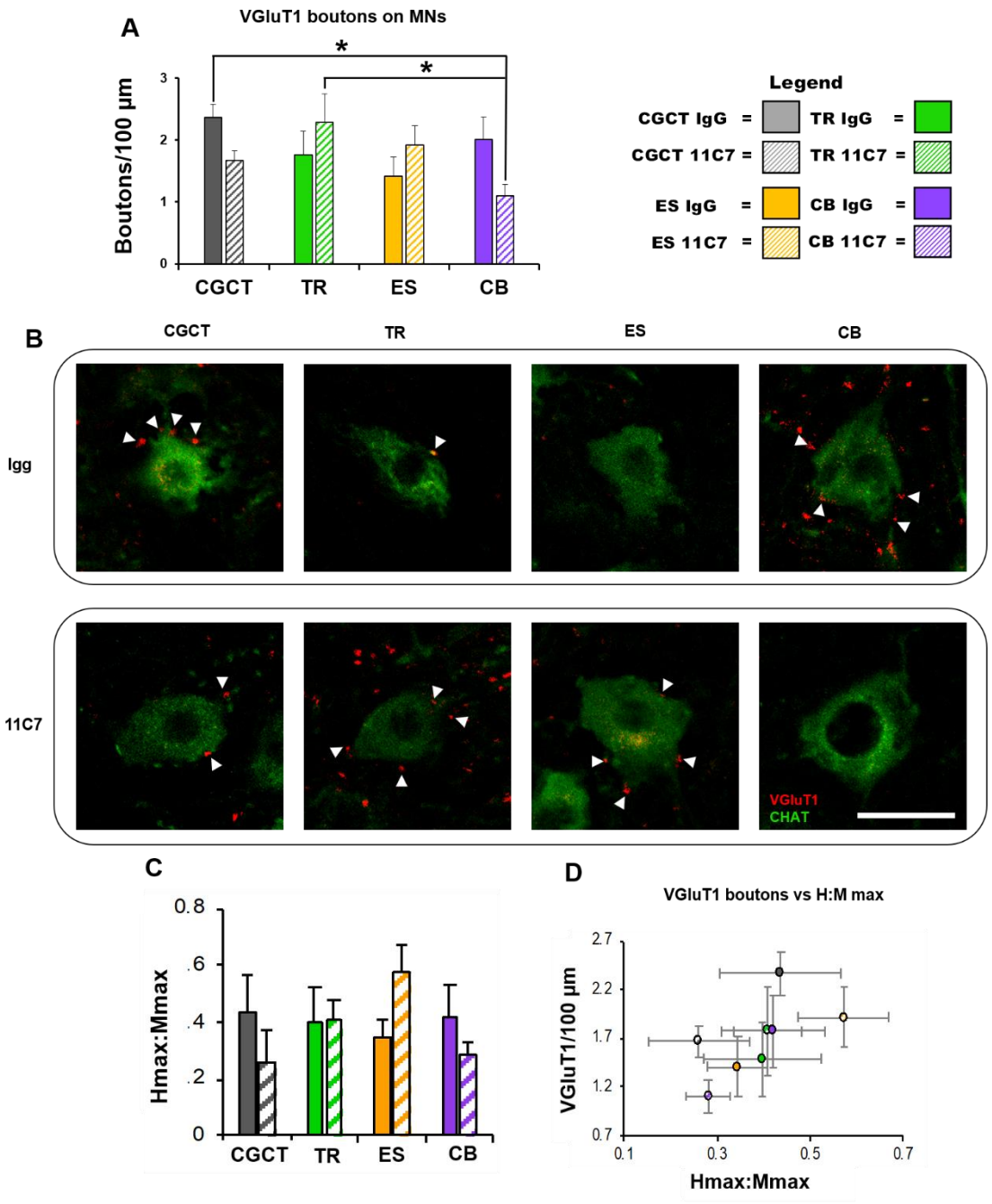

Figure 3.18 VGluT1 boutons on MNs

Boutons were counted on large (>100 µm perimeter) Chat+ MNs and on their proximal dendrites. There were less contacts in the CB 11C7 group compared to the TR 11C7 or CGCT IgG groups (A, B). This closely matched Hmax:Mmax ratios (C). And the group results were correlated (D). CGCT IgG (n=3), CGCT 11C7 (n=4), TR IgG (n=5), TR 11C7 (n=4), ES IgG (n=4), ES 11C7 (n=4), CB IgG (n=6), CB 11C7 (n=5). Scale bar = 50 µm. Error bars ±SEM. * p <.05

3.5.5 Presynaptic inhibition

Gad65 boutons on VGluT1 contacts in close apposition to large Chat+ α-MNs in the lateral motor pool of the ventral horn at the L5 level of the spinal cord. Images were taken with confocal Z stack (Figure 3.19A) and converted into 3D with IMARIS (Figure 3.19B). P boutons (in blue Figure 3.19A-C) in close apposition to VGluT1 sensory afferents (in red Figure 3.19A-C) close to MNs (in green Figure 3.19A-C) were counted. VGluT1 boutons in close apposition to MNs showed no size differences across groups (Figure 3.19D). P boutons per 10 μm^2 of VGluT1 surface were not significantly different across groups (Figure 3.19E) and neither were VGluT1 boutons with no P boutons (Figure 3.19F). There were more VGluT1 boutons with 3+ clusters of P boutons in the CB 11C7 group as compared to the CB IgG, ES IgG, TR IgG, and TR 11C7 ($p = .014, .003, .019$ and $.017$ respectively) (Figure 3.19G). The ES 11C7 group also had more afferent boutons with 3+ clusters of P boutons than the ES IgG group ($p = .019$). These data were not normally distributed, thus a Kruskal-Wallis with pairwise comparison was used to compare between groups.

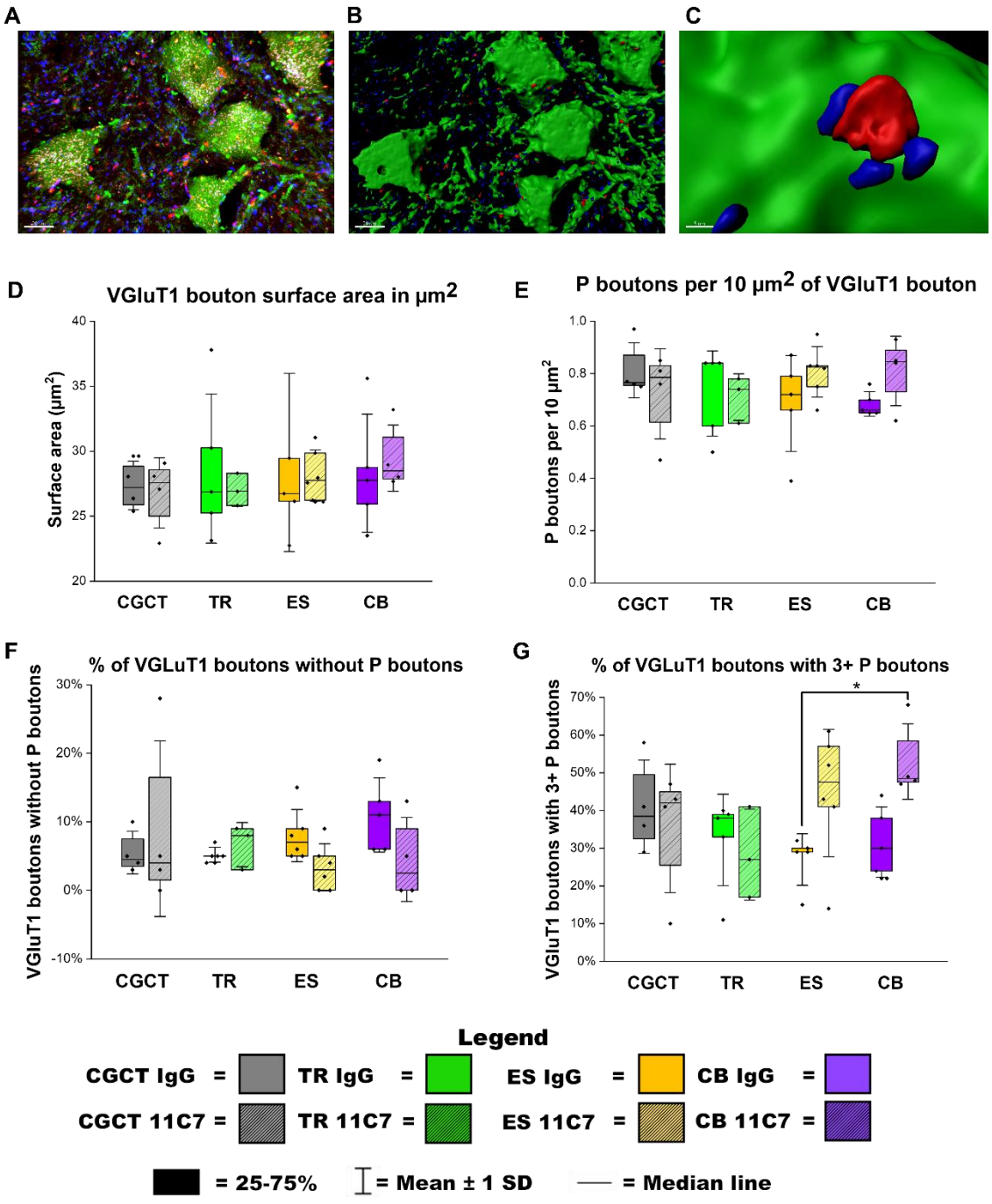

Figure 3.19 Pre-synaptic inhibition on MN contacting VGluT1 boutons

Images were taken with confocal Z stack (A) and converted into 3D with IMARIS (B). P boutons (in blue A-C) in close apposition to VGluT1 sensory afferents (in red A-C) close to MNs (in green A-C) were counted. VGluT1 boutons in close apposition to MNs showed no size differences across groups (D). P boutons per 10 µm^2 of VGluT1 surface and VGluT1 boutons with no P boutons were not statistically significantly different across groups. There were more VGluT1

boutons with 3+ clusters of P boutons in the CB 11C7 group as compared to the CB IgG, ES IgG, TR IgG, and TR 11C7. The ES 11C7 group also had more afferent boutons with 3+ clusters of P boutons than the Es IgG group (G). CGCT IgG (n=4), CGCT 11C7 (n=4), TR IgG (n=5), TR 11C7 (n=3), ES IgG (n=5), ES 11C7 (n=6), CB IgG (n=5), CB 11C7 (n=4). Scale bar in A,B = 20 μm, in C = 5 μm. * $p < .05$

3.5.6 5-HT expression in lumbar spinal cord

One way of measuring axonal growth after injury is to look at 5-HT expression below the lesion. This has been done previously measuring 5-HT varicosities on lumbar MNs (Chen et al., 2017) or ventral horn fibre density (Maier et al., 2009). In our study we have looked at both integrated density and contacts on MNs in the lumbar spinal cord.

Post hoc analysis of 5-HT expression in the ventral horn of L4 showed there were some group differences (Figure 3.20A). The TR 11C7 group had more 5-HT than either the CGCT 11C7 ($p = .046$) or the ES 11C7 ($p = .043$) groups. Data for 5-HT terminals in close apposition to α-MNs were not statistically significant (Figure 3.20B). Although the ES 11C7 group did have a trend for less contacts per 100 μm of cell perimeter than the TR 11C7 group ($p = .079$).

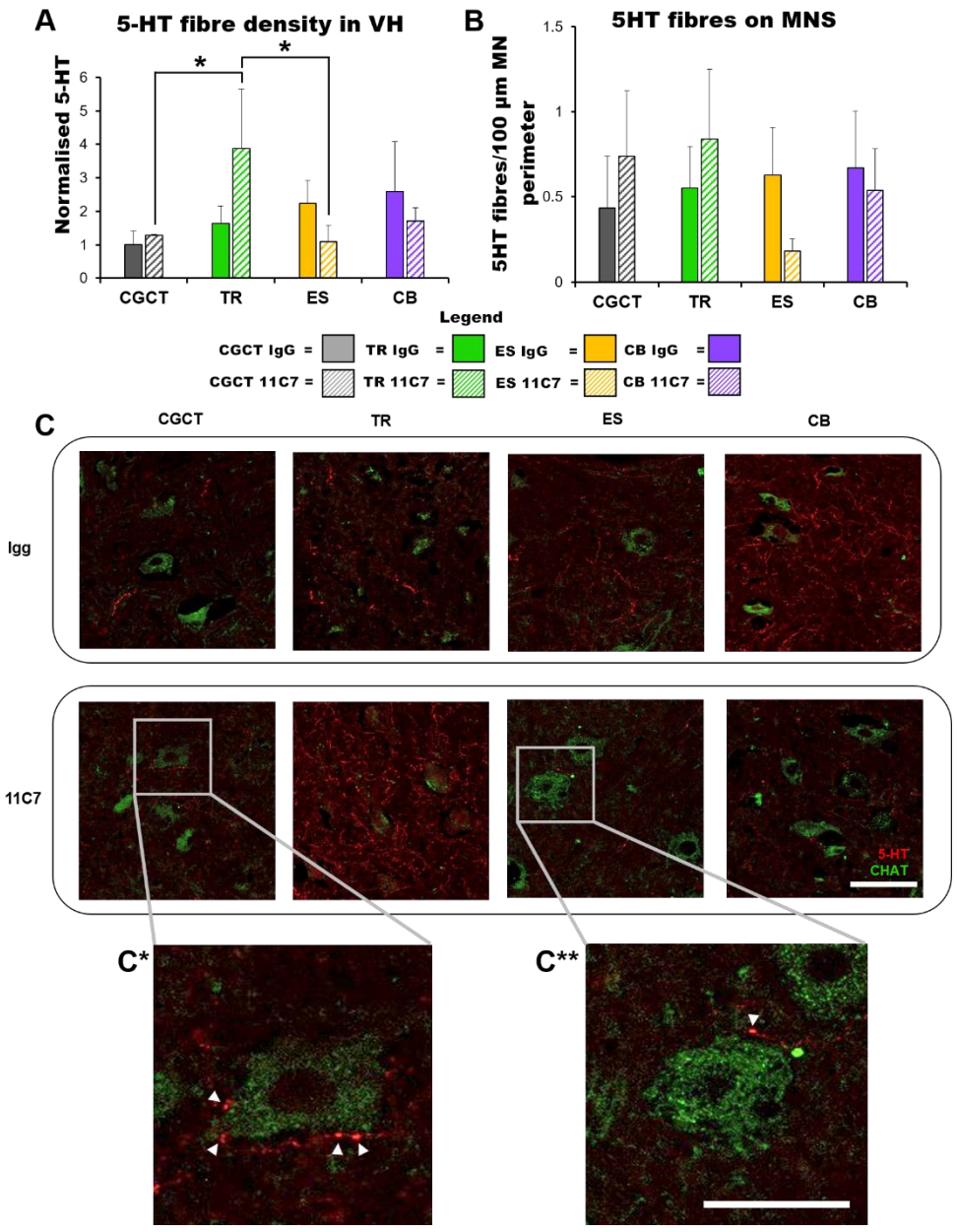

Figure 3.20 5-HT expression and MN contacts

5-HT expression analysis in the ventral horn of L4 showed that the TR 11C7 group had significantly more 5-HT than either the CGCT or ES 11C7 groups (A). 5-HT fibres in close apposition with large MNs showed no statistically significant differences (B). Although the ES 11C7 group did have a trend for less contacts per 100 µm of cell perimeter. Representative samples of ventral horn shown in C, with examples of 5-HT boutons (white arrows) in close apposition to MNs of the CGCT 11C7 and ES 11C7 groups. For 5-HT density in ventral horn CGCT IgG (n=3), CGCT 11C7 (n=3), TR IgG (n=6), TR 11C7 (n=3), ES IgG (n=4), ES 11C7 (n=6), CB IgG (n=4), CB 11C7 (n=4). For fibres per 100/µm, CGCT IgG (n=2), CGCT 11C7 (n=2), TR IgG (n=4), TR 11C7 (n=4), ES IgG (n=4), ES 11C7 (n=3),

CB IgG (n=3), CB 11C7 (n=4) Green = ChAT, red = 5-HT. Scale bar in C = 100 µm, in C* and C** scale bar = 50 µm. Error bars ± SEM

3.5.7 TH expression in lumbar spinal cord

One enzyme, tyrosine hydroxylase (TH), reliably marks both dopaminergic and noradrenergic projections. We studied the expression of TH in the lumbar spinal cord below lesion in a similar manner to the serotonergic integrated density analysis (Figure 3.21A). There were extremely sparse contacts on MNs, thus we did not analyse these contacts.

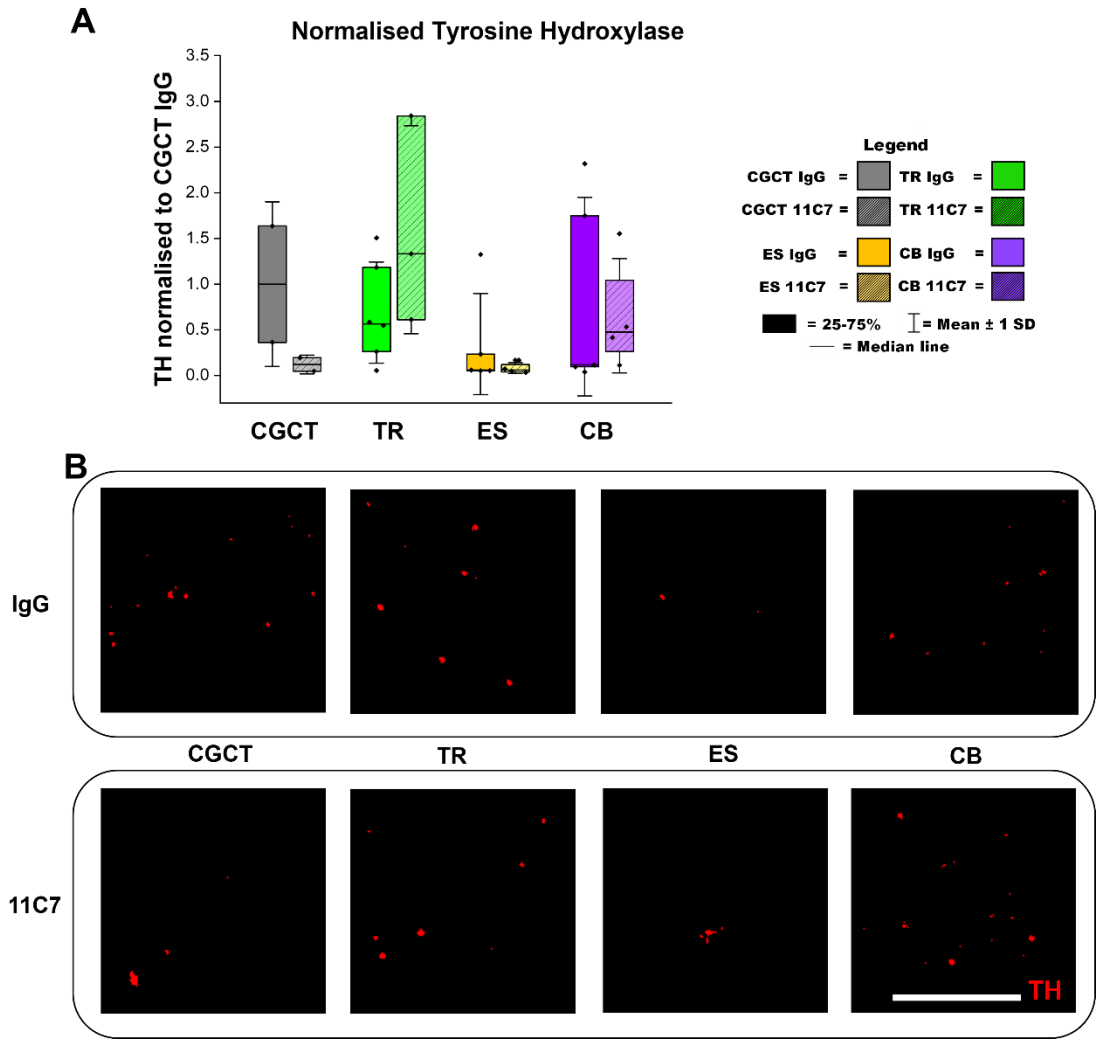

Figure 3.21 Tyrosine hydroxylase expression in lumbar spinal cord
Integrated density of tyrosine hydroxylase positive fibres in the ventral horn of L4 were measured (Data were normalized to CGCT IgG) (A). Axons were quantified after thresholding and were included for integrated density analysis if they were larger than 0.5 µm in total area and the entire ventral horn was analysed. CGCT IgG (n=2), CGCT 11C7 (n=2), TR IgG (n=6), TR 11C7 (n=3), ES IgG (n=5), ES 11C7 (n=4), CB IgG (n=5), CB 11C7 (n=4). Scale bar = 25 µm.

3.6 Discussion

There were a number of major findings within this study. These are summarised briefly below. In this study our primary aim was to demonstrate that the combined use of 11C7, locomotor training, and epidural stimulation would lead to the greatest functional recovery. Our secondary aim was to determine the structural and electrophysiological changes underpinning this recovery. The results show that the CB 11C7 group had the highest BBB scores although this result did not reach statistical significance (Figure 3.7). What was significant is that in the last four weeks of the study the CB 11C7 and TR 11C7 groups had the most animals weight supported stepping.

To further investigate detailed aspects of locomotor recovery we analysed joint kinematics and computed principal components from these data. For individual kinematic measurements, stride length was highest in the TR 11C7 group, swing height in the ES IgG group, while drag percentage was lowest in the CB 11C7 group (Figure 3.8). Step consistency scores were best for the TR and ES 11C7 groups, while being the lowest for the ES IgG group (Figure 3.9). PCA revealed two important principal components (Figure 3.10). The first PC was negatively correlated with consistency scores and positively correlated with gait time and kinematic variability while the second PC was highly correlated with toe drag variables (Figure 3.11A). For both PCs the naïve control group had a lower score than any of the SCI groups. For PC1, this was not significant for the TR, ES and CB 11C7 groups. Indicating the combination of 11C7 with all three of the treatments made them less dissimilar to naïve animals than the other groups (Figure 3.13). For PC2, the TR and CGCT 11C7 groups were statistically significantly different from the naïve controls while the other groups were not (Figure 3.13). Grouping the animals by drug, epidural stimulation and locomotor training showed there was a significant difference between all groups and naïve controls for PC1 (Figure 3.14, Figure 3.15 and Figure 3.16). For PC2 the difference between IgG treated animals or epidurally stimulated animals and naïve controls was not statistically significant while all the other groups were different to naïve controls.

We analysed local spinal changes below the lesion to determine if sensory changes were underlying the behavioural changes between groups. In the TR 11C7 group there is a

trend for increased proprioceptive afferent input to the premotor interneuronal area in Laminae V and VI (Figure 3.17C). Other VGluT1 differences between groups were not significant. There was a significant difference in direct proprioceptive afferent input to α-MNs. Here, the CB 11C7 group had the lowest VGluT1 contacts per MN perimeter (Figure 3.18A). The maximum H-reflex was also observed to be correlated with VGluT1 inputs to α-MNs. With the CB 11C7 and CGCT 11C7 having the lowest Hmax:Mmax ratio (Figure 3.18B-C).

We hypothesised that 11C7 and training would increase axonal sprouting of supraspinal inputs. Unfortunately, we have been unable to analyse CST sprouting as BDA analysis is being done by a lab in Beihang University, Beijing, and the data are not yet available. However, there were increased 5-HT fibres in the L4 ventral horn of the TR 11C7 group (Figure 3.20). There was a large variability in TH expression within groups, but the TR 11C7 group was also the highest here (Figure 3.21).

3.6.1 Combinational treatment with 11C7, treadmill training and epidural stimulation resulted in the highest recovery of locomotor function

We are the first group to investigate 11C7 therapy in a rat contusion injury, and the first to deliver a combinational treatment with sequential 11C7 therapy before epidural electrical stimulation and training. The results support our hypothesis that combinational treatment would lead to the greatest behavioural recovery. Thus, suggesting that there is potential for further investigation into this combination.

The plan for our combinational therapy was first to increase neural plasticity and axonal growth with 11C7, and second to guide this increased plasticity with locomotor training under electrical epidural stimulation. We know that increased plasticity and axonal growth does not always lead to behavioural recovery (Dickson et al., 2019). Therefore it was important for us to harness this with a previously proven training and epidural stimulation paradigm (Ichiyama et al., 2005). We are not the first to investigate plasticity enhancing therapies with behavioural training. Other groups have attempted combinatorial treatments with varying degrees of success. Reaching training is often combined with plasticity or growth promoting drugs for beneficial behavioural results (Liu et al., 2017b, Torres-Espín et al., 2018, Wei et al., 2016, Hollis Ii et al., 2016, Garcia-Alias et al., 2009).

Although this is rarer with locomotor training (Chen et al., 2017, Kubasak et al., 2007), where combinational treatment normally involves excitatory drug cocktails with training under epidural electrical stimulation (Ichiyama et al., 2008a, Courtine et al., 2009, van den Brand et al., 2012, Manohar et al., 2017, Asboth et al., 2018). Of course, the results of combined training and plasticity enhancing therapies do not always sum. For example, none of simultaneous training and 11C7 treatment (Maier et al., 2009), lumbar ChABC and training (Jakeman et al., 2011) or Nogo receptor deletion and training (Harel et al., 2010) resulted in enhanced behavioural recovery.

In our study we have observed some positive transfer from locomotor training under epidural stimulation to open field locomotor behaviour. This is not always the case, and sometimes there is even negative transfer from training one task to behaviour in another (De Leon et al., 1999, Garcia-Alias et al., 2009). Our kinematic measurements are also proof of positive transfer, as all our kinematic recordings were completed under no epidural stimulation. Thus, we have also shown that training under epidural stimulation transfers to treadmill performance without epidural stimulation. Namely in the form of reduced toe drag and increased weight supported stepping in this group.

While we observed some behavioural improvement, full locomotor recovery was not achieved. By delaying epidural stimulation and training we may have missed a critical period where training results in the highest recovery (Norrie et al., 2005). Although it should be noted this is not always the case, and starting training immediately rather than delaying treatment does not always improve behavioural outcomes (Smith et al., 2009). Another point to consider is the self-training which occurs after injury. The BBB score of all rats improved over the course of the study. Part of this recovery can probably be ascribed to self-training, as we know that immobilising rats after injury halts much of this spontaneous behavioural recovery (Caudle et al., 2011). Other studies have demonstrated this robust spontaneous recovery after thoracic contusion injury (Kuerzi et al., 2010), where they have suggested that rats self-training in their cages has led to reduced impact of their (swim) training regime on behavioural recovery. Discriminating the boundary between spontaneous and training induced recovery is a difficult but important problem. Our

training paradigm of twenty minutes per day five days a week may not be sufficient to increase recovery much above the normal spontaneous level.

While we have demonstrated some recovery following combinational treatment, it is important to understand the mechanisms underlying this and what each treatment is doing. In the following sections I have looked at what is causing the recovery observed. And what each treatment is doing individually and in concert with the others.

3.6.2 Locomotor training following 11C7 therapy is more effective than locomotor training with control antibody

In our study the trained group only increased in BBB score if 11C7 was given prior to locomotor training. The low impact of delayed training alone shows that it may not be as effective in a severe contusion injury such as ours. Thus reinforcing the idea that combinatorial treatments are necessary. Sequential 11C7 therapy with training led to increased step consistency where training alone did not. Reduced toe drag was not observed in either the TR IgG or TR 11C7 groups, unlike what has been reported previously (Chen et al., 2017). This may be due to the more severe lesion in our study. This severe lesion meant that not all rats were able to properly train, even with high amounts of body weight support.

The mechanisms of training induced recovery in the spinal cord are not fully understood. We do know the spinal cord is capable of learning in the absence of supraspinal input. This was proven with studies on spinally transected cats where treadmill training resulted in weight supported stepping on a treadmill (Lovely et al., 1986, Barbeau and Rossignol, 1987). We also know the role of sensory input is key, as without proprioceptive afferent input mice do not recover from SCI (Takeoka et al., 2014), and destruction of afferent input after spontaneous recovery resulted in a loss of the behavioural improvements (Takeoka and Arber, 2019). After transection of the CST there is an increase in afferent sprouting and connections to MNs in the cervical spinal cord (Tan et al., 2012). In some cases (Chen et al., 2017), but not all (Khalki et al., 2018), this increase in afferent input is reduced by training. There is a difference in training between studies, and in the latter study training is not uniform treadmill training, but rather a mix of enforced walking on a carousel, and physiotherapy stretching followed by a 5-HT agonist. In our study

training alone had no effect on afferent input to the intermediate zone of medial laminae IV-VI, whereas training following 11C7 therapy led to a small increase in afferent input to this area. This matches results by Chen et al. (2017), who showed similar afferent changes following training or sequential training and 11C7 therapy.

Training has been shown to increase sprouting of spared fibres from both the CST and serotonergic pathways. There is some evidence of increased CST sprouting following reach training (Girgis et al., 2007), and locomotor training (Chen et al., 2017). However, we have not yet been able to analyse the data for this. Post lesion 5-HT is increased following wheel running in a rat contusion injury (Engesser-Cesar et al., 2007). Although we have not seen similar increased 5-HT with training alone, this agrees with other data using a similar training paradigm to ours (Maier et al., 2009, Chen et al., 2017). The TR 11C7 group did have a higher density of 5-HT fibres in the ventral horn, indicating there are some synergistic effects from combinational treatments. The TR 11C7 group also had a higher density of tyrosine hydroxylase fibres in the ventral horn. This enzyme is present in both dopaminergic and noradrenergic fibres (Kuscha et al., 2012). Dopaminergic input may be important for micturition following SCI (Hou et al., 2016b), and noradrenergic sprouting has been observed following training after a contusion injury (Bose et al., 2012). In our study there was a large variation of TH expression between groups, and there did not appear to be a specific pattern of changes bar the increase in fibres in the TR 11C7 group.

There were some behavioural improvements in the TR 11C7 group, but not the TR IgG group. It is possible this is due to a ceiling effect. Where the training given was not sufficient to improve behaviour above that of spontaneous recovery and self-training. In a severe contusion such as the current study it appears that delayed training alone is not enough to result in weight supported plantar stepping in the final weeks of treatment. This was not the case for training after 11C7 therapy which did show improved BBB scores and averaged higher number of animals with weight supported plantar stepping. This adds contusion injury data to studies showing the benefit of delayed training after 11C7 therapy in targeted T-shaped lesions (Chen et al., 2017). Previous research has shown negative combinatorial effects of 11C7 with training (Maier et al., 2009). While increasing fibre sprouting with anti-Nogo-A before beginning intensive rehabilitative therapy is also found

to increase motor performance after stroke (Wahl et al., 2014). Our severe contusion injury model has added more clinically relevant evidence for sequential combinatorial therapy. The sequential nature of the combinational treatment has an added benefit in that SCI patients are not usually able to train immediately after injury. Therefore, a therapeutic timeline such as ours may be ideal for clinical interventions.

3.6.3 ES increased step height but not step consistency

ES has been used in humans with some promising results (Harkema et al., 2011, Angeli et al., 2014, Angeli et al., 2018, Wagner et al., 2018, Gill et al., 2018). There are a few hypotheses for how epidural electrical stimulation improves recovery after SCI. Electrical stimulation is known to increase BDNF expression in spinal cord neurons (Wenjin et al., 2011), and induce remyelination in peripheral nerves (Wan et al., 2010). In our study, ES alone did not lead to open field or kinematic behavioural improvement, but only did so when combined with 11C7, training, or both. This suggests that the actions of ES alone are not sufficient for behavioural recovery. It is the combination of training with ES which led to the greatest locomotor improvements. This tracks with the theory of state dependence which suggests that ES is simply putting the spinal cord into a state where proprioceptive feedback can initiate and control movement (Edgerton et al., 2008, Sławińska et al., 2012). Much of the research into this method has often combined ES with training and neuroexcitatory drugs such as quipazine (Gerasimenko et al., 2007, Ichiyama et al., 2008a, Ichiyama et al., 2008b, Courtine et al., 2009, van den Brand et al., 2012). This idea of increased spinal excitability modulated by sensory input also conforms with how we think ES is acting on the spinal cord. In humans, ES is found to primarily activate sensory afferents and ascending and descending dorsal column axons (Minassian et al., 2007). De-afferented spinal cords of rats are also unresponsive to ES, further confirming the importance of sensory fibres in ES (Lavrov et al., 2008). The suggestion of ES priming the spinal cord to respond to sensory input is also backed up by our data. Animals only had increased weight supported stepping when ES was combined with step training. Here, ES only improved performance when combined with coordinated afferent input from step training.

Looking at individual kinematic parameters it appears that ES alone increased step height while reducing stride length. This suggests that there is an exaggerated response to afferent input from the treadmill. Stride length is also reduced in this group, suggesting the response to afferent feedback is not leading to optimal behavioural results. In fact, the ES alone group was farthest from naïve controls for both swing height and stride length. The ES alone group also had some of the worst consistency scores, with toe, ankle, and knee consistency all low. Analysis of PC1 differences also showed ES alone to be the furthest from naïve controls. The coordinated sensory stimulation of step training is clearly required for locomotor improvements. Step training under ES led to improvements in stride length and step consistency as well as PC1 results more similar to naïve controls. We have demonstrated that ES alone cannot replace the necessary activity dependant plasticity from treadmill training.

We are not the first to suggest that training is needed alongside ES to tune spinal circuitry to produce appropriate motor behaviour (Shah and Lavrov, 2017). This is the idea of ES turning the non-functional spinal cord into a more functional state where the CPG is able to be activated. Earlier research has shown this using ES with training and 5-HT agonists after a full transection (Courtine et al., 2009). Variability in training under ES and 5-HT agonists is also shown to improve locomotor performance, where sidewards and backwards stepping under ES also improved forward stepping after a full transection (Shah et al., 2012). There is other evidence pointing to the role of ES in altering spinal networks to enable normal function. ES facilitates improved wheel running in a Parkinson's disease model where the nigrostriatal pathway is blocked (Zhong et al., 2019). In the above model there is also a decrease in excitatory descending input for which ES is able to compensate. Combined, these data suggest that the role of ES after SCI is to modulate the spinal network to a more functional state, a state where both voluntary supraspinal control and proprioceptive information result in meaningful motor output.

All the above studies test recovery during neuromodulation of the spinal cord with ES and/or 5-HT agonists. Indeed, even in humans, voluntary control of movement after SCI is possible with targeted epidural stimulation to facilitate this (Wagner et al., 2018). How these ES interventions affect normal behaviour in the absence of stimulation is not always

reported. In our study we have investigated the transfer of locomotor ability from treadmill walking under ES to open field behaviour and treadmill walking in the absence of ES. One other study has shown positive transfer from locomotor training under ES and 5-HT agonists to body weight supported stepping in the absence of stimulation after a severe contusion (Asboth et al., 2018). In the above study training with neuromodulation began just one week after injury. Our study on chronic SCI presents further challenges due to the delayed intervention where training under ES began three weeks after the initial injury. Most patients are unable to receive treatment or training immediately after SCI, therefore our model may be more clinically relevant, as humans are generally unable to begin rehabilitation early after SCI (Wernig et al., 1995).

3.6.4 11C7 improved behavioural outcomes in trained and combination groups, but not in cage control or ES alone

The spinal cord generally not permissive to axonal growth, factors such as CSPGs (Kwok et al., 2012), and myelin associated inhibitory factors act to limit neural plasticity. One of these myelin associated factors is Nogo-A. In order to overcome some of this inhibition we have used an antibody against Nogo-A. Anti-Nogo-A therapy has been found to increase neuronal sprouting and axonal regeneration (Schnell and Schwab, 1990). And sequential 11C7 therapy and training results in behavioural improvements following T-lesions (Chen et al., 2017). However, in our study 11C7 by itself did not improve locomotor behaviour. The reason for this unimpressive recovery is not entirely clear. We are the first to investigate Anti-Nogo-A therapy in a rat contusion injury, and the severity of our injury may have led to the modest behavioural improvements observed. The lack of behavioural improvement in the 11C7 alone group underlines the need for rehabilitation in combination with plasticity enhancing therapies (Dickson et al., 2019). While 11C7 by itself was unable to overcome the severe injury, behavioural improvements were observed when 11C7 was combined with locomotor training or training under ES.

Why 11C7 therapy alone did not improve locomotor recovery is unclear. There are still many questions regarding the role of Nogo-A in axonal growth and other processes. Many systems are changed by inhibiting Nogo-A with 11C7, some of which remain unknown. The extracellular domain of Nogo-A, Nogo-66, acts on the NgR1 receptor to

activate the RhoA pathway, which leads to cytoskeletal collapse of neurite outgrowth (Schmandke et al., 2007). This pathway appears straightforward in that if neurite outgrowth is disinhibited, then axonal sprouting should increase. Indeed, this is the case with most studies inhibiting Nogo-A or its receptors, where increased axonal sprouting and synapse formation is observed (Z'Graggen et al., 1998, Liebscher et al., 2005, Bregman et al., 1995, Chen et al., 2017, Maier et al., 2009, Petrinovic et al., 2013, Wills et al., 2012). There is another, more complex action of the 'amino-nogo' or nogo-Δ20 domain. This nogo-Δ20 domain is internalized into the nucleus, where it acts in a more diffuse manner to decrease axonal plasticity via transcriptional changes (Joset et al., 2010). When nogo-Δ20 is internalized there is a decrease in phosphorylated cAMP response element binding (CREB) levels in the soma of these cells. The activity of nogo-Δ20 appears to directly oppose that of growth associated factors such as nerve growth factor which increases CREB activity (Cox et al., 2008). Nogo-Δ20 also acts on the sphingosine 1-phosphate receptor 2 (Kempf et al., 2014), and was recently found to act on erythropoietin-producing hepatocellular (EphA4) (Wang et al., 2021), itself a target for axonal regeneration (Goldshmit et al., 2004). Nogo-Δ20 also inhibits microvascular endothelial cells (Wälchli et al., 2013), and Anti-Nogo-A was also recently observed to be pro-angiogenic following stroke (Rust et al., 2019). The above varied activity of Nogo-A makes discussion of its interactions with training and neuromodulation even more complex.

In our study it does appear that the disinhibition possible with anti-Nogo-A is insufficient to increase axonal sprouting below the lesion. Here again, combination of sequential 11C7 therapy followed by training shows additive effects. In our study 5-HT and TH did not increase with 11C7 therapy alone, but both did increase with sequential 11C7 therapy and training. While one study has shown increased serotonergic sprouting after SCI and 11C7 (Maier et al., 2009), another has not (Chen et al., 2017). This may be due to study timing, as in the latter study animals were trained for longer, and it is possible serotonergic fibre sprouting had been pruned. In our study animals were also trained for eight weeks before sacrificing around two weeks after that. It is also possible that there has been some retraction in serotonergic sprouting in the 11C7 therapy alone, but that continued locomotor training after 11C7 therapy was able to inhibit this retraction. The

difference in 5-HT expression may also be due to the tracts spared by each SCI. 5-HT fibres travel through the dorso-lateral and ventro-lateral funiculi (Bregman, 1987). While the T-lesion from the above studies leaves the ventro-lateral funiculus intact, our more severe contusion injury leads to almost complete destruction of this pathway.

Anti-Nogo-A therapy normally promotes CST sprouting after injury (Z'Graggen et al., 1998, Liebscher et al., 2005, Bregman et al., 1995). We have not yet quantified CST sprouting above or below the lesion, however both may be important for recovery. Even if there is limited sprouting below the lesion due to our severe injury, CST terminations on descending propriospinal neurons above the lesion may also be important for SCI recovery (Bareyre et al., 2004).

Our data on afferent input is in contradiction with other studies of 11C7 after SCI (Maier et al., 2009, Chen et al., 2017). In our study, 11C7 alone had no impact on afferent input to MNs. Again, the time between 11C7 therapy and tissue collection may also be important. Retraction of afferents could have occurred even if they had temporarily increased following 11C7 therapy. In our study 11C7 therapy and training under ES results in a decrease in afferent input in the CB 11C7 group. There is a general decrease in neuronal activity associated with locomotion following step training under ES (Ichiyama et al., 2008a). The reduced activity observed in the above study could be a function of reduced afferent input that we have observed in our data.

Our severe contusion injury has led to differential effects on recovery and axonal sprouting as compared to partial transection studies (Maier et al., 2009, Chen et al., 2017). There is very limited study of combinational treatments with 11C7, and none in rat contusion injuries. The contusion model, while more clinically relevant, has a great deal of secondary pathology and tissue damage associated with it (Rowland et al., 2008). This damage, and the severity of our injury, means that 11C7 alone did not have the effect of recovery observed in other studies with mild injuries (Zörner and Schwab, 2010, Chen et al., 2017, Maier et al., 2009). It is also likely that with prior 11C7 studies animals were able to self-train to a greater extent than in the current more severe and complex contusion injury. What we have found is that there are behavioural improvements following sequential 11C7 and training where there were none with 11C7 alone.

3.6.5 Drivers for afferent and presynaptic inhibitions changes

As mentioned before, afferent input is vital for recovery from SCI. Without proprioceptive muscle spindles mice are unable to recover from SCI (Takeoka et al., 2014). Training also relies on afferent activity to exert its effect on the H-reflex (Ollivier-Lanvin et al., 2010), and epidural stimulation requires intact afferents to result in CPG activation (Lavrov et al., 2008). The importance of sensory input for locomotor recovery suggests that changes in this sensory network could underpin recovery. However, the research on these afferent changes is not always clear.

Sensory input to MNs is increased following unilateral CST lesion in adult rats (Tan et al., 2012), and a lack of sensory retraction has also been noted in complete transection studies of neonatal rats (Smith et al., 2017). However, there is not always an increase in afferent sprouting after loss of descending input. Khalki et al. (2018) found a decrease in VGluT1 boutons on MNs of the ankle flexor tibialis anterior after a complete spinal transection. This reduction in afferent input was reversed after training with a 5-HT agonist. However, training does not always cause an increase in afferent to MN contacts after SCI (Chen et al., 2017). It is possible that different models of injury have led to different results for afferent input changes. Khalki et al. (2018) used a complete transection while the others used more targeted lesions (Tan et al., 2012, Chen et al., 2017). We have actually found a reduction in VGluT1 boutons in the CB 11C7 group. This suggests a retraction or refinement of sensory input due to combinational treatment. A refinement of activation patterns was noted by Ichiyama et al. (2008a), where training under ES and a 5-HT agonist led to a reduction in the number of active neurons during stepping. The reduction in afferent input observed in our study could be underlying the refinement in neural activity observed by Ichiyama et al. (2008a).

Another sensory change noted after SCI is a reduction in pre-synaptic inhibition (Caron et al., 2020). Pre-synaptic inhibition is caused by what are termed GABApre interneurons contacting sensory afferents, the somata of which reside in the deep medial dorsal horn (Hughes et al., 2005, Rudomin, 2009). They act to filter sensory information and without them oscillations in movement occur (Fink et al., 2014). Presynaptic inhibitory P boutons have decrease following sacral transection in a rat (Kapitza et al., 2012) and

training is found to increase P bouton density after spinal transection in a rat (Khalki et al., 2018), although there was no significant decrease in P boutons after SCI in Khalki et al. (2018). Further research after a spinal transection has demonstrated reduced pre-synaptic inhibition from afferent input, with treadmill training was able to reverse this (Caron et al., 2020). The mechanism for the increase in pre-synaptic inhibition and P boutons probably relies on increased afferent activity from training. This is because afferent glutamatergic activity is known to drive P bouton formation (Mende et al., 2016). Eliminating afferent glutamatergic activity decreased GABA synthesising GAD65 in P boutons and resulted in reduced presynaptic inhibition. The link between afferent input and P boutons is not always clear. In development there is a retraction of afferent input which coincides with an increase in P bouton coverage (Smith et al., 2017). In the above study a neonatal transection inhibited the sensory retraction, thus keeping afferent input hight, while at the same time stunting P bouton increases. Thus, the simple number of afferent inputs does not dictate the amount of P bouton coverage, even though afferent activity is one driver of their formation. In our study clusters of 3+ P boutons were only increased in the ES and CB 11C7 groups. The change in P boutons was not correlated with changes in VGluT1 afferent input to MNs, as the CB 11C7 group had the least afferent to MN input and the highest number of VGluT1 boutons with 3+ P boutons (Figure 3.22).

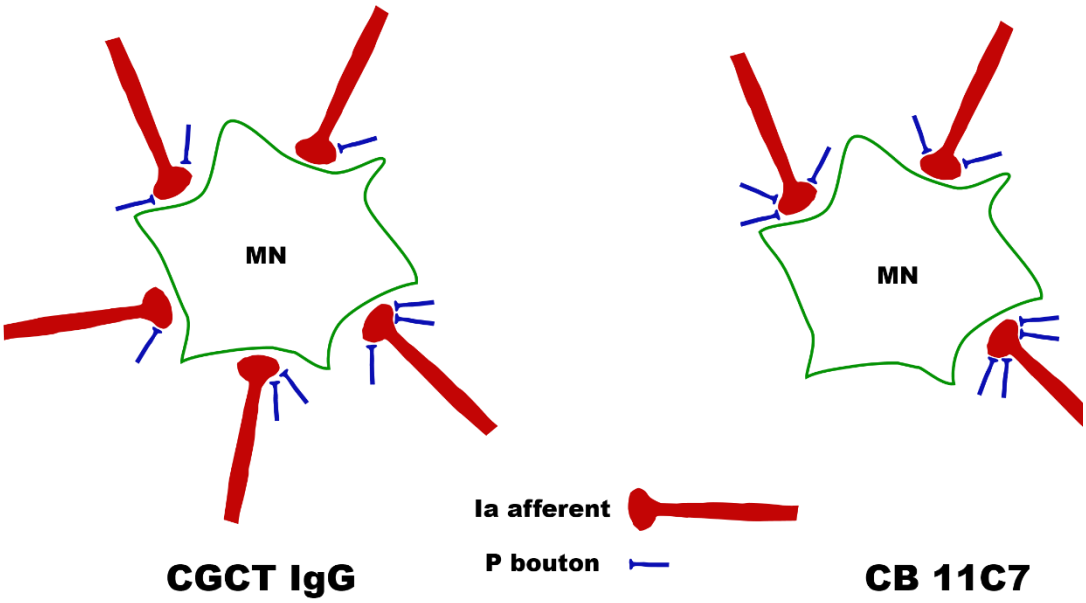

↑	**Afferent input to MNs**	↓
↓	**Afferent boutons to MNs with 3+ P boutons**	↑
↑	**H reflex**	↓

Figure 3.22 Summary of MN afferent and P bouton changes
Afferent input and the H reflex were reduced in the CB 11C7 group. However, the proportion of afferent terminals on MNs with 3+ P boutons were increased.

3.6.6 Delayed training may have stunted locomotor recovery

We have demonstrated some functional recovery following combinational treatment with sequential 11C7 therapy and training under ES. While recovery was best in these animals, it was still modest. The reason we have only observed modest recovery could be due to the timing of our intervention. Our model may be more clinically relevant, as training is normally delayed after SCI. However, the delay in training may mean we have missed the critical period of plasticity after injury. Delayed training does reduce the behavioural benefits observed from training soon after (1 week) injury (Norrie et al., 2005). Translational profiling has shown that after SCI, CST axons transiently express a regenerative transcriptome which is then downregulated after two weeks (Poplawski et al., 2020). Further research has underlined this critical period following SCI. The importance of activity dependant plasticity during this period was shown by Bradley et al. (2019). In

the above study the activity of descending propriospinal interneurons was inhibited from days 14-21 following a dorsal hemisection. This inhibition led to decreased CST contacts on these neurons and reduced recovery of locomotion. When these neurons were inhibited in normal animals, or 12 weeks after SCI there was no effect on CST to propriospinal neuron connections. It is not just propriospinal activity which has a time sensitive window to alter descending input connections. CST and propriospinal neurons have reduced post lesion sprouting in mice without proprioceptive afferents, however ablation of these afferents 7 weeks after injury does not alter below lesion sprouting (Takeoka and Arber, 2019). Taken together, these studies suggest a critical period for activity dependant plasticity of both afferents and propriospinal neurons which we may have missed using our delayed training intervention.

3.6.7 Conclusion

This study is the first to demonstrate the effectiveness of sequential 11C7 therapy and training under ES. Combinational rehabilitative therapy and plasticity enhancing treatments are necessary to achieve motor recovery following SCI (Dickson et al., 2019). Our study has demonstrated this, as none of the individual 11C7, training, or ES therapies alone led to improved locomotor function. Further, 11C7 alone did not lead to increased sprouting of afferents, TH or 5-HT fibres. Only when followed by locomotor training did TH and 5-HT fibre sprouting occur, this suggests that in a severe contusion injury such as ours 11C7 alone is insufficient, and therefore must be combined sequentially with activity based therapy. The current clinical trial of anti-Nogo-A therapy has shown it is well tolerated and thus can be continued (Kucher et al., 2018). We have presented evidence it could also be used with sequential training under ES for improved locomotor recovery.

4 Gamma motor neuron targeting and innervation

4.1 Introduction

We know that proprioceptive information is important for movement and motor learning. The role of muscle spindles in endogenous recovery from SCI has also been demonstrated (Takeoka et al., 2014). Sensory input is also vital in training mediated spinal changes and ES mediated locomotor recovery (Ollivier-Lanvin et al., 2010, Lavrov et al., 2008). ɣ-MNs exist to control the output from muscle spindles, and thus modulate the many functions which require sensory input. However, their role in learning or recovery from SCI is unclear, even though there is evidence of changes in their synaptic connectivity after SCI (Ichiyama et al., 2011).

The separate supraspinal and segmental control of ɣ-MNs poses further questions as to their role. If they existed just to maintain spindle sensitivity during muscle contraction then why even have ɣ-MNs, and not just the dual intrafusal and extrafusal fibre innervating β-MNs? Selective γ-MN control could be important in terms of 'fusimotor set', where either static or dynamic γ-MN control acts tonically to alter sensory output based on task specificity (Prochazka et al., 1985). Whereas α-MNs are only active if the muscle is required to move, γ-MNs may be tonically active during certain types of movements. Early evidence in cats suggested a role for selective γ-MN and not α-MN activity in novel or complex tasks (Prochazka et al., 1988). However, this has not been fully replicated in humans, where spindle output is often decreased when learning a visuomotor task (Jones et al., 2001). Although human studies have limitations with tasks constrained to small movements of only one limb in controlled settings, which thus may not be fully representative of the role of γ-MNs in normal movement.

How the spinal network learns is still highly debated. Much focus has been placed on the final common pathway of α-MNs, and on the last order interneurons directly contacting them (reviewed in the IN section of the general introduction). The second order actions of ɣ-MNs modulating spindle afferents has been ignored in favour of these pre-motor interneuron studies. We have targeted γ-MNs to discover their interneuronal, segmental

and supraspinal inputs. We did this to elucidate their potentially important role in motor learning suggested by earlier studies. This earlier evidence suggested increased dynamic γ-MN activity in novel or complex tasks (Prochazka et al., 1988) and a reduction in more routine walking and running tasks (Prochazka et al., 1985). Prochazka (1989) has suggested the above research shows that γ-MNs are necessary to deliver 'uncensored, unanalysed' information to the cortex in novel movements. The current human evidence actually suggests reduced proprioceptive output during visually guided learning (Jones et al., 2001), and pre-synaptic inhibition of afferent input to MNs is also increased during skill acquisition (Perez et al., 2005). The limits of recording from afferents in normal movement means that investigation of these circuitry in complex, multi joint, and faster movements is not currently possible.

The data from Prochazka suggest a pivotal role for γ-MNs in motor learning, however, further study and evidence is required to determine if this is really the case. Uncovering the inputs to these MNs could lead to a greater understanding of these phenomena, and shed new light on motor learning in the spinal cord. Below is a brief description of the gaps in our knowledge of the inputs and role of γ-MNs, summarised from the full description given in the first part of the general introduction.

4.1.1 Current understanding of γ-MNs, their inputs and role

γ-MNs control the sensitivity of the muscle spindle. The basic anatomy of the spindle was reviewed in the general introduction. Briefly, there are usually 1-2 primary afferents and 1-5 secondary afferents innervating the muscle spindle (Prochazka, 1996). The spindle has motor innervation from multiple γ-MNs and often a β-MN, and each β and γ MN innervate multiple spindles (Emonet-Denand et al., 1992). A β-MN is a motor neuron with axons innervating both the intrafusal and extrafusal muscle fibres. The typical spindle contains a dynamic bag fibre (b_1), a static bag fibre (b_2), and 2-10 chain fibres (c) (Matthews, 1964). There are two types of γ-MNs, dynamic and static. Excluding β-MNs, motor control of b_1 fibres is from dynamic γ-MNs (γ_d) and motor control of b_2 and c intrafusal fibres is from static γ-MNs (γ_s) (Barker et al., 1973). Primary muscle spindle afferents (Ia) have sensory terminals on b_1, b_2 and c intrafusal fibres and secondary spindle (group II) afferents have sensory terminals on b_2 and c spindle fibres (Emonet-Dénand et

al., 1977). Primary spindle afferents fire more during the application of stretch, while primary and secondary afferents signal the length of stretch and have a sustained higher firing rate until the return of the muscle to resting length (Harvey and Matthews, 1961).

The two types of γ-MNs have different and sometimes opposite effects on spindle afferent firing. Dynamic γ-MNs increase the sensitivity to stretch of the spindle primary afferents and lead to a pronounced drop in primary afferent firing after stretch termination (Emonet-Dénand et al., 1977). Static γ-MNs increase the base rate of spindle afferent firing (bias) while decreasing the stretch sensitivity (gain). Static γ-MN activity also attenuates the drop in firing after stretch termination. During muscle shortening γ_s activity acts to limit the decrease in spindle afferent firing (Prochazka et al., 1979). γ_s activity is able to occlude the effects of γ_d activity on Ia spindle afferents during small movements (Hulliger et al., 1977). There is some functional and spindle connectivity overlap between the two γ-MN types (Emonet-Dénand et al., 1977). The division of γ-MN activity means that just looking at the whole γ-MN population may not be as informative as looking at the individual sub-populations. Although at present there is no way to molecularly define them.

There have been many studies investigating the supraspinal and segmental inputs to γ-MNs. These are reviewed in the general introduction, however a brief description is provided here. The segmental inputs are diverse, however, there is not much evidence of direct sensory to γ-MN input bar a possible secondary afferent to γ_d connection in the cat (Gladden et al., 1998). γ-MNs are influenced by SA1 mechanoreceptors, secondary muscle spindle afferents, group III afferents responding to stretch or skin stimulation, and 5-HT and BK intramuscular injections probably via group III and IV afferents (Djupsjobacka et al., 1995, Jovanovic et al., 1990, Appelberg et al., 1977, Gladden et al., 1998, Davey and Ellaway, 1989). There are presumably many interneuronal connections, including Renshaw cells, and dorsal horn interneurons such as dI3 which are found to excite α and possibly γ-MNs in response to cutaneous stimulation (Bui et al., 2013). However, the identity and origin of the vast majority of the IN to γ-MN connections remain elusive.

For supraspinal input to γ-MNs there are structures such as the lateral vestibular nucleus, reticular formation, and certain areas in the MLR which have similar effects on α and γ motor neurons. Selective control of γ and not α-MNs has been observed from areas

including the subcoeruleus nucleus, SNpr, MesADC, and anterior cerebellum (Hulliger, 1984). MesADC stimulation excites only γ_d neurons, while only γ_s neurons are excited from stimulating the SNpr, vestibular nucleus or an area dorsal and caudal to the red nucleus. The separate areas of control for γ_s and γ_d appears logical, as the two γ-MN types often display opposite effects on spindle afferents. Controlling the spindle feedback to the locomotor network allows γ-MNs to alter the response of the motor system to proprioceptive stimuli. The separate control of γ_d, γ_s and α-MNs allows for adaptation of the reflexes responses in different environments and during different levels of arousal. This allows the dynamic ɣ-MNs to increase spindle responsiveness in resting states in order to counteract small postural differences, and allows the static ɣ-MNs to maintain spindle firing during contraction in order to assist in force production. There is an observed difference in dynamic and static γ-MN activity across flexors and extensors, where γ_d activity is dominant in extensors and γ_s activity is dominant in flexors (Cabelguen, 1981). The increased dynamic ɣ-MN activity in novel or complex tasks is another example of a demonstrable split in activity between the two different types (Prochazka et al., 1988).

The lack of recordings made from clearly identified static and dynamic ɣ-MNs in naturally moving animals or man has limited the conclusions that can be made as to their role. With the work by Taylor, Ellaway, Durbaba, and Rawlinson (Reviewed in Taylor et al. (2004)) providing the clearest picture of ɣ-MN function in movement. However, even the above studies were completed on decerebrate cats on treadmills, and thus are not fully representative of ɣ-MN activity in normal movement. Targeting ɣ-MNs and being able to control/record their activity in awake freely moving animals would provide much more robust information as to their role. At present there is limited clarity as to the role of ɣ-MNs in normal movement and locomotion, learning, and postural control. This may not be resolved soon, due to the technical difficulties involved in continuously recording from identified ɣ-MNs in awake normally moving animals or humans.

The advent of new viral targeting and with it the ability to trace inputs, modulate and record activity (Wickersham et al., 2007, Watakabe et al., 2017) has led us to investigate routes to molecularly identify and target γ-MNs. With this accomplished many questions about the innervation and function of γ-MNs could be solved

4.1.2 Aims

We know proprioceptive information is vital for SCI recovery as mice without muscle spindles were unable to recover any locomotor ability following a unilateral hemisection (Takeoka et al., 2014). It is currently unknown whether γ-MNs are also vital for this recovery, however it does seem likely, as they are responsible for the control of these spindles. Further hints at the role of γ-MNs in SCI include research by Ichiyama et al. (2011) who showed that there was a decrease in synaptic coverage on γ-MNs following neonatal transection. More research has shown γ-MNs lack plasticity restricting perineuronal nets (Smith et al., 2015), even after SCI (Al'joboori et al., 2020), and have a reduced amount of neurite outgrowth inhibitor Nogo-A as compared to α-MNs following SCI (unpublished observations). These observations have led us to believe that γ-MNs present a uniquely plastic and important target for SCI recovery. Our aim is to target γ-MNs in order to uncover their inputs and role.

In the absence of γ-MN specific targeting and tracing, we have also investigated the proportion of γ-MNs in various muscles to clarify the role of γ-MNs in the spinal locomotor system. Determining the distribution and proportion of γ-MNs in various muscles will uncover more information as to their role. Due to the multiple avenues of γ-MN investigation we have completed, this chapter is split into four separate short introductions, methods, results and discussions for each major hypothesis.

4.1.3 Hypotheses

i) The proportion of ɣ-MNs will vary per muscle

ii) An AAV targeted to the oestrogen related receptor γ (Err3) will selectively target ɣ-MNs
   (1) Err3 will selectively label γ-MNs
   (2) An AAV with an Err3 promotor will be selective for γ-MNs

iii) 5-HT_{1D} targeting will selectively label γ-MNs
   (1) *In-situ* hybridisation will show 5-HT_{1D} to be selective for γ-MNs
   (2) An AAV with a 5-HT_{1D} promotor will be selective for γ-MNs

iv) The small proximal branch of the soleus nerve will allow selective γ-MN targeting

4.2 Proportion of gamma motor neurons per muscle

Some insight into the role of γ-MNs can be found by looking at muscle spindle distribution. The number of spindles per muscle increases with size, however the density of spindles is lower in larger compared to smaller muscles (Peck et al., 1984). It was suggested that the relative excursion of small muscles means they act as motors for the detection of stretch. This does not appear to be case, and there is another explanation for increased density of spindles in smaller muscles. Banks and Stacey (1988) observed that small muscles in large animals, and large muscles in small animals have similar numbers of spindles (soleus of the cat (2.4 g, 56 spindles, 23 g−1;) abductor pollicis brevis of humans (2.7 g, 80 spindles, 29.3 g−1). The relationship of spindle numbers to muscle size is approximately 38 times the cube root of the muscle in grams (Prochazka, 1996). Taking size differences into account like this, the spindle density of each muscle still varies. The neck muscles have increased numbers of spindles while the shoulder girdle muscles have fewer spindles. The author (Banks) suggested the reason for the reduced number of spindles in the shoulder was due to the large range of motion and high number of degrees of freedom in the shoulder (Banks, 2006). He suggested the role of muscle spindles was more limited in shoulder girdle muscles due to this higher range of motion. This may be the reason for the lower density of spindles in shoulder girdle muscles. However, the fact that spindle density is not related to H-reflex amplitude (Berthoz et al., 1992) means this argument is not entirely convincing. There may be more afferents per spindle in the shoulder, just as there may be more γ-MNs per spindle. Thus, muscle spindle density may not fully explain the role of proprioception in control of the individual muscle.

While determining the number of spindles per muscle allows for a increased understanding of dynamic motor control, determining the number of γ-MNs in each muscle could be just as important. Variations in control of muscle spindles means that spindle density may not tell the whole picture. New labelling and analysis methods have allowed us to quantify the proportion of γ-MNs per muscle. The presence of ChAT and lack of NeuN has allowed us to reliably identify γ-MNs (Friese et al., 2009). Advances in 3D clearing and imaging of tissue means that this experiment is currently possible, with high spatial reliability compared to cryo-sectioning multiple spinal segments. Understanding the

distribution and proportion of γ-MNs in various muscles will provide more information as to their function. Therefore, we have studied the proportion of γ-MNs in various hindlimb and forelimb muscles in the rat.

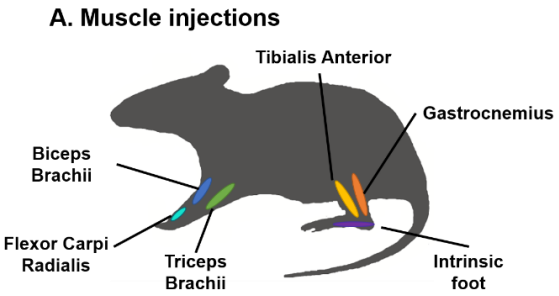

B. Animals injected

Animal	Muscles injected			
	Hindlimb		Forelimb	
1	Right TA	Left GS	Left Biceps	Right Triceps
2	Right TA	Left GS	Left Biceps	Right Triceps
3	Right intrinsic foot		Left wrist flexor	

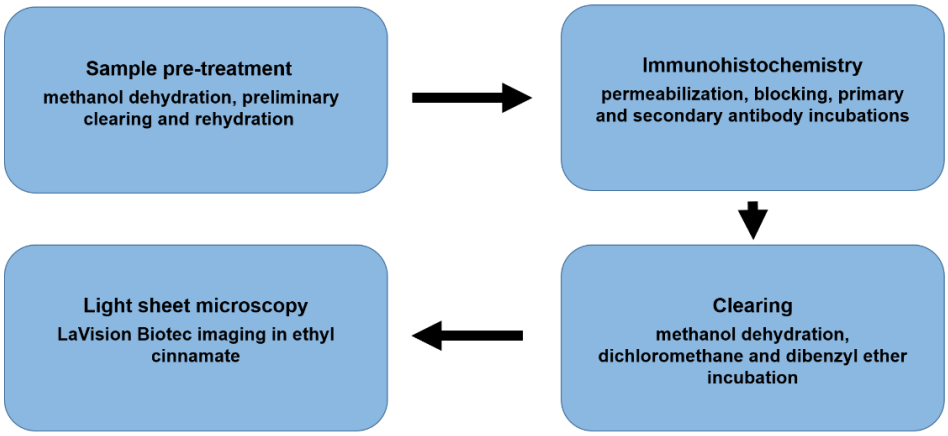

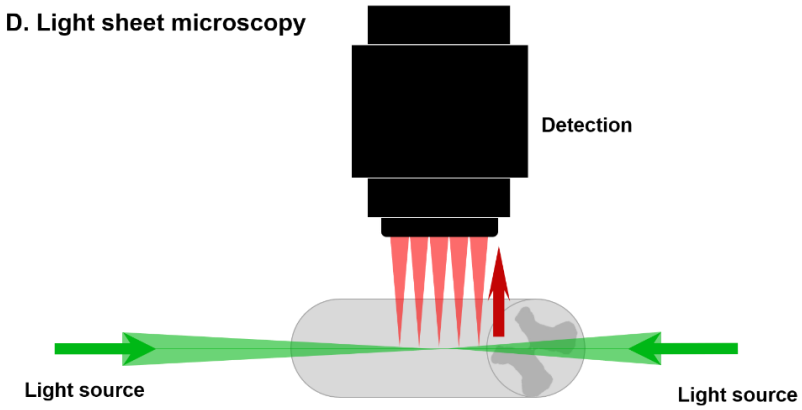

Figure 4.1 CTB injections, clearing and light sheet microscopy

Animals were injected with CTB in various muscles of the forelimb and hindlimb (A). Three animals were used for analysis (B). Tissue clearing and immunostaining protocol included dehydration, antibody incubation, and clearing (C) before imaging with light sheet microscopy (D).

4.2.1 Methods

4.2.1.1 Surgeries

Under isoflurane anaesthesia, the tracer CTB was injected into six different muscles of three animals (Figure 4.1A). Two of each Gastrocnemius (GS), Tibialis Anterior (TA), and Triceps Brachii (Triceps), and one of each Biceps Brachii (Biceps), Flexor Carpi Radialis (wrist flexor), and intrinsic foot (foot) were injected (Figure 4.1B). 5 µl of 1% CTB was injected into the GS and TA, 3 µl into the Biceps and Triceps, and 2 µl into the wrist flexor and intrinsic foot muscles. Animals were left 72 hours before perfusion.

4.2.1.2 Tissue clearing and light sheet microscopy

Rather than section thousands of sections, large segments of spinal cord were cleared for light sheet microscopy. The major issues for imaging thick sections is light scattering/translucence due to refractive index differences in heterogeneous tissue samples (Richardson and Lichtman, 2015). All clearing techniques aim to equilibrate the refractive index of a sample so that light scattering occurs in a uniform manner. The method we have chosen was a modified immunolabeling-enabled three-dimensional imaging of solvent-cleared organs (iDISCO) protocol (Renier et al., 2014). This solvent based clearing has a few different steps (Figure 4.1C). First, dehydration with lipid solvation, second, immunostaining, and finally further lipid solvation and clearing by refractive index matching before imaging.

Perfusions were as described in the Methods chapter. Spinal columns were post fixed overnight at 4^{o}C in 4% PFA in 1x PB, and then stored in 1x PB at 4^{o}C until further steps. All steps were conducted at room temperature and on a shaker unless otherwise stated. The room temperature antibody incubation steps were a modification to the iDISCO protocol in order to reduce non-specific staining. The lumbar and cervical enlargements were excised from the remainder of the spinal cord and washed 2x 30 minutes in PBS. Samples were dehydrated in a methanol/H_2O series of 25%, 50%, 75%, and 100% methanol for three hours each. There was a final 100% methanol step of 2 hours at 4^{o}C before samples

were incubated overnight in 66% dichloromethane (DCM)/33% methanol. Samples were then washed 2x10 minutes in 100% methanol before rehydration in a 100%, 75%, 50%, 25% methanol/H_2O series for three hours each. Samples were left to equilibrate in PBS for 2 hours before washing in PBST (0.2 % triton) 2x 1 hour.

Immunostaining began with 2 days permeabilization in 20% dimethyl sulfoxide (DMSO) and 10 µg/ml of glycine in PBST. Blocking was completed for 2 days with 6% NDS, 10% DMSO in PBST. Primary antibody incubation was four days with 1:500 anti-ChAT goat, 1:500 anti-NeuN mouse, and 1:500 anti-CTB rabbit (Sigma, USA) in a solution of 10µg/ml heparin, 5% DMSO, and 3%NDS in PBST. Samples were washed in 10 µg/ml heparin in PBST 4x 2 hours and overnight. Secondary antibody incubation was four days in 1:500 anti-goat-555, 1:500 anti-mouse-488, and 1:250 anti-rabbit-647 in a solution of 10 µg/ml heparin and 3%NDS in PBST. Samples were then washed in 10µg/ml heparin in PBST 4x 2 hours and left overnight.

A final dehydration step was completed in a methanol/H_2O series of 25%, 50%, 75%, and 100% methanol for three hours each and then overnight in 100% methanol. Following this there was a three-hour clearing step in 66% DCM/33% methanol. The methanol was washed off with 2x15 minutes washes in 100% DCM. The final clearing step was incubation in dibenzyl ether which resulted in visual clearing within 15 minutes. The samples were then stored in dibenzyl ether at room temperature until imaging the week after.

The UltraMicroscope II LaVision BioTec (Germany) with 2x objective was used for imaging. In light sheet microscopy light is projected orthogonally to the detection lens, in contrast to normal light microscopy or confocal microscopy (Figure 4.1D). Samples were imaged in ethyl cinnamate with 470, 560, and 630 nanometre wavelength light with a Z stack at 5 µm steps.

Files were processed using IMARIS 9.3, the files were batch processed to create 3D volumes and manual stitching was completed where necessary. 3D objects were created out of CTB staining (Figure 4.2A-A*). and α and γ-MNs were distinguished by the presence of CTB staining and lack of NeuN (Figure 4.2C-C**). Only cells with visible

dendritic staining with CTB were counted in order to minimise false positives (Figure 4.2B) (Tosolini and Morris, 2012). Objects were then labelled as α and γ-MNs before positional and MN type data were exported to excel for analysis (Figure 4.2D).

Statistical analysis between individual muscles was not completed due to small sample sizes. A one-way ANOVA was used to compare forelimb and hindlimb and flexor and extensor subgroups.

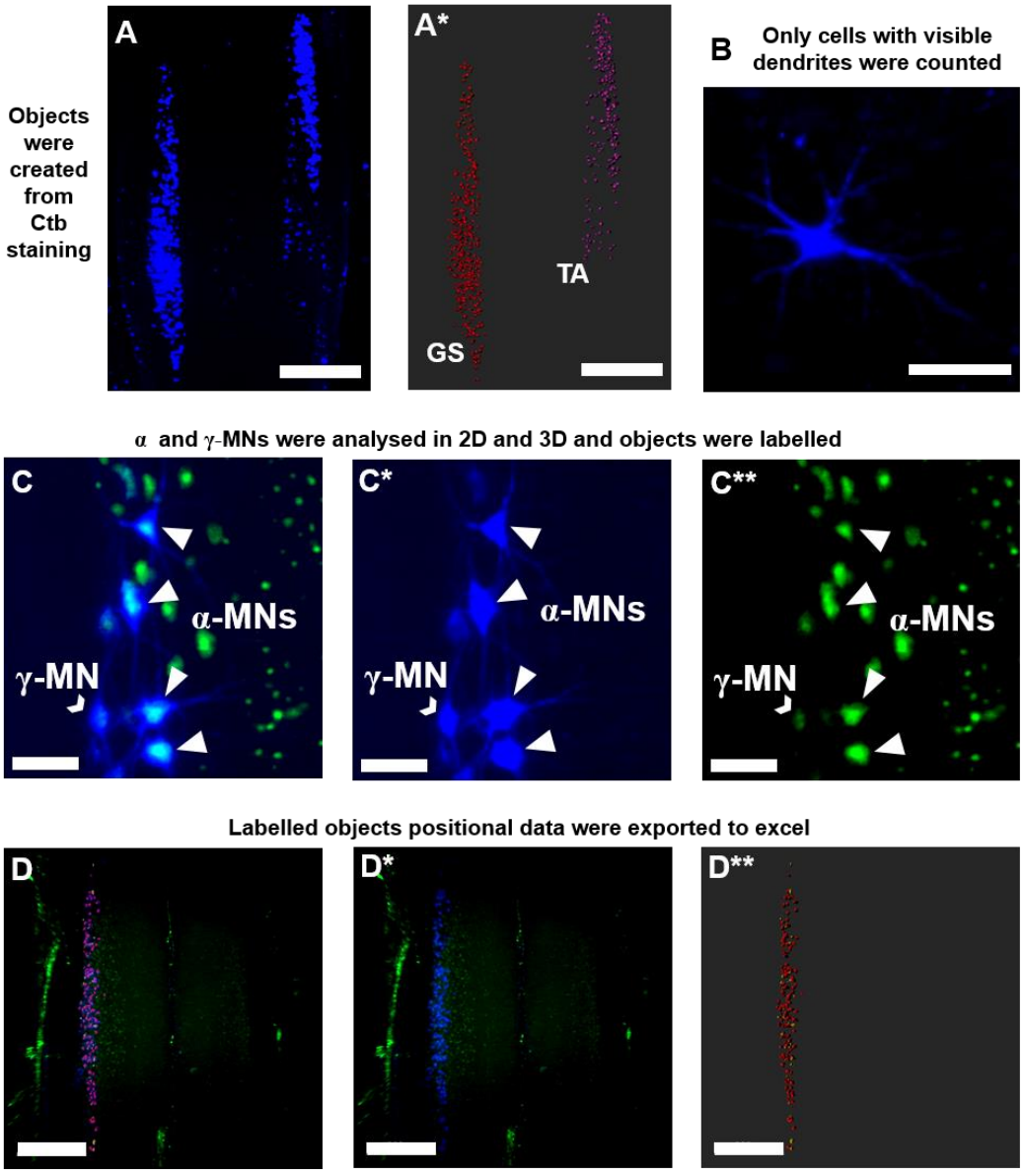

Figure 4.2 Image processing on IMARIS

Images were processed on IMARIS software. 3D objects were created out of CTB staining (A-A*). Only cells with visible dendrites were counted so as to exclude weak staining from CTB leakage (B). α and γ-MNs were identified by presence of CTB staining and lack of strong NeuN staining (C-C**) and labelled based on 2D and 3D analysis of staining (D-D**) before data were exported to excel. Blue = CTB, green = NeuN (A-D). Scale bar B-C = 100 µm. Scale bar A and D = 1000 µm.

4.2.2 Results/discussion

There were proportionally fewer γ-MNs in the triceps than in other muscles (Figure 4.3 A and B). However, statistical analysis between individual muscles was not completed

due to the small sample size. There was a lower proportion of γ-MNs in forelimb than hindlimb muscles (Figure 4.3C) ($F= 7.752$, $p = .027$). And a higher proportion of γ-MNs in flexor than extensor muscles (Figure 4.3D) ($F= 6.051$, $p = .043$).

We are the first to determine molecularly defined number and distribution of γ-MNs in various somatic muscles. Due to the lack of antibodies to determine the difference between α and γ-MNs this has not been completed previously. In prior studies, α and γ-MNs were defined simply by size differences. However, our data do concur with the earlier size-based analysis, as the proportion of γ-MNs was suggested to be roughly 25-30% of all MNs in the cat gastrocnemius (Burke et al., 1977). The number of MNs per muscle was higher than reported with earlier Fluorogold tracing studies for some lower limb muscles (Table 4.1) (Mohan et al., 2015), but were similar for some muscles such as the wrist flexor (Harrigan et al., 2019). Our method of whole tissue clearing could result in higher number of neurons counted as no sections are lost using this method. It is also possible nearby muscles were labelled, and further investigation of γ-MNs could include multiple retrograde tracers in different muscles to ensure only one motor pool is quantified (Han et al., 2019). There is less fascia separating nearby muscles such as the soleus from the gastrocnemius, therefore some overlap is possible (Han et al., 2019). However, it is unlikely our injections labelled unwanted motor pools given the distribution and shape of the labelled motor pools obtained (Fig. 1.2). Injections of tracer into the gastrocnemius and tibialis anterior show MN pools in the correct and separate positions for each muscle (Figure 4.2A*). Even if some of the injections labelled multiple muscles, the split between flexor and extensor and hindlimb and forelimb muscles will still be present as these muscles are not in the same muscle compartments.

Our data do not entirely conform to muscle spindle data, which, after correcting for size differences, show decreased spindles in the leg compared to the arm (Banks, 2006). However, the number of spindles per muscle does not necessarily restrict the amount of γ-MNs per muscle. Each muscle spindle can be contacted by multiple γ-MNs, and one γ-MN can innervate multiple spindles (Walro and Kucera, 1985), thus γ-MN numbers need not conform to spindle density data. Our data demonstrate the amount of control over the sensory information flow, rather than the total amount of sensory information possible.

In our study the proportion of γ-MNs is higher in flexors than extensors. Akay et al. (2014), found that Golgi tendon organs (GTOs) provided sufficient sensory feedback in extensors during normal walking and that the function of extensors was largely unaffected by the lack of muscle spindles. This suggests that there may be less need for muscle spindle afferent information in extensors. Looking at covariation in spindles and GTOs, one study found increased muscle spindles and concurrently decreased GTOs using a mouse knockout for the ETS transcription factor ER81 (Kucera et al., 2002). Although another study has found no correlation between increased GTOs and decreased muscle spindles in the mouse soleus (Sonner et al., 2017). It is possible that GTOs and muscle spindles are able to be modulated independently, but that in some circumstances, there are co-factors which can lead to the upregulation of muscle spindles and the concurrent downregulation of GTOs. As is often the case, the picture is somewhat complicated by the dynamic/static γ-MN divide. Extensors have been found to have more γ_d activity while flexors have more γ_s activity (Cabelguen, 1981). It is possible that differences in the main type of activity may influence the number of γ-MNs needed. Dynamic γ-MN activity may need relatively fewer γ-MNs to increase the stretch sensitivity of spindles. While the servo-assistance γ_s activity may require more γ-MNs to maintain spindle firing during rapid contractions. Although this is only a hypothesis and there is currently no evidence of differences in γ_d/γ_s ratio differences per muscle.

The reason we found a lower proportion of γ-MNs in the forelimb compared to hindlimb is unclear. It is possible that forelimb muscles require less afferent control due to the greater role of visual information to guide these muscles. Afferent input is reduced in visuomotor adaptation tasks in humans (Jones et al., 2001), where there may be a mismatch between visual information and proprioceptive input. This may explain some of the reduced proportion of γ-MNs in forelimb muscles. One clue could be found by looking at differences in spinal motor network INs between the hindlimb and forelimb, where spinal V2a INs show a graded connectivity array across the rostro caudal axis (Hayashi et al., 2018). There are more cervical V2a INs which project to supraspinal structures, while in the more caudal lumbar regions V2a INs do no project supraspinally, and instead form recurrent networks with local spinal neurons. It is possible that the increased proportion of

γ-MNs in the lumbar spinal cord is for a similar reason. Where in the lumbar spinal cord they are more important to control and coordinate local activity without as much supraspinal input as the cervical regions. This is slightly speculative and more work is needed to uncover the reasons for the forelimb hindlimb differences in γ-MN proportion we have demonstrated.

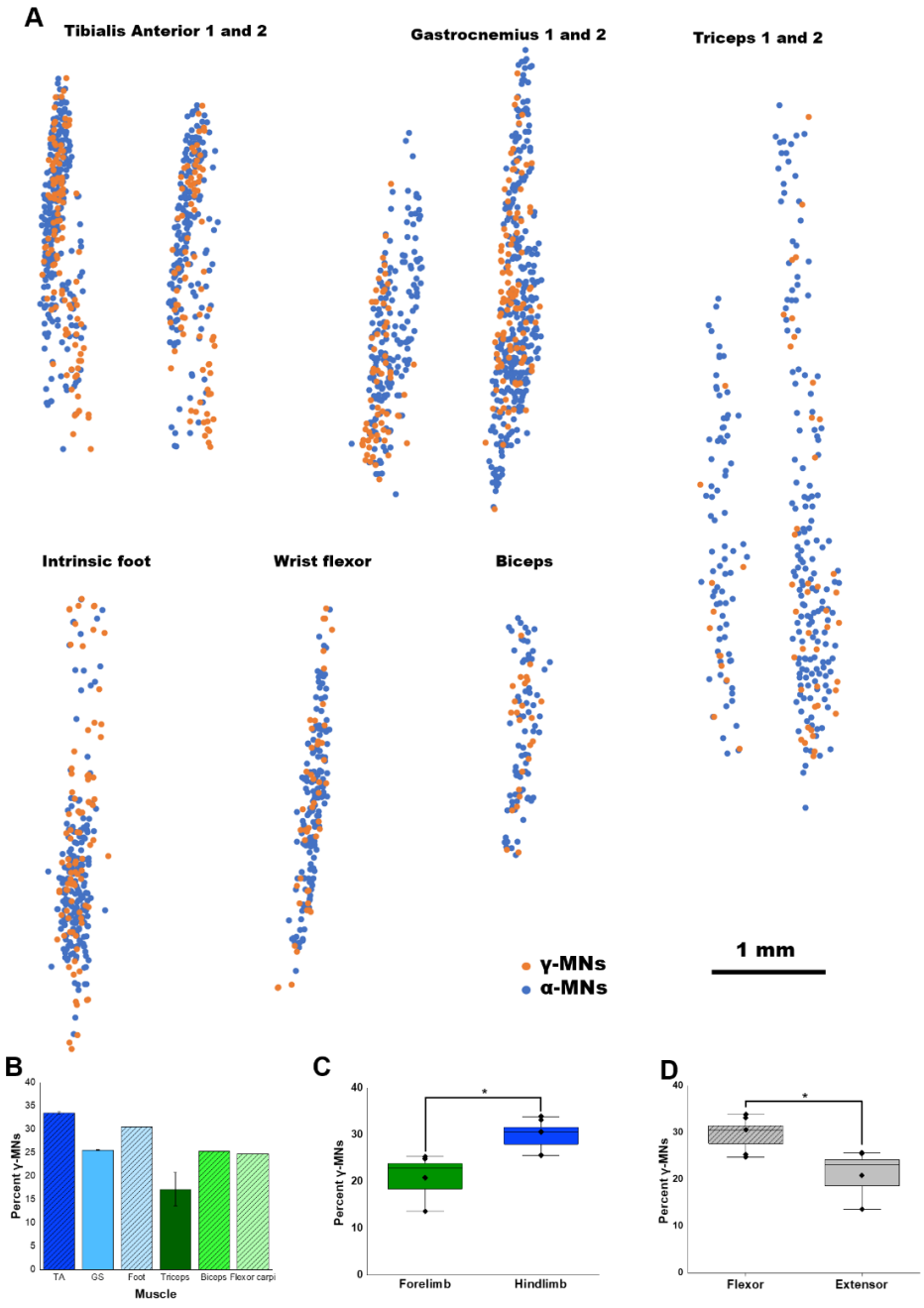

Figure 4.3 α and ɣ-MNs across muscles

There were no obvious distribution differences between α and ɣ-MNs across the motor pools of individual muscles (A). There were individual differences in ɣ-MNs as a percent of total MNs (B). However statistical tests were not completed due to limited data. There was a lower proportion of ɣ-MNs in forelimb muscles than hindlimb muscles (C). There was also a lower proportion of ɣ-MNs in extensors than flexors (D).

Table 4.1 Number of MNs per muscle

Muscle	Total MNs	α-MNs	γ-MNs	Percent γ-MN
Tibialis Anterior 1	331	221	110	33%
Tibialis Anterior 2	245	162	83	34%
Gastrocnemius 1	245	182	63	26%
Gastrocnemius 2	424	316	108	25%
Intrinsic foot	284	197	87	31%
Triceps 1	88	76	12	14%
Triceps 2	202	160	42	21%
Biceps	95	71	24	25%
Wrist flexor	202	152	50	25%

4.3 Targeting γ-MNs using an AAV

The many question marks around the innervation of ɣ-MNs led us to investigate these inputs by selectively targeting them for further tracing studies. To do this we targeted ɣ-MNs with AAVs specific only to them and not α-MNs. The ability to trace the inputs of ɣ-MNs will also be useful to study their changes before and after SCI and training.

A technique first demonstrated by Wickersham et al. (2007) found that it was possible to restrict a modified rabies virus to only monosynaptic inputs. Previously, rabies virus tracing resulted in polysynaptic virus transduction. Cells of interest for input tracing are induced to express the TVA viral receptor. This allows an EnvA pseudotyped modified rabies virus to enter only these cells for initial infection. The modified rabies virus unable to produce a specific ‘G’ protein and is therefore unable to enter other cells. The cells of interest are induced to produce this G protein along with the TVA receptor. The modified rabies virus is then able to assemble with the G protein and spread through synapses contacting the initial cell, but is not able to spread further due to the G protein deficiency.

The ability of this technique to monosynaptically trace inputs to specific populations led us to pursue this method. This plan for γ-MNs is shown in Figure 4.4.

The AAV technique to induce G protein expression was chosen for multiple reasons. One is that if we were able to target γ-MNs for G protein expression they could also be modified in other ways. As there is a large range of modifications which can be made using AAVs (Watakabe et al., 2017). The other main reason was to allow for investigations of neural circuitry in non-genetically modified rats. This would simplify experiments without the need for complex genetic modifications and would allow for more detailed behavioural assessments in rats as compared to mice.

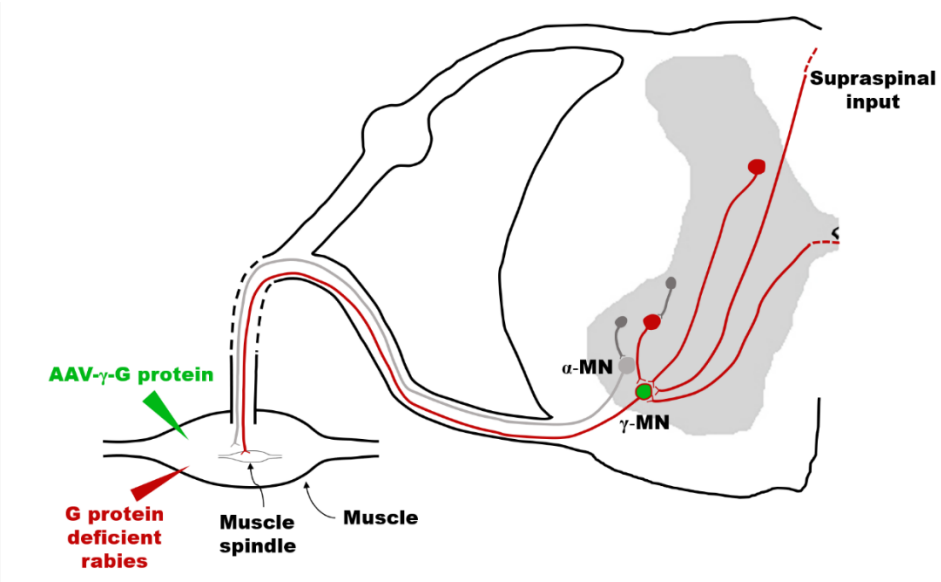

Figure 4.4 Plan for AAV targeting
The plan for AAV targeting was to inject an AAV with a γ-MN specific promotor into the chosen muscle. The AAV (green) would induce cells to produce G protein. A modified rabies virus deficient in G protein (red) would then be injected into the same muscle and transduce into γ-MNs and go precisely one synapse further. Thus identifying the monosynaptic connections to γ-MNs.

4.3.1 Err3 Background

Studies using AAV/modified rabies virus often use universal promotors with spatially defined regions of interest to target their neurons of interest (Stepien et al., 2010). Due to the colocalization of γ and α-MNs in the spinal cord (as demonstrated in Figure 4.1, 1.2 and 1.3), this method is unavailable to us. Other studies have used AAVs to target cells by

their birth date (Deshpande et al., 2013, Arenkiel et al., 2011) or with Cre expressing mouse lines for Cre dependant virus transduction (reviewed by Callaway and Luo (2015)). As mentioned earlier, we did not wish to use genetically modified mice due to the limited behavioural analysis and training possible with these animals. Therefore we investigated a γ-MN specific promotor for an AAV to be used in normal non-genetically modified rats.

Identifying specific markers for ɣ-MNs was the first step to progress with the techniques above. The transcription factor, oestrogen related receptor ɣ (Err3) was previously shown to be specific to ɣ-MNs (Friese et al., 2009). We investigated the exclusivity of Err3 to γ-MNs using the antibody from the above study. Simultaneous testing of an AAV with an Err3 promotor was completed alongside this, as the AAV-Err3-GFP had already been conjugated by Dr. Melissa Andrews (Southampton University).

4.3.2 IHC for Err3

Perfusions, tissue processing and IHC conformed to the methods chapter 2 unless otherwise stated. The Err3 antibody (R&D systems, USA) was the same as that of Friese et al. (2009). First trials with this antibody using 24-72 hour incubations were unsuccessful at producing clear nuclear staining (Figure 4.5A). Because of these negative results antigen retrieval (AR) techniques were attempted. AR is used to reverse the masking of epitopes which occurs during fixation/perfusion of the tissue. The AR protocol was 30 minutes incubation in 12 mM sodium citrate at 80 ^{o}C. On first inspection the AR appeared to have been successful with the nucleus of many cells stained (Figure 4.5B). Triple staining with ChAT and NeuN was the next step to confirm the identity of the cells stained, however, the results for this showed that the AR had led to staining in the nucleus of all cells regardless of primary antibody (Figure 4.5C). For this reason, AR was discontinued, as the method leading to universal staining did not appear reliable. Other research had shown success with the Err3 antibody using harsh antigen retrieval in paraffin sections of mice, but did not give the same results in our experiments (Yasvoina et al., 2013, Misawa et al., 2012). I then tried a series of trials with more concentrated detergent in order to achieve greater permeabilization of the cell and nuclear membrane. This was unsuccessful, with higher concentrations of Triton$^{x\text{-}100}$ leading to hugely increased non-specific staining, including white matter staining. These higher Triton$^{x\text{-}100}$ concentrations were also trialled

with tris buffered saline (TBS) with similarly negative results. Three other antibodies were also trialled. Neither an Err3 antibody from Proteintech (UK) nor GDNF receptor subunit-α1 antibodies from Proteintech (UK) or R&D systems (UK) resulted in specific γ-MN staining.

A

Primary antibody concentration	Permeabilization	Primary incubation time	Result
1:250 Err3	0.5 and 1% PBST	24 hr	No cellular staining
1:100 Err3	0.5% PBST	24 hr	No cellular staining
1:100 Err3	0.5% PBST	72 hr	Some unclear staining
1:100 Err3	0.2% PBST	24, 48, and 72 hr	Some unclear staining
1:100 Err3	0.2% PBST*	24 hr	Strong nuclear staining
1:100 Err3 1:250 ChAT 1:500 NeuN	0.2% PBST.*	Chat 48h, Err3 & NeuN 24h	All cells positive for all three antibodies
1:100 Err3 1:250 ChAT 1:500 NeuN	0.2% PBST	Err3 72 hr, Chat 48 hr, & NeuN 24 hr	Weak non-specific staining
1:100 Err3	0.5, 2.0, and 8.0% PBST	24 hr, 48 hr and 72 hr	Non-specific and white matter staining
1:100 Err3 1:250 ChAT 1:500 NeuN	0.5, 2.0, and 8.0% PBST	Err3 72h, Chat 48h, & NeuN 24h	White matter staining
1:100 Err3 1:500 NeuN	0.2% TBST	24h	No cellular staining
1:100 Err3	0.5, 2.0, and 8.0% TBST	24 hr and 48 hr	Some oligodendrocyte staining at 8.0% TBST

*antigen retrieval of 30 minutes in 12 mM sodium citrate solution at 80°C

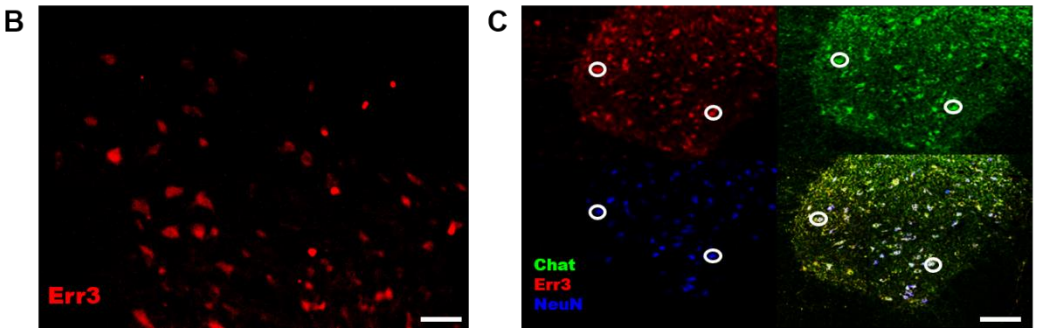

Figure 4.5 Err3 staining attempts
Multiple attempts were made to target γ-MNs with the Err3 antibody (R&D) (A). Some cellular staining was seen after antigen retrieval techniques were used (B). But further triple staining found that all cells were positive for all antibodies following this pre-treatment (C). Scale bar in B = 100 µm, in C = 200 µm

Looking for further targets is necessary to selectively target γ-MNs. The current method to distinguish α from γ-MNs is by lack of NeuN staining in γ-MNs (Friese et al., 2009). Using a negative marker does not allow for the design of specific ɣ-MN targeting viral vectors for tracing or modifying the neurons. Unfortunately, it does not look as if the

Err3 antibody is ready to be used to identify ɣ-MNs in rats. There are other potential targets for immunohistochemistry for ɣ-MNs , Wnt7a has been shown to be selective for ɣ-MNs, however that was using *in situ* hybridization and there has been no published data on a Wnt7a antibody used in the spinal cord (Ashrafi et al., 2012). Na^+/K^+ ATPase alpha 3 subunit (NKAα3), has been published as being selective for ɣ-MNs (Edwards et al., 2013). However, the results do not appear to be reliably conclusive regarding the exclusivity of NKAα3 to ɣ-MNs, as α-MNs also display some of this receptor on their cell membrane. It is probable that there is less of the NKAα3 subunit on α-MNs, but the evidence of its complete specificity is not convincing given the images in the above paper. The serotonin receptor 1d (5-ht1d) has been shown to be selective for ɣ-MNs (Enjin et al., 2012), however this too has only been accomplished using *in situ* hybridization and not immunohistochemistry.

4.3.3 AAV-Err3-GFP

AAV-Err3-GFP injections continued alongside the immunohistochemistry investigations above. The AAV serotype used was AAV-DJ, which is a hybrid of type 2, type 8, and type 9 AAVs (Lerch et al., 2012). The serotype is more easily transduced and escapes humoral neutralization and the immune response more effectively than any of its three precursors (AAV 2, 8, or 9) (Grimm et al., 2008). The AAV was designed and conjugated by Dr. Melissa Andrews (Figure 4.6A) and the Err3 promotor/reporter was produced by GenoCopoeia (USA). The promotor was conjugated to the AAV-DJ by Dr. Andrews and tested on cultured SKOV3 cells. SKOV3 cells are an ovarian cancer cell line which express high levels of Err3. The test was successful, with a number of cells expressing GFP 48 hours following AAV exposure (Figure 4.6B). Because the AAV-Err3-GFP was successful in transfecting SKOV3 cells it was decided to pursue an *in vivo* experiment to test the virus.

The AAV was diluted with sterile saline the night before surgery. Four animals received intramuscular injections and two received intraspinal injections. The intraspinal injections were in case the AAV was unable to be retrogradely transported from the periphery. The injection concentrations, location and volumes of AAV given to each animal are shown in Figure 4.6C. For intramuscular injections an incision was made to

reveal the muscle, the fascia was opened and injections were administered with a Hamilton syringe by manual pressure. For intraspinal injections an L1 dorsal laminectomy was performed and animals were injected with pulled glass pipettes. The Nanolitre 2000 with the Micro4 controller (World Precision Instruments, UK) was used for injections. Animals were left for 25 days before sacrificing as per the protocol for intramuscular AAV injections by Fortun et al. (2009). Animals were perfused and tissue was processed as per the general methods chapter.

Perfusions, tissue processing and IHC conformed to the methods chapter unless otherwise stated. Sections were incubated in primary antibody anti-ChAT (goat) (48 hr) and anti-NeuN (mouse) (24 hr) (as before, chapter 3), and anti-GFP (1:500, 24 hr) (rabbit, Abcam) in 3% NDS PBST. Secondary antibodies were anti-rabbit-488, anti-goat-555 and anti-mouse-647 (as before in chapter 3). Imaging was completed using the LSM 880 (Zeiss) at 63x with oil immersion.

Initial imaging of sections counterstained for GFP showed that the AAV had successfully transduced MNs in the ventral horn (Figure 4.6D). All spinal cord sections imaged showed a number of MNs positive for GFP indicating that the virus was transduced regardless of injection concentration. Sections from animals which received intraspinal or intramuscular injections both showed MNs which were positive for GFP. Unfortunately, it appeared as if both α and γ-MNs were labelled regardless of type. Counterstaining for NeuN and Chat confirmed this lack of transduction specificity as $Chat^{+}/NeuN^{+}$ (α-MNs) and $Chat^{+}/NeuN^{-}$ (ɣ-MNs) cells were transduced (Figure 4.6D). Thus, while the AAV is transducing the MNs, either the Err3 promotor is not functioning as it is supposed to, or both α and ɣ MNs contain Err3.

The Err3 promotor was chosen in order to selectively target ɣ and not α-MNs as it was shown to be specific for ɣ-MNs by Friese et al. (2009). Unfortunately, AAV-Err3-GFP has proven not to be specific for ɣ-MNs regardless of injection concentration. Either the Err3 promotor is not working in the AAV, or Err3 is not completely specific for ɣ-MNs. Further study of the literature has suggested the latter to be the case. Friese et al. (2009), Misawa et al. (2012), and Shneider et al. (2009) all state that Err3 is specific for ɣ-MNs. However, they also show that Err3 is present in α-MNs, only in smaller amounts than in ɣ-MNs. This

could be the cause for the non-specificity of the AAV used in the current experiment, where the presence of any amount of Err3 could be leading to the GFP being expressed in both α and ɣ-MNs.

A

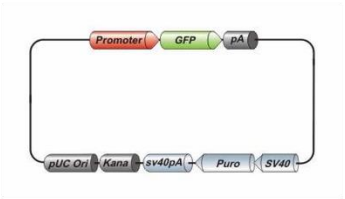

B

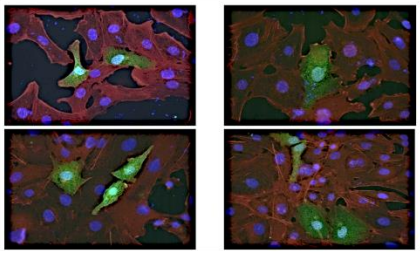

C

Animal	Dilution	Location and volume of injection
1	1:10	Medial gastrocnemius bilaterally, and left Biceps 4 x 1.5 µl
2	1:50	Medial gastrocnemius bilaterally, and left Biceps 4 x 1.5 µl
3	Pure	Medial gastrocnemius bilaterally, and left Biceps 4 x 1.5 µl
4	1:10	Medial gastrocnemius bilaterally 4 x 1.5 µl
5	1:10	Dorsal L4-L5 intraspinal bilaterally .5 mm from midline 1.0 mm deep. 2 x .5 µl
6	Pure	Dorsal L4-L5 intraspinal bilaterally .5 mm from midline 1.0 mm deep. 2 x .5 µl

D

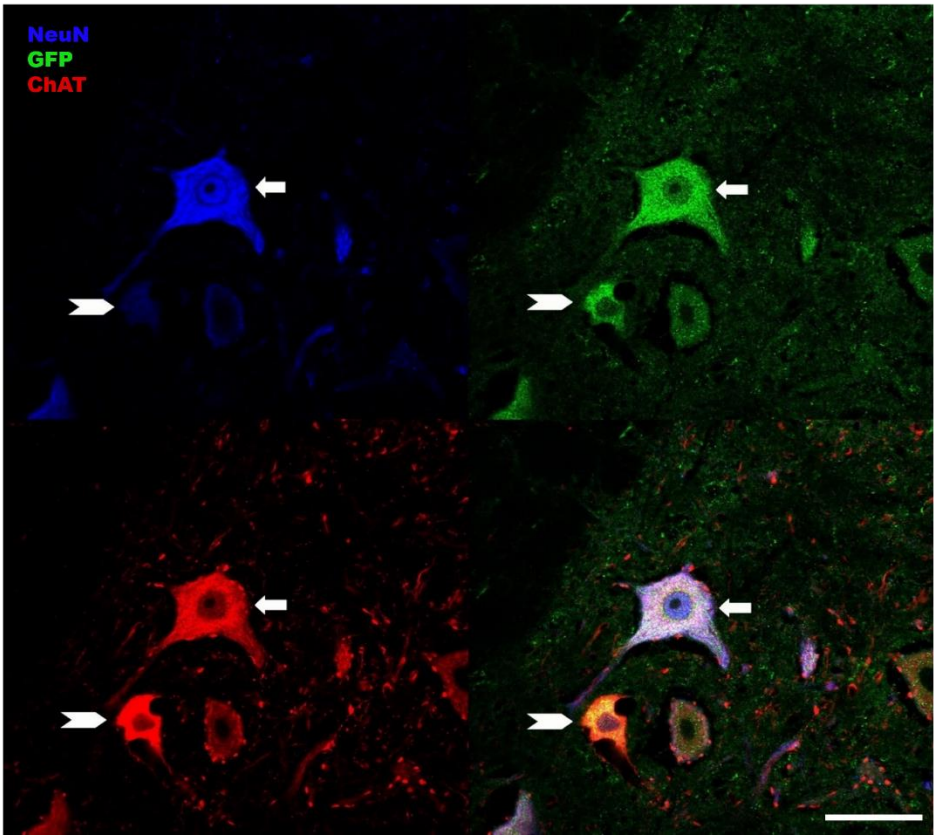

Figure 4.6 AAV-Err3-GFP intramuscular and intraspinal injections

An AAV viral vector with an Err3 promotor and a GFP insert was created by GenoCopoeia (A). The AAV successfully transduced SKOV3 cells with GFP (B). Six animals were injected in different locations with an array of viral concentrations (C). AAV-Err3-GFP successfully transduced MNs after intramuscular injection (D). However, both α-MNs (white arrow) and γ-MNs (white chevron) were transduced. Blue = NeuN, Green = GFP, Red =ChAT. Scale bar = 50 µm

4.4 Targeting ɣ-MNs using AAV-5ht1d-GFP

After the unsuccessful AAV-Err3-GFP targeting, we turned to the 5-HT_{1D} receptor. This receptor was found to be selective for ɣ-MNs by Enjin et al. (2012). They screened small MNs in the motor columns using the GENSAT database (http://www.gensat.org). A mouse line with GFP expression in 5-HT_{1D} expressing cells was found and *In situ* hybridisation discovered 5-HT_{1D} in small MNs of cranial motor pools. 5-HT_{1D} was found in cells in the abducens nucleus, which has ɣ-MNs, while it was not found in motor pools of the nucleus facialis which do not have ɣ-MNs. Early growth response 3 (Egr3) knockout animals lack muscle spindles and ɣ-MNs (Tourtellotte et al., 2001). In the study by Enjin et al. (2012), these Egr3 KO mice had greatly reduced numbers of 5-HT_{1D} positive cells, (~1 neuron per motor pool in Egr3 KO compared to ~11 in wild type mice). The evidence above suggests that 5-HT_{1D} is specific to ɣ-MNs in mice. Therefore, we decided to pursue this as a target for the next AAV experiments.

4.4.1 *In situ* hybridization probe production

Because of earlier trouble with on-specificity of targeting, we decided to confirm that 5-HT_{1D} is also specific to ɣ-MNs in rats. To do this, *in-situ* hybridisation was performed in combination with immunohistochemistry. A labelled RNA probe was created and the process for doing so is shown in Figure 4.7A. Methods were similar to those of Knoth et al. (2010) and are described below.

The Isolate II RNA mini kit (Bioline USA) was used to extract RNA from the rat olfactory bulb. First, 30 mg of tissue was homogenised with a scalpel blade and a large syringe. Then 600 µl of lysis buffer RLY was added to the sample before vortexing and further homogenisation with a syringe. Lysate was filtered by centrifuging at 11,000 g (g = centrifugal force of gravity) for one minute on a filter column, all centrifuge steps were

performed at 11,000 g unless otherwise stated. 600 µl of 70% ethanol was added before lysate was added to a binding column and centrifuged for 30 seconds. 350 µl of membrane desalting fluid was added to the column before centrifuging for a further 30 seconds. 100 µl of DNase I in reaction buffer was applied to the column and left to incubate at room temperature for 15 minutes. In order to inactivate the DNase, 200 µl of wash buffer 1 was added to the column and the sample was centrifuged for 30 seconds. 600 µl of wash buffer 2 was added before another centrifuge for 30 seconds. A final 250 µl of wash buffer 2 was added and the sample was centrifuged for two minutes. To elute the RNA, 60 µl of distilled H_2O was added to the column before centrifuging for 1 minute. The Nanodrop 2000 (Thermo Fisher, USA) was used to measure RNA concentration at 491 ng/µl and a 260:280 ratio of 2.0 indicating pure RNA.

cDNA was created from extracted RNA using the Tetro™ cDNA synthesis kit with MMLV reverse transcriptase with oligo $(dT)_{18}$ (Bioline, USA). For this process 4.9 µg of extracted RNA from above was added to 1 µl 10 mM of deoxynucleoside triphosphate (dNTP) mix, 4 µl of 5x reaction buffer, 1 µl of RNase inhibitor and 1 µl of 200 units/µl Tetro reverse transcriptase. Diethyl pyrocarbonate treated (DEPC) distilled H_2O (dH_2O) was added to top the reaction up to 20 µl before the sample was left to incubate for 30 minutes at $45^{O}C$. The reaction was terminated by leaving for five minutes at $80\ ^{O}C$ and the samples was then stored at $-20\ ^{O}C$.

The primers used for probe production were TCTTCACTCTGCTCGCTCAA forward and ATGGGGAGGACCAAGGATAC reverse for a probe with nucleotides 742-968 from the $5HT_{1D}$ gene (Genbank accession number NM_012852.1). The MangoTaq™ DNA polymerase kit (Bioline, USA) was used for polymerase chain reaction (PCR). A 50 µl reaction was set up with 10 µl or 5x reaction buffer, 1.5 µl of 50 mM $MgCl_2$, 5 µl of 10 mM dNTP mix, 1 µl of 20 µM forward primer, 1 µl of 20 µM reverse primer, 1 µl of 5 units/µl Mango Taq DNA polymerase, 1 µl of .5 µg/µl cDNA template from above, with 29.5 µl of dH_2O added to top the reaction up to 50 µl. The PCR mix was denatured for 5 minutes at 95ºC before 35 cycles of 30 seconds at 95ºC for denaturation, 30 seconds at 56ºC for annealing, and 30 seconds at 72ºC for elongation. The final annealing step was for 10 minutes at 72ºC.

The PCR product was run on a 1% agarose gel in Tris-acetate-Ethylenediaminetetraacetic acid (EDTA) (TAE) buffer with .02 % ethidium bromide for DNA detection. The gel containing the correct band of 226 base pairs was extracted and DNA was purified from this using the QIAquick Gel Extraction Kit (Qiagen, Germany). 1200 µl of a high salt buffer was added to 400 mg of extracted agarose gel and left for 10 minutes at 50^{o}C before 400 µl of isopropanol was added in order to precipitate the DNA. The mixture from above was added to the silica membrane from the kit. After centrifuging for 1 minute at 13,000 g, a further 500 µl of high salt buffer was added before another 1 minute centrifuge at 13,000 g. A further wash in 750 µl of a different buffer was completed before centrifuging for 1 minute at 13,000 g, discarding of waste, and another identical centrifuge. To elute the DNA 40 µl of dH_2O was added to the column and this was left for five minutes at room temperature before centrifuging for 1 minute.

The product from the gel extraction above was then added to a new PCR identical to that above. The only differences were in the different primers and the cDNA template from above replaced by the gel extraction product. The primers for the new PCR included the promotor sequences for SP6 and T7 RNA polymerases on the forward and reverse primers respectively. The SP6-forward sequence was ATTTAGGTGACACTATAGATCTTCA-CTCTGCTCGCTCAA, and the T7-reverse sequence was TAATACGACTCACTATA-GGATGGGGAGGACCAAGGATAC. The product of this PCR was then run on an identical gel to that above, and the band containing the DNA with the SP6/T7 primer sequences was extracted and purified in the same process as that above. The product was sequenced by Genewiz (Germany) which confirmed that the correct sequence was produced with no mutations.

The SP6/T7-Polymerase Digoxigenin (DIG) Labeling and Transcription Kit" (Roche Diagnostics, Germany) was used to create the RNA probe. To start, 13 µl of 79 ng/µl DNA with SP6/T7 primers from above was used as the template. 2 µl of 10x NTP labelling mix (10 mM ATP, 10 mM CTP, 10 mM GTP, 6.5 mM UTP, 3.5 mM DIG-11-UTP) was added with 2 µl of 10x transcription buffer and 1 µl of RNase inhibitor. Finally, 2 µl of either SP6 or T7 RNA polymerase (20 units/µl) was added to create the sense (control), or antisense probes respectively. These reactions were incubated for 2 hours at 37^{o}C, before 2 µl DNase

I was added to remove the template and 2 µl of EDTA was added to stop the reaction. The product of this reaction was then run on a gel to confirm successful probe creation.

To further purify the product from above it was run through the same RNA extraction protocol with the Isolate II RNA mini kit (Bioline USA). Briefly, the reaction from above was added to 60 µl of dH_2O, 300 µl of lysis buffer and 300 µl of 100% ethanol before being added to a binding column and centrifuged for 30 seconds. 350 µl of membrane desalting fluid was added to the column before centrifuging for a further 30 seconds. 200 µl of wash buffer 1 was added to the column and the sample was centrifuged for 30 seconds and 600 µl of wash buffer 2 was then added before another centrifuge for 30 seconds. A final 250 µl of wash buffer 2 was added and the sample was centrifuged for two minutes. To elute the probe, 40 µl of distilled H_2O was added to the column before centrifuging for 1 minute. The Nanodrop 2000 (Thermo Fisher, USA) was used to measure probe concentration at 370 ng/µl and control (SP6) sense probe at 140 ng/µl.

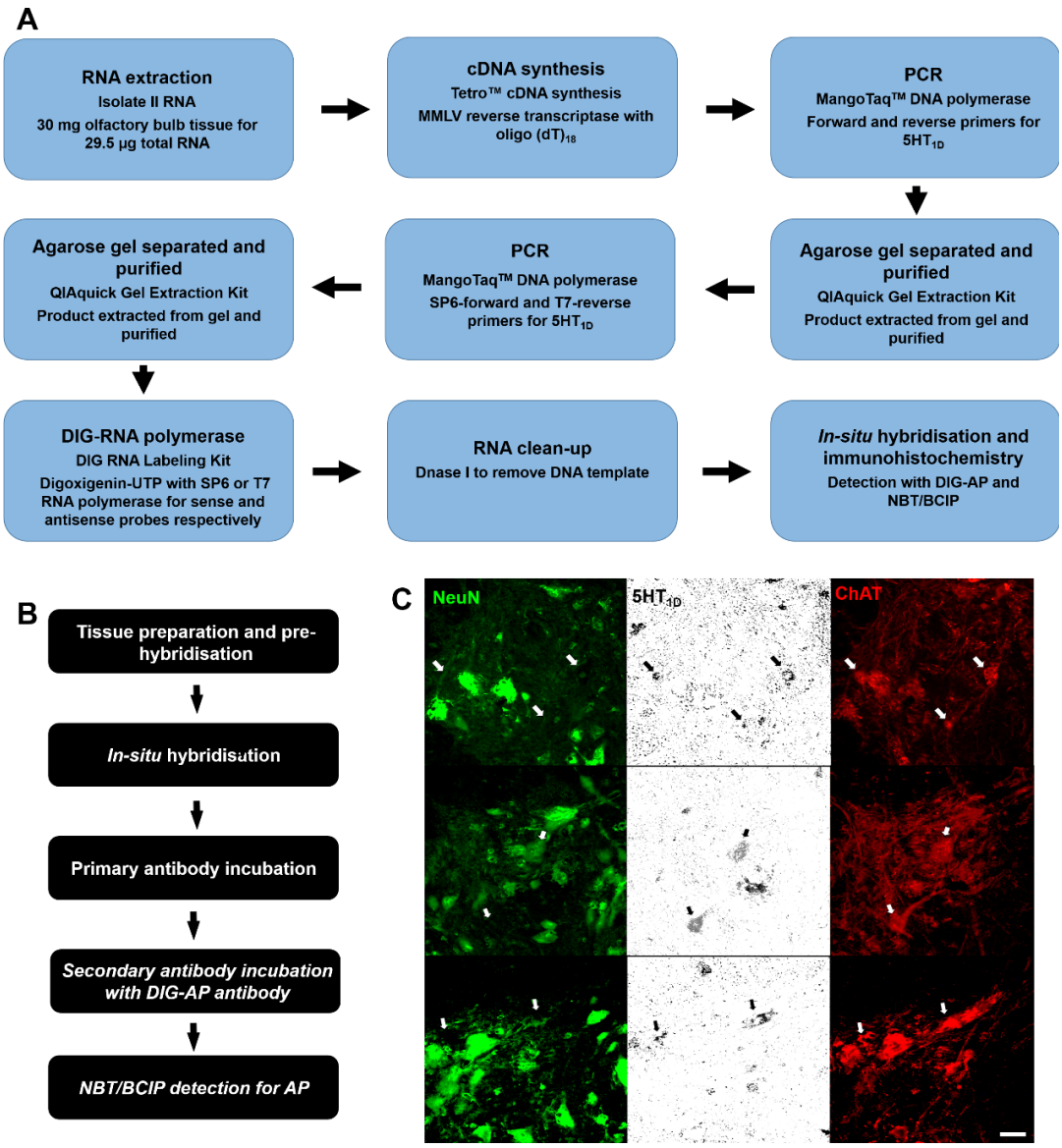

Figure 4.7 DIG-labelled probe production and *in-situ* hybridisation
A $5HT_{1D}$ DIG labelled probe was produced from olfactory bulb total RNA (A). In-situ hybridisation and immunohistochemistry (B) confirmed that $5HT_{1D}$ mRNA was mostly present in presumed γ-MNs (C). Scale bar = 50 µm

4.4.2 *In-situ* hybridization confirms 5ht1d is specific for gamma motor neurons

The protocol for *In-situ* hybridisation was similar to those of Knoth et al. (2010) and the major steps are outlined in Figure 4.7B. A single adult (200g) Sprague Dawley rat was perfused, and the tissue processed as per the methods chapter. The only difference was that spinal sections were placed directly on glass slides (SuperFrost Plus™, Fisher Scientific, UK) which were stored at -80°C. All buffers for perfusions, tissue processing, hybridisation

and immunostaining were prepared with sterilised and autoclaved .01% DEPC treated water to destroy any RNase which could undermine the protocol.

The following steps were all completed at room temperature unless otherwise stated. Slides were removed from the -80^{o}C freezer and left for 1 hour to thaw. Slides were then washed with PBS three times ten minutes (3x10) before permeabilization with 0.5% PBST and washed again three times ten minutes in PBS. Triethanolamine (1.4%) and acetic anhydride (0.25%) in dH_2O were added for ten minutes to repress non-specific structure formation before washing 3x 10 minutes in PBS. Slides were then left in pre-hybridisation mixture consisting of 50% formamide, and 50% 5x standard saline citrate buffer (SSC) (0.015 sodium citrate [pH 7.0], 0.15 M NaCl)) for two hours at 60^{o}C. Formamide lowers the melting point and annealing temperature of RNA to increase hybridisation rate and lower denaturation. The hybridisation solution consisted of 50% formamide, 25% 20x SSC, 20% blocking reagent from the DIG Nucleic Acid Detection Kit (Roche Diagnostics, Germany), 1% 0.5 mM EDTA, 0.1% Tween-20, 0.2% 200 µg/ml salmon sperm DNA, 0.5% CHAPS with topped up sense or anti-sense DIG-labelled probes at a final concentration of 0.5 µg/ml. 300 ul of hybridisation solution was placed on each slide and the slides were left overnight at 60^{o}C. The slides were then washed 2x15 minutes in 2x SSC at 60^{o}C, and then 1x15 minutes at room temperature in 0.1 x SSC. Slides were washed 2x10 minutes in PBS before proceeding to immunohistochemistry and detection steps.

Primary antibodies against ChAT (goat) and NeuN (rabbit) were used for triple staining the sections. First, slides were incubated overnight in 1:250 ChAT in PBS at 4^{o}C, then one further night in 1:250 ChAT and 1:500 NeuN in PBS at 4^{o}C. Sections were washed 3x10 minutes in PBS before a further 30 minutes in 1% blocking reagent from the DIG Nucleic Acid Detection Kit in Maleic acid buffer (0.1 M Maleic acid, 0.15 M NaCl; pH 7.5 adjusted with NaOH). Further antibodies were added to the 1% blocking reagent in Maleic acid buffer. These antibodies were 1:1000 anti-digoxigenin-alkaline phosphatase (Roche, Germany), 1:250 anti-goat-555 and 1:250 anti-rabbit-488. Sections were washed 3x10 minutes in PBS, and then 10 minutes in detection buffer (0.1 M Tris-HCl, 0.1 M NaCl, pH 9.5) to increase the pH. NBT/BCIP tablets (Roche, Germany) were used for detection. BCIP is an alkaline phosphatase substrate, after dephosphorylation BCIP is

oxidized by NBT to form a dark water insoluble indigo dye. The detection solution was left on the slides for two hours until clear staining was visible on the non-control slides. Sections were washed 2x10 minutes in PBS and then 2x10 minutes in TNS before mounting with Fluorsave (Merck, Germany).

Images were taken at 10x magnification on the fluorescence microscope (Nikon Eclipse E600) with Micro publisher 5.0 RTV used to take images and Aquis 2.0 software used for settings adjustments. Results showed that 5-HT_{1D} was present in ɣ-MNs and did not appear to be present in α-MNs (Figure 4.7C). Thus, we proceeded with plans for an AAV with a $5HT_{1D}$ specific promotor.

4.4.3 AAV-5ht1d injections

A $5HT_{1D}$-YFP plasmid was prepared by Dr. Melissa Andrews, from a sequence created by GenoCopoeia (USA). The AAV was produced by Viogene Biosciences (USA) who inserted the plasmid into the AAV-DJ serotype.

For the first experiment, 4 x 1.5 µl of $1x10^{12}$ genome copies/ml injections were made into the left gastrocnemius of two Sprague Dawley rats (Figure 4.8A). Animals were left for two weeks before perfusion and tissue preparation as per the methods chapter. Immunostaining with antibodies against ChAT, NeuN, and GFP (methods for this triple staining in section 4.3.3) revealed that no MNs were transduced by the injections (Figure 4.8B).

This lack of transduction with a 1:10 dilution of the AAV led us to use a higher concentration of AAV ($1x10^{13}$ genome copies/ml). We injected the AAV intraspinally to determine if the intramuscular point of entry did not allow CNS transduction with this virus. After two weeks animals were sacrificed and perfused as per the methods chapter with immunostaining as above. No MNs were transduced after intraspinal injections, and staining of any cells with GFP was sparse.

We then trialled a longer transduction time, this time waiting 4.5 weeks before perfusions and tissue preparation. Intraspinal or intramuscular injections with the higher concentration AAV ($1x10^{13}$ genome copies/ml) left for four and half weeks revealed no improvement in MN transduction (Figure 4.8C). Our viral concentration was higher and

our transduction time longer than other studies using intramuscular injections for tracing (Chen et al., 2020). Therefore neither the transduction time or viral concentration appear to be the problem.

The reason for this lack of transduction could be the lower levels of 5-HT_{1D} mRNA in cells as compared to other promotors such as CAG and CMV which are both highly expressed in all neurons. The targeting of individual neuron types by AAVs with specific promotors does not appear to be a widespread technique, with more universal and highly expressed cellular promotors normally used (Nieuwenhuis et al., 2021). Studies often use universal promotors with spatially defined regions of interest to target their neurons of interest (Stepien et al., 2010). Unfortunately, due to the colocalization of γ and α-MNs in the spinal cord, this method is unavailable to us. Other studies have used AAVs to target cells by their birth date (Deshpande et al., 2013, Arenkiel et al., 2011). Many other studies have targeted individual cell types via cell specific Cre recombinase expressing mouse lines with Cre dependant AAVs (reviewed by Callaway and Luo (2015)). This method is also unsuitable for our goals as there are no relevant Cre lines available with rats. There is one study virally targeting cells by receptor subtype. However, the study used a special bridge protein with the avian viral receptor TVB fused to the ligand for the specific receptor where the TVB receptor allowed a EnvB-pseudotyped virus to transduce only the cells of interest (Choi et al., 2010). This complex receptor-bridge protein technique is not currently viable for this project. Future studies using Cre mice with Cre dependent AAVs could be an option, even if the benefits of working with non-genetically altered rats are lost.

A

Animal	Dilution	Location and volume of injection	Transduction time
1	1:10	Left gastrocnemius 4 x 1.5 µl	2 weeks
2	1:10	Left gastrocnemius 4 x 1.5 µl	2 weeks
3	Pure	Thoracic intraspinal bilaterally .5 mm from midline 1.0 mm deep. 2 x .5 µl	2 weeks
4	Pure	Right gastrocnemius 4 x 1.5 µl Cervical intraspinal bilaterally .5 mm from midline 1.0 mm deep. 2 x .5 µl	4.5 weeks
5	Pure	Right gastrocnemius 4 x 1.5 µl	4.5 weeks

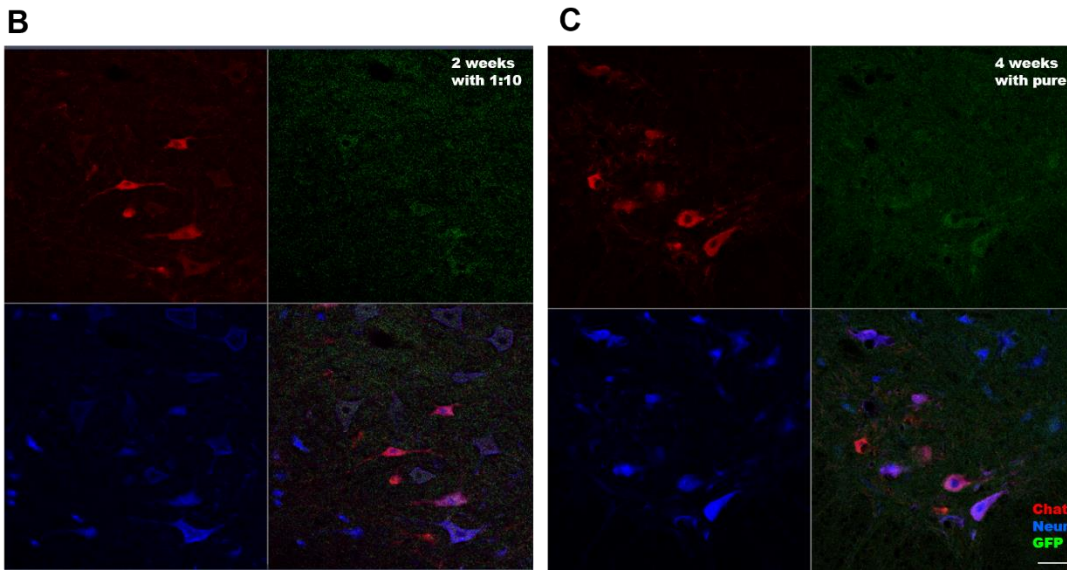

Figure 4.8 AAV-5HT$_{1D}$-YFP not transduced by MNs
AAV-5HT$_{1d}$-YFP was injected into the gastrocnemius of two animals and left for two weeks (A). After the AAV was not successfully transduced (B), more experiments were carried out (A). These experiments were similarly unsuccessful at transducing MNs (C). Scale bar = 50 µm

4.5 Targeting ɣ-MNs via the small nerve branch of the soleus

Attempts to create a ɣ-MN specific AAV were unsuccessful using either Err3 or 5-HT$_{1D}$. As mentioned previously, many AAV/rabies virus tracing attempts use location based targeting (Stepien et al., 2010). That method is unavailable to us due to the colocalization of ɣ and α-MNs. However, some anatomical separation may be possible. One study found that a branch of the rat soleus muscle nerve contained ɣ, but not α-MNs (Vult von Steyern et al., 1999). A proximal thin branch diverged from the main nerve prior

to entry, this branch was confirmed to contain ɣ but not α-MNs by anterograde and retrograde tracing. The lack of extrafusal muscle activity from the small proximal nerve branch was confirmed by electrical stimulation of the nerve after the larger distal nerve had been cut. One point about the above study is that retrograde tracing of ɣ-MNs was only completed by aspirating the small branch with a glass pipette filled with dextran dyes. Muscle injections with the large branch severed were not completed. Our method to trace ɣ-MN inputs require intramuscular injections rather than nerve preparations. This is because the rabies virus transduction requires more time than is available to keep an anaesthetised preparation going. Thus we have investigated the possibility of selectively tracing ɣ-MNs by cutting the large distal branch of the soleus and injecting tracers into the soleus.

4.5.1 Surgeries and immunohistochemistry

Animal were anaesthetised with isoflurane as per the methods chapter. Adult male Wistar rats were used for experiments as these were the same animals used by Vult von Steyern et al. (1999). A small skin incision was made and muscles were blunt dissected with one thin layer of the Gastrocnemius cut to expose the soleus muscle. The large branch of the soleus nerve was first tied with two sutures (Ethilon 9.0, Ethicon, USA). There was one suture close to the muscle and one close to the nerve bifurcation before the large branch was then cut between these sutures and 3M Vetbond Tissue Adhesive (3M, USA) was applied to both the cut ends of the large nerve branch (Figure 4.9A). Varying amounts of 1% CTB or 1 % fast blue were injected into the muscle using a Hamilton syringe (Hamilton Company, USA) under manual pressure (Figure 4.9B). The needle was left for two minutes after injection and the area was dried with a cotton bud following needle removal. 3M Vetbond Tissue Adhesive (3M, USA) was applied to the injection site and the fascia and skin incision of the animal was sutured. Animals received the normal post-operative care and were perfused 48-72 hours later as per the general methods.

Immunohistochemistry for all spinal sections was performed on free floating tissue as per the general methods. Primary incubation included antibodies against ChAT (48 hours), NeuN (24 hours), and CTB (24 hours) (Rabbit. Sigma, USA). Secondary antibodies were anti-goat-488, anti-rabbit-555, and anti-mouse-647 for unconjugated CTB injections. For

fast blue injections or other pre-conjugated CTB injections no CTB immunohistochemistry was completed, and non spectrally overlapping secondary antibodies anti-goat-488 or anti-goat-555 were used depending on the conjugated CTB. Imaging took place on the LSM 880 (Zeiss) at 20x.

A

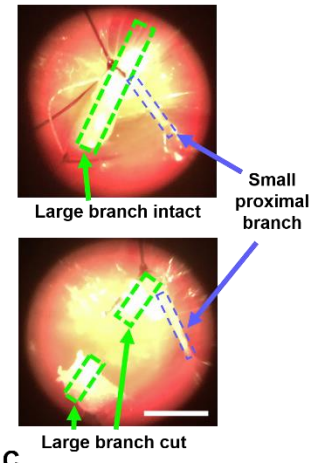

B

Animal	Time left	Injections	α or γ-MNs
1	72 hr	Left soleus 3 µl CTB	γ-MNs
2	72 hr	Left soleus 3 µl CTB	α and γ-MNs
3	72 hr	Left soleus 3 µl CTB	α and γ-MNs
4	72 hr	Left soleus 2 µl fast blue (1%), right soleus 3 µl CTB	α and γ-MNs
5	72 hr	Left soleus 2 µl fast blue (1%), right soleus 3 µl CTB	γ-MN in left
6	72 hr	Left soleus 3 µl fast blue (1%) and 2 µl of CTB-555, right soleus 3 µl CTB-488	α and γ-MNs
7	72 hr	Left soleus 3 µl fast blue (1%) and 2 µl of CTB-555, right soleus 3 µl CTB-488	γ-MN in left CTB-555
8	72 hr	Left soleus 3 µl fast blue (1%) and 2 µl of CTB-488, right soleus 3 µl CTB-555	α and γ-MNs
9-11	48 hr	Right soleus 3 µl CTB	α and γ-MNs

C

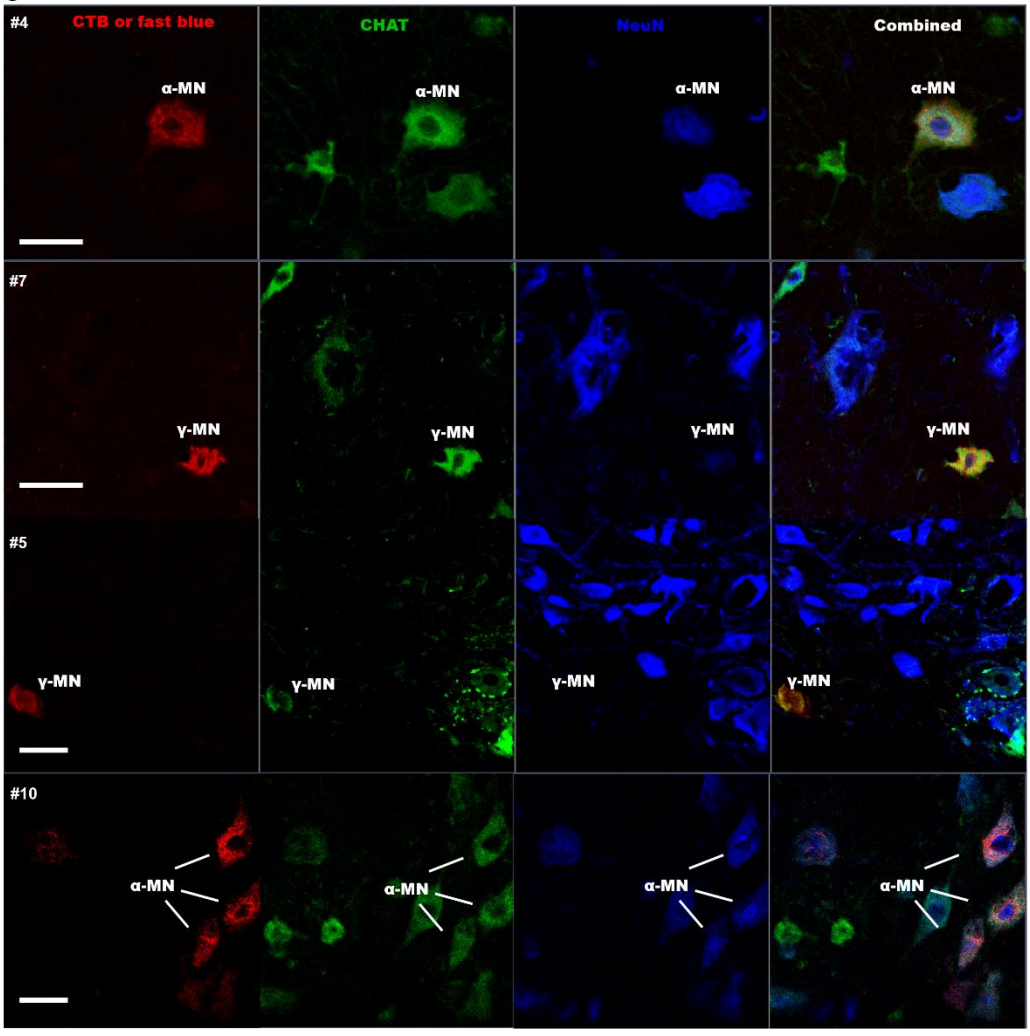

Figure 4.9 Soleus injections with distal branch cut and tied

The soleus nerve large distal branch was cut and tied (A). Injections with either CTB, conjugated CTB-488, conjugated CTB-555 or fast blue were injected into the soleus (B). Some animals had few α and ɣ-MNs traced following CTB

injections (C #4), others had ɣ-MNs only following CTB injections (C #7), or fast blue injections (C #5). Other animals had many neurons stained indicating more extensive staining potentially through other nerves or muscles (C#10). Scale bar in A = ~1 mm, scale bar in C = 50 µm.

4.5.2 Soleus small nerve branch tracing results

Small branch soleus tracing showed mixed results. Some animals had only γ-MNs traced from CTB or fast blue injections (animals #1, #5, and #7) (Figure 4.9C #5 fast blue, and #7 CTB). While many of the other animals had both α and γ-MNs labelled (Figure 4.9C #4 and #10 CTB). Why this is the case is not entirely evident. There are some anatomical differences between animals and the nerve is not always exactly the same. Vasculature and nerve branch structure vary considerably between animals. Possible leakage of intramuscular tracer is possible. It is known that damaged nerves are quite efficient at retrograde transfer (Todorova and Rodziewicz, 1995), so any small leakage may be quickly picked up by the proximal end of the cut large nerve branch. The current surgeries were completed with several precautions, the nerve was separated and cut, with care taken so as not to damage the muscle. Sutures and glue were used to prevent reconnection and accidental tracer uptake via the cut proximal end of the large branch. The injection needle was left for two minutes following tracer delivery to minimise any leakage, and the area was dried with cotton buds after.

Further surgeries may lead to more reliable results, however, rabies virus tracing is currently most effective in young animals (Callaway and Luo, 2015). The combined low success rate in adults in the current experiments, and potentially more difficult surgery in young rats with smaller nerves means that this method may need some more refining before the next steps are taken. This method would also only allow us to access one muscle which has lost its motor innervation, thus any studies of function would be limited. This method would, however, allow us to determine the inputs to γ-MNs through rabies virus tracing, therefore this avenue should continue to be pursued.

4.6 Discussion

To avoid repetition, there is no large discussion of the individual results from the different sections. To summarise the results, we have investigated the proportion of γ-MNs

across various muscles. There is a higher proportion of γ-MNs in flexors, and in hindlimb muscles, as compared to extensors and forelimb muscles. We have demonstrated the lack of γ-MN specificity of both an antibody against Err3, and an AAV with an Err3 promotor. The presence of 5-HT_{1D} mRNA in γ but not α-MNs of the rat has been confirmed. However, an AAV with a 5-HT_{1D} promotor does not transduce γ-MNs. We have also opened up a new avenue to selectively target γ-MNs by intramuscular injection in the soleus. These studies could lead to future experiments studying the innervation of γ-MNs if the technical difficulties of isolating γ-MNs alone can be resolved.

If γ-MN targeting is possible in the future, there are many avenues for further experiments. After the initial modified rabies tracing experiment, the plan was to create an inducible knockout for ɣ-MNs. An inducible silencing technique is necessary in order to study the role of different spinal network components. This is because transgenic knockouts have many developmental compensatory mechanisms which cloud the study of the true role of the component which has been knocked out. This has been demonstrated clearly in a congenital knockout involving Renshaw cells (Enjin et al., 2017b). In that model the spinal network was able to compensate for the lack of Renshaw cell activity in numerous ways, including reduced α-MN excitability and an increased number of proprioceptive afferent synapses on α-MNs. If this compensation is to be avoided in future studies then inducible knockouts will need to be used. Introducing diphtheria toxin receptors (DTR) into ɣ-MNs is one way of accomplishing this. Crossing a Cre inducible DTR transgenic mouse, (Buch et al., 2005), with a mouse which expresses Cre in only ɣ-MNs is a way this may be possible. The mutant mouse would express DTR in only ɣ-MNs, subsequent injections with diphtheria toxin would lead to the acute knockout of ɣ-MNs. This method would require the use of mutant mice which do not yet exist.

Another method which could be used to study the function of ɣ-MNs is using a designer receptor exclusively activated by a designer drug (DREADD) such as the receptor used in this study (Armbruster et al., 2007) which may be inhibitory or excitatory. The AAV would selectively insert a specific receptor into ɣ-MNs, this receptor would only be activated by specific non-endogenous drugs to turn off or on ɣ-MNs. In this way it would be possible to examine the changes in locomotion with and without ɣ-MN activity. This

could also be used to test the role of ɣ-MNs in motor learning, and spinal cord injury recovery. Introducing channelrhodopsin/halorhodopsin into the cell using an AAV to optogenetically control the cell is also a possibility (Rogan and Roth, 2011). However, due to the presence of large amounts of myelin in the spinal cord the light source would have to be very close to the target area, which would most likely preclude any chronic or awake studies of the role of ɣ-MNs in normal locomotion or learning. While we were unable to investigate these further, our experiments have opened up the possibility of further tracing studies using the soleus. Our negative results with potentially γ-MN specific AAV targeting suggests this may not be a viable method to selectively study the circuitry and function of γ-MNs.

5 General discussion

The two main experimental chapters on SCI and γ-MNs are not obviously connected. However, there are many reasons to think γ-MNs are important in locomotor recovery from SCI. I will first discuss these links before moving to more general theories of activity dependent plasticity and motor learning after SCI. To conclude I will discuss theories of motor learning in relation to γ-MNs.

5.1 Link between SCI and γ-MNs

The role of γ-MNs is to modulate sensory feedback by increasing the firing rate or the stretch sensitivity of spindle afferents. There is a clear and vital role for these spindle afferents in endogenous as well as intervention mediated locomotor recovery. The specific role of γ-MNs in recovery is currently unclear, but the importance of spindle afferents is clear and their control of these afferents suggest an important role for γ-MNs as well.

Clear evidence of spindle afferent contribution to recovery after SCI was demonstrated by Takeoka et al. (2014). The study demonstrated that mice without muscle spindles were unable to recover their locomotor function after a unilateral hemisection. In the above study lack of spindle afferent input not only inhibited locomotor recovery, but also restricted new circuit formation of descending reticulospinal fibres and of new propriospinal pathways. This lack of circuit formation is important as the reticulospinal pathway is a key target for locomotor recovery (Zörner et al., 2014), as are propriospinal detour circuits (Bareyre et al., 2004). The need for spindle afferent feedback was again confirmed by Takeoka and Arber (2019). The study found that proprioceptive afferent deletion inhibited recovery to the same extent as deletion of muscle spindles (Takeoka et al., 2014). The need for proprioceptive afferents both during and after recovery was demonstrated, as deleting afferents after full recovery at 7 weeks fully reversed locomotor recovery to a similar extent to the afferent deletion before the SCI (Takeoka and Arber, 2019). Propriospinal detour formation, however, did not change after the afferent deletion at 7 weeks. Thus indicating that following SCI there is an earlier stage where afferents can drive descending propriospinal plasticity.

Sensory feedback is also vital for training and ES mediated recovery. Again, while we are unsure of the role for γ-MNs in this, their control of the sensory spindle afferents mean they are likely important. The afferent dependence of ES was demonstrated by its inability to elicit stepping in spinally transected rats if sensory feedback is eliminated (Lavrov et al., 2008). Further modelling studies have proposed that large myelinated axons are the primary target of ES (Capogrosso et al., 2013). Increasing the sensitivity of afferents to sensory input from stepping/treadmill training is a key role of ES. As ES does not lead to stepping without sensory stimulation via paw placement on a treadmill (Ichiyama et al., 2005).

Primary spindle afferent activity also leads to other locomotor network changes. Ia afferent activity leads to an increase in P boutons mediating pre-synaptic inhibition (Mende et al., 2016). Pre-synaptic inhibition, first discovered by Frank and Fuortes (1957), is inhibition of Ia afferents on MNs. Pre-synaptic inhibition is increased during training of a visuo-motor task (Perez et al., 2005), and deletion of the 'GABA pre' neurons mediating this inhibition leads to errors and muscle oscillations during reaching (Fink et al., 2014). Locomotor training with 5-HT agonists, probably via sensory afferent activity, leads to an increase in the pre-synaptic inhibitory contacts of these GABA pre neurons (Khalki et al., 2018). There is clearer evidence suggesting afferent activity, (and thus potential γ-MN control), is needed for training induced modulation of the pre-synaptic inhibitory circuitry. Frequency dependent depression of the H-reflex is due to pre-synaptic inhibition, and this depression is lost after a SCI in humans or animals (Schindler-Ivens and Shields, 2000, Thompson et al., 1992). After spinal transection in a rat, cycle training returns this frequency dependent depression, but only if afferent activity is not inhibited during training (Ollivier-Lanvin et al., 2010).

As seen above, afferent activity has a large variety of impacts on spinal cord circuitry and behavioural recovery after SCI. The control of γ-MNs over this circuitry implicates them in detour circuit formation, supraspinal synaptic circuit formation, ES mediated recovery, training mediated recovery, and changes in pre-synaptic inhibitory circuitry. The exact role of γ-MNs in these processes is currently unknown, but their actions on muscle spindles and afferents suggest a role in the afferent activity dependent plasticity. γ-MNs

have been shown to increase afferent activity in an amyotrophic lateral sclerosis model (SOD1 mutants) whose MNs progressively degenerate (Lalancette-Hebert et al., 2016). Mice without muscle spindles, and thus no afferents to excite them, have less MN death. Further, selective deletion of half the population of γ-MNs resulted in a longer lifespan for the SOD1 mice. This is suggested, but not proven to be due to the reduction in afferent activity caused by γ-MNs. There is no direct study of this in animals with SCI, but it seems likely that γ-MNs play a similar role here, namely increasing afferent activity to MNs. However in the case of SCI, the increased afferent activity is mediating positive spinal circuitry changes and behavioural improvements.

The diffuse supraspinal and segmental inputs to γ-MNs (reviewed in the introduction Chapter 1) also suggest that they may be especially important following SCI. If specific supraspinal pathways are severed, then separate control of γ-MNs could allow for spared supraspinal input to activate the locomotor circuitry via γ-MNs rather than α-MNs. There is also some evidence to suggest γ-MNs have more synaptic plasticity potential and thus may present a good target for circuitry reorganization after injury. γ-MNs lack plasticity restricting perineuronal nets which are present on α-MNs in the spinal cord, and which increase after SCI (Smith et al., 2015, Al'joboori et al., 2020). After a neonatal transection there was a decrease in synaptic coverage on γ, but not α-MNs, with training found to restore much of this synaptic coverage loss (Ichiyama et al., 2011). We have also observed a reduced amount of Nogo-A in γ compared to α-MNs following SCI (unpublished observations), thus providing further indication of their potential for neural plasticity. To summarise, γ-MNs control the vital sensory afferents, are more plastic, and have separate control potentially leaving them with supraspinal control even when supraspinal control of α-MNs is limited. Taken together this suggests γ-MNs are an integral part of circuit reorganisation and recovery after SCI. Unfortunately, as we were unable to individually target γ-MNs and study their inputs before and after circuit reorganisation, we have not yet determined if this is the case.

5.2 Activity dependent plasticity after injury

Evidence suggests activation γ-MNs lead to enhanced spindle afferent activity, and that this activity is necessary to reconfigure spinal circuitry after injury. Given our somewhat modest synaptic changes and behavioural recovery, it is worth investigating under what conditions this enhanced sensory input leads to behavioural recovery and synaptic plasticity. From the evidence it appears the timing of intervention is key, and our activity based therapy may be happening after the critical period for neural plasticity is over.

During neural development much of the circuitry is guided by various transcription factors with gradients of chemoattractants and chemorepellents (Introduction section 1.2.2). However, activity dependent circuit formation is also evident for certain descending pathways such as the CST. Evidence for CST activity dependant plasticity comes from cat developmental studies inhibiting either the motor cortex or specific muscles (Martin et al., 2007). There is a loss of stable synaptic connection between the motor cortex and motor neurons by inhibiting either one or the other during critical periods of development. Activity dependent plasticity in development is well evidenced, however this plasticity declines in adults. After development there is an upregulation of plasticity inhibiting molecules such as Krüppel-like factor-4, and a downregulation of plasticity enhancing pathways such as the mTOR pathway (He and Jin, 2016). Following a spinal dorsal column lesion, the transcriptional state of many neurons is returned to a developmental phenotype (Poplawski et al., 2020). In the above study there was a transient increase in levels of cAMP mediated signalling, mTOR signalling, and mitogen-activated protein kinase (MAPK) signalling, which was then reduced by day 21 following injury.

This activity dependent plasticity during the critical period appears to be mediated by NMDA receptors. These receptors are critical for cortical organisation and without them mice somatosensory cortex layer IV granule cells do not aggregate to their normal ‘barrels’ (Iwasato et al., 2000). Cortical neuron dendritic density is also reduced in mice lacking NMDA receptors (Ultanir et al., 2007). NMDA receptor deletion in descending propriospinal neurons restricted the cortical synapse formation which normally occurs after unilateral hemisection (Bradley et al., 2019). A downstream effector of NMDA receptor

activity is CREB, and inhibition of CREB in descending propriospinal neurons also decreases the number of these cells receiving new cortical connections after a lateral hemisection (Bradley et al., 2019). The nogo-Δ20 unit of Nogo-A reduces CREB levels, thus inhibition of Nogo-A should lead to enhanced plasticity via this mechanism as well as its other well documented effects on the Rho/ROCK pathway. Both ES and training lead to activation of this pathway via their direct increase of neuronal activity and via their action to increase BDNF. Dendritic BDNF application leads to long term potentiation and Ca^{2+} transients in a process that also requires NMDA receptors (Kovalchuk et al., 2002). Thus all three of 11C7, training, and ES indirectly act on activity dependent pathways to increase neural plasticity.

The importance of activity dependent plasticity during the critical period after SCI (Poplawski et al., 2020) was recently shown by Bradley et al. (2019). In that study the activity of descending propriospinal interneurons was inhibited from days 14-21 following a dorsal hemisection. This inhibition led to decreased CST contacts on these neurons and reduced recovery of locomotion. When these neurons were inhibited in normal animals, or 12 weeks after SCI there was no effect on CST to propriospinal neuron connections. It is not just propriospinal activity which has a time sensitive window to alter descending input connections. After a unilateral hemisection, both CST and propriospinal neurons have reduced post lesion sprouting in mice without proprioceptive afferents, however ablation of these afferents 7 weeks after injury does not alter below lesion sprouting (Takeoka and Arber, 2019). Taken together, these studies suggest a critical period for activity dependant plasticity of both afferents and propriospinal neurons. We have observed some neural plasticity in the form of increased 5-HT and TH sprouting in the TR 11C7 group, modulated VGluT1 in the CB 11C7 groups, and increased 3+ P boutons in the ES 11C7 and CB 11C7 groups. However, the lack of differences between the other groups, and the only subtle differences even in those groups that did change, does suggest we have missed a critical period of plasticity.

5.3 Individual treatments effects on recovery

5.3.1 Anti-Nogo-A therapy

Why 11C7 therapy alone did not improve locomotor recovery is unclear. There are still many questions regarding the role of Nogo-A in axonal growth. The extracellular domain of Nogo-A, Nogo-66, acts on the NgR1 receptor to activate the RhoA pathway, leading to cytoskeletal collapse of neurite outgrowth (Schmandke et al., 2007). Many studies inhibiting Nogo-A or its receptors see increased axonal sprouting and synapse formation (Z'Graggen et al., 1998, Liebscher et al., 2005, Bregman et al., 1995, Chen et al., 2017, Maier et al., 2009, Petrinovic et al., 2013, Wills et al., 2012). There are still many questions about the complex actions of the nogo-Δ20 domain which is internalized into the nucleus, and acts in a more diffuse manner to decrease axonal plasticity via transcriptional changes (Joset et al., 2010). When nogo-Δ20 is internalized there is a decrease in CREB activity in these cells, this activity is directly opposed to that of growth associated factors such as nerve growth factor which increases CREB activity (Cox et al., 2008). Nogo-Δ20 also acts on the sphingosine 1-phosphate receptor 2 (Kempf et al., 2014), and was recently found to act on erythropoietin-producing hepatocellular (EphA4) (Wang et al., 2021), itself a target for axonal regeneration (Goldshmit et al., 2004). Nogo-Δ20 also inhibits microvascular endothelial cells and anti-Nogo-A is pro-angiogenic following stroke (Rust et al., 2019, Wälchli et al., 2013). The many downstream effects of Nogo-A inhibition make understanding how it is reacting with other treatments complex.

Our data on afferent input is in contradiction with another study of 11C7 after SCI (Chen et al., 2017) where 11C7 alone increased afferent sprouting, in our study, 11C7 alone had no impact on afferent input to MNs. Our more severe contusion injury as compared to the more selective partial transection is most likely behind this difference in afferent input. In our study 11C7 therapy and training under ES results in a decrease in afferent input in the CB 11C7 group. There is a general decrease in the number of active cells associated with locomotion following step training under ES (Ichiyama et al., 2008a). The reduced activity observed in the above study could be a function of reduced afferent input that we have observed in our data. The idea of relative synaptic efficacy may be applicable in this situation. This idea was demonstrated in neuromuscular junctions (NMJ) during the

retraction phase of development where fibres innervated by multiple MN axons lose all but one NMJ. If specific MNs have more ChAT (thus more influence on the muscle fibre) than other MNs, they then take over control of the muscle fibre, and those with less ChAT lose their NMJs (Buffelli et al., 2003). This may be happening in our study where the relative activity of certain afferents is leading to a retraction of inactive afferents and thus a lower overall total number of afferent to MN inputs. At this stage this is more theoretical than evidenced, but relative synaptic efficacy has also been observed in other systems (Bradley et al., 2019, Burrone et al., 2002).

In our study 5-HT and TH did not increase with 11C7 therapy alone, but both did increase with sequential 11C7 therapy and training. While one study has shown increased serotonergic sprouting after SCI and 11C7 (Maier et al., 2009), another has not (Chen et al., 2017). This may be due to study timing, as in the latter study animals were trained for longer, and it is possible serotonergic fibre sprouting had been pruned. The difference in 5-HT expression may be due to the tracts spared by each SCI. 5-HT fibres travel through the dorso-lateral and ventro-lateral funiculi (Bregman, 1987). While the T-lesion from the above studies leaves the ventro-lateral funiculus intact, our more severe contusion injury leads to almost complete destruction of this pathway.

We are the first to investigate 11C7 in an animal contusion injury. Our injury is also more severe than any other study investigating Nogo-A inhibition. It appears that 11C7 alone is not enough to either increase axonal sprouting, or improve behavioural recovery. However, sequential 11C7 therapy and locomotor training with or without ES does lead to increased weight supported stepping and sequential 11C7 with training increased 5-HT and TH fibre sprouting. The current clinical trial of anti-Nogo-A therapy has shown it is well tolerated and thus the trial is continuing (Kucher et al., 2018). We have presented evidence it could also be used with sequential training under ES for improved locomotor recovery. However, in our severe contusion injury model, 11C7 alone is insufficient for locomotor recovery. These data suggest locomotor rehabilitative training should also be given sequentially following Anti-Nogo-A therapy in humans.

5.3.2 Epidural stimulation

ES has been used in human SCI patients with some promising results (Harkema et al., 2011, Angeli et al., 2014, Angeli et al., 2018, Wagner et al., 2018, Gill et al., 2018). There are a few hypotheses for how epidural electrical stimulation improves recovery after SCI. Electrical stimulation is known to increase BDNF expression in spinal cord neurons (Wenjin et al., 2011). Effects on myelination are also observed, as electrical stimulation of corticospinal axons increases oligodendrocytes proliferation and differentiation of oligodendrocyte progenitor cells (Li et al., 2010) and induces remyelination in peripheral nerves (Wan et al., 2010). Electrical stimulation also leads to neurite outgrowth in cells treated with nerve growth factor (Chang et al., 2013). These direct effects of ES may have some benefits, however, in our study ES alone did not lead to any functional improvements or increased axonal sprouting. Behavioural improvements were only observed when ES was combined with step training. This supports the theory that the main mechanism of ES mediated recovery is by changing the state of the spinal cord to allow afferent input to elicit functional behaviour. The main pathway for ES to change the spinal cord state is via afferents and through these afferents to modulate the CPG (Lavrov et al., 2008, Capogrosso et al., 2013). These have been discussed in the above section on afferent changes in relation to γ-MNs and activity dependent plasticity.

The convergence of descending input with afferent input via training and ES is hypothesised to be responsible for the motor learning and locomotor recovery observed after training under ES in SCI animals and humans (recently reviewed by Eisdorfer et al. (2020)). The idea of concurrent stimulation in learning is not new and concurrent cortical and spinal stimulation has been shown to improve CST sprouting following a cervical contusion (Martin, 2016). In our study, the ES stimulation alone may not be activating pathways in the coordinated manner needed for motor learning. Continuous stimulation has recently been shown to result in antidromic collisions with afferent input (Formento et al., 2018), thus even our ES with training may not be leading to the most effective recovery. Further studies with spatiotemporally targeted stimulation that selectively modulates flexor and then extensor muscles during locomotion has shown improved results over continuous stimulation (Wenger et al., 2016). There is debate as to whether targeted or continuous

stimulation is more effective (McPherson et al., 2015), and we have demonstrated locomotor improvements from step training under continuous ES. Activity dependent ES in rats is now a possibility which should lead to more studies of its effectiveness (Rascoe et al., 2018).

5.3.3 Locomotor training

The mechanisms of training induced recovery in the spinal cord are not fully understood. Afferent input is necessary for locomotor recovery, and this afferent driven activity dependent plasticity is covered in the above sections and was recently reviewed by Takeoka (2020). In our study training alone did not lead to changes in afferent input to MNs. Although this afferent to MN input is not the only connections afferents have with the spinal locomotor circuitry. Low threshold cutaneous afferents connect to MN contacting Di3 INs which are necessary for recovery following a spinal transection (Bui et al., 2016). These Di3 neurons appear to be part of the spinal comparator networks which compare sensory feedback with motor commands. Other sensory contacted INs include V3 INs which can generate spasms after SCI (Lin et al., 2019), and V2a INs which are needed for afferent driven locomotor like activity in fictive locomotion (Crone et al., 2008). Changes in connections to these sensory networks, as well as the effect of afferents on propriospinal neurons (Takeoka and Arber, 2019) are likely to be important in training induced recovery. However, further markers of these INs in adult animals are needed to determine plasticity in this network in response to training. We have not seen any significant differences in afferent input to the areas where these INs reside, but this does not rule out the possibility that afferent to IN synaptic plasticity is important following training.

Training alone did not lead to any locomotor recovery in this study. There are a couple of possible reasons for this. One, we missed the critical period where training would lead to the greatest functional recovery. Two, our injury was so severe that locomotor training was unable to elicit a functional spinal response without other stimulation. Training under ES did lead to greater functional recovery, thus indicating this second reason may be why training alone was unsuccessful. It is also possible that if training was started earlier we would have seen greater recovery, thus both reasons remain possible. The low volume of

training in our study may also have limited the behavioural improvements possible, the 20 minutes of training per day may not have been sufficient to improve locomotor performance above the potential self-training animals could have been doing in their home cages. Recent meta analysis of rehabilitative training in humans has shown that treadmill training in very severe SCI (AISA A) does not improve locomotor performance (Duan et al., 2021). Our severe contusion injury has shown similar negative results, thus supporting the need for combinational therapies for locomotor improvements.

5.4 The role of γ-MNs

5.4.1 AAV targeting

γ-MNs present an attractive target for SCI studies due their role in modulation of vital sensory afferents, their potential plasticity, and their separate descending pathway control. However, the role of γ-MNs in awake, freely moving, uninjured animals or humans is still largely unknown. The many question marks around the innervation of ɣ-MNs led us to investigate these inputs by selectively targeting them for further tracing studies. To do this we targeted ɣ-MNs with AAVs specific only to them and not α-MNs. We chose AAVs for multiple reasons, including the large range of modifications which can be made with AAVs (Watakabe et al., 2017). The other main reason was to allow for investigations of neural circuitry in non-genetically modified rats. This would simplify experiments without the need for complex genetic modifications, and would allow for more detailed behavioural assessments in rats as compared to mice.

A technique first demonstrated by Wickersham et al. (2007) found that it was possible to restrict a modified rabies virus to only monosynaptic inputs as opposed to previous polysynaptic rabies virus transduction. In this method, cells of interest for input tracing are induced to express the TVA viral receptor and a specific ‘G’ protein. A modified EnvA pseudotyped rabies virus lacking this G protein is then able to enter only those cells expressing the TVA receptor, and in the cell is able to assemble with the G protein and spread through synapses contacting the initial cell, but no further. Unfortunately our AAV targeting studies were unsuccessful, we have demonstrated the lack of γ-MN specificity of both an antibody against Err3, and an AAV with an Err3 promotor. The presence of 5-

HT_{1D} mRNA in γ but not α-MNs of the rat was confirmed, however, an AAV with a 5-HT_{1D} promotor does not transduce γ-MNs. Our negative results with potentially γ-MN specific AAV targeting suggests this may not be a viable method to selectively study the circuitry and function of γ-MNs.

The targeting of individual neuron types by AAVs with specific promotors does not appear to be a widespread technique, with more universal and highly expressed cellular promotors such as CAG and CMV normally used (Nieuwenhuis et al., 2021). Studies often use universal promotors with spatially defined regions of interest to target their neurons of interest (Stepien et al., 2010), however, due to the colocalization of γ and α-MNs in the spinal cord, this method was unavailable to us. Other studies have used AAVs to target cells by their birth date (Deshpande et al., 2013, Arenkiel et al., 2011) or via cell specific Cre recombinase expressing mouse lines with Cre dependant AAVs (reviewed by Callaway and Luo (2015)). This method was also unsuitable for our goals as there are no relevant Cre lines available with rats. Future studies using Cre mice with Cre dependent AAVs could be an option, even if the benefits of working with non-genetically altered rats are lost.

We have had some success selectively targeting γ-MNs by intramuscular injection of the soleus muscle after severing the larger α-MN axon containing larger nerve branch. Further surgeries may lead to more reliable results, however, rabies virus tracing is currently most effective in young animals (Callaway and Luo, 2015). The combined low success rate of our surgeries in adults and potentially more difficult surgery in young rats with smaller nerves means that this method may need some more refining before the next steps are taken. This method would allow us to determine the inputs to γ-MNs through combined AAV and modified rabies virus tracing, therefore this avenue should continue to be pursued. However, any studies of function would be limited as this method would only allow us to access to the γ-MNs of one muscle which has lost its motor innervation.

5.4.2 What the relative proportion of γ-MNs indicates

We have investigated the proportion of γ-MNs across various muscles using tissue clearing and imaging of whole spinal enlargements to maintain spatial accuracy. We found a higher proportion of γ-MNs in flexors vs extensor, and in hindlimb vs forelimb muscles.

The reasons for this difference in γ-MN proportion are not entirely clear. Our data point to differential control of muscle spindle activity in different muscles and do not necessarily reflect total amount of afferent input as spindles receive multiple γ-MN innervation each.

The higher proportion of γ-MNs in flexors vs extensors could be explained by the increased role of GTOs in extensors. When spindle afferents are deleted there is very little change in extensor EMG activity (Akay et al., 2014). GTOs are hypothesised to ensure this continuation of function as in an unloaded activity such as swimming there are significant dysfunctions in extensor activity (Akay et al., 2014). In the above study the EMG activity of flexors is altered significantly, indicating spindle afferent information is more important here, and thus suggesting the higher proportion of γ-MNs is appropriate for flexors. The reason we found a lower proportion of γ-MNs in the forelimb compared to hindlimb is unclear. It is possible that forelimb muscles require less afferent control due to the greater role of visual information to guide these muscles. Afferent input is reduced in visuomotor adaptation tasks in humans (Jones et al., 2001), where there may be a mismatch between visual information and proprioceptive input. In the hindlimb γ-MNs may control and coordinate local activity without as much supraspinal input as the forelimb with their more visually directed movements. This is speculative at present, but there is evidence for other rostro caudal connectivity gradients in pre-motor networks. There are more cervical V2a INs which project to supraspinal structures, while in the more caudal lumbar regions V2a INs do no project supraspinally, and instead form recurrent networks with local spinal neurons (Hayashi et al., 2018). It is possible that the increased proportion of γ-MNs in the lumbar spinal cord is for a similar reason.

5.4.3 Role of γ-MNs in movement and learning

Human studies of the muscle spindle have shown some conflicting results regarding the separate control of γ and not α-MNs and there is still debate as to the separate control of spindle gain (Burke, 2021, Dimitriou, 2021). There is not much evidence of increased spindle sensitivity in preparation for movement (Burke et al., 1980), but there is evidence of reduced spindle sensitivity in muscles which will be stretched by the movement (Papaioannou and Dimitriou, 2021). An earlier study demonstrated attention mediated modulation of afferent firing during an imposed movement task (Hospod et al., 2007).

There was some reduction in activity as well as increases and changes in spontaneous activity. The modulatory activities of γ-MNs in humans are not yet clear; our understanding of their activity and function in animals is also incomplete.

If γ-MNs are not activated differently than α-MNs, then why even have γ-MN and not just α or β-MNs? One reason could be for the lack of direct Ia input to γ-MNs. This ensure there is not too much resistance to stretch in muscles. If γ-MNs received direct Ia excitation this would cause them to increase the firing of Ia afferents, which would in turn increase the firing of γ-MNs in a positive feedback loop which would also increase the firing of α-MNs due to the monosynaptic stretch reflex. The modulation in afferent firing during visual attention to imposed movements indicate that reduced afferent feedback is a strategy used by the motor system, potentially to restrict unwanted activity from muscles which would oppose this movement (Hospod et al., 2007). γ-MNs may be important in this system to reduce muscle stiffness, as dynamic γ-MN activity may be lower in antagonist muscles prior to movement (Papaioannou and Dimitriou, 2021). This may be one form of differential control, with some recent evidence suggesting lower γ-MN activity if one wants to reduce muscle stiffness and allow for stretching of muscles which would otherwise interfere with the task if they were active.

Study of the fusimotor system has often focused on cats, human and rodent fusimotor systems may not fulfil exactly the same function as in felines. The cat spinal cord is potentially more independent than humans, as afferent feedback from a moving treadmill results in functional stepping in cats, where it does not result in the same quality of movements in humans (Lovely et al., 1986). Our evidence has suggested γ-MNs may be more prevalent in lumbar spinal cord circuitry, where more independent and less supraspinally modulated movement occurs. The proprioceptive system and segmental inputs from afferents may be more important in the lumbar circuitry, and animals with less direct supraspinal control of movement may also rely upon this system more.

Role of γ-MNS in learning is unclear, obviously afferent input is needed for learning after SCI (Takeoka et al., 2014). But does afferent output need to be increased or decreased selectively during learning? Some studies in humans have demonstrated reduced Ia afferent

activity during learning (Jones et al., 2001) and have shown reductions in H reflex, probably mediated by increased pre-synaptic inhibition (Perez et al., 2005). The reduced afferent output and reduced H reflex does not necessarily mean less sensory input is travelling supraspinally, as sensory evoked potentials in the cortex were not reduced even with a reduction in H-reflex (Perez 2005). This touches on the potential triple function of γ-MNs, to modulate afferent to α-MN activity, to modulate afferent to local CPG activity, and to modulate afferent output to supraspinal regions. The role of γ-MNs in each of these tasks could be different. There may be a difference between spinal motor learning and supraspinal based motor learning, although there is likely a component of both in most activities.

I have not really touched on the role of γ-MNs in providing an internal copy of movement allowing the motor system to update movement as required. According to Burke (2021), "It is conceivable that selective changes in fusimotor drive play an important role in kinaesthesia and in providing the feedback necessary for performing and updating a movement". Where normal spindle afferent output during movement does not change behaviour, but alterations in afferent response indicate something has not gone according to plan. This is slightly beyond the scope of this thesis, but further targeting and modulation of γ-MN activity could supply answers regarding the role of γ-MNs in kinaesthesia and the internal copy of movement. Further studies of the activity of γ-MNs in awake and freely moving animals are needed for a fuller understanding of not only γ-MNs, but also afferent directed learning in general, and afferent directed learning after SCI in particular.

5.5 Clinical implications

The limited structural plasticity changes in any of our treatments suggest we may have missed a crucial period of plasticity to begin our activity based therapy. It is possible the injury type and severity require an earlier activity based intervention than previous studies also beginning training after three weeks (Chen et al., 2017). Sequential 11C7 therapy and training under ES did lead to an increase in the proportion of sensory to MN inputs which had 3+ clusters of P boutons, and an opposing decrease in the number of these sensory to MN inputs. Together these changes suggest that afferent input is being selectively

modulated in response to coordinated input from training under continuous epidural stimulation. Further studies of this afferent network are needed to determine if these changes are specific to contusion injury, or if afferent retraction/modulation is a general feature of activity based rehabilitative therapy.

The current clinical trial of anti-Nogo-A therapy has shown it is well tolerated and thus can be continued (Kucher et al., 2018). We have presented evidence it could also be used with sequential training under ES for improved locomotor recovery. In our hands 11C7 therapy only induced functional behavioural improvements when used with sequential training, or training under ES. This could be due to our severe contusion model, where descending tracts needed for recovery are destroyed in our injury when they are not in other partial transections studies (Chen et al., 2017, Maier et al., 2009). The current clinical trial includes only severe injuries (ASIA A) (Kucher et al., 2018), our evidence suggests that in these severe patients anti-Nogo-A therapy must be followed by rehabilitative training in order to achieve behavioural improvements.

6 Reference list

AKAY, T., TOURTELLOTTE, W. G., ARBER, S. & JESSELL, T. M. 2014. Degradation of mouse locomotor pattern in the absence of proprioceptive sensory feedback. 111**,** 16877-16882.

AL'JOBOORI, Y. D. 2016. Maximising Recovery of Function after Severe Spinal Cord Injury by Combining Electrical Epidural Stimulation, Locomotor Training and Intraspinal Lentiviral- Mediated Chondroitinase-ABC Delivery. PhD Thesis, University of Leeds.

AL'JOBOORI, Y. D., EDGERTON, V. R. & ICHIYAMA, R. M. 2020. Effects of Rehabilitation on Perineural Nets and Synaptic Plasticity Following Spinal Cord Transection. 10**,** 824.

ALSTERMARK, B., OGAWA, J. & ISA, T. 2004. Lack of Monosynaptic Corticomotoneuronal EPSPs in Rats: Disynaptic EPSPs Mediated Via Reticulospinal Neurons and Polysynaptic EPSPs Via Segmental Interneurons. 91**,** 1832-1839.

ALVAREZ, F. J., DEWEY, D. E., HARRINGTON, D. A. & FYFFE, R. E. 1997. Cell-type specific organization of glycine receptor clusters in the mammalian spinal cord. *J Comp Neurol,* 379**,** 150-70.

ALVAREZ, F. J., JONAS, P. C., SAPIR, T., HARTLEY, R., BERROCAL, M. C., GEIMAN, E. J., TODD, A. J. & GOULDING, M. 2005. Postnatal phenotype and localization of spinal cord V1 derived interneurons. 493**,** 177-192.

ANDERSON, K. D. 2004. Targeting recovery: priorities of the spinal cord-injured population. *J Neurotrauma,* 21**,** 1371-83.

ANDERSON, M. A., BURDA, J. E., REN, Y., AO, Y., O'SHEA, T. M., KAWAGUCHI, R., COPPOLA, G., KHAKH, B. S., DEMING, T. J. & SOFRONIEW, M. V. 2016. Astrocyte scar formation aids central nervous system axon regeneration. *Nature,* 532**,** 195.

ANDERSON, M. A., O'SHEA, T. M., BURDA, J. E., AO, Y., BARLATEY, S. L., BERNSTEIN, A. M., KIM, J. H., JAMES, N. D., ROGERS, A., KATO, B., WOLLENBERG, A. L., KAWAGUCHI, R., COPPOLA, G., WANG, C., DEMING, T. J., HE, Z., COURTINE, G. & SOFRONIEW, M. V. 2018. Required growth facilitators propel axon regeneration across complete spinal cord injury. *Nature,* 561**,** 396-400.

ANDERSSON, L. S., LARHAMMAR, M., MEMIC, F., WOOTZ, H., SCHWOCHOW, D., RUBIN, C.-J., PATRA, K., ARNASON, T., WELLBRING, L., HJÄLM, G., IMSLAND, F., PETERSEN, J. L., MCCUE, M. E., MICKELSON, J. R., COTHRAN, G., AHITUV, N., ROEPSTORFF, L., MIKKO, S., VALLSTEDT, A., LINDGREN, G., ANDERSSON, L. & KULLANDER, K. 2012. Mutations in DMRT3 affect locomotion in horses and spinal circuit function in mice. *Nature,* 488**,** 642-646.

ANGELI, C. A., BOAKYE, M., MORTON, R. A., VOGT, J., BENTON, K., CHEN, Y., FERREIRA, C. K. & HARKEMA, S. J. 2018. Recovery of Over-Ground Walking after Chronic Motor Complete Spinal Cord Injury. 379**,** 1244-1250.

ANGELI, C. A., EDGERTON, V. R., GERASIMENKO, Y. P. & HARKEMA, S. J. J. B. 2014. Altering spinal cord excitability enables voluntary movements after chronic complete paralysis in humans. 137**,** 1394-1409.

APPELBERG, B., HULLIGER, M., JOHANSSON, H. & SOJKA, P. 1983a. Actions on gamma-motoneurones elicited by electrical stimulation of group I muscle afferent fibres in the hind limb of the cat. *The Journal of Physiology,* 335**,** 237-253.

APPELBERG, B., HULLIGER, M., JOHANSSON, H. & SOJKA, P. 1983b. Actions on gamma-motoneurones elicited by electrical stimulation of group II muscle afferent fibres in the hind limb of the cat. *The Journal of Physiology,* 335**,** 255-273.

APPELBERG, B., HULLIGER, M., JOHANSSON, H. & SOJKA, P. 1983c. Actions on gamma-motoneurones elicited by electrical stimulation of group III muscle afferent fibres in the hind limb of the cat. *J Physiol,* 335**,** 275-92.

APPELBERG, B., HULLIGER, M., JOHANSSON, H. & SOJKA, P. 1983d. Recurrent actions on gamma-motoneurones mediated via large and small ventral root fibres in the cat. *The Journal of Physiology,* 335**,** 293-305.

APPELBERG, B. & JENESKOG, T. 1969. A Dorso-lateral Spinal Pathway Mediating Information from the Mesencephalon to Dynamic Fusimotor Neurones. *Acta Physiologica Scandinavica,* 77**,** 159-171.

APPELBERG, B. & JENESKOG, T. 1972. Mesencephalic fusimotor control. *Experimental Brain Research,* 15**,** 97-112.

APPELBERG, B., JENESKOG, T. & JOHANSSON, H. 1975. Rubrospinal Control of Static and Dynamic Fusimotor Neurones. *Acta Physiologica Scandinavica,* 95**,** 431-440.

APPELBERG, B., JOHANSSON, H. & KALISTRATOV, G. 1977. The influence of Group II muscle afferents and low threshold skin afferents on dynamic fusimotor neurones to the triceps surae of the cat. *Brain Research,* 132**,** 153-158.

APPELBERG, B. & MOLANDER, C. 1967. A rubro-olivary pathway I. identification of a descending system for control of the dynamic sensitivity of muscle spindles. *Experimental Brain Research,* 3**,** 372-381.

APPENTENG, K., MORIMOTO, T. & TAYLOR, A. 1980. Fusimotor activity in masseter nerve of the cat during reflex jaw movements. *The Journal of Physiology,* 305**,** 415-431.

ARENKIEL, B. R., HASEGAWA, H., YI, J. J., LARSEN, R. S., WALLACE, M. L., PHILPOT, B. D., WANG, F. & EHLERS, M. D. 2011. Activity-Induced Remodeling of Olfactory Bulb Microcircuits Revealed by Monosynaptic Tracing. *PLOS ONE,* 6**,** e29423.

ARMBRUSTER, B. N., LI, X., PAUSCH, M. H., HERLITZE, S. & ROTH, B. L. 2007. Evolving the lock to fit the key to create a family of G protein-coupled receptors potently activated by an inert ligand. *Proc Natl Acad Sci U S A,* 104**,** 5163-8.

ASBOTH, L., FRIEDLI, L., BEAUPARLANT, J., MARTINEZ-GONZALEZ, C., ANIL, S., REY, E., BAUD, L., PIDPRUZHNYKOVA, G., ANDERSON, M. A., SHKORBATOVA, P., BATTI, L., PAGÈS, S., KREIDER, J., SCHNEIDER, B. L., BARRAUD, Q. & COURTINE, G. 2018. Cortico–reticulo–spinal circuit reorganization enables functional recovery after severe spinal cord contusion. *Nature Neuroscience,* 21**,** 576-588.

ASHRAFI, S., LALANCETTE-HÉBERT, M., FRIESE, A., SIGRIST, M., ARBER, S., SHNEIDER, N. A. & KALTSCHMIDT, J. A. 2012. Wnt7A Identifies Embryonic γ-Motor Neurons and Reveals Early Postnatal Dependence of γ-Motor Neurons on a Muscle Spindle-Derived Signal. *The Journal of Neuroscience,* 32**,** 8725-8731.

BAKER, J. R., CATLEY, M. C., DAVEY, N. J. & ELLAWAY, P. H. 1991. Influence of the pontine and medullary reticular formation on synchrony of gamma motoneurone discharge in the cat. *Experimental Brain Research,* 87**,** 604-614.

BAKER, S. N., ZAAIMI, B., FISHER, K. M., EDGLEY, S. A. & SOTEROPOULOS, D. S. 2015. Chapter 18 - Pathways mediating functional recovery. *In:* DANCAUSE, N., NADEAU, S. & ROSSIGNOL, S. (eds.) *Progress in Brain Research.* Elsevier.

BALASKAS, N., RIBEIRO, A., PANOVSKA, J., DESSAUD, E., SASAI, N., PAGE, KAREN M., BRISCOE, J. & RIBES, V. 2012. Gene Regulatory Logic for Reading the Sonic Hedgehog Signaling Gradient in the Vertebrate Neural Tube. *Cell,* 148**,** 273-284.

BANKS, R. & STACEY, M. 1988. Quantitative Studies on Mammalian Muscle Spindles and their Sensory Innervation. *In:* HNÍK, P., SOUKUP, T., VEJSADA, R. & ZELENÁ, J. (eds.) *Mechanoreceptors: Development, Structure, and Function.* Boston, MA: Springer US.

BANKS, R. W. 2006. An allometric analysis of the number of muscle spindles in mammalian skeletal muscles. *Journal of Anatomy,* 208**,** 753-768.

BARBEAU, H. & ROSSIGNOL, S. 1987. Recovery of locomotion after chronic spinalization in the adult cat. *Brain Research,* 412**,** 84-95.

BAREYRE, F. M., KERSCHENSTEINER, M., RAINETEAU, O., METTENLEITER, T. C., WEINMANN, O. & SCHWAB, M. E. 2004. The injured spinal cord spontaneously forms a new intraspinal circuit in adult rats. *Nature Neuroscience,* 7**,** 269-277.

BARKER, D. 1948. The innervation of the muscle-spindle. *Journal of Cell Science,* 3**,** 143-185.

BARKER, D., EMONET-DÉNAND, F., LAPORTE, Y., PROSKE, U. & STACEY, M. J. 1973. Morphological identification and intrafusal distribution of the endings of static fusimotor axons in the cat. *The Journal of Physiology,* 230**,** 405-427.

BARKER, D., HUNT, C. C. & MCINTYRE, A. K. 1974. *Muscle receptors,* New York, Springer Science & Business Media.

BASSO, D. M., BEATTIE, M. S. & BRESNAHAN, J. 1995. A sensitive and reliable locomotor rating scale for open field testing in rats. *Journal of neurotrauma,* 12**,** 1-21.

BAUMANN, T. K., EMONET-DE´NAND, F. & HULLIGER, M. 1982. After-effects of fusimotor stimulation on spindle la afferents' dynamic sensitivity, revealed during slow movements. *Brain Research,* 232**,** 460-465.

BAUMANN, T. K. & HULLIGER, M. 1991. The dependence of the response of cat spindle Ia afferents to sinusoidal stretch on the velocity of concomitant movement. *The Journal of Physiology,* 439**,** 325-350.

BEAUPARLANT, J., VAN DEN BRAND, R., BARRAUD, Q., FRIEDLI, L., MUSIENKO, P., DIETZ, V. & COURTINE, G. J. B. 2013. Undirected compensatory plasticity contributes to neuronal dysfunction after severe spinal cord injury. 136**,** 3347-3361.

BENNETT, D. J., DE SERRES, S. J. & STEIN, R. B. 1996. Regulation of soleus muscle spindle sensitivity in decerebrate and spinal cats during postural and locomotor activities. *The Journal of Physiology,* 495**,** 835.

BERES-JONES, J. A., JOHNSON, T. D. & HARKEMA, S. J. 2003. Clonus after human spinal cord injury cannot be attributed solely to recurrent muscle-tendon stretch. *Experimental Brain Research,* 149**,** 222-236.

BERGMANS, J. & GRILLNER, S. 1968. Monosynaptic control of staticγ-motoneurones from the lower brain stem. *Experientia,* 24**,** 146-147.

BERTHOZ, A., GRAF, W. & VIDAL, P. P. 1992. *The head-neck sensory motor system,* Oxford University Press, USA.

BETLEY, J. N., WRIGHT, C. V. E., KAWAGUCHI, Y., ERDÉLYI, F., SZABÓ, G., JESSELL, T. M. & KALTSCHMIDT, J. A. 2009. Stringent Specificity in the Construction of a GABAergic Presynaptic Inhibitory Circuit. *Cell,* 139**,** 161-174.

BOROWSKA, J., JONES, C. T., ZHANG, H., BLACKLAWS, J., GOULDING, M. & ZHANG, Y. 2013. Functional subpopulations of V3 interneurons in the mature mouse spinal cord. *J Neurosci,* 33**,** 18553-65.

BOSE, P., HOU, J., PARMER, R., REIER, P. & THOMPSON, F. 2012. Altered Patterns of Reflex Excitability, Balance, and Locomotion Following Spinal Cord Injury and Locomotor Training. 3.

BOURANE, S., GROSSMANN, KATJA S., BRITZ, O., DALET, A., DEL BARRIO, MARTA G., STAM, FLOOR J., GARCIA-CAMPMANY, L., KOCH, S. & GOULDING, M. 2015. Identification of a Spinal Circuit for Light Touch and Fine Motor Control. *Cell,* 160**,** 503-515.

BOYCE, V. S., PARK, J., GAGE, F. H. & MENDELL, L. M. 2012. Differential effects of brain-derived neurotrophic factor and neurotrophin-3 on hindlimb function in paraplegic rats. 35**,** 221-232.

BOYD, I. 1981. The muscle spindle controversy. *Science Progress* 67**,** 205-221.

BOYD, I. A. 1986. Two types of static γ-axon in cat muscle spindles. *Quarterly Journal of Experimental Physiology,* 71**,** 307-327.

BRADBURY, E. J., MOON, L. D., POPAT, R. J., KING, V. R., BENNETT, G. S., PATEL, P. N., FAWCETT, J. W. & MCMAHON, S. B. 2002. Chondroitinase ABC promotes functional recovery after spinal cord injury. *Nature,* 416**,** 636-40.

BRADLEY, P. M., DENECKE, C. K., ALJOVIC, A., SCHMALZ, A., KERSCHENSTEINER, M. & BAREYRE, F. M. 2019. Corticospinal circuit remodeling after central nervous system injury is dependent on neuronal activity. *Journal of Experimental Medicine,* 216**,** 2503-2514.

BREGMAN, B. S. 1987. Development of serotonin immunoreactivity in the rat spinal cord and its plasticity after neonatal spinal cord lesions. *Developmental Brain Research,* 34**,** 245-263.

BREGMAN, B. S., KUNKEL-BAGDEN, E., SCHNELL, L., DAI, H. N., GAO, D. & SCHWAB, M. E. 1995. Recovery from spinal cord injury mediated by antibodies to neurite growth inhibitors. *Nature,* 378**,** 498-501.

BREGMAN, B. S., MCATEE, M., DAI, H. N. & KUHN, P. L. 1997. Neurotrophic Factors Increase Axonal Growth after Spinal Cord Injury and Transplantation in the Adult Rat. *Experimental Neurology,* 148**,** 475-494.

BROWN, M. C. 1971. The responses of frog muscle spindles and fast and slow muscle fibres to a variety of mechanical inputs. *The Journal of Physiology,* 218**,** 1-17.

BROWN, T. G. J. P. O. T. R. S. O. L. S. B., CONTAINING PAPERS OF A BIOLOGICAL CHARACTER 1911. The intrinsic factors in the act of progression in the mammal. 84**,** 308-319.

BUCH, T., HEPPNER, F. L., TERTILT, C., HEINEN, T. J., KREMER, M., WUNDERLICH, F. T., JUNG, S. & WAISMAN, A. 2005. A Cre-inducible diphtheria toxin receptor mediates cell lineage ablation after toxin administration. *Nat Methods,* 2**,** 419-26.

BUFFELLI, M., BURGESS, R. W., FENG, G., LOBE, C. G., LICHTMAN, J. W. & SANES, J. R. 2003. Genetic evidence that relative synaptic efficacy biases the outcome of synaptic competition. *Nature,* 424**,** 430-4.

BUI, TUAN V., AKAY, T., LOUBANI, O., HNASKO, THOMAS S., JESSELL, THOMAS M. & BROWNSTONE, ROBERT M. 2013. Circuits for Grasping: Spinal dI3 Interneurons Mediate Cutaneous Control of Motor Behavior. *Neuron,* 78**,** 191-204.

BUI, T. V., STIFANI, N., AKAY, T. & BROWNSTONE, R. M. 2016. Spinal microcircuits comprising dI3 interneurons are necessary for motor functional recovery following spinal cord transection. *eLife,* 5**,** e21715.

BURKE, D. 2021. Independent fusimotor control of muscle spindles in humans: there is little to gain. *J Physiol*.

BURKE, D., MCKEON, B., SKUSE, N. F. & WESTERMAN, R. A. 1980. Anticipation and fusimotor activity in preparation for a voluntary contraction. *J Physiol,* 306**,** 337-48.

BURKE, R. E., STRICK, P. L., KANDA, K., KIM, C. C. & WALMSLEY, B. 1977. Anatomy of medial gastrocnemius and soleus motor nuclei in cat spinal cord. *Journal of Neurophysiology,* 40**,** 667-680.

BURRONE, J., O'BYRNE, M. & MURTHY, V. N. 2002. Multiple forms of synaptic plasticity triggered by selective suppression of activity in individual neurons. *Nature,* 420**,** 414-418.

BYRNE, A. B., MCWHIRTER, R. D., SEKINE, Y., STRITTMATTER, S. M., MILLER, D. M., III & HAMMARLUND, M. 2016. Inhibiting poly(ADP-ribosylation) improves axon regeneration. *eLife,* 5**,** e12734.

CABELGUEN, J.-M. 1981. Static and dynamic fusimotor controls in various hindlimb muscles during locomotor activity in the decorticate cat. *Brain Research,* 213**,** 83-97.

CAGGIANO, A. O., ZIMBER, M. P., GANGULY, A., BLIGHT, A. R. & GRUSKIN, E. A. 2005. Chondroitinase ABCI improves locomotion and bladder function following contusion injury of the rat spinal cord. *J Neurotrauma,* 22**,** 226-39.

CALDEIRA, V., DOUGHERTY, K. J., BORGIUS, L. & KIEHN, O. 2017. Spinal Hb9::Cre-derived excitatory interneurons contribute to rhythm generation in the mouse. *Scientific Reports,* 7**,** 41369.

CALLAWAY, E. M. & LUO, L. 2015. Monosynaptic Circuit Tracing with Glycoprotein-Deleted Rabies Viruses. 35**,** 8979-8985.

CAPOGROSSO, M., WENGER, N., RASPOPOVIC, S., MUSIENKO, P., BEAUPARLANT, J., BASSI LUCIANI, L., COURTINE, G. & MICERA, S. 2013. A Computational Model for Epidural Electrical Stimulation of Spinal Sensorimotor Circuits. 33**,** 19326-19340.

CARON, G., BILCHAK, J. N. & CÔTÉ, M.-P. 2020. Direct evidence for decreased presynaptic inhibition evoked by PBSt group I muscle afferents after chronic SCI and recovery with step-training in rats. 598**,** 4621-4642.

CATELA, C., SHIN, M. M. & DASEN, J. S. 2015. Assembly and function of spinal circuits for motor control. *Annu Rev Cell Dev Biol,* 31**,** 669-98.

CAUDLE, K. L., BROWN, E. H., SHUM-SIU, A., BURKE, D. A., MAGNUSON, T. S., VOOR, M. J., MAGNUSON, D. S. J. N. & REPAIR, N. 2011. Hindlimb immobilization

in a wheelchair alters functional recovery following contusive spinal cord injury in the adult rat. 25**,** 729-739.

CHAKRABARTY, S., SHULMAN, B. & MARTIN, J. H. 2009. Activity-Dependent Codevelopment of the Corticospinal System and Target Interneurons in the Cervical Spinal Cord. 29**,** 8816-8827.

CHANG, Y. J., HSU, C. M., LIN, C. H., LU, M. S. & CHEN, L. 2013. Electrical stimulation promotes nerve growth factor-induced neurite outgrowth and signaling. *Biochim Biophys Acta,* 1830**,** 4130-6.

CHAU, C., BARBEAU, H. & ROSSIGNOL, S. 1998. Early Locomotor Training With Clonidine in Spinal Cats. 79**,** 392-409.

CHEN, K., MARSH, B. C., COWAN, M., AL'JOBOORI, Y. D., GIGOUT, S., SMITH, C. C., MESSENGER, N., GAMPER, N., SCHWAB, M. E. & ICHIYAMA, R. M. 2017. Sequential therapy of anti-Nogo-A antibody treatment and treadmill training leads to cumulative improvements after spinal cord injury in rats. *Experimental Neurology,* 292**,** 135-144.

CHEN, Z., FAN, G., LI, A., YUAN, J. & XU, T. 2020. rAAV2-Retro Enables Extensive and High-Efficient Transduction of Lower Motor Neurons following Intramuscular Injection. *Molecular Therapy - Methods & Clinical Development,* 17**,** 21-33.

CHOI, J., YOUNG, J. A. T. & CALLAWAY, E. M. 2010. Selective viral vector transduction of ErbB4 expressing cortical interneurons in vivo with a viral receptor–ligand bridge protein. 107**,** 16703-16708.

CIPOLLONE, L. T. 1898. Nuove ricerche sul fuso neuro-muscolare. *Richerche. n. lab. anat. norm. r. Univ. Roma,* 6**,** 157-200.

CLOUGH, J. F. M., PHILLIPS, C. G. & SHERIDAN, J. D. 1971. The short-latency projection from the baboon's motor cortex to fusimotor neurones of the forearm and hand. *The Journal of Physiology,* 216**,** 257-279.

CONRADI, S. 1969. Ultrastructure and distribution of neuronal and glial elements on the motoneuron surface in the lumbosacral spinal cord of the adult cat. *Acta Physiol Scand,* 332**,** 5-48.

CÔTÉ, M.-P., GANDHI, S., ZAMBROTTA, M. & HOULÉ, J. D. 2014. Exercise Modulates Chloride Homeostasis after Spinal Cord Injury. 34**,** 8976-8987.

COURTINE, G., GERASIMENKO, Y., VAN DEN BRAND, R., YEW, A., MUSIENKO, P., ZHONG, H., SONG, B., AO, Y., ICHIYAMA, R. M., LAVROV, I., ROY, R. R., SOFRONIEW, M. V. & EDGERTON, V. R. 2009. Transformation of nonfunctional spinal circuits into functional states after the loss of brain input. *Nat Neurosci,* 12**,** 1333-42.

COX, L. J., HENGST, U., GURSKAYA, N. G., LUKYANOV, K. A. & JAFFREY, S. R. 2008. Intra-axonal translation and retrograde trafficking of CREB promotes neuronal survival. *Nat Cell Biol,* 10**,** 149-59.

CRONE, S. A., QUINLAN, K. A., ZAGORAIOU, L., DROHO, S., RESTREPO, C. E., LUNDFALD, L., ENDO, T., SETLAK, J., JESSELL, T. M., KIEHN, O. & SHARMA, K. 2008. Genetic Ablation of V2a Ipsilateral Interneurons Disrupts Left-Right Locomotor Coordination in Mammalian Spinal Cord. *Neuron,* 60**,** 70-83.

CULLHEIM, S. & KELLERTH, J. O. 1978. A morphological study of the axons and recurrent axon collaterals of cat sciatic α-motoneurons after intracellular staining with horseradish peroxidase. *The Journal of Comparative Neurology,* 178**,** 537-557.

DAVEY, N. J. & ELLAWAY, P. H. 1988. Control from the brainstem of synchrony of discharge between gamma motoneurones in the cat. *Experimental Brain Research,* 72**,** 249-263.

DAVEY, N. J. & ELLAWAY, P. H. 1989. Facilitation of individual gamma-motoneurones by the discharge of single slowly adapting type 1 mechanoreceptors in cats. *The Journal of Physiology,* 411**,** 97-114.

DE LEON, R., TAMAKI, H., HODGSON, J., ROY, R. & EDGERTON, V. 1999. Hindlimb locomotor and postural training modulates glycinergic inhibition in the spinal cord of the adult spinal cat. *Journal of Neurophysiology,* 82**,** 359-369.

DESHPANDE, A., BERGAMI, M., GHANEM, A., CONZELMANN, K.-K., LEPIER, A., GÖTZ, M. & BERNINGER, B. 2013. Retrograde monosynaptic tracing reveals the temporal evolution of inputs onto new neurons in the adult dentate gyrus and olfactory bulb. 110**,** E1152-E1161.

DETLOFF, M. R., SMITH, E. J., QUIROS MOLINA, D., GANZER, P. D. & HOULÉ, J. D. 2014. Acute exercise prevents the development of neuropathic pain and the sprouting of non-peptidergic (GDNF- and artemin-responsive) c-fibers after spinal cord injury. *Experimental Neurology,* 255**,** 38-48.

DICKSON, R. G., LALL, V. & ICHIYAMA, R. M. 2019. Enhancing plasticity in spinal sensorimotor circuits following injuries to facilitate recovery of motor control. *Current Opinion in Physiology,* 8**,** 152-160.

DIMITRIOU, M. 2021. Crosstalk proposal: there is much to gain from the independent control of human muscle spindles. *J Physiol*.

DITUNNO, J. F., LITTLE, J. W., TESSLER, A. & BURNS, A. S. 2004. Spinal shock revisited: a four-phase model. *Spinal Cord,* 42**,** 383-395.

DJUPSJOBACKA, M., JOHANSSON, H., BERGENHEIM, M. & WENNGREN, B. I. 1995. Influences on the gamma-muscle spindle system from muscle afferents stimulated by increased intramuscular concentrations of bradykinin and 5-HT. *Neurosci Res,* 22**,** 325-33.

DONGA, R., TAYLOR, A. & JUCH, P. J. 1993. The use of midbrain stimulation to identify the discharges of static and dynamic fusimotor neurones during reflex jaw movements in the anaesthetized cat. *Experimental Physiology,* 78**,** 15-23.

DOUGHERTY, KIMBERLY J., ZAGORAIOU, L., SATOH, D., ROZANI, I., DOOBAR, S., ARBER, S., JESSELL, THOMAS M. & KIEHN, O. 2013. Locomotor Rhythm Generation Linked to the Output of Spinal Shox2 Excitatory Interneurons. *Neuron,* 80**,** 920-933.

DU BEAU, A., SHAKYA SHRESTHA, S., BANNATYNE, B. A., JALICY, S. M., LINNEN, S. & MAXWELL, D. J. 2012. Neurotransmitter phenotypes of descending systems in the rat lumbar spinal cord. *Neuroscience,* 227**,** 67-79.

DUAN, R., QU, M., YUAN, Y., LIN, M., LIU, T., HUANG, W., GAO, J., ZHANG, M. & YU, X. 2021. Clinical Benefit of Rehabilitation Training in Spinal Cord Injury: A Systematic Review and Meta-Analysis. *Spine,* 46.

DYCK, J., LANUZA, G. M. & GOSGNACH, S. 2012. Functional characterization of dI6 interneurons in the neonatal mouse spinal cord. 107**,** 3256-3266.

ECCLES, J. C., ECCLES, R. M., IGGO, A. & ITO, M. 1961. Distribution of recurrent inhibition among motoneurones. *The Journal of Physiology,* 159**,** 479-499.

ECCLES, J. C., ECCLES, R. M., IGGO, A. & LUNDBERG, A. 1960. Electrophysiological studies on gamma motoneurones. *Acta Physiol Scand,* 50**,** 32-40.

EDGERTON, V. R., COURTINE, G., GERASIMENKO, Y. P., LAVROV, I., ICHIYAMA, R. M., FONG, A. J., CAI, L. L., OTOSHI, C. K., TILLAKARATNE, N. J. K., BURDICK, J. W. & ROY, R. R. 2008. Training locomotor networks. *Brain Research Reviews,* 57**,** 241-254.

EDWARDS, I. J., BRUCE, G., LAWRENSON, C., HOWE, L., CLAPCOTE, S. J., DEUCHARS, S. A. & DEUCHARS, J. 2013. Na(+)/K(+) ATPase α1 and α3 Isoforms Are Differentially Expressed in α- and γ-Motoneurons. *The Journal of Neuroscience,* 33**,** 9913-9919.

EISDORFER, J. T., SMIT, R. D., KEEFE, K. M., LEMAY, M. A., SMITH, G. M. & SPENCE, A. J. 2020. Epidural Electrical Stimulation: A Review of Plasticity Mechanisms That Are Hypothesized to Underlie Enhanced Recovery From Spinal Cord Injury With Stimulation. 13.

ELDRED, E. & FUJIMORI, B. 1958. Relations of the reticular formation to muscle spindle activation. *Reticular formation of the brain***,** 275-283.

ELDRED, E., GRANIT, R. & MERTON, P. A. 1953. Supraspinal control of the muscle spindles and its significance. *J Physiol,* 122**,** 498-523.

ELLAWAY, P., FRIEDLAND, C. & WEBSTER, R. 1989. Synchrony of gamma motoneuron discharge and monoamines in the spinal-cord of the anesthetized rat. *Journal of Physiology***,** 59.

ELLAWAY, P. H. & MURPHY, P. R. 1981. A comparison of the recurrent inhibition of alpha- and gamma-motoneurones in the cat. *The Journal of Physiology,* 315**,** 43-58.

ELLAWAY, P. H., MURPHY, P. R. & TRIPATHI, A. 1982. Closely coupled excitation of γ-motoneurones by group III muscle afferents with low mechanical threshold in the cat. *The Journal of Physiology,* 331**,** 481-498.

EMONET-DÉNAND, F., LAPORTE, Y., MATTHEWS, P. B. & PETIT, J. 1977. On the subdivision of static and dynamic fusimotor actions on the primary ending of the cat muscle spindle. *The Journal of Physiology,* 268**,** 827-861.

EMONET-DENAND, F., PETIT, J. & LAPORTE, Y. 1992. Comparison of skeleto-fusimotor innervation in cat peroneus brevis and peroneus tertius muscles. *The Journal of Physiology,* 458**,** 519.

ENGESSER-CESAR, C., ICHIYAMA, R. M., NEFAS, A. L., HILL, M. A., EDGERTON, V. R., COTMAN, C. W. & ANDERSON, A. J. 2007. Wheel running following spinal cord injury improves locomotor recovery and stimulates serotonergic fiber growth. *Eur J Neurosci,* 25**,** 1931-9.

ENJIN, A., LEÃO, K. E., MIKULOVIC, S., LE MERRE, P., TOURTELLOTTE, W. G. & KULLANDER, K. 2012. Sensorimotor function is modulated by the serotonin receptor 1d, a novel marker for gamma motor neurons. *Molecular and Cellular Neuroscience,* 49**,** 322-332.

ENJIN, A., PERRY, S., HILSCHER, M. M., NAGARAJA, C., LARHAMMAR, M., GEZELIUS, H., ERIKSSON, A., LEÃO, K. E. & KULLANDER, K. 2017a. Developmental Disruption of Recurrent Inhibitory Feedback Results in Compensatory Adaptation in the Renshaw Cell–Motor Neuron Circuit. 37**,** 5634-5647.

ENJIN, A., PERRY, S., HILSCHER, M. M., NAGARAJA, C., LARHAMMAR, M., GEZELIUS, H., ERIKSSON, A., LEÃO, K. E. & KULLANDER, K. 2017b. Developmental disruption of recurrent inhibitory feedback results in compensatory adaptation in the Renshaw cell - motor neuron circuit. *The Journal of Neuroscience*.

FAULKNER, J. R., HERRMANN, J. E., WOO, M. J., TANSEY, K. E., DOAN, N. B. & SOFRONIEW, M. V. 2004. Reactive astrocytes protect tissue and preserve function after spinal cord injury. *J Neurosci,* 24**,** 2143-55.

FILLI, L., ENGMANN, A. K., ZÖRNER, B., WEINMANN, O., MORAITIS, T., GULLO, M., KASPER, H., SCHNEIDER, R. & SCHWAB, M. E. 2014. Bridging the Gap: A Reticulo-Propriospinal Detour Bypassing an Incomplete Spinal Cord Injury. *The Journal of Neuroscience,* 34**,** 13399-13410.

FILOUS, A. R. & SCHWAB, J. M. 2018. Determinants of Axon Growth, Plasticity, and Regeneration in the Context of Spinal Cord Injury. *The American Journal of Pathology,* 188**,** 53-62.

FINK, A. J. P., CROCE, K. R., HUANG, Z. J., ABBOTT, L. F., JESSELL, T. M. & AZIM, E. 2014. Presynaptic inhibition of spinal sensory feedback ensures smooth movement. *Nature,* 509**,** 43-48.

FINK, K. L., LÓPEZ-GIRÁLDEZ, F., KIM, I.-J., STRITTMATTER, S. M. & CAFFERTY, W. B. J. 2017. Identification of Intrinsic Axon Growth Modulators for Intact CNS Neurons after Injury. *Cell reports,* 18**,** 2687-2701.

FONG, A. J., CAI, L. L., OTOSHI, C. K., REINKENSMEYER, D. J., BURDICK, J. W., ROY, R. R. & EDGERTON, V. R. 2005. Spinal Cord-Transected Mice Learn to Step in Response to Quipazine Treatment and Robotic Training. 25**,** 11738-11747.

FORMENTO, E., MINASSIAN, K., WAGNER, F., MIGNARDOT, J. B., LE GOFF-MIGNARDOT, C. G., ROWALD, A., BLOCH, J., MICERA, S., CAPOGROSSO, M. & COURTINE, G. 2018. Electrical spinal cord stimulation must preserve proprioception to enable locomotion in humans with spinal cord injury. *Nature Neuroscience,* 21**,** 1728-1741.

FORSSBERG, H., GRILLNER, S., HALBERTSMA, J. & ROSSIGNOL, S. J. A. P. S. 1980. The locomotion of the low spinal cat. II. Interlimb coordination. 108**,** 283-295.

FORTUN, J., PUZIS, R., PEARSE, D. D., GAGE, F. H. & BUNGE, M. B. 2009. Muscle injection of AAV-NT3 promotes anatomical reorganization of CST axons and improves behavioral outcome following SCI. *J Neurotrauma,* 26**,** 941-53.

FOURNIER, A. E., TAKIZAWA, B. T. & STRITTMATTER, S. M. 2003. Rho kinase inhibition enhances axonal regeneration in the injured CNS. *J Neurosci,* 23**,** 1416-23.

FRANCIUS, C., HARRIS, A., RUCCHIN, V., HENDRICKS, T. J., STAM, F. J., BARBER, M., KUREK, D., GROSVELD, F. G., PIERANI, A., GOULDING, M. & CLOTMAN, F. 2013. Identification of Multiple Subsets of Ventral Interneurons and Differential Distribution along the Rostrocaudal Axis of the Developing Spinal Cord. *PLOS ONE,* 8**,** e70325.

FRANK, K. & FUORTES, M. 1957. Presynaptic and postsynaptic inhibition of monosynaptic reflexes. *Federation proceedings,* 16**,** 39-40.

FREUND, P., SCHMIDLIN, E., WANNIER, T., BLOCH, J., MIR, A., SCHWAB, M. E. & ROUILLER, E. M. 2009. Anti-Nogo-A antibody treatment promotes recovery of manual dexterity after unilateral cervical lesion in adult primates--re-examination and extension of behavioral data. *Eur J Neurosci,* 29**,** 983-96.

FRIEL, K., CHAKRABARTY, S., KUO, H.-C. & MARTIN, J. 2012. Using Motor Behavior during an Early Critical Period to Restore Skilled Limb Movement after Damage to the Corticospinal System during Development. 32**,** 9265-9276.

FRIESE, A., KALTSCHMIDT, J. A., LADLE, D. R., SIGRIST, M., JESSELL, T. M. & ARBER, S. 2009. Gamma and alpha motor neurons distinguished by expression of transcription factor Err3. *Proceedings of the National Academy of Sciences,* 106**,** 13588-13593.

GAJEWSKA-WOŹNIAK, O., SKUP, M., KASICKI, S., ZIEMLIŃSKA, E. & CZARKOWSKA-BAUCH, J. 2013. Enhancing Proprioceptive Input to Motoneurons Differentially Affects Expression of Neurotrophin 3 and Brain-Derived Neurotrophic Factor in Rat Hoffmann-Reflex Circuitry. *PLOS ONE,* 8**,** e65937.

GANZER, P. D., MANOHAR, A., SHUMSKY, J. S. & MOXON, K. A. 2016. Therapy induces widespread reorganization of motor cortex after complete spinal transection that supports motor recovery. *Experimental Neurology,* 279**,** 1-12.

GARCIA-ALIAS, G., BARKHUYSEN, S., BUCKLE, M. & FAWCETT, J. W. 2009. Chondroitinase ABC treatment opens a window of opportunity for task-specific rehabilitation. *Nat Neurosci,* 12**,** 1145-51.

GEOFFROY, C. G., LORENZANA, A. O., KWAN, J. P., LIN, K., GHASSEMI, O., MA, A., XU, N., CREGER, D., LIU, K., HE, Z. & ZHENG, B. 2015. Effects of PTEN and Nogo Codeletion on Corticospinal Axon Sprouting and Regeneration in Mice. *The Journal of Neuroscience,* 35**,** 6413-6428.

GERASIMENKO, Y. P., ICHIYAMA, R. M., LAVROV, I. A., COURTINE, G., CAI, L., ZHONG, H., ROY, R. R. & EDGERTON, V. R. 2007. Epidural Spinal Cord Stimulation Plus Quipazine Administration Enable Stepping in Complete Spinal Adult Rats. 98**,** 2525-2536.

GILL, M. L., GRAHN, P. J., CALVERT, J. S., LINDE, M. B., LAVROV, I. A., STROMMEN, J. A., BECK, L. A., SAYENKO, D. G., VAN STRAATEN, M. G., DRUBACH, D. I., VEITH, D. D., THORESON, A. R., LOPEZ, C., GERASIMENKO, Y. P., EDGERTON, V. R., LEE, K. H. & ZHAO, K. D. 2018. Neuromodulation of lumbosacral spinal networks enables independent stepping after complete paraplegia. *Nature Medicine,* 24**,** 1677-1682.

GILMAN, S. & EBEL, H. C. 1970. Fusimotor neuron responses to natural stimuli as a function of prestimulus fusimotor activity in decerebellate cats. *Brain Research,* 21**,** 367-384.

GIRGIS, J., MERRETT, D., KIRKLAND, S., METZ, G. A. S., VERGE, V. & FOUAD, K. 2007. Reaching training in rats with spinal cord injury promotes plasticity and task specific recovery. *Brain,* 130**,** 2993-3003.

GLADDEN, M. H. 1981. The activity of intrafusal muscle fibres during central stimulation in the cat. *In:* TAYLOR, A. & PROCHAZKA, A. (eds.) *Muscle Receptors and Movement: Proceedings of a Symposium held at the Sherrington School of Physiology, St Thomas's Hospital Medical School, London, on July 8th and 9th, 1980.* London: Palgrave Macmillan UK.

GLADDEN, M. H., JANKOWSKA, E. & CZARKOWSKA-BAUCH, J. 1998. New observations on coupling between group II muscle afferents and feline γ-motoneurones. *The Journal of Physiology,* 512**,** 507-520.

GOLDSHMIT, Y., GALEA, M. P., WISE, G., BARTLETT, P. F. & TURNLEY, A. M. 2004. Axonal Regeneration and Lack of Astrocytic Gliosis in EphA4-Deficient Mice. 24**,** 10064-10073.

GONZENBACH, R. R., ZOERNER, B., SCHNELL, L., WEINMANN, O., MIR, A. K. & SCHWAB, M. E. 2012. Delayed Anti-Nogo-A Antibody Application after Spinal Cord Injury Shows Progressive Loss of Responsiveness. *J Neurotrauma,* 29**,** 567-578.

GOSGNACH, S., LANUZA, G. M., BUTT, S. J. B., SAUERESSIG, H., ZHANG, Y., VELASQUEZ, T., RIETHMACHER, D., CALLAWAY, E. M., KIEHN, O. & GOULDING, M. 2006. V1 spinal neurons regulate the speed of vertebrate locomotor outputs. *Nature,* 440**,** 215-219.

GRAHAM, B. A. & HUGHES, D. I. 2020. Defining populations of dorsal horn interneurons. *Pain,* 161**,** 2434-2436.

GRANIT, R. & HOLMGREN, B. 1955. Two pathways from brain stem to gamma ventral horn cells. *Acta Physiologica Scandinavica,* 35**,** 93-108.

GRANIT, R., HOLMGREN, B. & MERTON, P. 1955. The two routes for excitation of muscle and their subservience to the cerebellum. *The Journal of physiology,* 130**,** 213-224.

GRANIT, R. & KAADA, B. R. 1953. Influence of Stimulation of Central Nervous Structures on Muscle Spindles in Cat1. *Acta Physiologica Scandinavica,* 27**,** 130-160.

GRANIT, R., PASCOE, J. E. & STEG, G. 1957. The behaviour of tonic α and γ motoneurones during stimulation of recurrent collaterals. *The Journal of Physiology,* 138**,** 381-400.

GREER, J. J. & STEIN, R. B. 1990. Fusimotor control of muscle spindle sensitivity during respiration in the cat. *The Journal of physiology,* 422**,** 245.

GRILLNER, S., HONGO, T. & LUND, S. 1969. Descending Monosynaptic and Reflex Control of γ-Motoneurones. *Acta Physiologica Scandinavica,* 75**,** 592-613.

GRILLNER, S., HONGO, T. & LUNDBERG, A. 1967. The Effect of DOPA on the Spinal Cord 7. Reflex activation of static γ-motoneurones from the flexor reflex afferents. *Acta Physiologica Scandinavica,* 70**,** 403-411.

GRIMM, D., LEE, J. S., WANG, L., DESAI, T., AKACHE, B., STORM, T. A. & KAY, M. A. 2008. In Vitro and In Vivo Gene Therapy Vector Evolution via Multispecies Interbreeding and Retargeting of Adeno-Associated Viruses. *Journal of Virology,* 82**,** 5887-5911.

GROSSMAN, S. D., ROSENBERG, L. J. & WRATHALL, J. R. 2001. Temporal–Spatial Pattern of Acute Neuronal and Glial Loss after Spinal Cord Contusion. *Experimental Neurology,* 168**,** 273-282.

HADLEY, W., ROMAIN, F., LIONEL, H. & KIRILL, M. 2020. dplyr: A Grammar of Data Manipulation. *R package version 1.0.2*.

HAGBARTH, K., WALLIN, G., LÖFSTEDT, L. & AQUILONIUS, S. 1975. Muscle spindle activity in alternating tremor of Parkinsonism and in clonus. *Journal of Neurology, Neurosurgery & Psychiatry,* 38**,** 636-641.

HAGBARTH, K. E., WALLIN, G. & LOFSTEDT, L. 1973. Muscle spindle responses to stretch in normal and spastic subjects. *Scand J Rehabil Med,* 5**,** 156-9.

HAN, S., LI, D., KOU, Y., FU, Z. & YIN, X. 2019. Multiple retrograde tracing methods compatible with 3DISCO clearing. *Artificial Cells, Nanomedicine, and Biotechnology,* 47**,** 4240-4247.

HAREL, N. Y., SONG, K.-H., TANG, X. & STRITTMATTER, S. M. J. J. O. N. 2010. Nogo receptor deletion and multimodal exercise improve distinct aspects of recovery in cervical spinal cord injury. 27**,** 2055-2066.

HARKEMA, S., GERASIMENKO, Y., HODES, J., BURDICK, J., ANGELI, C., CHEN, Y., FERREIRA, C., WILLHITE, A., REJC, E., GROSSMAN, R. G. & EDGERTON, V. R. 2011. Effect of epidural stimulation of the lumbosacral spinal cord on voluntary movement, standing, and assisted stepping after motor complete paraplegia: a case study. *The Lancet,* 377**,** 1938-1947.

HARKEMA, S. J., WANG, S., ANGELI, C. A., CHEN, Y., BOAKYE, M., UGILIWENEZA, B. & HIRSCH, G. A. 2018. Normalization of Blood Pressure With Spinal Cord Epidural Stimulation After Severe Spinal Cord Injury. 12.

HARRIGAN, M. E., FILOUS, A. R., TOSOLINI, A. P., MORRIS, R., SCHWAB, J. M. & ARNOLD, W. D. 2019. Assessing Rat Forelimb and Hindlimb Motor Unit Connectivity as Objective and Robust Biomarkers of Spinal Motor Neuron Function. *Scientific Reports,* 9**,** 16699.

HARVEY, R. & MATTHEWS, P. 1961. The response of de-efferented muscle spindle endings in the cat's soleus to slow extension of the muscle. *The Journal of Physiology,* 157**,** 370.

HAUSMANN, O. N. 2003. Post-traumatic inflammation following spinal cord injury. *Spinal Cord,* 41**,** 369-378.

HAYASHI, M., HINCKLEY, C. A., DRISCOLL, S. P., MOORE, N. J., LEVINE, A. J., HILDE, K. L., SHARMA, K. & PFAFF, S. L. 2018. Graded Arrays of Spinal and Supraspinal V2a Interneuron Subtypes Underlie Forelimb and Hindlimb Motor Control. *Neuron,* 97**,** 869-884.e5.

HE, Z. & JIN, Y. 2016. Intrinsic Control of Axon Regeneration. *Neuron,* 90**,** 437-451.

HELMS, A. W. & JOHNSON, J. E. 2003. Specification of dorsal spinal cord interneurons. *Current Opinion in Neurobiology,* 13**,** 42-49.

HENNEMAN, E., SOMJEN, G. & CARPENTER, D. O. 1965. Functional significance of cell size in spinal moroneurons *Journal of Neurophysiology,* 28**,** 560-580.

HERRITY, A. N., WILLIAMS, C. S., ANGELI, C. A., HARKEMA, S. J. & HUBSCHER, C. H. 2018. Lumbosacral spinal cord epidural stimulation improves voiding function after human spinal cord injury. *Scientific Reports,* 8**,** 8688.

HILDE, K. L., LEVINE, A. J., HINCKLEY, C. A., HAYASHI, M., MONTGOMERY, J. M., GULLO, M., DRISCOLL, S. P., GROSSCHEDL, R., KOHWI, Y., KOHWI-SHIGEMATSU, T. & PFAFF, S. L. 2016. Satb2 Is Required for the

Development of a Spinal Exteroceptive Microcircuit that Modulates Limb Position. *Neuron,* 91**,** 763-776.

HILTON, B. J., ANENBERG, E., HARRISON, T. C., BOYD, J. D., MURPHY, T. H. & TETZLAFF, W. 2016. Re-Establishment of Cortical Motor Output Maps and Spontaneous Functional Recovery via Spared Dorsolaterally Projecting Corticospinal Neurons after Dorsal Column Spinal Cord Injury in Adult Mice. *The Journal of Neuroscience,* 36**,** 4080-4092.

HINSEY, J. C. 1934. The innervation of skeletal muscle. *Physiological Reviews,* 14**,** 514-585.

HOFFMANN, P. J. Z. B. 1918. Uber die Beziehungen der Sehnenreflexe zur willkurlichen Bewegung und zum Tonus. 68**,** 351-370.

HOLLIS II, E. R., ISHIKO, N., YU, T., LU, C.-C., HAIMOVICH, A., TOLENTINO, K., RICHMAN, A., TURY, A., WANG, S.-H., PESSIAN, M., JO, E., KOLODKIN, A. & ZOU, Y. 2016. Ryk controls remapping of motor cortex during functional recovery after spinal cord injury. *Nature Neuroscience,* 19**,** 697.

HOSPOD, V., AIMONETTI, J. M., ROLL, J. P. & RIBOT-CISCAR, E. 2007. Changes in human muscle spindle sensitivity during a proprioceptive attention task. *J Neurosci,* 27**,** 5172-8.

HOU, S., CARSON, D. M., WU, D., KLAW, M. C., HOULÉ, J. D. & TOM, V. J. 2016a. Dopamine is produced in the rat spinal cord and regulates micturition reflex after spinal cord injury. *Experimental neurology,* 285**,** 136-146.

HOU, S., CARSON, D. M., WU, D., KLAW, M. C., HOULÉ, J. D. & TOM, V. J. 2016b. Dopamine is produced in the rat spinal cord and regulates micturition reflex after spinal cord injury. *Experimental Neurology,* 285**,** 136-146.

HUBER, A. B., WEINMANN, O., BRÖSAMLE, C., OERTLE, T. & SCHWAB, M. E. 2002. Patterns of Nogo mRNA and Protein Expression in the Developing and Adult Rat and After CNS Lesions. 22**,** 3553-3567.

HUGHES, D. I., MACKIE, M., NAGY, G. G., RIDDELL, J. S., MAXWELL, D. J., SZABÓ, G., ERDÉLYI, F., VERESS, G., SZŰCS, P., ANTAL, M. & TODD, A. J. 2005. P boutons in lamina IX of the rodent spinal cord express high levels of glutamic acid decarboxylase-65 and originate from cells in deep medial dorsal horn. 102**,** 9038-9043.

HULLIGER, M. 1984. The mammalian muscle spindle and its central control. *Reviews of Physiology, Biochemistry and Pharmacology.* Springer.

HULLIGER, M., MATTHEWS, P. B. & NOTH, J. 1977. Effects of combining static and dynamic fusimotor stimulation on the response of the muscle spindle primary ending to sinusoidal stretching. *The Journal of Physiology,* 267**,** 839-856.

HUNT, C. C. & KUFFLER, S. W. 1951. Further study of efferent small-nerve fibers to mammalian muscle spindles; multiple spindle innervation and activity during contraction. *J Physiol,* 113**,** 283-97.

HUNT, C. C. & WILKINSON, R. S. 1980. An analysis of receptor potential and tension of isolated cat muscle spindles in response to sinusoidal stretch. *The Journal of Physiology,* 302**,** 241-262.

HUTCHINSON, K. J., GÓMEZ-PINILLA, F., CROWE, M. J., YING, Z. & BASSO, D. M. 2004. Three exercise paradigms differentially improve sensory recovery after spinal cord contusion in rats. *Brain,* 127**,** 1403-1414.

ICHIYAMA, R., POTUZAK, M., BALAK, M., KALDERON, N. & EDGERTON, V. R. 2009. Enhanced motor function by training in spinal cord contused rats following radiation therapy. *PLoS One,* 4**,** e6862.

ICHIYAMA, R. M., BROMAN, J., EDGERTON, V. R. & HAVTON, L. A. 2006. Ultrastructural synaptic features differ between alpha- and gamma-motoneurons innervating the tibialis anterior muscle in the rat. *J Comp Neurol,* 499**,** 306-15.

ICHIYAMA, R. M., BROMAN, J., ROY, R. R., ZHONG, H., EDGERTON, V. R. & HAVTON, L. A. 2011. Locomotor Training Maintains Normal Inhibitory Influence on Both Alpha- and Gamma-Motoneurons after Neonatal Spinal Cord Transection. *The Journal of neuroscience : the official journal of the Society for Neuroscience,* 31**,** 26-33.

ICHIYAMA, R. M., COURTINE, G., GERASIMENKO, Y. P., YANG, G. J., VAN DEN BRAND, R., LAVROV, I. A., ZHONG, H., ROY, R. R. & EDGERTON, V. R. 2008a. Step training reinforces specific spinal locomotor circuitry in adult spinal rats. *J Neurosci,* 28**,** 7370-5.

ICHIYAMA, R. M., GERASIMENKO, Y., JINDRICH, D. L., ZHONG, H., ROY, R. R. & EDGERTON, V. R. 2008b. Dose dependence of the 5-HT agonist quipazine in facilitating spinal stepping in the rat with epidural stimulation. *Neuroscience Letters,* 438**,** 281-285.

ICHIYAMA, R. M., GERASIMENKO, Y. P., ZHONG, H., ROY, R. R. & EDGERTON, V. R. 2005. Hindlimb stepping movements in complete spinal rats induced by epidural spinal cord stimulation. *Neuroscience Letters,* 383**,** 339-344.

IWAHARA, T., ATSUTA, Y., GARCIA-RILL, E. & SKINNER, R. D. 1991. Locomotion Induced by Spinal Cord Stimulation in the Neonate Rat In Vitro. *Somatosensory & Motor Research,* 8**,** 281-287.

IWAHARA, T., ATSUTA, Y., GARCIA-RILL, E. & SKINNER, R. D. 1992. Spinal cord stimulation-induced locomotion in the adult cat. *Brain Research Bulletin,* 28**,** 99-105.

IWASATO, T., DATWANI, A., WOLF, A. M., NISHIYAMA, H., TAGUCHI, Y., TONEGAWA, S., KNÖPFEL, T., ERZURUMLU, R. S. & ITOHARA, S. 2000. Cortex-restricted disruption of NMDAR1 impairs neuronal patterns in the barrel cortex. *Nature,* 406**,** 726-731.

JAKEMAN, L. B., HOSCHOUER, E. L. & BASSO, D. M. J. B. R. B. 2011. Injured mice at the gym: review, results and considerations for combining chondroitinase and locomotor exercise to enhance recovery after spinal cord injury. 84**,** 317-326.

JAMI, L., MURTHY, K. S. & PETIT, J. 1982. A quantitative study of skeletofusimotor innervation in the cat peroneus tertius muscle. *The Journal of Physiology,* 325**,** 125-144.

JANKOWSKA, E., GLADDEN, M. H. & CZARKOWSKA-BAUCH, J. 1998. Modulation of responses of feline γ-motoneurones by noradrenaline, tizanidine and clonidine. *The Journal of Physiology,* 512**,** 521-531.

JESSELL, T. M. 2000. Neuronal specification in the spinal cord: inductive signals and transcriptional codes. *Nature Reviews Genetics,* 1**,** 20-29.

JIN, D., LIU, Y., SUN, F., WANG, X., LIU, X. & HE, Z. 2015. Restoration of skilled locomotion by sprouting corticospinal axons induced by co-deletion of PTEN and SOCS3. *Nature Communications,* 6**,** 8074.

JOHNSON, I. P. 1986. A quantitative ultrastructural comparison of alpha and gamma motoneurons in the thoracic region of the spinal cord of the adult cat. *J Anat,* 147**,** 55-72.

JONES, K. E., WESSBERG, J. & VALLBO, Å. 2001. Proprioceptive feedback is reduced during adaptation to a visuomotor transformation: preliminary findings. *NeuroReport,* 12.

JOSET, A., DODD, D. A., HALEGOUA, S. & SCHWAB, M. E. 2010. Pincher-generated Nogo-A endosomes mediate growth cone collapse and retrograde signaling. *J Cell Biol,* 188**,** 271-85.

JOVANOVIC, K., ANASTASIJEVIC, R. & VUCO, J. 1990. Reflex effects on gamma fusimotor neurones of chemically induced discharges in small-diameter muscle afferents in decerebrate cats. *Brain Research,* 521**,** 89-94.

KAKULAS, B. A. 2004. Neuropathology: the foundation for new treatments in spinal cord injury. *Spinal Cord,* 42**,** 549-63.

KAPITZA, S., ZÖRNER, B., WEINMANN, O., BOLLIGER, M., FILLI, L., DIETZ, V. & SCHWAB, M. E. 2012. Tail spasms in rat spinal cord injury: changes in interneuronal connectivity. *Exp Neurol,* 236**,** 179-89.

KEMM, R. E. & WESTBURY, D. R. 1978. Some properties of spinal gamma-motoneurones in the cat, determined by micro-electrode recording. *J Physiol,* 282**,** 59-71.

KEMPF, A., TEWS, B., ARZT, M. E., WEINMANN, O., OBERMAIR, F. J., PERNET, V., ZAGREBELSKY, M., DELEKATE, A., IOBBI, C., ZEMMAR, A., RISTIC, Z., GULLO, M., SPIES, P., DODD, D., GYGAX, D., KORTE, M. & SCHWAB, M. E. 2014. The Sphingolipid Receptor S1PR2 Is a Receptor for Nogo-A Repressing Synaptic Plasticity. *PLOS Biology,* 12**,** e1001763.

KERSCHNER, L. 1888. Bemerkungen über ein besonderes Muskelsystem im willkürlichen Muskel. *Anat. Anz,* 3**,** 126-132.

KHALKI, L., SADLAOUD, K., LEROND, J., COQ, J.-O., BREZUN, J.-M., VINAY, L., COULON, P. & BRAS, H. 2018. Changes in innervation of lumbar motoneurons and

organization of premotor network following training of transected adult rats. *Experimental Neurology,* 299**,** 1-14.

KIEHN, O. 2006. LOCOMOTOR CIRCUITS IN THE MAMMALIAN SPINAL CORD. 29**,** 279-306.

KISER, T. S., REESE, N. B., MARESH, T., HEARN, S., YATES, C., SKINNER, R., PAIT, T. G. & GARCIA-RILL, E. 2005. Use of a Motorized Bicycle Exercise Trainer to Normalize Frequency-Dependent Habituation of the H-reflex in Spinal Cord Injury. *The Journal of Spinal Cord Medicine,* 28**,** 241-245.

KNOTH, R., SINGEC, I., DITTER, M., PANTAZIS, G., CAPETIAN, P., MEYER, R. P., HORVAT, V., VOLK, B. & KEMPERMANN, G. 2010. Murine Features of Neurogenesis in the Human Hippocampus across the Lifespan from 0 to 100 Years. *PLOS ONE,* 5**,** e8809.

KORONFEL, L. M., KANNING, K. C., ALCOS, A., HENDERSON, C. E. & BROWNSTONE, R. M. J. B. 2021. Elimination of glutamatergic transmission from Hb9 interneurons does not impact treadmill locomotion. *BioRxiv*.

KOVALCHUK, Y., HANSE, E., KAFITZ, K. W. & KONNERTH, A. 2002. Postsynaptic Induction of BDNF-Mediated Long-Term Potentiation. *Science,* 295**,** 1729-34.

KRAJACIC, A., GHOSH, M., PUENTES, R., PEARSE, D. D. & FOUAD, K. 2009. Advantages of delaying the onset of rehabilitative reaching training in rats with incomplete spinal cord injury. 29**,** 641-651.

KUBASAK, M. D., JINDRICH, D. L., ZHONG, H., TAKEOKA, A., MCFARLAND, K. C., MUÑOZ-QUILES, C., ROY, R. R., EDGERTON, V. R., RAMÓN-CUETO, A. & PHELPS, P. E. 2007. OEG implantation and step training enhance hindlimb-stepping ability in adult spinal transected rats. *Brain,* 131**,** 264-276.

KUCERA, J., COONEY, W., QUE, A., SZEDER, V., STANCZ-SZEDER, H. & WALRO, J. 2002. Formation of supernumerary muscle spindles at the expense of golgi tendon organs in ER81-deficient mice. 223**,** 389-401.

KUCERA, J. & HUGHES, R. 1983. Histological study of motor innervation to long nuclear chain intrafusal fibers in the muscle spindle of the cat. *Cell and Tissue Research,* 228**,** 535-547.

KUCHER, K., JOHNS, D., MAIER, D., ABEL, R., BADKE, A., BARON, H., THIETJE, R., CASHA, S., MEINDL, R., GOMEZ-MANCILLA, B., PFISTER, C., RUPP, R., WEIDNER, N., MIR, A., SCHWAB, M. E. & CURT, A. 2018. First-in-Man Intrathecal Application of Neurite Growth-Promoting Anti-Nogo-A Antibodies in Acute Spinal Cord Injury. *Neurorehabil Neural Repair,* 32**,** 578-589.

KÜCHLER, M., FOUAD, K., WEINMANN, O., SCHWAB, M. E. & RAINETEAU, O. 2002. Red nucleus projections to distinct motor neuron pools in the rat spinal cord. 448**,** 349-359.

KUERZI, J., BROWN, E. H., SHUM-SIU, A., SIU, A., BURKE, D., MOREHOUSE, J., SMITH, R. R. & MAGNUSON, D. S. K. 2010. Task-specificity vs. ceiling effect: Step-training in shallow water after spinal cord injury. *Experimental Neurology,* 224**,** 178-187.

KUSCHA, V., BARREIRO-IGLESIAS, A., BECKER, C. G. & BECKER, T. 2012. Plasticity of tyrosine hydroxylase and serotonergic systems in the regenerating spinal cord of adult zebrafish. *J Comp Neurol,* 520**,** 933-51.

KUYPERS, H. G. J. M. 1981. Anatomy of the Descending Pathways. *Comprehensive Physiology.*

KWOK, J. C. F., WARREN, P. & FAWCETT, J. W. 2012. Chondroitin sulfate: A key molecule in the brain matrix. *The International Journal of Biochemistry & Cell Biology,* 44**,** 582-586.

LAGERBACK, P. A., CULLHEIM, S. & ULFHAKE, B. 1986. Electron microscopic observations on the synaptology of cat sciatic gamma-motoneurons after intracellular staining with horseradish peroxidase. *Neurosci Lett,* 70**,** 23-7.

LALANCETTE-HEBERT, M., SHARMA, A., LYASHCHENKO, A. K. & SHNEIDER, N. A. 2016. Gamma motor neurons survive and exacerbate alpha motor neuron degeneration in ALS. 113**,** E8316-E8325.

LAPORTE, Y., EMONET-DÉNAND, F. & JAMI, L. 1981. The skeletofusimotor or β-innervation of mammalian muscle spindles. *Trends in Neurosciences,* 4**,** 97-99.

LAVROV, I., COURTINE, G., DY, C. J., VAN DEN BRAND, R., FONG, A. J., GERASIMENKO, Y., ZHONG, H., ROY, R. R. & EDGERTON, V. R. 2008. Facilitation of Stepping with Epidural Stimulation in Spinal Rats: Role of Sensory Input. 28**,** 7774-7780.

LAVROV, I., GERASIMENKO, Y. P., ICHIYAMA, R. M., COURTINE, G., ZHONG, H., ROY, R. R. & EDGERTON, V. R. 2006. Plasticity of Spinal Cord Reflexes After a Complete Transection in Adult Rats: Relationship to Stepping Ability. 96**,** 1699-1710.

LEE, H., MCKEON, R. J. & BELLAMKONDA, R. V. 2010. Sustained delivery of thermostabilized chABC enhances axonal sprouting and functional recovery after spinal cord injury. *Proceedings of the National Academy of Sciences of the United States of America,* 107**,** 3340-3345.

LEE, T. D. & GENOVESE, E. D. 1988. Distribution of Practice in Motor Skill Acquisition: Learning and Performance Effects Reconsidered. *Research Quarterly for Exercise and Sport,* 59**,** 277-287.

LEMON, R. N. 2008. Descending Pathways in Motor Control. *Annual Review of Neuroscience,* 31**,** 195-218.

LEON, R. D. D., HODGSON, J. A., ROY, R. R. & EDGERTON, V. R. 1998. Full Weight-Bearing Hindlimb Standing Following Stand Training in the Adult Spinal Cat. 80**,** 83-91.

LERCH, T. F., O'DONNELL, J. K., MEYER, N. L., XIE, Q., TAYLOR, K. A., STAGG, S. M. & CHAPMAN, M. S. 2012. Structure of AAV-DJ, a Retargeted Gene Therapy Vector: Cryo-Electron Microscopy at 4.5Å resolution. *Structure (London, England : 1993),* 20**,** 1310-1320.

LESKELL, L. 1945. The action potential and excitatory effects of the small ventral root fibers to skeletal muscle. *Acta physiol. scand,* 10.

LI, Q., BRUS-RAMER, M., MARTIN, J. H. & MCDONALD, J. W. 2010. Electrical stimulation of the medullary pyramid promotes proliferation and differentiation of oligodendrocyte progenitor cells in the corticospinal tract of the adult rat. *Neurosci Lett,* 479**,** 128-33.

LIEBSCHER, T., SCHNELL, L., SCHNELL, D., SCHOLL, J., SCHNEIDER, R., GULLO, M., FOUAD, K., MIR, A., RAUSCH, M., KINDLER, D. J. A. O. N. O. J. O. T. A. N. A. & SOCIETY, T. C. N. 2005. Nogo-A antibody improves regeneration and locomotion of spinal cord–injured rats. 58**,** 706-719.

LIN, S., LI, Y., LUCAS-OSMA, A. M., HARI, K., STEPHENS, M. J., SINGLA, R., HECKMAN, C. J., ZHANG, Y., FOUAD, K., FENRICH, K. K. & BENNETT, D. J. 2019. Locomotor-related V3 interneurons initiate and coordinate muscles spasms after spinal cord injury. 121**,** 1352-1367.

LITTLE, J. W. & HALAR, E. M. 1985. H-reflex changes following spinal cord injury. *Archives of Physical Medicine and Rehabilitation,* 66**,** 19-22.

LIU, G., DETLOFF, M. R., MILLER, K. N., SANTI, L. & HOULÉ, J. D. 2012. Exercise modulates microRNAs that affect the PTEN/mTOR pathway in rats after spinal cord injury. *Experimental Neurology,* 233**,** 447-456.

LIU, Y., WANG, X., LI, W., ZHANG, Q., LI, Y., ZHANG, Z., ZHU, J., CHEN, B., WILLIAMS, P. R., ZHANG, Y., YU, B., GU, X. & HE, Z. 2017a. A Sensitized IGF1 Treatment Restores Corticospinal Axon-Dependent Functions. *Neuron,* 95**,** 817-833.e4.

LIU, Z. H., YIP, P. K., ADAMS, L., DAVIES, M., LEE, J. W., MICHAEL, G. J., PRIESTLEY, J. V. & MICHAEL-TITUS, A. T. 2015. A Single Bolus of Docosahexaenoic Acid Promotes Neuroplastic Changes in the Innervation of Spinal Cord Interneurons and Motor Neurons and Improves Functional Recovery after Spinal Cord Injury. *J Neurosci,* 35**,** 12733-52.

LIU, Z. H., YIP, P. K., PRIESTLEY, J. V. & MICHAEL-TITUS, A. T. 2017b. A Single Dose of Docosahexaenoic Acid Increases the Functional Recovery Promoted by Rehabilitation after Cervical Spinal Cord Injury in the Rat. *J Neurotrauma,* 34**,** 1766-1777.

LOVELY, R. G., GREGOR, R. J., ROY, R. R. & EDGERTON, V. R. 1986. Effects of training on the recovery of full-weight-bearing stepping in the adult spinal cat. *Experimental Neurology,* 92**,** 421-435.

MACEFIELD, V. G. 2013. Discharge rates and discharge variability of muscle spindle afferents in human chronic spinal cord injury. *Clinical Neurophysiology,* 124**,** 114-119.

MACIAS, M., NOWICKA, D., CZUPRYN, A., SULEJCZAK, D., SKUP, M., SKANGIEL-KRAMSKA, J. & CZARKOWSKA-BAUCH, J. 2009. Exercise-induced motor improvement after complete spinal cord transection and its relation to expression of brain-derived neurotrophic factor and presynaptic markers. *BMC Neuroscience,* 10**,** 144.

MAIER, I. C., ICHIYAMA, R. M., COURTINE, G., SCHNELL, L., LAVROV, I., EDGERTON, V. R. & SCHWAB, M. E. 2009. Differential effects of anti-Nogo-A antibody treatment and treadmill training in rats with incomplete spinal cord injury. *Brain,* 132**,** 1426-1440.

MANOHAR, A., FOFFANI, G., GANZER, P. D., BETHEA, J. R. & MOXON, K. A. 2017. Cortex-dependent recovery of unassisted hindlimb locomotion after complete spinal cord injury in adult rats. *Elife,* 6.

MARTIN, J. H. 2016. Harnessing neural activity to promote repair of the damaged corticospinal system after spinal cord injury. *Neural regeneration research,* 11**,** 1389-1391.

MARTIN, J. H., FRIEL, K. M., SALIMI, I. & CHAKRABARTY, S. 2007. Activity- and use-dependent plasticity of the developing corticospinal system. *Neuroscience & Biobehavioral Reviews,* 31**,** 1125-1135.

MATTHEWS, P. B. 1972. Mammalian muscle receptors and their central actions, London, Edward Arnold ltd.

MATTHEWS, P. B. C. 1964. Muscle Spindles and Their Motor Control. *Physiological Reviews,* 44**,** 219-288.

MAY, Z., FENRICH, K. K., DAHLBY, J., BATTY, N. J., TORRES-ESPÍN, A. & FOUAD, K. 2017. Following Spinal Cord Injury Transected Reticulospinal Tract Axons Develop New Collateral Inputs to Spinal Interneurons in Parallel with Locomotor Recovery. *Neural plasticity,* 2017.

MCALLISTER, A. K., LO, D. C. & KATZ, L. C. 1995. Neurotrophins regulate dendritic growth in developing visual cortex. *Neuron,* 15**,** 791-803.

MCCREA, D. A. & RYBAK, I. A. 2008. Organization of mammalian locomotor rhythm and pattern generation. *Brain Research Reviews,* 57**,** 134-146.

MCDAID, D., PARK, A. L., GALL, A., PURCELL, M. & BACON, M. 2019. Understanding and modelling the economic impact of spinal cord injuries in the United Kingdom. *Spinal Cord,* 57**,** 778-788.

MCPHERSON, J. G., MILLER, R. R. & PERLMUTTER, S. I. 2015. Targeted, activity-dependent spinal stimulation produces long-lasting motor recovery in chronic cervical spinal cord injury. 112**,** 12193-12198.

MCWILLIAM, P. N. 1975. The incidence and properties of β axons to muscles spindles in the cat hindlimb. *Quarterly Journal of Experimental Physiology and Cognate Medical Sciences,* 60**,** 25-36.

MÉNARD, A., LEBLOND, H. & GOSSARD, J. P. 1999. The modulation of presynaptic inhibition in single muscle primary afferents during fictive locomotion in the cat. *J Neurosci,* 19**,** 391-400.

MENDE, M., FLETCHER, EMILY V., BELLUARDO, JOSEPHINE L., PIERCE, JOSEPH P., BOMMAREDDY, PRAVEEN K., WEINRICH, JARRET A., KABIR, ZEEBA D., SCHIERBERL, KATHRYN C., PAGIAZITIS, JOHN G., MENDELSOHN, ALANA I., FRANCESCONI, A., EDWARDS, ROBERT H., MILNER, TERESA A., RAJADHYAKSHA, ANJALI M., VAN ROESSEL, PETER J., MENTIS, GEORGE Z. & KALTSCHMIDT, JULIA A. 2016. Sensory-Derived Glutamate Regulates Presynaptic Inhibitory Terminals in Mouse Spinal Cord. *Neuron,* 90**,** 1189-1202.

MENSE, S. & MEYER, H. 1988. Bradykinin-induced modulation of the response behaviour of different types of feline group III and IV muscle receptors. *The Journal of Physiology,* 398**,** 49-63.

MILES, G. B., HARTLEY, R., TODD, A. J. & BROWNSTONE, R. M. 2007. Spinal cholinergic interneurons regulate the excitability of motoneurons during locomotion. 104**,** 2448-2453.

MINASSIAN, K., PERSY, I., RATTAY, F., PINTER, M. M., KERN, H. & DIMITRIJEVIC, M. R. 2007. Human lumbar cord circuitries can be activated by extrinsic tonic input to generate locomotor-like activity. *Human Movement Science,* 26**,** 275-295.

MISAWA, H., HARA, M., TANABE, S., NIIKURA, M., MORIWAKI, Y. & OKUDA, T. 2012. Osteopontin is an alpha motor neuron marker in the mouse spinal cord. *Journal of Neuroscience Research,* 90**,** 732-742.

MOHAN, R., TOSOLINI, A. P. & MORRIS, R. 2015. Segmental distribution of the motor neuron columns that supply the rat hindlimb: A muscle/motor neuron tract-tracing analysis targeting the motor end plates. *Neuroscience,* 307**,** 98-108.

MOLANDER, C., XU, Q. & GRANT, G. 1984. The cytoarchitectonic organization of the spinal cord in the rat. I. The lower thoracic and lumbosacral cord. *Journal of Comparative Neurology,* 230**,** 133-141.

MOSCHOVAKIS, A. K., BURKE, R. E. & FYFFE, R. E. 1991. The size and dendritic structure of HRP-labeled gamma motoneurons in the cat spinal cord. *J Comp Neurol,* 311**,** 531-45.

MÜLLNER, A., GONZENBACH, R. R., WEINMANN, O., SCHNELL, L., LIEBSCHER, T. & SCHWAB, M. E. 2008. Lamina-specific restoration of serotonergic projections after Nogo-A antibody treatment of spinal cord injury in rats. 27**,** 326-333.

MURPHY, P. R. & HAMMOND, G. R. 1993. The locomotor discharge characteristics of ankle flexor gamma-motoneurones in the decerebrate cat. *The Journal of Physiology,* 462**,** 59-70.

MURPHY, P. R., STEIN, R. B. & TAYLOR, J. 1984. Phasic and tonic modulation of impulse rates in gamma-motoneurons during locomotion in premammillary cats. *Journal of Neurophysiology,* 52**,** 228.

MURRAY, K. C., NAKAE, A., STEPHENS, M. J., RANK, M., D'AMICO, J., HARVEY, P. J., LI, X., HARRIS, R. L. W., BALLOU, E. W., ANELLI, R., HECKMAN, C. J., MASHIMO, T., VAVREK, R., SANELLI, L., GORASSINI, M. A., BENNETT, D. J. & FOUAD, K. 2010. Recovery of motoneuron and locomotor function after spinal cord injury depends on constitutive activity in 5-HT2C receptors. *Nat Med,* 16**,** 694-700.

NIEUWENHUIS, B., HAENZI, B., HILTON, S., CARNICER-LOMBARTE, A., HOBO, B., VERHAAGEN, J. & FAWCETT, J. W. 2021. Optimization of adeno-associated viral vector-mediated transduction of the corticospinal tract: comparison of four promoters. *Gene Therapy,* 28**,** 56-74.

NOBLE, L. J. & WRATHALL, J. R. 1989. Distribution and time course of protein extravasation in the rat spinal cord after contusive injury. *Brain Res,* 482**,** 57-66.

NORRIE, B. A., NEVETT-DUCHCHERER, J. M. & GORASSINI, M. A. 2005. Reduced Functional Recovery by Delaying Motor Training After Spinal Cord Injury. 94**,** 255-264.

NOTH, J. 1981. Autogenetic and antagonistic group II effects on extensor gamma motoneurons of the decerebrate cat. *In:* TAYLOR, A. & PROCHAZKA, A. (eds.) *Muscle Receptors and Movement: Proceedings of a Symposium held at the Sherrington School of Physiology, St Thomas's Hospital Medical School, London, on July 8th and 9th, 1980.* London: Palgrave Macmillan UK.

OERTLE, T., VAN DER HAAR, M. E., BANDTLOW, C. E., ROBEVA, A., BURFEIND, P., BUSS, A., HUBER, A. B., SIMONEN, M., SCHNELL, L., BRÖSAMLE, C., KAUPMANN, K., VALLON, R. & SCHWAB, M. E. 2003. Nogo-A Inhibits Neurite Outgrowth and Cell Spreading with Three Discrete Regions. 23**,** 5393-5406.

OKADA, S., HARA, M., KOBAYAKAWA, K., MATSUMOTO, Y. & NAKASHIMA, Y. 2018. Astrocyte reactivity and astrogliosis after spinal cord injury. *Neuroscience Research,* 126**,** 39-43.

OLLIVIER-LANVIN, K., KEELER, B. E., SIEGFRIED, R., HOULÉ, J. D. & LEMAY, M. A. 2010. Proprioceptive neuropathy affects normalization of the H-reflex by exercise after spinal cord injury. *Experimental Neurology,* 221**,** 198-205.

PAIXÃO, S., LOSCHEK, L., GAITANOS, L., ALCALÀ MORALES, P., GOULDING, M. & KLEIN, R. 2019. Identification of Spinal Neurons Contributing to the Dorsal Column Projection Mediating Fine Touch and Corrective Motor Movements. *Neuron,* 104**,** 749-764.e6.

PAPAIOANNOU, S. & DIMITRIOU, M. 2021. Goal-dependent tuning of muscle spindle receptors during movement preparation. *Science Advances,* 7.

PARK, K. K., LIU, K., HU, Y., SMITH, P. D., WANG, C., CAI, B., XU, B., CONNOLLY, L., KRAMVIS, I., SAHIN, M. & HE, Z. 2008. Promoting Axon Regeneration in the Adult CNS by Modulation of the PTEN/mTOR Pathway. 322**,** 963-966.

PAXINOS, G. & WATSON, C. 2006. The rat brain in stereotaxic coordinates: hard cover edition, Elsevier.

PECK, D., BUXTON, D. F. & NITZ, A. 1984. A comparison of spindle concentrations in large and small muscles acting in parallel combinations. 180**,** 243-252.

PEREZ, M. A., LUNGHOLT, B. K. S. & NIELSEN, J. B. 2005. Presynaptic control of group Ia afferents in relation to acquisition of a visuo-motor skill in healthy humans. *The Journal of physiology,* 568**,** 343-354.

PERRY, S., LARHAMMAR, M., VIEILLARD, J., NAGARAJA, C., HILSCHER, M. M., TAFRESHIHA, A., ROFO, F., CAIXETA, F. V. & KULLANDER, K. 2019. Characterization of Dmrt3-Derived Neurons Suggest a Role within Locomotor Circuits. 39**,** 1771-1782.

PETRINOVIC, M. M., HOUREZ, R., ALOY, E. M., DEWARRAT, G., GALL, D., WEINMANN, O., GAUDIAS, J., BACHMANN, L. C., SCHIFFMANN, S. N., VOGT, K. E. & SCHWAB, M. E. 2013. Neuronal Nogo-A negatively regulates dendritic morphology and synaptic transmission in the cerebellum. 110**,** 1083-1088.

PHADKE, C. P., THOMPSON, F. J., KUKULKA, C. G., NAIR, P. M., BOWDEN, M. G., MADHAVAN, S., TRIMBLE, M. H. & BEHRMAN, A. L. 2010. Soleus H-reflex modulation after motor incomplete spinal cord injury: effects of body position and walking speed. *The journal of spinal cord medicine,* 33**,** 371-378.

PIERANI, A., MORAN-RIVARD, L., SUNSHINE, M. J., LITTMAN, D. R., GOULDING, M. & JESSELL, T. M. 2001. Control of Interneuron Fate in the Developing Spinal Cord by the Progenitor Homeodomain Protein Dbx1. *Neuron,* 29**,** 367-384.

PILLAI, A., MANSOURI, A., BEHRINGER, R., WESTPHAL, H. & GOULDING, M. 2007. Lhx1 and Lhx5 maintain the inhibitory-neurotransmitter status of interneurons in the dorsal spinal cord. 134**,** 357-366.

PINEAU, I. & LACROIX, S. 2007. Proinflammatory cytokine synthesis in the injured mouse spinal cord: multiphasic expression pattern and identification of the cell types involved. *J Comp Neurol,* 500**,** 267-85.

POPLAWSKI, G. H. D., KAWAGUCHI, R., VAN NIEKERK, E., LU, P., MEHTA, N., CANETE, P., LIE, R., DRAGATSIS, I., MEVES, J. M., ZHENG, B., COPPOLA, G. & TUSZYNSKI, M. H. 2020. Injured adult neurons regress to an embryonic transcriptional growth state. *Nature,* 581**,** 77-82.

POWERS, R. K., CAMPBELL, D. L. & RYMER, W. Z. 1989. Stretch reflex dynamics in spastic elbow flexor muscles. *Annals of Neurology,* 25**,** 32-42.

PROCHAZKA, A. 1989. Sensorimotor gain control: A basic strategy of motor systems? *Progress in Neurobiology,* 33**,** 281-307.

PROCHAZKA, A. 1996. Proprioceptive feedback and movement regulation. *In:* SHEPHERD, R. L. B. A. J. T. (ed.) *Handbook of Physiology*. Oxford: American Physiological Society.

PROCHAZKA, A., HULLIGER, M., TREND, P. & DÜRMÜLLER, N. 1988. Dynamic and Static Fusimotor Set in Various Behavioural Contexts. *In:* HNÍK, P., SOUKUP, T., VEJSADA, R. & ZELENÁ, J. (eds.) *Mechanoreceptors: Development, Structure, and Function.* Boston, MA: Springer US.

PROCHAZKA, A., HULLIGER, M., ZANGGER, P. & APPENTENG, K. 1985. 'Fusimotor set': new evidence for α-independent control of γ-motoneurones during movement in the awake cat. *Brain Research,* 339**,** 136-140.

PROCHAZKA, A., STEPHENS, J. A. & WAND, P. 1979. Muscle spindle discharge in normal and obstructed movements. *The Journal of Physiology*, 287**,** 57-66.

PROCHAZKA, A. & WAND, P. 1981. Independence of fusimotor and skeletomotor systems during voluntary movement. *In:* TAYLOR, A. & PROCHAZKA, A. (eds.) *Muscle Receptors and Movement: Proceedings of a Symposium held at the Sherrington School of Physiology, St Thomas's Hospital Medical School, London, on July 8th and 9th, 1980.* London: Palgrave Macmillan UK.

R CORE TEAM 2020. R: A language and environment for statistical computing. Vienna, Austria: R Foundation for Statistical Computing.

RASCOE, A., SHARMA, P. & SHAH, P. K. 2018. Development of an Activity-Dependent Epidural Stimulation System in Freely Moving Spinal Cord Injured Rats: A Proof of Concept Study. 12.

RASOULI, A., BHATIA, N., DINH, P., CAHILL, K., SURYADEVARA, S. & GUPTA, R. 2009. Resection of glial scar following spinal cord injury. 27**,** 931-936.

REESE, N. B., SKINNER, R. D., MITCHELL, D., YATES, C., BARNES, C. N., KISER, T. S. & GARCIA-RILL, E. 2006. Restoration of frequency-dependent depression of the H-reflex by passive exercise in spinal rats. *Spinal Cord,* 44**,** 28-34.

RENIER, N., WU, Z., SIMON, DAVID J., YANG, J., ARIEL, P. & TESSIER-LAVIGNE, M. 2014. iDISCO: A Simple, Rapid Method to Immunolabel Large Tissue Samples for Volume Imaging. *Cell,* 159**,** 896-910.

REXED, B. 1952. The cytoarchitectonic organization of the spinal cord in the cat. 96**,** 415-495.

RIBAK, C., DE LA HOZ, C., JONES, E., LARRIVA SAHD, J. & SWANSON, L. 2008. From Development to Degeneration and Regeneration of the Nervous System.

RICHARDSON, D. S. & LICHTMAN, J. W. 2015. Clarifying Tissue Clearing. *Cell,* 162**,** 246-257.

RIDDLE, C. N., EDGLEY, S. A. & BAKER, S. N. 2009. Direct and Indirect Connections with Upper Limb Motoneurons from the Primate Reticulospinal Tract. 29**,** 4993-4999.

ROGAN, S. C. & ROTH, B. L. 2011. Remote Control of Neuronal Signaling. *Pharmacological Reviews,* 63**,** 291-315.

ROWLAND, J. W., HAWRYLUK, G. W., KWON, B. & FEHLINGS, M. G. 2008. Current status of acute spinal cord injury pathophysiology and emerging therapies: promise on the horizon. *Neurosurg Focus,* 25**,** E2.

RUDOMIN, P. 2009. In search of lost presynaptic inhibition. *Experimental Brain Research,* 196**,** 139.

RUFFINI, A. 1898. On the minute anatomy of the neuromuscular spindles of the cat, and on their physiological significance. *The Journal of Physiology,* 23**,** 190.

RUSCHEL, J., HELLAL, F., FLYNN, K. C., DUPRAZ, S., ELLIOTT, D. A., TEDESCHI, A., BATES, M., SLIWINSKI, C., BROOK, G., DOBRINDT, K., PEITZ, M., BRÜSTLE, O., NORENBERG, M. D., BLESCH, A., WEIDNER, N., BUNGE, M. B., BIXBY, J. L. & BRADKE, F. 2015. Systemic administration of epothilone B promotes axon regeneration after spinal cord injury. *Science,* 348**,** 347-352.

RUST, R., WEBER, R. Z., GRÖNNERT, L., MULDERS, G., MAURER, M. A., HOFER, A.-S., SARTORI, A. M. & SCHWAB, M. E. 2019. Anti-Nogo-A antibodies prevent vascular leakage and act as pro-angiogenic factors following stroke. *Scientific Reports,* 9**,** 20040.

RYBAK, I. A., SHEVTSOVA, N. A., LAFRENIERE-ROULA, M. & MCCREA, D. A. 2006. Modelling spinal circuitry involved in locomotor pattern generation: insights from deletions during fictive locomotion. 577**,** 617-639.

SARUHASHI, Y., YOUNG, W. & PERKINS, R. 1996. The Recovery of 5-HT Immunoreactivity in Lumbosacral Spinal Cord and Locomotor Function after Thoracic Hemisection. *Experimental Neurology,* 139**,** 203-213.

SATOH, D., PUDENZ, C. & ARBER, S. 2016. Context-Dependent Gait Choice Elicited by EphA4 Mutation in Lbx1 Spinal Interneurons. *Neuron,* 89**,** 1046-1058.

SCHEFF, S. W., RABCHEVSKY, A. G., FUGACCIA, I., MAIN, J. A. & LUMPP JR, J. E. J. J. O. N. 2003. Experimental modeling of spinal cord injury: characterization of a force-defined injury device. 20**,** 179-193.

SCHINDLER-IVENS, S. & SHIELDS, R. K. 2000. Low frequency depression of H-reflexes in humans with acute and chronic spinal-cord injury. *Exp Brain Res,* 133**,** 233-41.

SCHMANDKE, A., SCHMANDKE, A. & STRITTMATTER, S. M. 2007. ROCK and Rho: biochemistry and neuronal functions of Rho-associated protein kinases. *The Neuroscientist : a review journal bringing neurobiology, neurology and psychiatry,* 13**,** 454-469.

SCHMIDT, B. J. & JORDAN, L. M. 2000. The role of serotonin in reflex modulation and locomotor rhythm production in the mammalian spinal cord. *Brain Research Bulletin,* 53**,** 689-710.

SCHNELL, L. & SCHWAB, M. E. J. N. 1990. Axonal regeneration in the rat spinal cord produced by an antibody against myelin-associated neurite growth inhibitors. 343**,** 269-272.

SCHWAB, M. E. 2004. Nogo and axon regeneration. *Current Opinion in Neurobiology,* 14**,** 118-124.

SCHWAB, M. E. 2010. Functions of Nogo proteins and their receptors in the nervous system. *Nature Reviews Neuroscience,* 11**,** 799-811.

SCHWAB, M. E. & STRITTMATTER, S. M. 2014. Nogo limits neural plasticity and recovery from injury. *Current Opinion in Neurobiology,* 27**,** 53-60.

SCHWARZ, M., SONTAG, K. H. & WAND, P. 1984a. Non-dopaminergic neurones of the reticular part of substantia nigra can gate static fusimotor action onto flexors in cat. *The Journal of Physiology,* 354**,** 333-344.

SCHWARZ, M., SONTAG, K. H. & WAND, P. 1984b. Sensory-motor processing in substantia nigra pars reticulata in conscious cats. *The Journal of Physiology,* 347**,** 129-147.

SEVERIN, F., ORLOVSKIĬ, G. & SHIK, M. 1967. Work of muscle receptors during controlled locomotion. *Biofizika,* 12**,** 502.

SHAH, P. K., GERASIMENKO, Y., SHYU, A., LAVROV, I., ZHONG, H., ROY, R. R. & EDGERTON, V. R. 2012. Variability in step training enhances locomotor recovery after a spinal cord injury. 36**,** 2054-2062.

SHAH, P. K. & LAVROV, I. 2017. Spinal Epidural Stimulation Strategies: Clinical Implications of Locomotor Studies in Spinal Rats. *Neuroscientist,* 23**,** 664-680.

SHARPLES, S. A., KOBLINGER, K., HUMPHREYS, J. M. & WHELAN, P. J. 2014. Dopamine: a parallel pathway for the modulation of spinal locomotor networks. *Frontiers in neural circuits,* 8**,** 55-55.

SHERRINGTON, C. S. 1894. On the Anatomical Constitution of Nerves of Skeletal Muscles; with Remarks on Recurrent Fibres in the Ventral Spinal Nerve-root. *The Journal of Physiology,* 17**,** 210-258.

SHNEIDER, N. A., BROWN, M. N., SMITH, C. A., PICKEL, J. & ALVAREZ, F. J. 2009. Gamma motor neurons express distinct genetic markers at birth and require muscle spindle-derived GDNF for postnatal survival. *Neural development,* 4**,** 1.

SIEGEL, C. S., FINK, K. L., STRITTMATTER, S. M. & CAFFERTY, W. B. J. 2015. Plasticity of Intact Rubral Projections Mediates Spontaneous Recovery of Function after Corticospinal Tract Injury. *The Journal of Neuroscience,* 35**,** 1443-1457.

SIMONS, D. G. 1988. Myofascial pain syndromes: where are we? Where are we going? *Arch Phys Med Rehabil,* 69**,** 207-12.

SJÖSTRÖM, A. & ZANGGER, P. 1976. Muscle Spindle Control during Locomotor Movements Generated by the Deafferented Spinal Cord. *Acta Physiologica Scandinavica,* 97**,** 281-291.

SKINNER, R. D., HOULE, J. D., REESE, N. B., BERRY, C. L. & GARCIA-RILL, E. 1996. Effects of exercise and fetal spinal cord implants on the H-reflex in chronically spinalized adult rats. *Brain Research,* 729**,** 127-131.

SŁAWIŃSKA, U., ROSSIGNOL, S., BENNETT, D. J., SCHMIDT, B. J., FRIGON, A., FOUAD, K. & JORDAN, L. M. 2012. Comment on “Restoring Voluntary Control of Locomotion After Paralyzing Spinal Cord Injury”. 338**,** 328-328.

SMITH, C. C., MAURICIO, R., NOBRE, L., MARSH, B., WUST, R. C., ROSSITER, H. B. & ICHIYAMA, R. M. 2015. Differential regulation of perineuronal nets in the brain and spinal cord with exercise training. *Brain Res Bull,* 111**,** 20-6.

SMITH, C. C., PATON, J. F. R., CHAKRABARTY, S. & ICHIYAMA, R. M. 2017. Descending Systems Direct Development of Key Spinal Motor Circuits. *J Neurosci,* 37**,** 6372-6387.

SMITH, R. R., BROWN, E. H., SHUM-SIU, A., WHELAN, A., BURKE, D. A., BENTON, R. L. & MAGNUSON, D. S. 2009. Swim training initiated acutely after spinal cord injury is ineffective and induces extravasation in and around the epicenter. *J Neurotrauma,* 26**,** 1017-27.

SONNER, M. J., WALTERS, M. C. & LADLE, D. R. 2017. Analysis of Proprioceptive Sensory Innervation of the Mouse Soleus: A Whole-Mount Muscle Approach. *PLOS ONE,* 12**,** e0170751.

STEBBINS, C. L., CARRETERO, O. A., MINDROIU, T. & LONGHURST, J. C. 1990. Bradykinin release from contracting skeletal muscle of the cat. *Journal of Applied Physiology,* 69**,** 1225-1230.

STEPIEN, A. E., TRIPODI, M. & ARBER, S. 2010. Monosynaptic Rabies Virus Reveals Premotor Network Organization and Synaptic Specificity of Cholinergic Partition Cells. *Neuron,* 68**,** 456-472.

SZUMSKI, A. J., BURG, D., STRUPPLER, A. & VELHO, F. 1974. Activity of muscle spindles during muscle twitch and clonus in normal and spastic human subjects. *Electroencephalography and Clinical Neurophysiology,* 37**,** 589-597.

TAKAKUSAKI, K. 2013. Neurophysiology of gait: From the spinal cord to the frontal lobe. 28**,** 1483-1491.

TAKEOKA, A. 2020. Proprioception: Bottom-up directive for motor recovery after spinal cord injury. *Neuroscience Research,* 154**,** 1-8.

TAKEOKA, A. & ARBER, S. 2019. Functional Local Proprioceptive Feedback Circuits Initiate and Maintain Locomotor Recovery after Spinal Cord Injury. *Cell Reports,* 27**,** 71-85.e3.

TAKEOKA, A., VOLLENWEIDER, I., COURTINE, G. & ARBER, S. 2014. Muscle spindle feedback directs locomotor recovery and circuit reorganization after spinal cord injury. *Cell,* 159**,** 1626-1639.

TALPALAR, A. E., BOUVIER, J., BORGIUS, L., FORTIN, G., PIERANI, A. & KIEHN, O. 2013. Dual-mode operation of neuronal networks involved in left–right alternation. *Nature,* 500**,** 85-88.

TAN, A. M., CHAKRABARTY, S., KIMURA, H. & MARTIN, J. H. 2012. Selective Corticospinal Tract Injury in the Rat Induces Primary Afferent Fiber Sprouting in the Spinal Cord and Hyperreflexia. 32**,** 12896-12908.

TASHIRO, S., NISHIMURA, S., IWAI, H., SUGAI, K., ZHANG, L., SHINOZAKI, M., IWANAMI, A., TOYAMA, Y., LIU, M., OKANO, H. & NAKAMURA, M. 2016. Functional Recovery from Neural Stem/Progenitor Cell Transplantation Combined with Treadmill Training in Mice with Chronic Spinal Cord Injury. *Scientific Reports,* 6**,** 30898.

TAYLOR, A., DONGA, R. & JÜCH, P. J. W. 1993. Fusimotor effects of midbrain stimulation on jaw muscle spindles of the anaesthetized cat. *Experimental Brain Research,* 93**,** 37-45.

TAYLOR, A., DURBABA, R. & ELLAWAY, P. H. 2004. Direct and indirect assessment of gamma-motor firing patterns. *Can J Physiol Pharmacol,* 82**,** 793-802.

TAYLOR, A., DURBABA, R., ELLAWAY, P. H. & RAWLINSON, S. 2006. Static and dynamic γ-motor output to ankle flexor muscles during locomotion in the decerebrate cat. *The Journal of Physiology,* 571**,** 711-723.

TAYLOR, A., ELLAWAY, P. H., DURBABA, R. & RAWLINSON, S. 2000. Distinctive patterns of static and dynamic gamma motor activity during locomotion in the decerebrate cat. *The Journal of Physiology,* 529**,** 825-836.

TEDESCHI, A. & BRADKE, F. J. C. O. I. N. 2017. Spatial and temporal arrangement of neuronal intrinsic and extrinsic mechanisms controlling axon regeneration. 42**,** 118-127.

TESTER, N. J. & HOWLAND, D. R. 2008. Chondroitinase ABC improves basic and skilled locomotion in spinal cord injured cats. *Exp Neurol,* 209**,** 483-96.

THOMPSON, F. J., REIER, P. J., LUCAS, C. C. & PARMER, R. 1992. Altered patterns of reflex excitability subsequent to contusion injury of the rat spinal cord. *J Neurophysiol,* 68**,** 1473-86.

TODOROVA, N. & RODZIEWICZ, G. S. 1995. Biotin-dextran: fast retrograde tracing of sciatic nerve motoneurons. *Journal of Neuroscience Methods,* 61**,** 145-150.

TORRES-ESPÍN, A., FORERO, J., FENRICH, K. K., LUCAS-OSMA, A. M., KRAJACIC, A., SCHMIDT, E., VAVREK, R., RAPOSO, P., BENNETT, D. J., POPOVICH, P. G. & FOUAD, K. 2018. Eliciting inflammation enables successful rehabilitative training in chronic spinal cord injury. *Brain,* 141**,** 1946-1962.

TOSOLINI, A. P. & MORRIS, R. 2012. Spatial characterization of the motor neuron columns supplying the rat forelimb. *Neuroscience,* 200**,** 19-30.

TOURTELLOTTE, W. G., KELLER-PECK, C., MILBRANDT, J. & KUCERA, J. 2001. The Transcription Factor Egr3 Modulates Sensory Axon–Myotube Interactions during Muscle Spindle Morphogenesis. *Developmental Biology,* 232**,** 388-399.

ULFHAKE, B. & CULLHEIM, S. 1981. A quantitative light microscopic study of the dendrites of cat spinal gamma -motoneurons after intracellular staining with horseradish peroxidase. *J Comp Neurol,* 202**,** 585-96.

ULTANIR, S. K., KIM, J.-E., HALL, B. J., DEERINCK, T., ELLISMAN, M. & GHOSH, A. 2007. Regulation of spine morphology and spine density by NMDA receptor signaling in vivo. 104**,** 19553-19558.

VAN BUUREN, S. & GROOTHUIS-OUDSHOORN, K. 2011. mice: Multivariate Imputation by Chained Equations. *R. Journal of Statistical Software,* 45**,** 1-67.

VAN DEN BRAND, R., HEUTSCHI, J., BARRAUD, Q., DIGIOVANNA, J., BARTHOLDI, K., HUERLIMANN, M., FRIEDLI, L., VOLLENWEIDER, I., MORAUD, E. M., DUIS, S., DOMINICI, N., MICERA, S., MUSIENKO, P. & COURTINE, G. 2012. Restoring Voluntary Control of Locomotion after Paralyzing Spinal Cord Injury. 336**,** 1182-1185.

VAN NIEKERK, E. A., TUSZYNSKI, M. H., LU, P., DULIN, J. N. J. M. & PROTEOMICS, C. 2016. Molecular and cellular mechanisms of axonal regeneration after spinal cord injury. 15**,** 394-408.

VARGAS, M. E. & BARRES, B. A. 2007. Why Is Wallerian Degeneration in the CNS So Slow? 30**,** 153-179.

VU, V. Q. 2011. ggbiplot: A ggplot2 based biplot. *R package version 0.55*.

VULT VON STEYERN, F., MARTINOV, V., RABBEN, I., NJÅ, A., DE LAPEYRIÈRE, O. & LØMO, T. 1999. The homeodomain transcription factors Islet 1 and HB9 are expressed in adult alpha and gamma motoneurons identified by selective retrograde tracing. *Eur J Neurosci,* 11**,** 2093-102.

WAGNER, F. B., MIGNARDOT, J.-B., LE GOFF-MIGNARDOT, C. G., DEMESMAEKER, R., KOMI, S., CAPOGROSSO, M., ROWALD, A., SEÁÑEZ, I., CABAN, M., PIRONDINI, E., VAT, M., MCCRACKEN, L. A., HEIMGARTNER, R., FODOR, I., WATRIN, A., SEGUIN, P., PAOLES, E., VAN DEN KEYBUS, K., EBERLE, G., SCHURCH, B., PRALONG, E., BECCE, F., PRIOR, J., BUSE, N., BUSCHMAN, R., NEUFELD, E., KUSTER, N., CARDA, S., VON ZITZEWITZ, J., DELATTRE, V., DENISON, T., LAMBERT, H., MINASSIAN, K., BLOCH, J. & COURTINE, G. 2018. Targeted neurotechnology restores walking in humans with spinal cord injury. *Nature,* 563**,** 65-71.

WAHL, A.-S., OMLOR, W., RUBIO, J., CHEN, J., ZHENG, H., SCHRÖTER, A., GULLO, M., WEINMANN, O., KOBAYASHI, K. & HELMCHEN, F. J. S. 2014. Asynchronous therapy restores motor control by rewiring of the rat corticospinal tract after stroke. 344**,** 1250-1255.

WÄLCHLI, T., PERNET, V., WEINMANN, O., SHIU, J.-Y., GUZIK-KORNACKA, A., DECREY, G., YÜKSEL, D., SCHNEIDER, H., VOGEL, J., INGBER, D. E., VOGEL, V., FREI, K. & SCHWAB, M. E. 2013. Nogo-A is a negative regulator of CNS angiogenesis. 110**,** E1943-E1952.

WALRO, J. M. & KUCERA, J. 1985. Motor innervation of intrafusal fibers in rat muscle spindles: Incomplete separation of dynamic and static systems. 173**,** 55-68.

WALRO, J. M. & KUCERA, J. 1987. Sharing of sensory terminals between the dynamic bag1 and static bag2 fibers in the rat muscle spindle. *Brain Research,* 425**,** 311-318.

WAN, L. D., XIA, R. & DING, W. L. 2010. Electrical stimulation enhanced remyelination of injured sciatic nerves by increasing neurotrophins. *Neuroscience,* 169**,** 1029-38.

WAND, P., SCHWARZ, M., KOLASIEWICZ, W. & SONTAG, K.-H. 1981. Nigral output neurons are engaged in regulation of static fusimotor action onto flexors in cat. *Pflügers Archiv,* 391**,** 255-257.

WANG, D., ICHIYAMA, R. M., ZHAO, R., ANDREWS, M. R. & FAWCETT, J. W. 2011. Chondroitinase Combined with Rehabilitation Promotes Recovery of Forelimb Function in Rats with Chronic Spinal Cord Injury. *The Journal of Neuroscience,* 31**,** 9332-9344.

WANG, H., LIU, N.-K., ZHANG, Y. P., DENG, L., LU, Q.-B., SHIELDS, C. B., WALKER, M. J., LI, J. & XU, X.-M. 2015a. Treadmill training induced lumbar motoneuron dendritic plasticity and behavior recovery in adult rats after a thoracic contusive spinal cord injury. *Experimental Neurology,* 271**,** 368-378.

WANG, J.-L., CHEN, W.-G., ZHANG, J.-J. & XU, C.-J. J. J. O. M. H. 2021. Nogo-A-Δ20/EphA4 interaction antagonizes apoptosis of neural stem cells by integrating p38 and JNK MAPK signaling. 1-17.

WANG, Z., REYNOLDS, A., KIRRY, A., NIENHAUS, C. & BLACKMORE, M. G. 2015b. Overexpression of Sox11 Promotes Corticospinal Tract Regeneration after Spinal Injury While Interfering with Functional Recovery. *The Journal of Neuroscience,* 35**,** 3139-3145.

WATAKABE, A., SADAKANE, O., HATA, K., OHTSUKA, M., TAKAJI, M. & YAMAMORI, T. 2017. Application of viral vectors to the study of neural connectivities and neural circuits in the marmoset brain. *Developmental neurobiology,* 77**,** 354-372.

WEI, D., HURD, C., GALLEGUILLOS, D., SINGH, J., FENRICH, K. K., WEBBER, C. A., SIPIONE, S. & FOUAD, K. 2016. Inhibiting cortical protein kinase A in spinal cord injured rats enhances efficacy of rehabilitative training. *Experimental Neurology,* 283**,** 365-374.

WEISMANN, A. 1861. Über die Muskulatur des Herzens beim Menschen und im Tierreiche. *Arch. f. Anat. u. wiss. Med*.

WENGER, N., MORAUD, E. M., GANDAR, J., MUSIENKO, P., CAPOGROSSO, M., BAUD, L., LE GOFF, C. G., BARRAUD, Q., PAVLOVA, N., DOMINICI, N., MINEV, I. R., ASBOTH, L., HIRSCH, A., DUIS, S., KREIDER, J., MORTERA, A., HAVERBECK, O., KRAUS, S., SCHMITZ, F., DIGIOVANNA, J., VAN DEN BRAND, R., BLOCH, J., DETEMPLE, P., LACOUR, S. P., BÉZARD, E., MICERA, S. &

COURTINE, G. 2016. Spatiotemporal neuromodulation therapies engaging muscle synergies improve motor control after spinal cord injury. *Nature Medicine,* 22**,** 138-145.

WENJIN, W., WENCHAO, L., HAO, Z., FENG, L., YAN, W., WODONG, S., XIANQUN, F. & WENLONG, D. 2011. Electrical stimulation promotes BDNF expression in spinal cord neurons through Ca(2+)- and Erk-dependent signaling pathways. *Cell Mol Neurobiol,* 31**,** 459-67.

WERNIG, A., MÜLLER, S., NANASSY, A. & CAGOL, E. 1995. Laufband Therapy Based on'Rules of Spinal Locomotion'is Effective in Spinal Cord Injured Persons. 7**,** 823-829.

WESTBURY, D. R. 1982. A comparison of the structures of α- and γ-spinal motoneurones of the cat. *The Journal of Physiology,* 325**,** 79-91.

WHITEHEAD, J., KELLER-PECK, C., KUCERA, J. & TOURTELLOTTE, W. G. 2005. Glial cell-line derived neurotrophic factor-dependent fusimotor neuron survival during development. *Mech Dev,* 122**,** 27-41.

WICKERSHAM, I. R., LYON, D. C., BARNARD, R. J. O., MORI, T., FINKE, S., CONZELMANN, K.-K., YOUNG, J. A. T. & CALLAWAY, E. M. 2007. Monosynaptic Restriction of Transsynaptic Tracing from Single, Genetically Targeted Neurons. *Neuron,* 53**,** 639-647.

WILLS, ZACHARY P., MANDEL-BREHM, C., MARDINLY, ALAN R., MCCORD, ALEJANDRA E., GIGER, ROMAN J. & GREENBERG, MICHAEL E. 2012. The Nogo Receptor Family Restricts Synapse Number in the Developing Hippocampus. *Neuron,* 73**,** 466-481.

WILSON, J. M., BLAGOVECHTCHENSKI, E. & BROWNSTONE, R. M. 2010. Genetically defined inhibitory neurons in the mouse spinal cord dorsal horn: a possible source of rhythmic inhibition of motoneurons during fictive locomotion. *J Neurosci,* 30**,** 1137-48.

WRATHALL, J. R., TENG, Y. D. & CHOINIERE, D. 1996. Amelioration of functional deficits from spinal cord trauma with systemically administered NBQX, an antagonist of non-N-methyl-D-aspartate receptors. *Exp Neurol,* 137**,** 119-26.

YAMAMOTO, K., RUUSKANEN, J. O., WULLIMANN, M. F. & VERNIER, P. 2011. Differential expression of dopaminergic cell markers in the adult zebrafish forebrain. 519**,** 576-598.

YASVOINA, M. V., GENÇ, B., JARA, J. H., SHEETS, P. L., QUINLAN, K. A., MILOSEVIC, A., SHEPHERD, G. M. G., HECKMAN, C. J. & ÖZDINLER, P. H. 2013. eGFP Expression under UCHL1 Promoter Genetically Labels Corticospinal Motor Neurons and a Subpopulation of Degeneration-Resistant Spinal Motor Neurons in an ALS Mouse Model. *The Journal of Neuroscience,* 33**,** 7890-7904.

YIN, X., JONES, N., YANG, J., ASRAOUI, N., MATHIEU, M.-E., CAI, L. & CHEN, S. X. 2021. Delayed motor learning in a 16p11.2 deletion mouse model of autism is rescued by locus coeruleus activation. *Nature Neuroscience*.

Z'GRAGGEN, W. J., METZ, G. A., KARTJE, G. L., THALLMAIR, M. & SCHWAB, M. E. J. J. O. N. 1998. Functional recovery and enhanced corticofugal plasticity after unilateral pyramidal tract lesion and blockade of myelin-associated neurite growth inhibitors in adult rats. 18**,** 4744-4757.

ZAGORAIOU, L., AKAY, T., MARTIN, J. F., BROWNSTONE, R. M., JESSELL, T. M. & MILES, G. B. 2009. A Cluster of Cholinergic Premotor Interneurons Modulates Mouse Locomotor Activity. *Neuron,* 64**,** 645-662.

ZHANG, J., LANUZA, GUILLERMO M., BRITZ, O., WANG, Z., SIEMBAB, VALERIE C., ZHANG, Y., VELASQUEZ, T., ALVAREZ, FRANCISCO J., FRANK, E. & GOULDING, M. 2014. V1 and V2b Interneurons Secure the Alternating Flexor-Extensor Motor Activity Mice Require for Limbed Locomotion. *Neuron,* 82**,** 138-150.

ZHANG, S., FUJITA, Y., MATSUZAKI, R. & YAMASHITA, T. 2018. Class I histone deacetylase (HDAC) inhibitor CI-994 promotes functional recovery following spinal cord injury. *Cell Death & Disease,* 9**,** 460.

ZHANG, Y., NARAYAN, S., GEIMAN, E., LANUZA, G. M., VELASQUEZ, T., SHANKS, B., AKAY, T., DYCK, J., PEARSON, K., GOSGNACH, S., FAN, C.-M. & GOULDING, M. 2008. V3 Spinal Neurons Establish a Robust and Balanced Locomotor Rhythm during Walking. *Neuron,* 60**,** 84-96.

ZHAO, R. R., ANDREWS, M. R., WANG, D., WARREN, P., GULLO, M., SCHNELL, L., SCHWAB, M. E. & FAWCETT, J. W. 2013. Combination treatment with anti-Nogo-A and chondroitinase ABC is more effective than single treatments at enhancing functional recovery after spinal cord injury. *Eur J Neurosci,* 38**,** 2946-61.

ZHONG, H., ZHU, C., MINEGISHI, Y., RICHTER, F., ZDUNOWSKI, S., ROY, R. R., VISSEL, B., GAD, P., GERASIMENKO, Y., CHESSELET, M.-F. & EDGERTON, V. R. 2019. Epidural Spinal Cord Stimulation Improves Motor Function in Rats With Chemically Induced Parkinsonism. 33**,** 1029-1039.

ZIMMERMANN, D. R. & DOURS-ZIMMERMANN, M. T. 2008. Extracellular matrix of the central nervous system: from neglect to challenge. *Histochemistry and Cell Biology,* 130**,** 635-653.

ZÖRNER, B., BACHMANN, L. C., FILLI, L., KAPITZA, S., GULLO, M., BOLLIGER, M., STARKEY, M. L., RÖTHLISBERGER, M., GONZENBACH, R. R. & SCHWAB, M. E. 2014. Chasing central nervous system plasticity: the brainstem's contribution to locomotor recovery in rats with spinal cord injury. *Brain,* 137**,** 1716-1732.

ZÖRNER, B. & SCHWAB, M. E. 2010. Anti-Nogo on the go: from animal models to a clinical trial. *Annals of the New York Academy of Sciences,* 1198**,** E22-E34.

7 Appendix

7.1 Kinematic measurements

Number	Variable title	Description	Calculation
1	SwingDM (s)	Swing Duration Mean (Toe)	count # of frames in swing phase -> convert to time (s) -> mea
2	StanceDM (s)	Stance Duration Mean (Toe)	count # of frames in stance phase -> convert to time (s) -> me
3	CycleDM (s)	Cycle Duration Mean(Toe)	SwingD (s) + StanceD (s) -> mean
4	DutyCM (%)	Duty Cycle Mean(Toe)	StanceD (s) / CycleD (s) -> convert to % -> mean
5	SwingLM (mm)	Stride Length Mean (Toe)	final y value of swing phase (mm) - first y value of swing phase (r > mean
6	SwingSM (mm/s)	Swing Speed Mean (Toe)	SwingL (s) / SwingD (s) -> mean
7	SwingDV (s)	Swing Duration Standard Deviation (Toe)	same as 1 for standard deviation
8	StanceDV (s)	Stance Duration Standard Deviation (Toe)	same as 2 for standard deviation
9	CycleDV (s)	Cycle Duration Standard Deviation (Toe)	same as 3 for standard deviation
10	DutyCV (%)	Duty Cycle Standard Deviation (Toe)	same as 4 for standard deviation
11	SwingLV (mm)	Stride Length Standard Deviation (Toe)	same as 5 for standard deviation
12	SwingSV (mm/s)	Swing Speed Standard Deviation (Toe)	same as 6 for standard deviation
25	CrestSwingHM (mm)	Crest Swing Height Mean (Crest)	mean z value of crest in swing phase (mm) -> mean
26	HipSwingHM (mm)	Hip Swing Height Mean (Hip)	same for hip
27	KneeSwingHM (mm)	Knee Swing Height Mean (Knee)	same for knee
28	AnkleSwingHM (mm)	Ankle Swing Height Mean (Ankle)	same for ankle
29	ToeSwingHM (mm)	Toe Swing Height Mean (Toe)	same for toe
35	CrestSwingHV (mm)	Crest Swing Height Standard Deviation (Crest)	same as 25 for standard deviation
36	HipSwingHV (mm)	Hip Swing Height Standard Deviation (Hip)	same as 26 for standard deviation
37	KneeSwingHV (mm)	Knee Swing Height Standard Deviation (Knee)	same as 27 for standard deviation
38	AnkleSwingHV (mm)	Ankle Swing Height Standard Deviation (Ankle)	same as 28 for standard deviation
39	ToeSwingHV (mm)	Toe Swing Height Standard Deviation (Toe)	same as 29 for standard deviation
65	CrestWM (mm)	Crest Width Mean (Crest)	z value of right crest - z value of left crest -> mean over the ent performance
66	HipWM (mm)	Hip Width Mean (Hip)	same for hip
67	KneeWM (mm)	Knee Width Mean (Knee)	same for knee
68	AnkleWM (mm)	Ankle Width Mean (Ankle)	same for ankle
69	ToeWM (mm)	Toe Width Mean (Toe)	same for toe
70	CrestWV (mm)	Crest Width Standard Deviation (Crest)	same as 65 for standard deviation
71	HipWV (mm)	Hip Width Standard Deviation (Hip)	same as 66 for standard deviation
72	KneeWV (mm)	Knee Width Standard Deviation (Knee)	same as 67 for standard deviation
73	AnkleWV (mm)	Ankle Width Standard Deviation (Ankle)	same as 68 for standard deviation
74	ToeWV (mm)	Toe Width Standard Deviation (Toe)	same as 69 for standard deviation
75	HipSwingAM (°)	Hip Swing Angle Mean (Crest Hip Knee)	convert x,y,z value of crest,hip,knee in swing phase to 2 vectors calculate the angle between the vectors -> mean
76	KneeSwingAM (°)	Knee Swing Angle Mean (Hip Knee Ankle)	same for knee
77	AnkleSwingAM (°)	Ankle Swing Angle Mean (Knee Ankle Foot)	same for ankle
78	HipStanceAM (°)	Hip Stance Angle Mean (Crest Hip Knee)	convert x,y,z value of crest,hip,knee in stance phase to 2 vector calculate the angle between the vectors -> mean
79	KneeStanceAM (°)	Knee Stance Angle Mean (Hip Knee Ankle)	same for knee
80	AnkleStanceAM (°)	Ankle Stance Angle Mean (Knee Ankle Foot)	same for ankle
81	HipSwingAV (°)	Hip Swing Angle Standard Deviation (Crest Hip Knee)	same as 75 for standard deviation
82	KneeSwingAV (°)	Knee Swing Angle Standard Deviation (Hip Knee Ankle)	same as 76 for standard deviation
83	AnkleSwingAV (°)	Ankle Swing Angle Standard Deviation (Knee Ankle Foot)	same as 77 for standard deviation
84	HipStanceAV (°)	Hip Stance Angle Standard Deviation (Crest Hip Knee)	same as 78 for standard deviation
85	KneeStanceAV (°)	Knee Stance Angle Standard Deviation (Hip Knee Ankle)	same as 79 for standard deviation
86	AnkleStanceAV (°)	Ankle Stance Angle Standard Deviation (Knee Ankle Foot)	same as 80 for standard deviation
99	DragDM1 (s)	Drag Duration Mean - 1 mm nail (Toe)	count # of frames that z value of toe is ≤ 1 mm in swing phase convert to time (s) -> mean
100	DragDM2 (s)	Drag Duration Mean - 2 mm nail (Toe)	same for 2 mm
101	DragDM3 (s)	Drag Duration Mean - 3 mm nail (Toe)	same for 3 mm
102	DragLM1 (mm)	Drag Length Mean - 1 mm nail (Toe)	final y value of toe - first y value of toe that z value of toe is ≤ 1 m swing phase -> mean

Figure 7.1 Kinematic variables

Number	Variable title	Description	Calculation
103	DragLM2 (mm)	Drag Length Mean - 2 mm nail (Toe)	same for 2 mm
104	DragLM3 (mm)	Drag Length Mean - 3 mm nail (Toe)	same for 3 mm
105	DragPDM1 (%)	Drag Percent Duration Mean - 1 mm nail (Toe)	DragD / SwingD -> convert to % -> mean
106	DragPDM2 (%)	Drag Percent Duration Mean - 2 mm nail (Toe)	same for 2 mm
107	DragPDM3 (%)	Drag Percent Duration Mean - 3 mm nail (Toe)	same for 3 mm
108	DragPLM1 (%)	Drag Percent Length Mean - 1 mm nail (Toe)	DragL / SwingL -> convert to % -> mean
109	DragPLM2 (%)	Drag Percent Length Mean - 2 mm nail (Toe)	same for 2 mm
110	DragPLM3 (%)	Drag Percent Length Mean - 3 mm nail (Toe)	same for 3 mm
147	AnklePAM (°)	Ankle Plantar Angle Mean (Ankle Toe)	convert x,y value of ankle,toe,a (0,1) line to 2 vectors -> calcu angle between the vectors -> mean
148	AnkleSwingPAM (°)	Ankle Swing Plantar Angle Mean (Ankle Toe)	convert x,y value of ankle,toe,a (0,1) line in swing phase to 2 v calculate the angle between the vectors -> mean
149	AnkleStancePAM (°)	Ankle Stance Plantar Angle Mean (Ankle Toe)	convert x,y value of ankle,toe,a (0,1) line in stance phase to 2 > calculate the angle between the vectors -> mean
150	AnklePAV (°)	Ankle Plantar Angle Standard Deviation (Ankle Toe)	same as 147 for standard deviation
151	AnkleSwingPAV (°)	Ankle Swing Plantar Angle Standard Deviation (Ankle Toe)	same as 148 for standard deviation
152	AnkleStancePAV (°)	Ankle Stance Plantar Angle Standard Deviation (Ankle Toe)	same as 149 for standard deviation
153	AnklePALiftM (°)	Ankle Plantar Angle at Lift Off Mean (Ankle Toe)	same as 147 but only in the beginning of swing phase
154	AnklePALiftV (°)	Ankle Plantar Angle at Lift Off Standard Deviation (Ankle Toe)	same as 153 for standard deviation
155	AnklePAContactM (°)	Ankle Plantar Angle at Initial Contact Mean (Ankle Toe)	same as 147 but only in the beginning of stance phase
156	AnklePAContactV (°)	Ankle Plantar Angle at Initial Contact Standard Deviation (Ankle Toe)	same as 155 for standard deviation
167	WaddleNAM (°)	Waddle N? Angle Mean (Crest)	find the mean line between left and right crest -> calulate the the line with respect to the ground in x-axis -> calculate the difference from the mean line -> mean
168	WaddleNAV (°)	Waddle N? Angle Standard Deviation (Crest)	same as 167 for standard deviation
169	RLCouplingsM (%)	Right to Left Couplings Mean (Toe)	See p89-95 in CatWalk manual for calculating couplings ->
170	RLCouplingsDM (%)	Right to Left Couplings Different from 50% Mean (Toe)	See p89-95 in CatWalk manual for calculating couplings -> m absolute of the mean value - 50%
171	RLCouplingsV (%)	Right to Left Couplings Standard Deviation (Toe)	same as 169 for standard deviation
172	RLCouplingsDV (%)	Right to Left Couplings Different from 50% Standard Deviation (Toe)	same as 170 for standard deviation
176	LRCouplingsM (%)	Left to Right Couplings Mean (Toe)	See p89-95 in CatWalk manual for calculating couplings ->
177	LRCouplingsDM (%)	Left to Right Couplings Different from 50% Mean (Toe)	See p89-95 in CatWalk manual for calculating couplings -> m absolute of the mean value - 50%
178	LRCouplingsV (%)	Left to Right Couplings Standard Deviation (Toe)	same as 176 for standard deviation
179	LRCouplingsDV (%)	Left to Right Couplings Different from 50% Standard Deviation (Toe)	same as 177 for standard deviation
183	CouplingsM (%)	Couplings Mean (Toe)	mean of 169 and 176
184	CouplingsDM (%)	Couplings Different from 50% Mean (Toe)	mean of 170 and 177
185	CouplingsV (%)	Couplings Standard Deviation (Toe)	mean of 171 and 178
186	CouplingsDV (%)	Couplings Different from 50% Standard Deviation (Toe)	mean of 172 and 179
190	CouplingsMD (%)	Couplings Mean Difference (Toe)	absolute difference of 169 and 176
191	CouplingsDMD (%)	Couplings Different from 50% Mean Difference (Toe)	absolute difference of 170 and 177
192	CouplingsVD (%)	Couplings Standard Deviation Difference (Toe)	absolute difference of 171 and 178
193	CouplingsDVD (%)	Couplings Different from 50% Standard Deviation Difference (Toe)	absolute difference of 172 and 179
197	ToeScoreM (%)	%Toe Consistency Score Mean (Toe)	x,y,z of toe -> resample() each step -> arrange in matrix -> p read the explained value
198	AnkleScoreM (%)	%Ankle Consistency Score Mean (Ankle)	same for ankle
199	KneeScoreM (%)	%Knee Consistency Score Mean (Knee)	same for knee
200	HipScoreM (%)	%Hip Consistency Score Mean (Hip)	same for hip
201	CrestScoreM (%)	%Crest Consistency Score Mean (Crest)	same for crest
202	ScoreM (%)	%Consistency Score Mean (Toe Ankle Knee Hip Crest)	mean of 197-201

Figure 7.2 Kinematics variables continued

7.2 'R' scripts

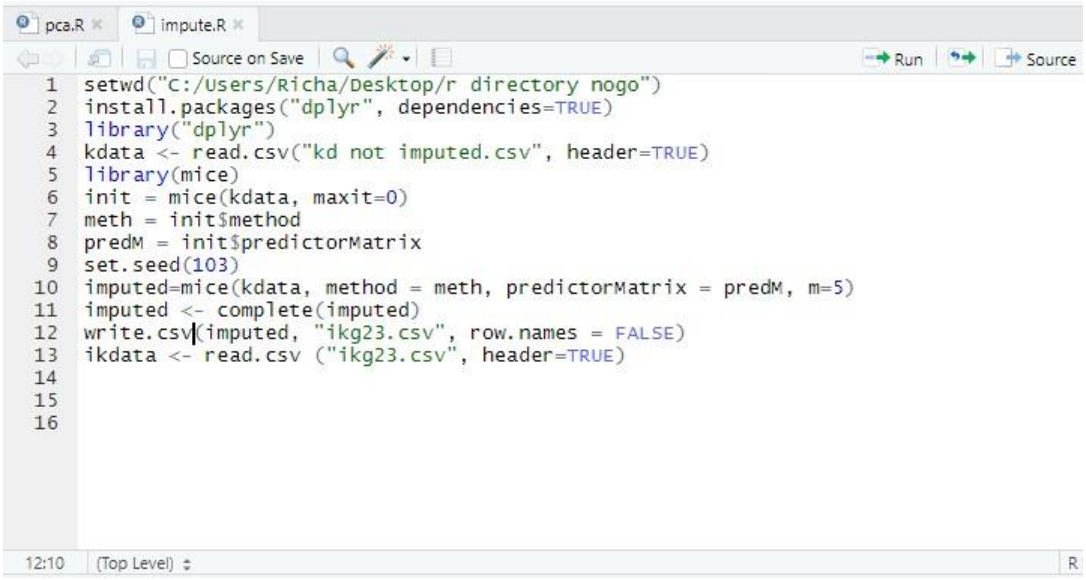

Figure 7.3 mice package

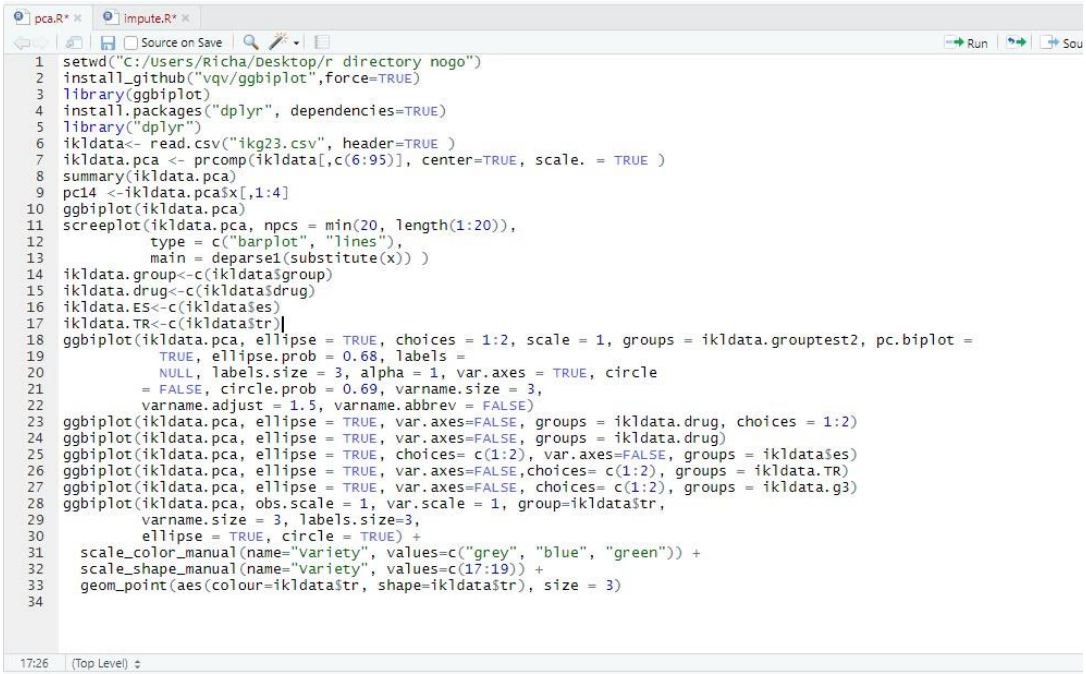

Figure 7.4 ggbiplot package